RATE, AMOUNT, AND STYLE OF LATE CENOZOIC DEFORMATION OF SOUTHERN NINGXIA, NORTHEASTERN MARGIN OF TIBETAN PLATEAU, CHINA

BY

Peizhen Zhang

B. S. Changchun Geological College (1979)
M. S. Chinese University of Science and Technology (1982)

SUBMITTED TO THE DEPARTMENT OF
EARTH, ATMOSPHERIC, AND PLANETARY SCIENCES
IN PARTIAL FULFILLMENT OF THE REQUIREMENTS FOR THE DEGREE OF

DOCTOR OF PHILOSOPHY

at the
MASSACHUSETTS INSTITUTE OF TECHNOLOGY
October 1987

Signature of Author_____
Department of Earth, Atmospheric, and Planetary Sciences

Certified by_____
Peter Molnar
Thesis Supervisor

Certified by_____
B. C. Burchfiel
Thesis Supervisor

Accepted by_____
Chairman, Department of Earth, Atmosphiric,
and Planetary Sciences

RATE, AMOUNT, AND STYLE OF LATE CENOZOIC DEFORMATION OF SOUTHERN NINGXIA, NORTHEASTERN MARGIN OF TIBETAN PLATEAU, CHINA

PEIZHEN ZHANG

Submitted to the Department of Earth, Atmospheric and Planetary Sciences on Oct. 6, 1987, in partial fulfillment of the requirement for the degree of Doctor of Philosophy at the Massachusetts Institute of Technology

ABSTRACT

Continental deformation significantly deviates from the principles of plate tectonics. In order to understand the dynamics of continental deformation, one first must understand its geometry and kinematics. The Tibetan Plateau, which comprises a large part of the 2000 km wide zone of collision between India and Eurasia, provides a natural laboratory to study continental deformation. The Ningxia Autonomous region of China is located along the northeastern margin of Tibetan Plateau, and its neotectonics is characterized by several arcuate active thrust and strike-slip fault zones. All of these fault zones contribute to uplift and to left-lateral motion of that part of the Tibetan Plateau with respect to the area farther northeast.

The style of Cenozoic deformation in the Haiyuan and Liupan Shan fault zone seems to be northeast-southwest shortening followed by left-slip displacement along west-northwest-trending faults. In the Haiyuan area, the oldest Cenozoic structures consist of N30-40°W-trending folds and strike-slip faults and involve most, if not totally, pre-Quaternary rocks. These structures and all of the Quaternary rocks are cut by the Haiyuan strike-slip fault zone that generally trends N60°-65°W and is nearly vertical. In the Liupan Shan area, the structural history can be divided into three overlapping phases. The earliest Cenozoic deformational phase probably occurred between late Pliocene and early Quaternary time, and produced the folds and thrust faults in the Liupan Shan and Yueliang Shan. During this phase, deformation apparently was the result of approximately N50°E shortening, and the Liupan Shan thrust fault apparently acted as a thrust fault with a right-slip component. The second phase of deformation is dominated by left-slip on the N60°W-striking Haiyuan fault zone and shortening in the Liupan Shan area caused by transfer of the left-slip displacement to shortening on north-south-trending structures located farther east. During the second phase, the orientation of shortening in the Liupan Shan area changed to N60°W, and the Madong Shan fold zone began to develop. During the third phase of deformation, deformation in the Madong Shan and Xiaoguan Shan ceased, or was reduced to a very slow rate. The present, active left-slip on the Haiyuan fault zone is accommodated by shortening and left-slip along the Xiaokou fault and the Liupan Shan thrust fault.

Furthermore, most of the shortening in the Liupan Shan area can be shown quantitatively to be associated with the left-slip on the Haiyuan fault zone. The total left-slip displacement on the Haiyuan fault is 10.5 to 15.5 km. The amounts of shortening in the Madong Shan and Liupan Shan before the youngest phase of deformation are 5.7 ± 0.75 and 6.8 - 7.8 km respectively. Combining the 5.7 - 6.9 km shortening in

the Xiaoguan Shan east of them and the 1 - 2 km horizontal shortening during the most recent phase of deformation yields a total shortening of 12.4 - 16.7 km in the direction parallel to the Haiyuan fault zone.

The Haiyuan and Liupan Shan fault zone is the most active among the arcuate zones in the Ningxia region. The 1920 Haiyuan earthquake (M = 8.7), associated with a 220 km long surface rupture zone, was responsible for the death of 220,000 people. Evaluation of the earthquake hazard in these fault zones is intimately tied to the determination of rate of slip on the major fault. To estimate the Holocene slip rate on the Haiyuan fault, the offsets of six streams have been measured to be 30 - 90 m and their minimum ages have been determined. The average Holocene slip rate of the Haiyuan fault is larger than 6 mm/yr. If the average Quaternary slip rate of 5 to 10 mm/yr is applicable to Holocene time, the rate is 8 ± 2 mm/yr. To determine the average displacement associated with the 1920 Haiyuan earthquake, a plane table and an alidade have been used to construct detailed topographic maps of offset features along the surface rupture zone. The average displacement associated with the earthquake was about 8 m. If the Holocene slip rate is 8 ± 2 mm/yr, the recurrence interval for events similar to that in 1920 would be 800 to 1400 years, if all displacement occurred by slip during great earthquakes. Evidence of surface rupture prior to 1920 has been found in trenches across the Haiyuan fault, but neither provides tight constraints on the age of previous events. It is clear that there has been at least one event during the last 2560 ± 210 years ago, and there probably was another event between 1490 ± 175 years ago and 1920. The results from the trenches are consistent with that obtained by using the Holocene slip rate.

Deformational evolution similar to the Haiyuan and Liupan Shan fault zone is also found in other arcuate fault zones in the Ningxia region. For example, the Tianjin Shan - Mibo Shan fault zone consists of thrust faults, reverse faults, and associated ramp folds. The north-northwest-trending major thrust faults along the foot of Tianjin Shan became a strike-slip fault with total left-lateral offset of 3.6 ± 1 km during Quaternary period, whereas at its southeastern end the north-south-trending faults and folds along the Mibo Shan have experienced continued convergence. Even extension within the Yinchuan graben, north of the arcuate zones, can be at least partly related to the left-slip on the Niushou Shan and Dalou Shan fault zone. Thus, all data suggest that the northeastern margin of Tibetan Plateau began to form in late Pliocene time, and early northeastward convergence is followed by later left-slip on west-northwest-trending faults. The left-slip displacement is transferred into crustal shortening on the north-south-trending fault zones. The rates of deformation, however, can be inferred to be less in the northern range than in the southern ranges. The tectonic evolution of the Haiyuan - Liupan Shan fault zone may be a foreshadow the future deformation in the northern arcuate zones.

Thesis Advisors:

Peter Molnar	Senior Research Scientist (Formerly, Professor of Geophysics)
B. C. Burchfiel	Professor of Geology

ACKNOWLEDGEMENT

First and foremost, I would like to deeply express my thanks to my advisors: Peter Molnar and B. C. Burchfiel. They have been a constant source of stimulations, encouragement and ideas during the last 5 years. From them, I have learn not only a great deal of geology and geophysics, but also many basic skills for scientific research. I especially thank their time and patience in improving my English grammar and logic. Their influence will benefit my entire scientific career, the only thing that I regret is my inability to take full advantage of their knowledge and experience when it was the time.

I would like to thank Kip Hodges, John Southard, Peter Molnar, and Clark Burchfiel from M.I.T., and Gary Johnson from Dartmouth College for being in my thesis committee.

I am grateful to Deng Qidong, Institute of Geology, State Seismological Bureau of China, who used to be my advisor when I was in China. Without his arrangement and financial support, the whole project and this thesis would not be possible. I appreciate his encouragement, advice, and help. I hope he is satisfied by this thesis.

Zhang Weiqi, from Ningxia seismological Bureau of China, Wang Yipeng and Song Fangmin, from Institute of Geology, State Seismological Bureau of China, helped me a lot during my field work. I am grateful for their advice and encouragements. Special thanks to Jiao Decheng, one of my best friends, for being my field assistant. I will never forget our mapping in the unusually early-snow covered mountains and in those

constantly raining days.

I would like to thanks Leigh Royden, Kip Hodges, and John Southard for their help and encouragement. Thanks also go to Robert McCaffrey, John Nabelek, Eric Bergman, and Steve Roecker for their kindly help.

There have been many Chinese students and visiting scientists in the Department during my five years at M.I.T., their help and friendship helped me through some difficult times. I would like to express my thanks to Rushan Wu, Tianqing Cao, Paul Huang, Tianwen Lo, Xiaoming Tang and his wife Xiaoming Zhao, Yian Song, Jiadong Qian, Ansu Jin, Jinzhong Zhang, Qiming Wang and Ye Hong.

My fellow students gave me all the help that I asked for. Among them I would like to thank Laurence Page, David Dinter, Barbara Sheffels, James Knapp, Liz Schermer, Cynthia Ebinger, Joann Stock, Peter Wilcock, Mary Hubbard, Sang-Mook Lee, Craig Jones, Mike Nelson, Jeoffrey Abers, Peter Tilke, Dave Klepacki, Doug Walker, and Peter Crowley.

Finally, I would like to thank my wife, Fengying Mao, and my family in China.

PREFACE

This section describes the contribution of the co-authors in the co-authored papers in Chapter II, III, IV, V, and VI. The project has been a collaboration under a protocol between the State Seismological Bureau of China and the U. S. Geological Survey and National Academy of Sciences of the United States; in keeping with the spirit of the collaboration, all earth scientists who participated individually in the aspects of this project are co-authors regardless of the extent of the work that each has done.

In Chapter II, Jiao Decheng and I are responsible for all the plane table mapping of the offset features. Peter Molnar participated in the mapping at Luzigou, and Zhang Weiqi taught us how to make the plane table maps and participated in the mapping at Luzigou, Tangjiapo and west of Fangjiahe. I did all the drafting, analysis, and writing. The reason for putting Zhang Weiqi and Jiao Decheng as the first authors was to balance the credit for the collective work among the Institute of Geology, State Seismological Bureau of China, the Ningxia Seismological Bureau of China, and the Massachusetts Institute of Technology. In 1984, Peter Molnar wrote a paper that was first-authored by scientists from the Institute of Geology, State Seismological Bureau. We decided to have the paper given here as Chapter II first-authored by the Ningxia Seismological Bureau. The remaining papers are to be first-authored by the Massachusetts Institute of Technology.

Peter Molnar and I measured most of the offsets and collected

the samples of organic material for radiocarbon dating. The trenches were dug by local people that we hired, and the trenches were logged by Peter Molnar, Deng Qidong, Zhang Weiqi, and me. I did the drafting, analysis, and writing of the two papers in Chapter III and IV.

In Chapter V, I mapped most of the area of Madong Shan, and the Liupan Shan fault zone, while I was assisted by Jiao Decheng. B. C. Burchfiel, Peter Molnar, Leigh Royden, Wang Yipeng, Zhang Weiqi who mapped the area east of Sikouzi in the Madong Shan. In Chapter VI, Peter Molnar, Leigh Royden, Wang Yipeng, and Zhang Weiqi mapped the Lijiapuzi and Qingeda areas along the Tianjin Shan - Mibo Shan fault zone. B. C. Burchfiel, Jiao Decheng, and I mapped Hong Gou Liang and Xiao Hong Gou areas. Once again, I am responsible for drafting, analysis, and writing.

TABLE OF CONTENTS

Chapter I

INTRODUCTION

Plate tectonics has been successful in explaining much of present and past deformation of oceanic regions of the earth. The assumption that the plates are essentially rigid bodies well describes the behavior of the oceanic regions. However, it has been recognized for many years that the deformation of the continents represents a significant departure from the principles of plate tectonics (McKenzie, 1972, 1977; Molnar and Tapponnier, 1975; Tapponnier and Molnar, 1976; England and McKenzie, 1982, 1983). For example, the Tibetan Plateau, the zone of collision between India and Asia, is more than 2000 km wide (Figure 1). The crustal thickness beneath the Tibetan Plateau is very thick, 70 ± 5 or 10 km (Chen and Molnar, 1981; Molnar et al., 1987a,b). Although some of the seismicity and deformation in Tibetan Plateau appears to occur in narrow linear zones, much of it is diffuse in nature and cannot be adequately accounted for in terms of the relative motion of the large plates, or even of a great number of small plates.

The Cenozoic deformation of the Tibetan Plateau includes a full spectrum of styles and structural orientations and is distributed over a vast area (Figure 1). Much, if not all, of the deformation can be attributed to the collision of the Indian plate with Eurasia. The collision and subsequent penetration of India into Eurasia resulted in the folding and over-thrusting of the northern margin of India to form the Himalaya, and India's penetration caused a thickening of Tibet's crust. The rise of the Tian Shan since Oligocene time is also easily ascribable to this collision. At the present, much of the active

tectonics and most of the major earthquakes north or east of the Himalaya reflect strike-slip and some normal faulting. Slip on those faults seems to reflect an eastward extrusion of the material in Tibetan Plateau north of Himalaya. Thus, the Tibetan Plateau becomes a natural laboratory for studies of the dynamics of collision-related continental deformation. However, in order to achieve this aim, one must first understand the geometry of the structures and their kinematics.

Two questions are especially important in understanding the geometry, kinematics and dynamics of continental deformation in the Tibetan Plateau, and central and eastern Asia.

1, How is the convergence between India and Eurasia partitioned into deformation of different kinds and at different rates in the various parts of Asia, if the deformation is related to the collision between India and Eurasia? This question is crucial in determining whether the crustal thickening underneath the Tibetan Plateau is by underthrusting of the Indian continental lithosphere or by the deformation within the wide area of the Tibetan Plateau, and northern and eastern Asia. From Minster and Jordan's (1978) angular velocity the convergence of India with Eurasia at 90°E is calculated to be 58 ± 6 mm/yr. Neogene underthrusting of India beneath the front of the Himalaya has been occurring at a rate of 15 ± 5 mm/yr (Lyon-Caen and Molnar, 1985). Even if crustal shortening at a rate of as much as 5 mm/yr were occurring within the Himalaya (Molnar, 1987), making a total of about 18 ± 7 mm/yr between southern Tibet and India, the amount would be less than half of the total. Including an additional 13 ± 7 mm/yr of crustal shortening within the Tian Shan (Molnar and Deng, 1984), the sum

of these average values, about 36 mm/yr, is still much less than the theoretical angular velocity of 58 ± 6 mm/yr (Figure 1) (Minster and Jordan, 1978; Molnar at al., 1987b). Some of the convergence is probably absorbed by strike-slip faulting on the major fault zones, such as the Altyn Tagh, Haiyuan, Kunlun, and Xianshuihe faults. The first step in evaluating how deformation is distributed is to place constraints on the rates of slip on major fault zones. In this thesis the slip rate on the Haiyuan fault will be constrained.

2, How has the style of deformation evolved with time? As a specific example some extreme possibilities will be considered. The strike-slip faulting and eastward extrusion may have begun shortly after the collision and may have been an important phenomenon in Asia throughout the middle and later Tertiary. This inference was implicitly accepted, if cautiously stated, in the early studies by Molnar and Tapponnier (1975) and was an explicit conclusion of Tapponnier et al. (1982). In the other extreme, the collision of India with Eurasia may have first created thick crust in Tibet, so that most of the deformation may have originally involved thrust or reverse faulting and folding. The strike-slip faulting might have developed (or become important) late in the evolution of the collision. This is the conclusion predicted by England and Houseman (1986) from numerical experiments of continental deformation between India and Eurasia. Distinguishing between these two possibilities might be difficult if major strike-slip faults were active for only short durations (a few million years), and if zones with significant strike-slip displacement in the late Tertiary were no longer active. In any case, evaluating how Asia has evolved in the last 50

million years will require more time and energy than we will have in our lifetimes. Accordingly, progress is likely to be most rapid if carefully selected areas are examined in detail in order to define how deformation has evolved in these areas.

Present hypotheses of Cenozoic and active intracontinental deformation within Asia relate it to the collision of Asia with the Indian subcontinent about 40 to 55 million years ago and the continued convergence within continental crust between India and Asia (for example, see Molnar and Tapponnier, 1975, 1978; and Tapponnier and Molnar, 1976, 1977; England and McKenzie, 1982, 1983). These hypotheses are based largely on the study of Landsat imagery, seismological studies of earthquakes, numerical experiments and what little geological information is available in the literature. There is very little direct geological ground truth available for most of the region. Our study in the Ningxia region is an attempt to begin to provide geological data to address the questions of continental deformation and dynamics in Tibetan Plateau.

The Ningxia Autonomous region is located along the northeastern margin of the Tibetan Plateau of north-central China, and spans part of the transition zone between active crustal shortening and strike-slip faulting to active crustal extension (Figure 2). This margin of the Tibetan Plateau drops irregularly in elevation from 3600 m in the south to 1200 m along the Huang He (Yellow River) in the north and Qinshuihe in the east (Figure 3). To the north lies the Gobi desert, the Helan Shan and the Yinchuan Valley, and to the east is the Ordos Plateau. The land surface in this part of the Tibetan Plateau is

characterized by smooth rounded slopes with narrow, steep-walled stream valleys. This morphology is the result of deposition of a blanket of windblown Pleistocene loess that has only recently been incised by present day streams that generally follow the more ancient loess-buried valleys. The loess cover makes mapping difficult because exposure of older rocks is commonly discontinuous and present only beneath the loess in the valleys.

The Ningxia region is characterized by numerous active faults and contains the transition from strike-slip and thrust faulting within the broad northeastern margin of the Tibetan Plateau to normal faulting that dominates the tectonics of northeastern China (Figure 3). Thrust faulting dominates the northern boundary of the western Qinling mountains in the southeastern part of the region. Left-slip strike-slip faults are present in the west-central part of the region. All of these active faults contribute to the continuing uplift of the northeastern margin of the Tibetan Plateau. The thrust faults in the Yanton Shan, Dalou Shan and Niushou Shan lie northeast of the main topographic front of the Plateau and may foreshadow future northeastward migration of the Plateau. The Helan Shan in the northeastern part of the region is bounded by normal faults, and the Yinchuan valley is underlain by a graben with at least 1600 m of Quaternary sediment. This area of active extension is only part of the regional area of extension that surrounds three sides of the Ordos Plateau and that extends farther into Northeast China. Three major earthquakes with $M > 6$ are known from historical records to have occurred within the Yinchuan basin (Lee et al., 1976; Li et al., 1960; Tapponnier and Molnar, 1977). Of specific interest to the

present study was the December 16, 1920, Haiyuan earthquake (M = 8.7), which was associated with a surface rupture 220 km long and was followed by an aftershock of M = 7.5 in the region west of Salt Lake basin.

The purpose of work in this part of China is focused on answering several regional and local questions. Regionally we would like to know 1) how the Tibetan Plateau is built; 2) when deformation began in this part of the plateau; 3) what are the past and present rates of plateau uplift and lateral motion; 4) how the total displacement within the region is partitioned among various faults; 5) how the fault-bounded blocks of crust interact with one another; and 6) how the strike-slip displacement along the west northwest-trending faults is transformed to north-south convergence and crustal shortening. Locally we wish to know 1) the evolution of the fault zones in this region; 2)their times of formation; 3) the total offsets along the strike-slip fault zones and the amount of shortening in convergent zones; 4) Quaternary and Holocene slip rates along the fault zones, and 5) the recurrence interval of great earthquakes occurring in these zones. These are important questions that need to be addressed in order to understand the processes of intracontinental deformation in this particular region. Studies in this region will form a basis for extrapolation to the Asian region in general. Only through detailed field studies of such areas as the Ningxia region will we be able to obtain constraints needed to reconstruct quantitatively the evolution of deformation within Asia.

Chapter two of this thesis concerns the displacement along the Haiyuan fault associated with the great 1920 Haiyuan, China, earthquake (M = 8.7). We used several methods to demonstrate that the smallest

offset features are associated with the 1920 earthquake. A plane table and an alidade have been used to construct detailed topographic maps of offset features (stream channels, dry gullies, and old terrace walls) along the fault zone that ruptured during the earthquake. The measured displacements range from possibly as little as 4.4 m to as much as 11 m. The maximum displacement that can be demonstrated convincingly is about 10 m. The reliable average slip probably was 8 ± 2 m during the earthquake. This amount of displacement appears to be the characteristic amount of slip for 1920-type events.

In chapter three we measured the 30 - 90 m offsets of six streams along the Haiyuan fault and determined minimum ages of these offsets to set the lower bounds for the Holocene slip rate. The bounds range from 3.5 ± 0.8 to 16.4 ± 5.9 mm/yr with the five that we consider most reliable to be less than 7.6 ± 1.0 mm/yr. Careful studies indicate that the average Holocene slip rate of the Haiyuan fault is larger than 6 mm/yr. If it is less than 10 mm/yr, or in another form, 8 ± 2 mm/yr, then this rate is comparable to the 5 to 10 mm/yr average slip rate over Quaternary time.

Chapter four mainly describes the evidence of surface rupture prior to 1920 observed from trenches across the Haiyuan fault zone. Although neither provides tight constraints on the age of previous earthquakes, it is clear that faulting occurred since 2560 ± 210 years ago, and there probably was another faulting event that occurred since 1520 ± 175 years ago, but before 1920. If we assume that the average displacement associated with pre-1920 event was also 8 m, the Holocene slip rate is 8 ± 2 mm/yr. The resulting average recurrence interval for

earthquakes with slips of 8 m would be from 800 years to 1400 years. The historical record also suggests that the earthquake recurrence interval along the Haiyuan fault is probably not less than 800 years. Therefore the results from the trenches, from the historical record, and from the Holocene and Quaternary slip rate are consistent with one other.

Chapter five discusses the amount and style of late Cenozoic deformation of the Liupan Shan area based on detailed geological mapping in that area. The Liupan Shan area is located in the southernmost part of Ningxia and the eastern end of the Haiyuan fault zone. Its kinematics and strain evolution is tightly related to the evolution of the adjacent areas. Most of the magnitude of the deformation quantitatively can be shown to have been the result of left-slip displacement on the Haiyuan fault zone. The observed amount of shortening in the Liupan Shan area (12.4 - 16.7 km) is consistent with a total left-lateral displacement of 10.5 to 15.5 km on the Haiyuan fault. The structures in the Liupan Shan area also suggest a thin-skinned deformation. The geological interpretation at this area can be extended to all of southern Ningxia, which forms the developing northeastern margin of the Tibetan Plateau.

In chapter six, we synthesized our field mapping and studies all over the Ningxia region, particularly the late Cenozoic tectonics along the Tianjin Shan - Mibo Shan zone. It seems that the late Cenozoic deformation in Ningxia region began in late Pliocene or earliest Pleistocene time. The style of deformation is left-slip along the west northwest-trending faults followed by convergence in a northeast direction. The rates of Cenozoic deformation appear to be irregular. Extension in northern Ningxia region is probably related to left-slip

faulting along the Niushou Shan - Dalou Shan fault, which bounds the Yinchuan graben on the south.

REFERENCES

Armijo, R., P. Tapponnier, J. -L. Mercier, and T. Han, Quaternary extension in southern Tibet: Field observations and tectonic implications, J. Geophys. Res., 91, 13,803-13,872, 1986.

Burchfiel, B. C., Zhang P., Wang Y., Zhang W., Jiao D., Song F., Deng Q., Molnar P., and L. Royden, Geology of the Haiyuan fault zone, Ningxia Autonomous Region, China and its relation to evolution of the northeastern margins of the Tibetan Plateau, submitted to J. Geophys. Res., 1987.

Chen, W.-P., and P. Molnar, Constraints on the seismic wave velocity structure beneath the Tibetan Plateau and their tectonic implications, J. Geophys. Res., 86, 5937-5962, 1981.

England, P.C., and D.P. McKenzie, A thin viscous sheet model for continental deformation, Geophys. J. R. Astron. Soc., 70, 295-231, 1982.

England, P.C., and D.P. McKenzie, Correction to: A thin viscous model for continental deformation, Geophys. J. R. Astron. Soc., 73, 523-532, 1983.

England, P.C., and G.A. Houseman, Finite strain calculations of continental deformation; 2. Comparison with the India-Asia collision, J. Geophys. Res., 91, 3664-3676, 1986.

Lee, W.H.K., Wu, F.T., and C. Jacobsen, A catalog of historical earthquake in China compiled from recent Chinese publications, Bull. Seismol. Soc. Am., 66, 2003-2016, 1976.

Li, S. et al., A catalogue of earthquake in China, (in Chinese), Science Press, Beijing, 1960.

Lyon-Caen, H., and P. Molnar, Gravity anomalies, flexure of the Indian plate, and the structure, support and evolution of the Himalaya and Ganga basin, Tectonics, 4, 513-538, 1985

McKenzie, D.P., Active tectonics of the Mediterranean region, Geophys. J. R. Astron. Soc., 30, 109-185, 1972.

McKenzie, D.P., Can plate tectonics describe continental deformation? In Bijn-Duval, B. and Montadert, L. (eds.), Structural history of the Mediterranean basins, Editions Technip, Paris, 189-196, 1977.

Minster, J.B., and T.H. Jordan, Present-day plate motions, J. Geophys. Res., 83, 5331-5354, 1978.

Molnar, P., Inversion of profiles of uplift rates for the geometry of dip-slip faults at depth, with examples from Alps and the Himalaya, Ann. Geophysicae, (in press), 1987.

Molnar, P. and W.-P Chen, Focal depths and fault plane solutions of earthquakes under the Tibetan Plateau, J. Geophys. Res., 88, 1180-1196, 1983.

Molnar, P., and Deng Qidong, Faulting associated with large earthquakes and the average rate of deformation in central and eastern Asia, J. Geophys. Res., 89, 6203-6227, 1984.

Molnar, P., Burchfiel, B.C., Zhao Ziyun, Liang K'uangyi, Wang Shuji, and Huang Minmin, Geological evolution of northern Tibet: Results of an expedition to Ulugh Muztagh, Science, 235, 299-304,1987a.

Molnar, P., Burchfiel, B.C., Liang K'uangyi, and Zhao Ziyun, Geomorphic evidence for active faulting in the Altyn Tagh and northern Tibet and qualitative estimates of its contribution to the convergence of India and Eurasia, Geology, 15, 249-253, 1987b.

Molnar P., and P. Tapponnier, Cenozoic tectonics of Asia: Effects of a continental collision, Science, 189, 419-426, 1975.

Tapponnier, P., and P. Molnar, Slip-line field theory and large scale continental tectonics, Nature, 264, 319-324, 1976.

Tapponnier P., and P. Molnar, Active faulting and Cenozoic tectonics of China, J. Geophys. Res., 82, 2905-2930, 1977.

Tapponnier, P., G. Pelzer, A.Y. Le Dain, R. Armijo, and P. Cobbold, Propagating extrusion tectonics in Asia: New insights from simple plasticine experiment, Geology, 10, 611-616, 1982.

Zhang P., Molnar P., Burchfiel B.C., Royden L., Wang Y., Deng Q., Song F., Zhang W., and Jiao D., Bounds on the Holocene slip rate of the Haiyuan fault, north-central China, submitted to Quaternary Research, 1987.

Figure Captions

Figure 1. Simplified tectonic map of the Tibetan Plateau, the deformational zone produced by collision between the Indian plate and Eurasia from Molnar et al., (1987). This map summarizes inferred rates of slip along major faults and of deformation across this broad intracontinental deformational zone. Rates for Himalaya are from Lyon-Caen and Molnar (1985), modified by Molnar (1986); for Tibet, from Armijo et al. (1986), Molnar and Chen (1983), and Molnar and Deng (1984); for Kunlun faults, from unpublished work of W.S.F. Kidd and P. Molnar; for Tian Shan and for Xianshuihe fault, from Molnar and Deng, and for Haiyuan fault, from Burchfiel et al., (1987), Zhang et al., (1987). The lines with solid triangles are thrust or reverse faults, the lines with arrows are strike-slip faults, and the lines with ticks are normal faults.

Figure 2. Simplified map of tectonic setting of the Ningxia Region.

Figure 3. Map of the major structural features and epicenters of large earthquakes in the Ningxia Autonomous region, northeastern margin of the Tibetan Plateau. Dotted area is the northeastern margin of the Tibetan Plateau.

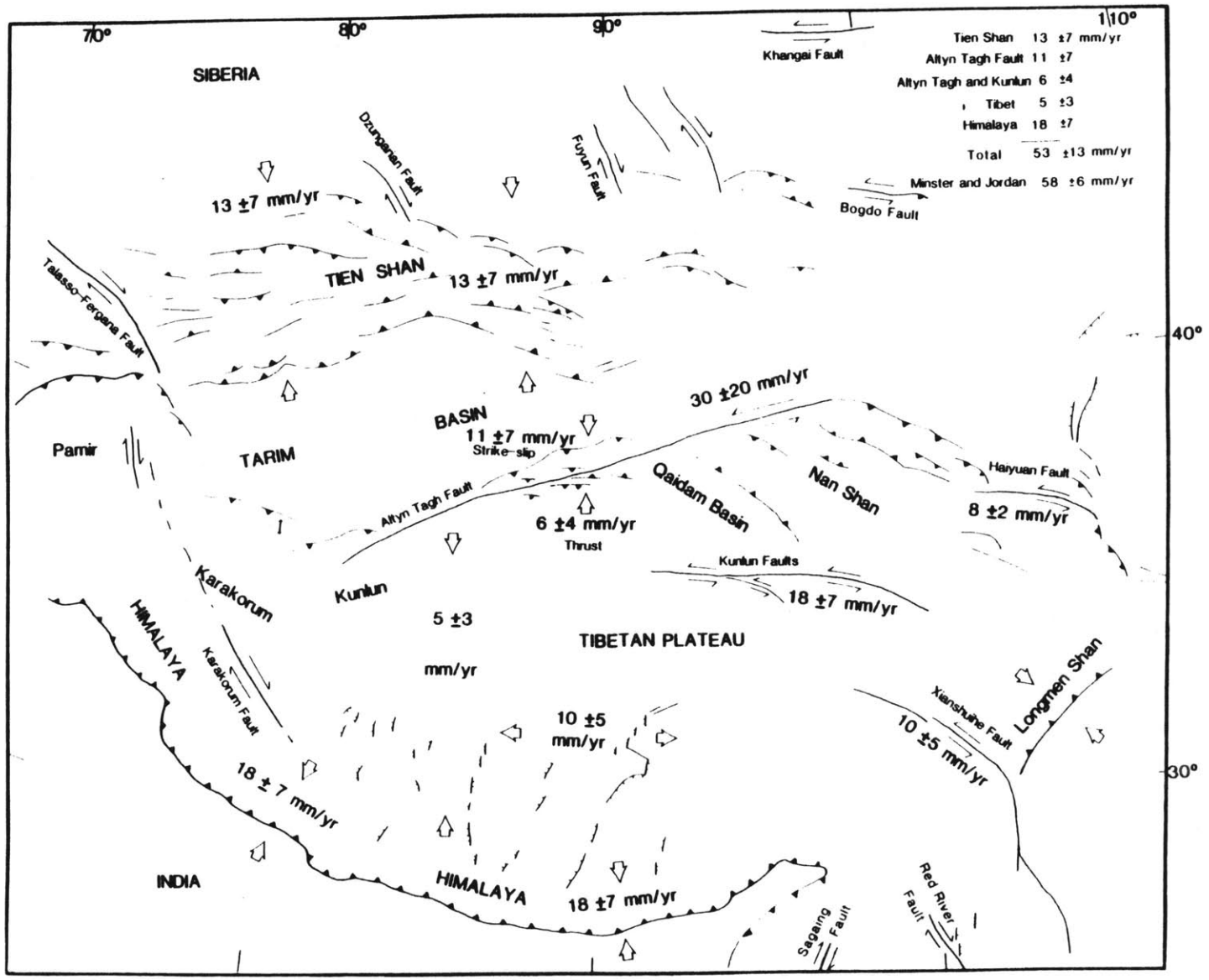
70°
80°
90°
110°
40°
30°
SIBERIA
Khangai Fault
Tien Shan 13 ±7 mm/yr
Altyn Tagh Fault 11 ±7
Altyn Tagh and Kunlun 6 ±4
Tibet 5 ±3
Himalaya 18 ±7
Total 53 ±13 mm/yr
Minster and Jordan 58 ±6 mm/yr
Dzungarian Fault
Fuyun Fault
Bogdo Fault
13 ±7 mm/yr
TIEN SHAN
13 ±7 mm/yr
Talasso-Fergana Fault
30 ±20 mm/yr
BASIN
11 ±7 mm/yr
Strike-slip
Pamir
TARIM
Altyn Tagh Fault
6 ±4 mm/yr
Thrust
Qaidam Basin
Nan Shan
Haryuan Fault
8 ±2 mm/yr
Kunlun Faults
18 ±7 mm/yr
Karakorum
Kunlun
5 ±3
mm/yr
TIBETAN PLATEAU
HIMALAYA
Karakorum Fault
10 ±5
mm/yr
Xianshuihe Fault
10 ±5 mm/yr
Longmen Shan
18 ±7 mm/yr
INDIA
HIMALAYA
18 ±7 mm/yr
Sagaing Fault
Red River Fault

Figure 1

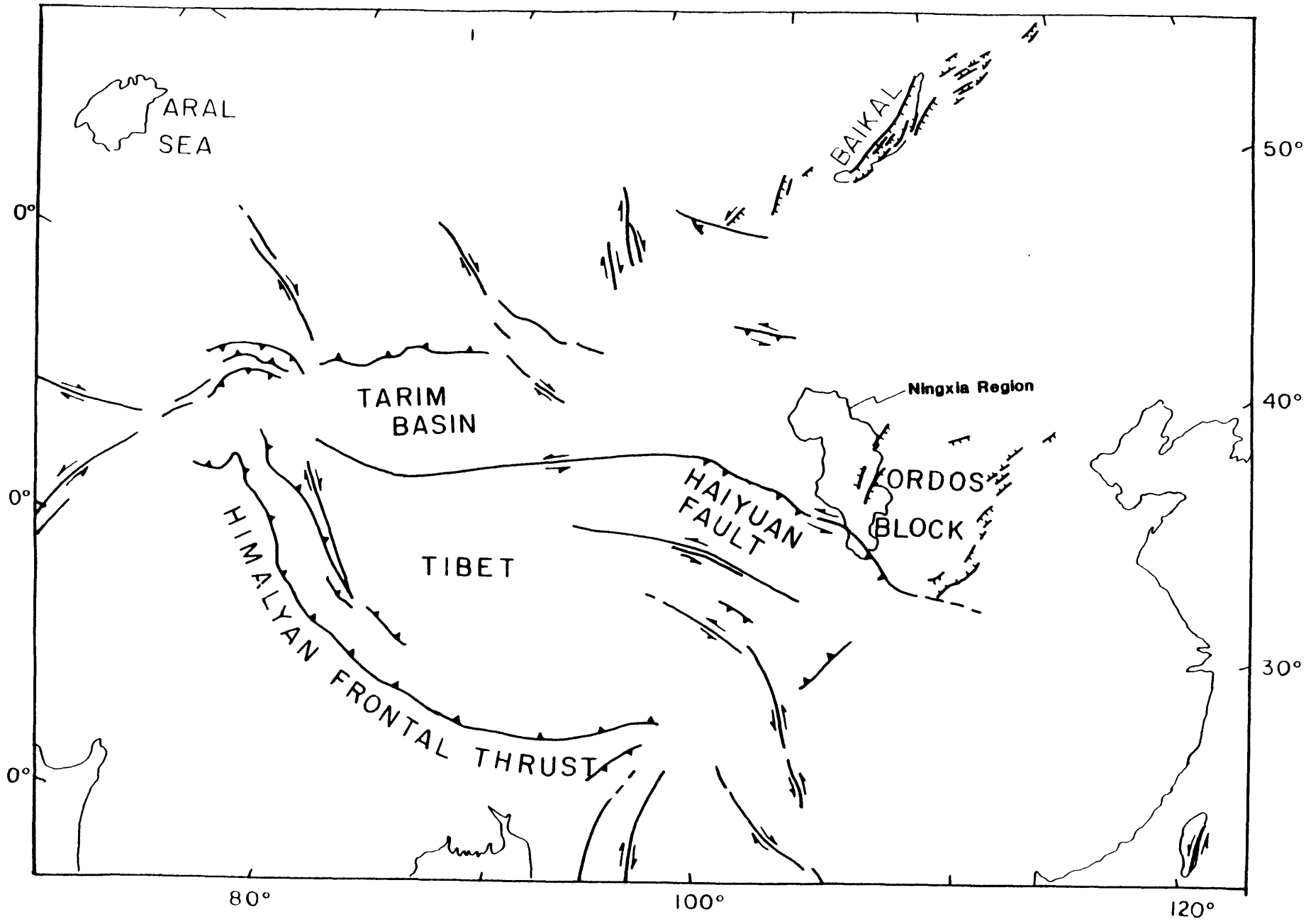
ARAL
SEA
BAIKAL
50°
0°
TARIM
BASIN
Ningxia Region
40°
0°
HAIYUAN
FAULT
ORDOS
BLOCK
TIBET
HIMALYAN FRONTAL THRUST
30°
0°
80°
100°
120°

Figure 2

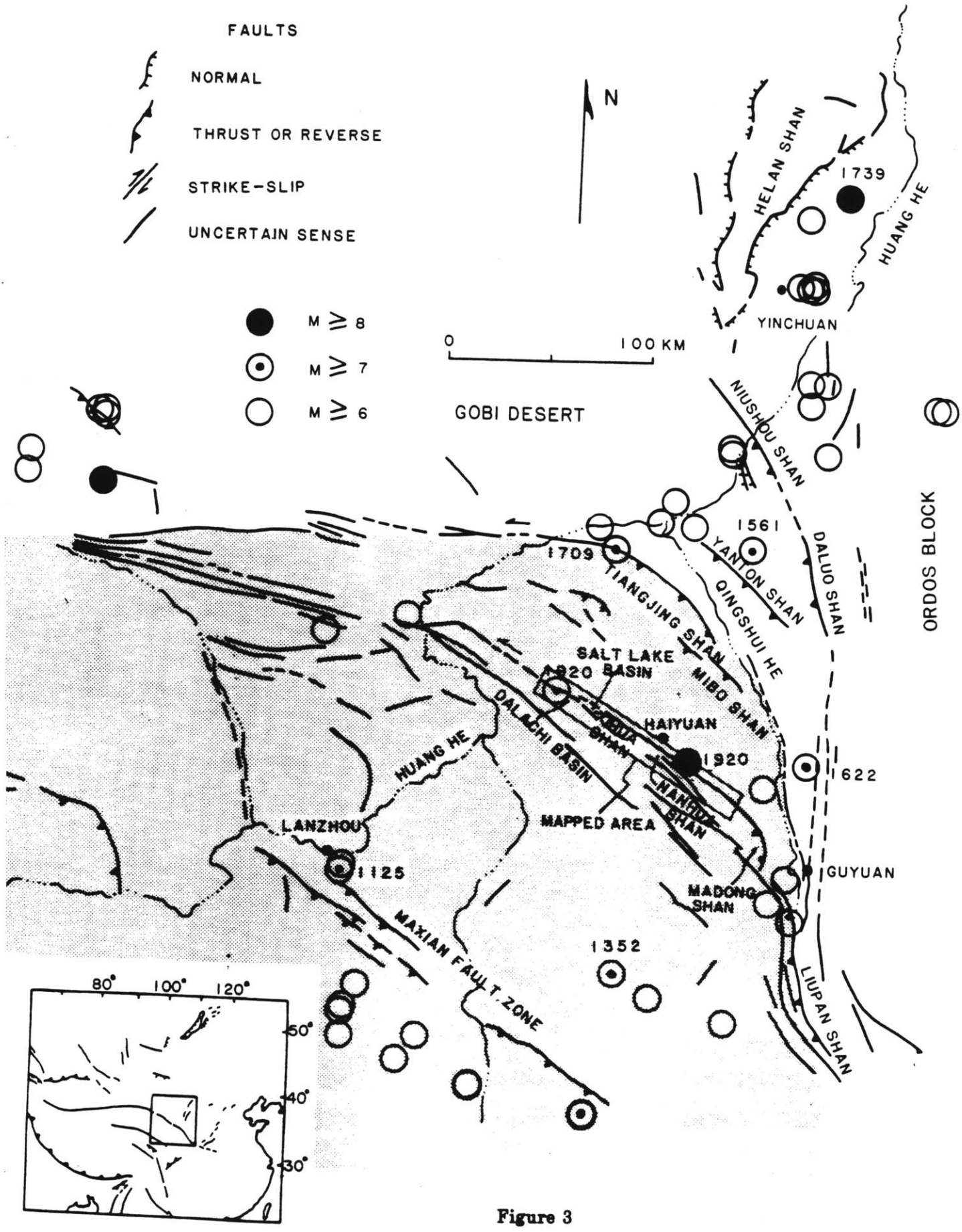
FAULTS
NORMAL
THRUST OR REVERSE
STRIKE-SLIP
UNCERTAIN SENSE
N
M ≥ 8
M ≥ 7
M ≥ 6
0
100 KM
GOBI DESERT
HELAN SHAN
1739
HUANG HE
YINCHUAN
NIUSHOU SHAN
1561
YANTON SHAN
DALUO SHAN
ORDOS BLOCK
1709
TIANGJING SHAN
QINGSHUI HE
SALT LAKE BASIN
MIBO SHAN
DALIANHI BASIN
HAIYUAN
1920
1622
HUANG HE
LANZHOU
1125
MAPPED AREA
GUYUAN
MADONG SHAN
1352
MAXIAN FAULT ZONE
LIUPAN SHAN
80°
100°
120°
50°
40°
30°

Figure 3

Chapter II

Displacement along the Haiyuan Fault Associated with the Great 1920 Haiyuan, China, Earthquake

Zhang Weiqi and Jiao Decheng

Ninxia Seismological Bureau

Ningxia-Hui Autonomous Region

Yinchuan, China

Zhang Peizhen, Peter Molnar, and B. C. Burchfiel

Department of Earth, Atmospheric and Planetary Sciences

Massachusetts Institute of Technology

Cambridge, Massachusetts 02139

and

Deng Qidong, Wang Yipeng and Song Fangmin

Institute of Goelogy

State Seismological Bureau

Beijing, China

Abstract

We used a plane table and an alidade to construct detailed topographic maps of offset features (stream channels, dry gullies, and old terrace walls) along the fault zone that ruptured during the 1920 Haiyuan earthquake (M = 8.7) in Ningxia and Gansu, China. The maximum displacement appears to have reached 10 m at Shikaguangou between the Salt Lake and Xianzhou basins in southern Ningxia. The average displacement along the 100 km of the fault that we studied was about 8 meters. Assuming the average Holocene slip rate to be 8 ± 2 mm/year, the recurrence interval for events similar to that in 1920 would be about 800 to 1400 years.

Introduction

A basic premise in the evaluation of earthquake hazards is that a knowledge of the characteristics of past seismicity will allow us to predict at least some aspects of future seismicity. Allen (1968) postulated that the historical seismicity of the San Andreas fault may reflect the long-term behavior, such that future large earthquakes will occur where they have in the past. Moreover, the concept of a meaningful average recurrence intervals (e.g. Wallace, 1970) is based on the assumption that the amount of slip that occurred in a past earthquake will reoccur in future earthquake, with the interval between them equal to that amount of slip divided by the long term average rate of slip in the absence of fault-creep. Measurements of displacement and recurrence intervals for earthquakes that are associated with surface faulting along the Wasatch fault zone suggest that most of the slip has occurred during earthquakes of essentially the same size and therefore with a relatively narrow range of magnitudes (Schwartz et al., 1981; Schwartz and Coppersmith, 1984). The studies of displacements of historical earthquakes and earthquake recurrence intervals along the San Andreas fault zone suggest that the displacements during one earthquake may differ from one segment to another along the fault zone, and that different segments rupture with earthquakes of different magnitude (Sieh, 1978a, 1978b, 1984; Sieh and Jahns, 1984). Nevertheless, offsets at particular localities recur with similar amounts from one event to the next. If the slip rate over a long time period is constant

throughout the length of the fault, earthquakes will occur more frequently on segments with small amounts of displacement than those with large amounts of displacement. To discern such variability, however, requires relatively accurate knowledge of the amounts of displacement associated with historical earthquakes.

A 200 km long left-lateral surface rupture zone formed during the Haiyuan earthquake (M = 8.7) of December 16, 1920 in northcentral China. This earthquake was responsible for 220,000 deaths and the destruction of thousands of towns and villages (Lanzhou Institute of Seismology and Ninxia Seismological Bureau, 1980). The surface displacement of 1920 earthquake represented renewed activity along the Haiyuan fault zone, one of the most important left-lateral fault zones in central Asia (e.g. Molnar and Tapponnier, 1975; Tapponnier and Molnar, 1977.).

Our study was carried out only in the eastern half of this fault zone (Figure 1). The average strike of the Haiyuan fault is about N65W. At the western end of this area, the Haiyuan fault zone follows the southern foot of Huangjiawa Shan and is marked by a relatively narrow zone along which a series of small streams and ridges are displaced. Where the fault enters the southwest side of the Salt Lake basin, a small pull-apart basin (Figure 1), the displacement along this strand steps over to another strand north of the basin (Burchfiel et al., 1987; Deng et al, 1984, 1986; Zhang et al., 1983). Among these strands, displacements were observed only within the step-over zone near Tangjiapo. From the Salt Lake basin to the southeast, the Haiyuan fault follows the northern foot of the Xihua Shan and Nanhua Shan (Figure 1). The surface rupture zone is commonly defined by small scarps and

grabens, but in some places it is very difficult to recognize on the ground. From east of Luzigou to the eastern end of the fault zone, surface ruptures become increasingly difficult to recognize and eventually a continuous trace cannot be seen. A fault trace trending N35°W intersects the main Haiyuan fault zone southeast of Luzigou where the surface ruptures of the Haiyuan fault zone become more obscure to the east. The intersecting fault can be followed more than 40 km to the south-southeast. The displacement at the eastern end of the Haiyuan fault zone probably has been partly absorbed by slip on this fault, but we do not call it the Haiyuan fault because its trend differs considerably from that of the main Haiyuan fault zone.

The general geometry of the surface rupture zone and the distribution of displacement during the 1920 earthquake were described preliminarily by Deng et al. (1984, 1986) and by Song et al. (1982). The variability of their tape-measured offsets probably is due to the inclusion of offsets on only one strand where several subparallel strands were active. The goal of this paper is to present more objective data on the amount of left-lateral displacement.

Displacements associated with 1920 Haiyuan Earthquake

Although the earthquake occurred 65 years prior to our study, and the loess-covered area has undergone rapid erosion, some of fault scarps of the rupture zone and some offset features are still visible. Along the zone of surface rupture associated with the 1920 earthquake, many reference features such as stream channels, alluvial fans, topographic

surfaces and some man-made features have been offset. The smallest offsets are probably the result of the 1920 event. This presumes that these topographic features were created prior to the 1920 event but after the youngest previous event. We think that this is a reasonable assumption for the following reasons.

First, we know that a rupture zone that displaced these features was formed during 1920 earthquake. During our studies several old local people pointed out that those ruptures were associated with the 1920 earthquake. In 1983, Ma Jinchao, then an 82-year-old man who is one of the two survivors of the earthquake in Caiyuan (Figure 1), said that the rupture could be traced along northern foot of Nanhua Shan all the way to the Yuan river. Tian Bai-you, an 87-year-old man who lived in Luzigou, said that some "cracks" formed from Luzigou to Shanmen during the earthquake. These "cracks" are, in fact, a combination of grabens, troughs and fault scarps. In 1983, an unidentified, 82-year-old man who moved to Shaojiazhuang three years after the earthquake, said that the newly formed scarps could be followed continuously from Tangjiapo to Shaojiazhuang, and his neighbors told him that those scarps were formed during the 1920 earthquake. In addition, we found a fresh portion of the south face of the fault scarp with very little vegetation on it at the western end of a dry stream east of Shaomayin (Figure 2). Its exposure was probably produced by slip during the 1920 earthquake, for the sharp contrast in vegetation could not be due to fault creep or displacement several hundred years ago. The amount of displacement is 8 to 9 meters. We will discuss it in the following section.

Second, the reference features that have been offset are newly

formed. In the loess-covered area, the small channels that we studied, which are about one meter wide and less than half a meter deep, could have been formed within several hundred years. Similar channels cross the boundaries of now unused farming terraces that, according to the local historical documents, probably were ploughed 200 to 300 years ago in the late Qing Dynasty (Figure 3). Because the sizes of these channels are about the same as, or even larger than, the channel offsets about 10 m. Thus the ages of these offset channels probably are no more a few hundred years.

Third, the first historical earthquake documented in this area was in 1219 with magnitude 5.0 (Li, 1960). No large earthquake ($M > 7$) is reported in this area between 1219 and 1920. Perhaps no significant large earthquake occurred 400 to 500 years before 1219, because the area is only 300 km from Xian--the capital city and cultural center of China during that time. If large earthquakes occurred in this area, people probably would have known and recorded them in the documents.

Finally, the seismic moment of the 1920 Haiyuan earthquake was calculated to be 1.2×10^{21} Nm from spectral densities measured by Chen and Molnar (1977) from long-period Rayleigh waves at two stations (Deng et al., 1984). For a fault area of $A = 220\text{km} \times 20\text{km} = 4.4 \times 10^{8}$ m^2 and shear modulous $\mu = 33$ GPa, this value of seismic moment corresponds to an average slip $\Delta u = Mo / \mu A = 8.3$ m. Although uncertain by a factor of two or more, the amount is consistent with the smallest offsets that we measured along the Haiyuan fault. Therefore we think that the smallest offsets of several to 11 m, along the rupture zone result from left-lateral slip during the 1920 Haiyuan earthquake.

None of these arguments prove that all of the displacements that we measured could not include fault creep before or after the 1920 earthquake, but the sharpness of most offset features suggests that offsets were abrupt and not gradual. Thus, we are confident that the major portions of each offset occurred in 1920, and we suspect that if fault creep has contributed to the offsets, it has been small and probably negligible.

To measure the displacements associated with the 1920 earthquake, we used a plane table and alidade to construct topographic maps of offset features at six widely spaced sites along the surface rupture zone (Figure 1). These sites were chosen because offsets were relatively clear, because only one or two principal strands of the fault seemed to have been active in 1920, and because the amounts of offset are believed to have formed during the 1920 earthquake.

Site 1. The western offset that we mapped is about 3 km west of Gaowenzi (Figure 1) where an offset stream channel is clearly present (Figure 4). The fault scarp at this channel is still identifiable in most places at this site. The upper stream channel is located on northern side of the fault; it is straight, sharply incised, and aligned almost perpendicular to the fault. A downstream channel can be found 4.4 ± 0.5 m along the fault scarp to the east. Both its depth and its width, however, are two or three times smaller than the upstream channel.

Another, beheaded channel is presented on the downstream side of the fault, 11.6 m southeast of the upstream channel (Figure 4). The size of this beheaded downstream channel begins about 4 m downslope from the fault scarp; a small landslide on the northern side of the fault has

buried the part of the stream channel near the fault scarp. It is unlikely that before the small landslide formed there was a preexisting channel upstream of the fault from the place where the landslide is located now, and that later the preexisting channel was buried or destroyed by the landslide. Morever, because the landslide is located at the nose of a ridge, the channel cannot have formed at such a location. Because the channel has not incised into the landslide material, but instead the landslide material has filled in and covered on the buried part of channel, it is also unlikely that the channel is newly formed and that its head reaches only to the landslide. Therefore we think this downstream channel was beheaded from the main upstream channel and offset about 11.6 ± 1 m from it.

A small ridge that blocks the upstream channel to form a sag pond lies about 3.9 m west-southwest of the ridge making the west bank of the upstream channel, but because of the irregularity of the small hill an accurate measurement of offset is impossible. The similarity of the distance of 3.9 m to the offset of the neighboring stream may be fortuitous, but we did obtain several offsets of 4 to 6 m nearby.

Since we do not know the age of the small downstream channel, two possibilities exist. The first is that this beheaded channel was displaced 7.2 ± 1.5 m from the upstream channel during a pre-1920 event, and 4.4 m in 1920. A second possibility is that the total offset of 11.7 ± 2 m was associated with 1920 earthquake, a point of view supported by the similar sizes of the upstream and beheaded downstream channels. The apparent offset of the small ridge and the other offsets of 4 to 6 m, however, are inconsistent with this inference. The choice of the

possibilities depends on the assumption that before the 1920 event, or perhaps before the previous large event, no deflection of this channel existed. At present no evidence requires a definite choice, and among ourselves, we are undecided whether only 4 m of slip occurred in this area in 1920 or as much as 10 m occurred.

Site 2. About 700 m east of Gaowanzi, a small stream channel incised into the Haiyuan group of metamorphic rocks has been offset 9 ± 3 m (Figures 1 and 5). An offset small ridge has blocked the upstream channel to form a sag pond. The length of offset ridge forming the southern wall of the sag pond is about 9 m, which is comparable to the amount of offset of the stream in the same place. Both probably formed during the 1920 earthquake. Because both upstream and downstream channels are not perpendicular to the fault, part of the displacement may be due to meandering of the stream. Thus the amount of the offset at this site cannot be measured as well as at some other sites.

Site 3. About 1.5 km west of Tangjiapo, a village 2 km west of the Salt Lake (Figure 1), the main strand of the surface rupture zone displaces a series of stone walls that bound old, now unused farming terraces (Figure 6). There are 18 walls in the mapped area, as well as some other features such as stream channels, that cross the rupture zone and were offset. In places the walls are clearly offset by narrow strands of the fault, but in others the fault zone is complicated by the existence of tension cracks and mole tracks (Figure 6). Most of the walls were offset at two or more localities, with the combined offset of 6 to 8 m. For each, our estimate of the displacement was obtained by measuring the distance between the crests of the walls at the ruptures.

The edges of the walls were not used to determine the displacement because modification of them is much greater than that of the crests. The uncertainty for each offset was estimated to be either the width or half-width of the wall depending upon how clear the crest of the wall was and how extensive the modification has been. Obtaining an exact or precise estimate of the offset at this locality is very difficult because the walls were not initially straight. Consequently, if the measurements were taken only at the places where the rupture displaced segments of the wall from one another, we probably obtained a minimum amount of displacement, because we failed to include simple shear strain across the fault zone.

According to the local county historical documents, many people immigrated into this area to farm in the late part of the Qing Dynasty (200-300 years ago). The walls were probably built by those people. The walls were offset during 1920 earthquake; in the early 1970's some of the older people in Tangjiapo told some geologists working in this area that the offset of those farming walls occurred at the time of the 1920 earthquake (Lanzhou Institute of Seismology and Ninxia Seismological Bureau, 1980).

In middle part of Figure 6a, a very young alluvial fan represents the outwash from a small and deeply incised young channel to the northeast. The fault scarp of 1920 earthquake has been covered by this young fan, which has not been offset at all. This probably implies that there is at least no significant offset along the rupture zone since 1920 earthquake. Fault-creep has not been reported at any locality along the Haiyuan fault. Furthermore, the walls were unlikely to have been

offset more than 200-300 years before 1920 because they probably had not been built by then. Since there have been no large earthquakes reported in this area in the 200-300 years before 1920, we think that the entire offset of the walls can be associated with the 1920 earthquake.

Site 4. About 1.5 km north west-west Fangjiahe, a small village located next to the Haiyuan fault (Figure 1), there are several small stream channels that have been offset apparently during the 1920 earthquake (see Figure 6 in Deng et al.,1984). Three among them were mapped (Figure 7), and the observed amount of displacement is about 10 meters.

All of these offset channels are located geomorphically on the surface of a terrace above a westward-flowing large stream. The fault scarp that formed during the 1920 earthquake has not been preserved, but a series of offsets of stream channels and some depressions clearly delineate a narrow zone of surface rupture. The small stream channels are displaced left laterally so that the drainage has been blocked, and the runoff periodically has ponded on the upstream (south) side of the fault.

The stream on the right (west) side of figure 7 has the largest channel and the smallest sag pond among these streams. It has deeply incised the terrace and the slope of the hill. The upstream channel is clear and well defined. Its downstream channel is wide and shallow, but the main channel is clearly present. The match of the main channels gives 10 ± 1 m of left lateral offset. The northwest edge of this channel is also offset, and one can argue that there has been 20 ± 5 m of offset.

The other two stream channels are much smaller than the one in the west (Figure 7), and their associated sag ponds are shallow and large. Springs developed at the heads of both of these gullies, so that centers of the channels are clearly defined. The match of the channels yields 9.6 ± 1.0 m and 10.2 ± 1.0 m of left-lateral offset for the eastern and central channels, respectively. Moreover, the two gullies have well-defined banks, and the matches of them also give about 10 meters of displacement, but with large uncertainties.

We think that the 10-meter offsets of these three gullies probably occurred during the 1920 earthquake, largely because we associate comparable offsets farther east with that earthquake. The 20 ± 5 m offset of the western wall of the western stream channel might represent two offsets of 10 m, one associated with the 1920 earthquake and the other with its predecessor. This is the only place where we may have found multiple offsets, but the evidence is not very convincing. Thus we cannot be certain that the 1920 earthquake was typical of major earthquakes on the Haiyuan fault.

Site 5. Between Shaomayin and Dagoumen along the Haiyuan fault, offsets of minor streams and dry stream beds also clearly show 8-9 meters of left-lateral offset. About 700 m east of Shaomayin (Figure 1), a minor dry stream appears to be offset about 30 meters (Figures 2 and 8). Both the upstream channel on the southwestern side and downstream channel on the northeastern side of the fault trend about N30E, almost perpendicular to the fault. As the stream reaches the fault, it turns to N60W, the general orientation of the Haiyuan fault. A well-defined fault scarp forms the northern bank of the stream, and to

the east it connects with the boundary fault of a small graben associated with the 1920 earthquake rupture zone. Only 0.4 to 0.5 meters of vertical displacement were measured at the flat place east of the stream (Figure 8); thus the slip along this part of the fault was almost entirely strike-slip. There is very little vegetation on a fresh portion of the south face of the scarp at the western end of the dry stream valley, but to the east beyond the fresh face the vegetation covered all the slope of the channel bank, so the boundary between them is very sharp (Figure 2 and Figure 10 in Deng et al.,1984). Its exposure was probably produced by slip during the 1920 earthquake. If there has been fault-creep, the boundary between the vegetation and bare segments of the scarp would not be so sharp. The horizontal distance between the northwest end of the escarpment and the edge of the vegetation to its southeast gives a displacement of 8 to 9 m.

Site 6. At Luzigou, a small village located about 7 km from the eastern end of the west-northwest striking portion of the Haiyuan fault (Figure 1), the fault scarp still can be recognized in the farming fields. Several small channels along the scarp have been offset, and we mapped two of them (Figure 9). The upstream channel of the eastern gully is deeply incised and well defined, but its downstream continuation from the fault is very shallow and poorly defined. North of the scarp, there appear to be two small, shallow channels, which join 4-5 m from the scarp. If we matched the eastern channel with the upstream gully, then the displacement would be 5.2 ± 1 m. Otherwise, matching the western channel yields 9.2 ± 1.5 m.

The fault scarp to the west seems to curve to the west-northwest,

and a small ridge that defines it has blocked a small gully flowing from south to north and caused a small sag pond to form (Figure 9). The offsets of the gully and the ridge are 4.8 ± 0.5 m and 5.6 ± 1 m, respectively. To the north the deflection of same gully may be due to faulting but could also be due to meandering of the stream that has no tectonic significance. Thus the total offset in this site is poorly defined and could be as little as 4.5 m or as large as 10.5 m.

Site 7. About 7.5 km southeast of Luzigou, another strand of the fault developed with an average orientation of about N35°W. This strand crosses the Nanhua Shan, and extends about 40 km southeast to a small pull-apart basin on the south side of Nanhua Shan. We mapped a stream offset on a strike-slip fault strand just north of this pull-apart basin (Figure 1). According to the local people the well-defined fault scarp in this place is associated with the 1920 earthquake. A straight stream channel has been offset 7.5 ± 1.0 m where it crosses the fault scarp (Figures 10 and 11). The widths of the bottoms of the channels, both upstream and downstream from the fault, are typically about 1 m, and depths are about 0.5 m. The segment of the channel parallel to the fault has a typical width of only about 0.5 m and a depth of 0.2 m or even less. It is clear that this segment of the channel formed after the offset occurred, which we think was in 1920.

Conclusion

The smallest offsets along the Haiyuan fault are probably associated with the 1920 earthquake. This assumption is supported by several reasons. Three old local people who lived in western, middle and eastern parts of our studied area respectively pointed out that the ruptures that offset the smallest reference features were formed during the 1920 earthquake. By comparing with the channels of known age, the smallest offset channels are probably formed within the several hundred years before 1920. The historical seismicity studies (Li, 1960) show that no large earthquake occurred in this area between 1219 and 1920, and probably no great earthquakes occurred 400 to 500 years before 1219. The seismic moment studies (Chen and Molnar, 1977; Deng et al.,1984) suggests that the average slip during the 1920 earthquake is about 8 m, a value consistent with the amounts of the smallest offset that we measured along the Haiyuan fault.

The displacements associated with 1920 earthquake in Ningxia and westernmost Gansu range from possibly as little as 4.4 m to as much as 11 m. The maximum displacement that can be demonstrated convincingly is about 10 m, at Shikaguangou between the Salt Lake and Xianzhou basins. From Gaowenzi to the Xianzhou basin the amount of displacement associated with 1920 earthquake is probably between 7 and 10 meters. Smaller amounts may have occurred southeast of Caiyuan and northwest of Gaowenzi, but the evidence is not clear. Thus the average slip probably was 8 $\pm$ 2 m.

Zhang et al. (1987) found that the average Holocene rate of left-lateral slip on the Haiyuan fault during Quaternary time was about 8 $\pm$ 2 mm/year, which is consistent with the 5 - 10 mm/yr of slip rate over

whole Quaternary period obtained by Burchfiel et al. (1987). For an average amount of displacement for 1920-type events of 8 ± 2 meters, the recurrence interval of this type of event would be about 1000 years: less than 1400 years and more than 800 years.

Acknowledgements: We thank Zhang Yuzheng and Wang Zhenguang, for their help in the field with the plane table mapping, and S. Gardner for her help in the preparation of the manuscript. We are grateful to an anonymous referee for his/her comments and suggestions that improved this paper greatly. This work was part of an exchange between the People's Republic of China and the United States on seismological studies of earthquake hazards and has been supported by the National Science Foundation through grant EAR-8306863 and by the State Seismological Bureau of China.

References

Allen, C. R., The tectonic environments of seismically active and inactive areas along the San Andreas fault system, in Proceedings of the Conference on Geologic Problems of the San Andreas Fault System, Edited by W. R. Dickinson and A. Grantz, Stanford Univ. Publ Geol. Sci, 11, 70-82, 1968.

Burchfiel, B. C., Zhang P., Wang Y., Zhang W., Jiao D., Song F., Deng Q., Molnar, P., Royden,L., Geology of the Haiyuan fault zone, Ninxia Autonomous Region, China and its relation to the evolution of the northeastern margins of the Tibetan Plateau, submitted to J. Geophys. Res., 1987.

Chen, W.P. and P. Molnar, Seismic moments of major earthquakes and average rate of slip in central Asia, J. Geophys. Res., 82, 2954-2969, 1977.

Deng Q., Song F., Zhu S., Li M., Wang T., Zhang W., B. C. Burchfiel, P. Molnar, and Zhang P., Active faulting and tectonics of the Ninxia Hui Autonomous Region, China. J. Geophys. Res., 89, 4427-4445, 1984.

Deng Q., Chen S., Song F., Zhu S., Wang Y., Zhang W., Jiao D., B. C. Burchfiel, P. Molnar, L. Royden, and Zhang, P., Variation in the geometry and amount of slip on the Haiyuan fault zone, China and the surface rupture of the 1920 Haiyuan earthquake, Maurice Ewing Series 6, Amer. Geophys. Un., Washington, D. C., in press, 1986.

Lanzhou Institute of Seismology and the Seismological Bureau of Ninxia-

Hui Autonomous Region, The Haiyuan Earthquake in 1920 (in Chinese), Seismology Publishing House, Beijing, 1980.

Molnar, P. and P. Tapponnier, Cenozoic tectonics of Asia: effects of a continental collision, Science,189, 419-426, 1975.

Schwartz, D. P., K. J. Coppersmith, F. H. Swan III, P. Somerville, and W. U. Savage, Characteristic earthquakes on intraplate normal faults (abstract). Earthquake Notes,52, 71, 1981.

Schwartz, D. P. and K. J. Coppersmith, Fault behavior and Characteristic Earthquakes: Examples from the Wasatch and San Andreas Fault Zones, J. Geophys. Res.,89, 5681-5698, 1984.

Sieh, K. E., Slip along the San Andreas fault associated with the great 1857 earthquake, Bull. Seism. Soc. Am.,68, 1421-1448, 1978a.

Sieh, K. E., Prehistoric large earthquakes produced by slip on the San Andreas fault at Pallett Creek, California, J. Geophys. Res.,83, 3907-3939, 1978b.

Sieh, K. E., Lateral offsets and revised dates of large earthquakes at Pallett Creek, California, J. Geophys. Res., 89, 7641-7670, 1984.

Sieh, K. E., and R. Jahns, Holocene activity of the San Andreas fault at Wallace Creek, California, Geol. Soc. Am. Bull.,95, 883-896, 1984.

Tapponnier P. and P. Molnar, Active faulting and Cenozoic tectonics of China, J. Geophys. Res.,82, 2905-2930, 1977.

Song F., Zhu S., Wang Y., Deng Q. and Zhang W., The maximum horizontal displacement in the Haiyuan earthquake of 1920 and estimates of earthquake recurrence in northern marginal fault of the Xihuashan (in Chinese), Seismology and Geology, 4, 1983.

Wallace, R. E. Earthquake recurrence intervals on the San Andreas fault,

Geol. Soc. Am. Bull.,81, 2875-2890, 1970.

Zhang, W., Deng Q., B.C.Burchfiel, and Zhang P., Active faulting and the formation of a pull-apart basin along the western part of the Haiyuan fault, China (abstract), Eos, Trans. AGU, 64, 861, 1983.

Zhang P., P. Molnar, B.C. Burchfiel, L. Royden, Wang Y., Deng Q., Song F., Zhang W., Jiao D., Bounds on the Holocene slip rate of the Haiyuan fault, north central China, submitted to Quaternary Research, 1987.

Figure Captions

Figure 1. The rupture zone associated with 1920 earthquake plotted on a topographic map of Haiyuan area and showing the locations of features and villages mentioned in the text. Contour interval is 100 m.

Figure 2. Left-lateral offset of the east side of a small dry stream that begins in the lower right, passes across the photo and then flows northeast across the Haiyuan fault at the left edge of the photo. View is toward the north. The fault passes along the opposite bank of the stream, and is marked by the ridge in the center of the photo. The fault scarp produced during the 1920 Haiyuan earthquake can be seen on the bare area in the left center of the photo. The fresh face near the left end of the gully with very little vegetation on it was formed by left-lateral displacement of 8 to 9 meters, which is the horizontal distance between the top of the escarpment and the edge of the vegetation to the right.

Figure 3. Channels developed across the boundaries of farming fields. According to local documents these fields probably were ploughed 200 to 300 year ago (late Qing Dynasty). The age of these channels must be younger than those boundaries.

Figure 4. Contour map of an offset stream channel and a small ridge west of Gaowenzi (Site 1). A small stream flows south and is separated by 4.4 m from its present downstream channel. A

second downstream channel, another 7.2 m to the southeast, is buried by a recent landslide. This channel probably was offset either once in 1920 by 11 m or twice, 4.4 m in 1920 and 7 m in a previous event. The elevation in the plane table map is arbitrary.

Figure 5. Contour map of an offset stream channel and a small ridge east of Gaowenzi (Site 2). A small stream flowing south has been blocked by a ridge, which apparently lay west of its present position before the 1920 earthquake. The deflection of the stream is about 9 m but with a large uncertainty (3 m). The elevation in the plane table map is arbitrary.

Figure 6. Map of offset stone walls once used to support farming terraces in Tangjiapo (Site 3). This detailed map of 18 stone walls that have been offset in 1920 shows two or three splays of the fault. Offsets at particular localities are probably underestimates because permanent strain near the walls could not be detected. Sums give both offsets at particular strands and the total for each wall.

Figure 7. Contour map of offset stream channels at Shikaguangou (Site 4). Three gullies have been displaced about 10 m, presumably in 1920. The larger of the three, the western gully, may have been displaced by an earlier event; the northwest bank is offset about 20 m at the fault trace. The elevation in the plane table map is arbitrary.

Figure 8. Contour map of an offset stream channel and the Haiyuan fault about 700 m east of Shaomayin (Site 5). A small stream flows

northeast but is deflected at a small ridge that marks the Haiyuan fault. This channel is displaced about 30 m. East of the stream the fault scarp traverses a low saddle and the surface rupture there has defined a small graben. The vertical component of slip is only about 0.5 m. Thus the displacement was primarily strike-slip. At the northwest end of the ridge that marks the scarp the southwest side of the ridge is bare of vegetation (Figure 2). We presume that this bare region formed by left-lateral slip in 1920, and from its dimensions we estimate that 8 to 9 m of slip occurred. The elevation in the plane table map is arbitrary.

Figure 9. Contour map of offset stream channels and a small ridge near Luzigou (Site 6). The fault in the eastern part of the area shown seems to consist of only one strand, but in the western part there seem to be two strands. A deeply incised channel in the eastern part seems to be offset left-laterally, but the low relief in the field north of the scarp makes it difficult to determine the total offset accurately. A small gully in the western part is clearly offset nearly 5 m by the southern strand, and possibly another 3.6 m at the northern strand. The elevation in the plane table map is arbitrary.

Figure 10. Contour map of offset stream southeast of Luzigou (site 7). A well-defined stream channel is offset about 7.5 m at a southwest-facing scarp (see Figure 11). The elevation in the plane table map is arbitrary.

Figure 11. Photograph of the stream offset shown in Figure 10. The fault

scarp in the middle of the photo formed during the 1920 earthquake. The offset stream can clearly be seen on the left side of the photo. The measured amount of offset is 7.5 meters.

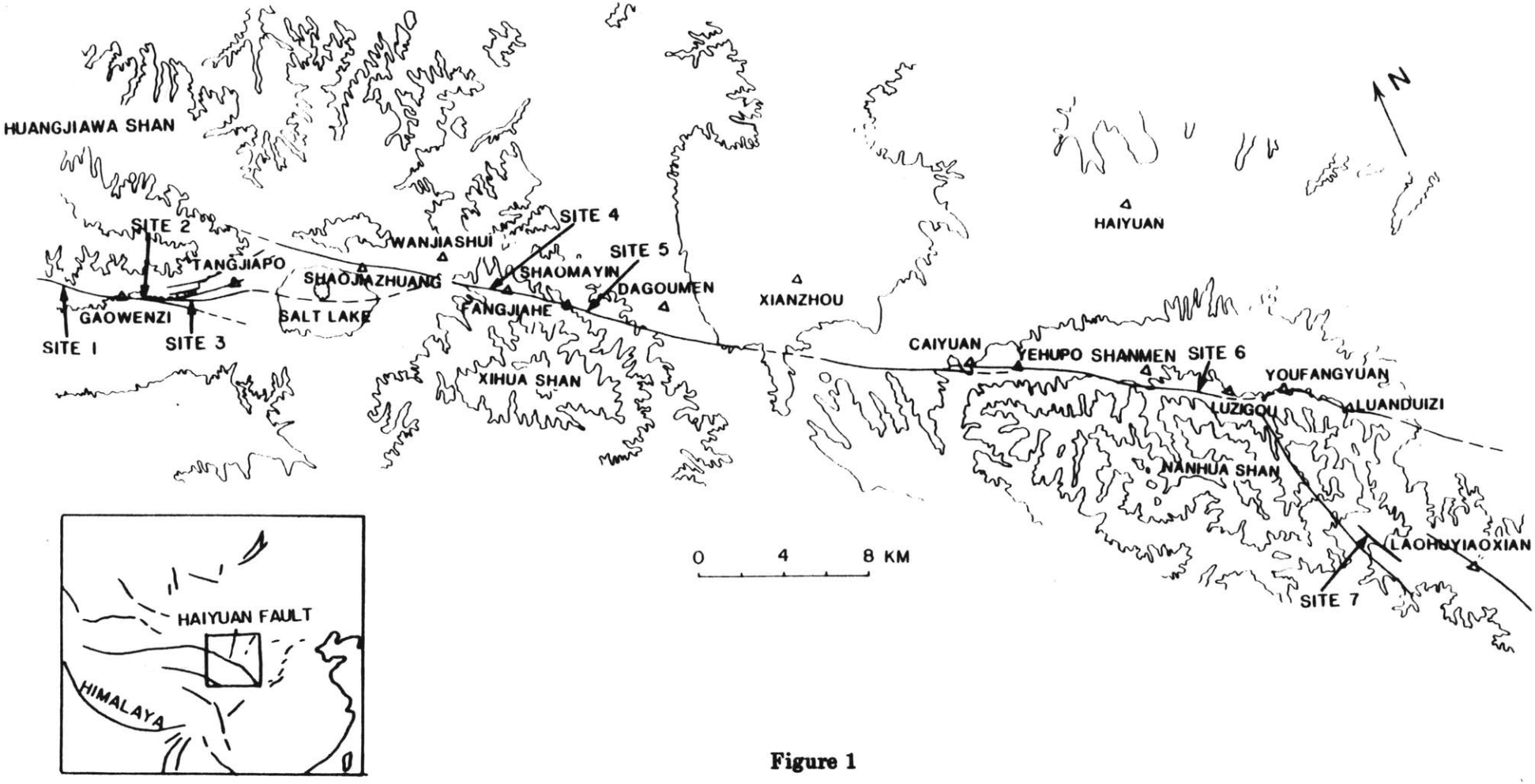
HUANGJIAWA SHAN
SITE 2
TANGJIAPO
SHAOJIAZHUANG
SALT LAKE
GAOWENZI
SITE 1
SITE 3
WANJIASHUI
SITE 4
SITE 5
SHAOMAYIN
FANGJIAHE
DAGOUMEN
XIANZHOU
HAIYUAN
N
CAIYUAN
YEHUPO SHANMEN
SITE 6
YOUFANGYUAN
LUANDUIZI
LUZIGOU
XIHUA SHAN
NANHUA SHAN
LAOHUYIAOXIAN
SITE 7
0 4 8 KM
HAIYUAN FAULT
HIMALAYA

Figure 1

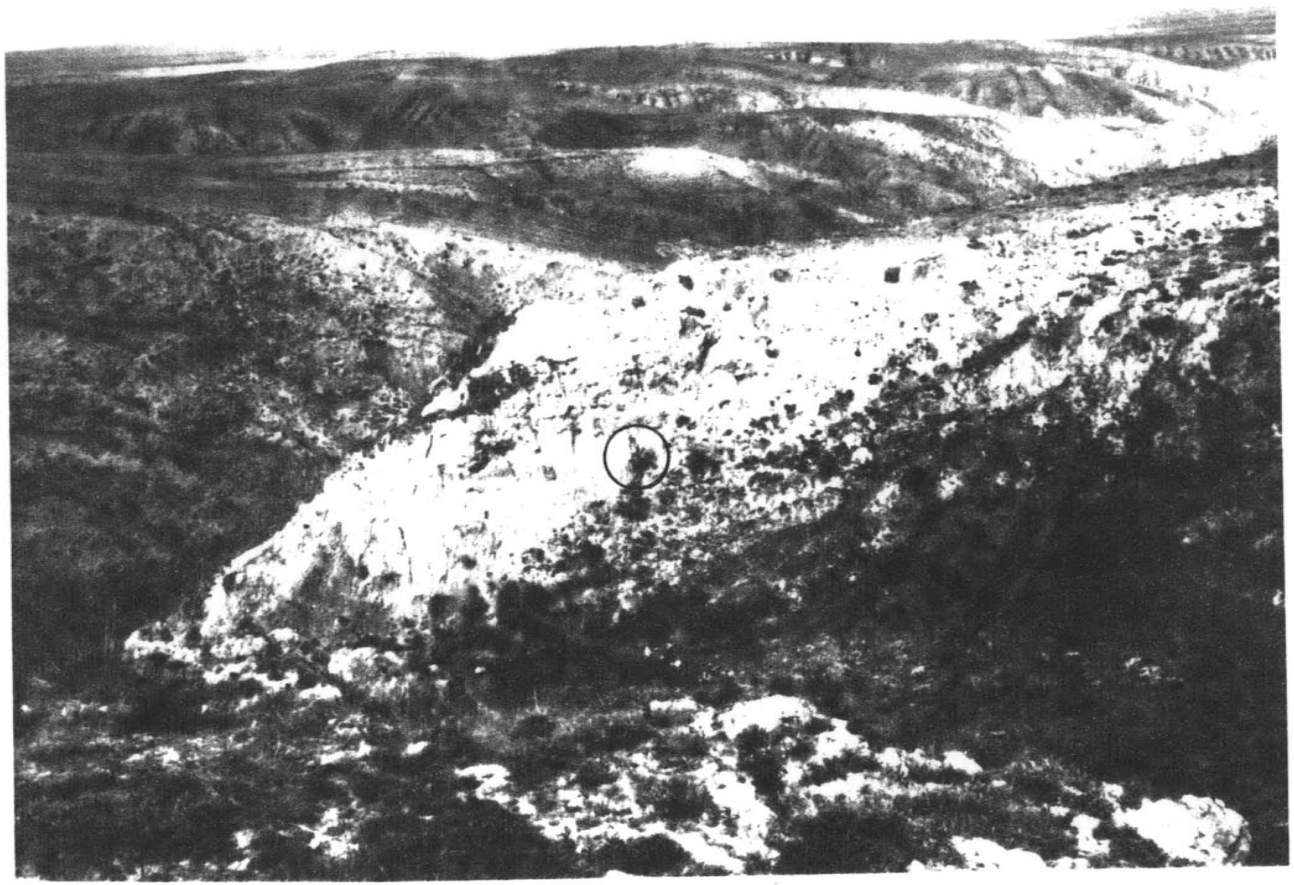

Figure 2

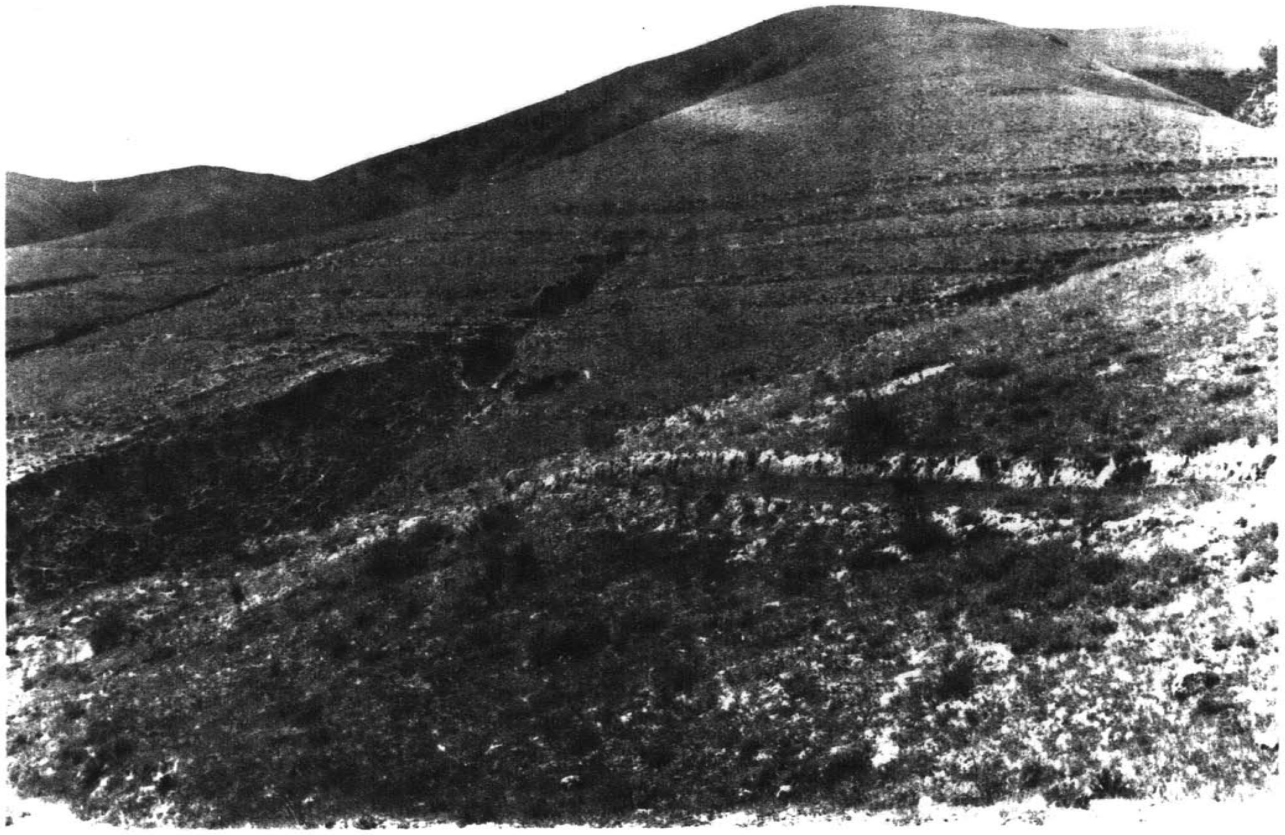

Figure 3

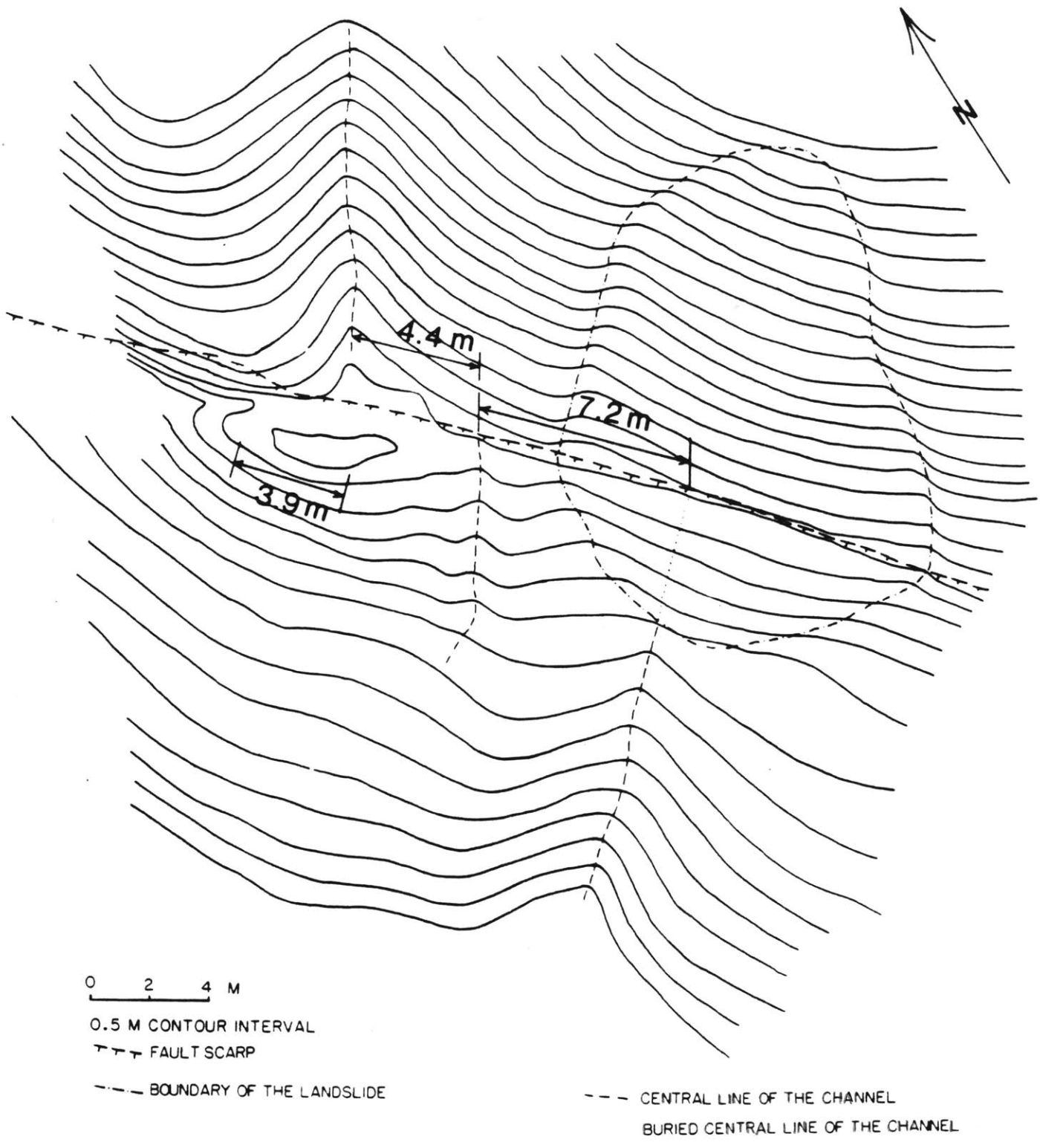
N
4.4 m
7.2 m
3.9 m
0 2 4 M
0.5 M CONTOUR INTERVAL
FAULT SCARP
BOUNDARY OF THE LANDSLIDE
CENTRAL LINE OF THE CHANNEL
BURIED CENTRAL LINE OF THE CHANNEL

Figure 4

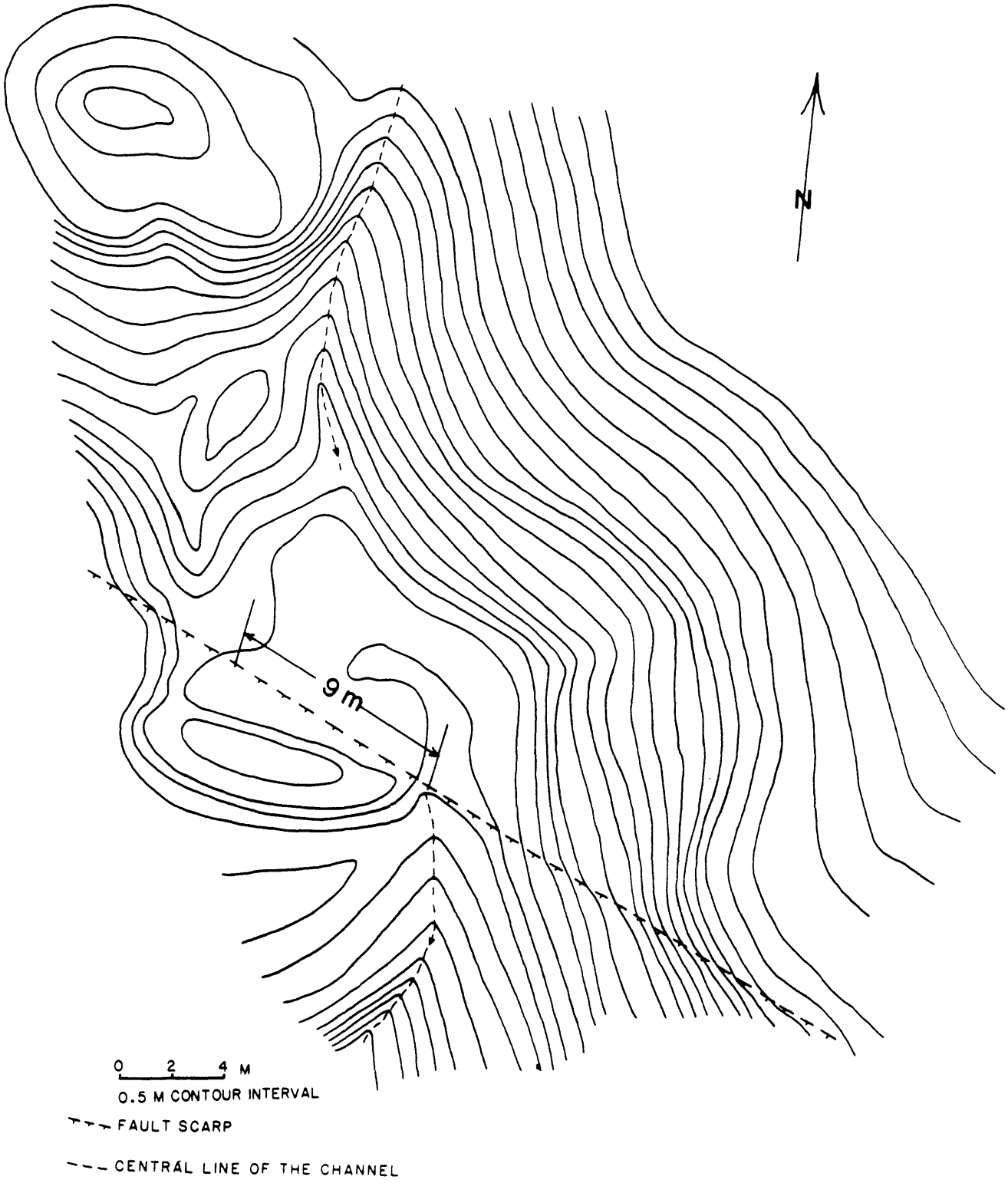
N
9m
0 2 4 M
0.5 M CONTOUR INTERVAL
FAULT SCARP
CENTRAL LINE OF THE CHANNEL

Figure 5

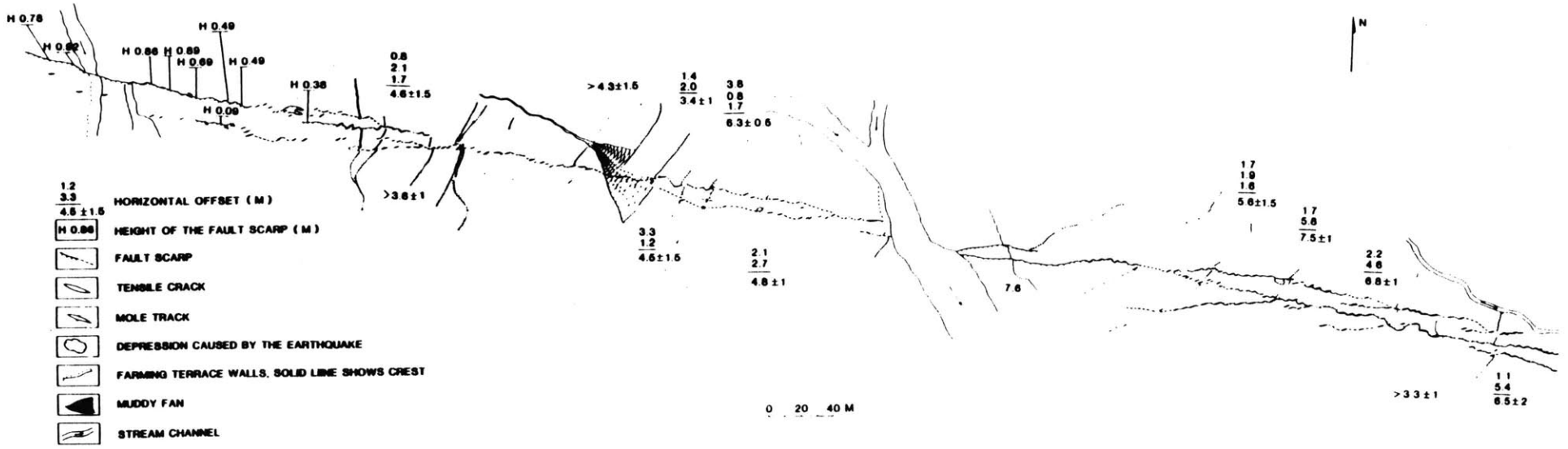
H 0.78
H 0.49
H 0.86
H 0.89
H 0.89
H 0.49
H 0.36
H 0.09
0.8
2.1
1.7
4.6±1.5
>3.6±1
>4.3±1.5
1.4
2.0
3.4±1
3.8
0.8
1.7
6.3±0.6
3.3
1.2
4.6±1.5
2.1
2.7
4.8±1
7.6
1.7
1.9
1.6
5.6±1.5
1.7
5.6
7.5±1
2.2
4.6
6.8±1
>3.3±1
1.1
5.4
6.5±2
N
0 20 40 M
1.2
3.3
4.8±1.5
HORIZONTAL OFFSET (M)
H 0.86
HEIGHT OF THE FAULT SCARP (M)
FAULT SCARP
TENSILE CRACK
MOLE TRACK
DEPRESSION CAUSED BY THE EARTHQUAKE
FARMING TERRACE WALLS, SOLID LINE SHOWS CREST
MUDDY FAN
STREAM CHANNEL

Figure 6

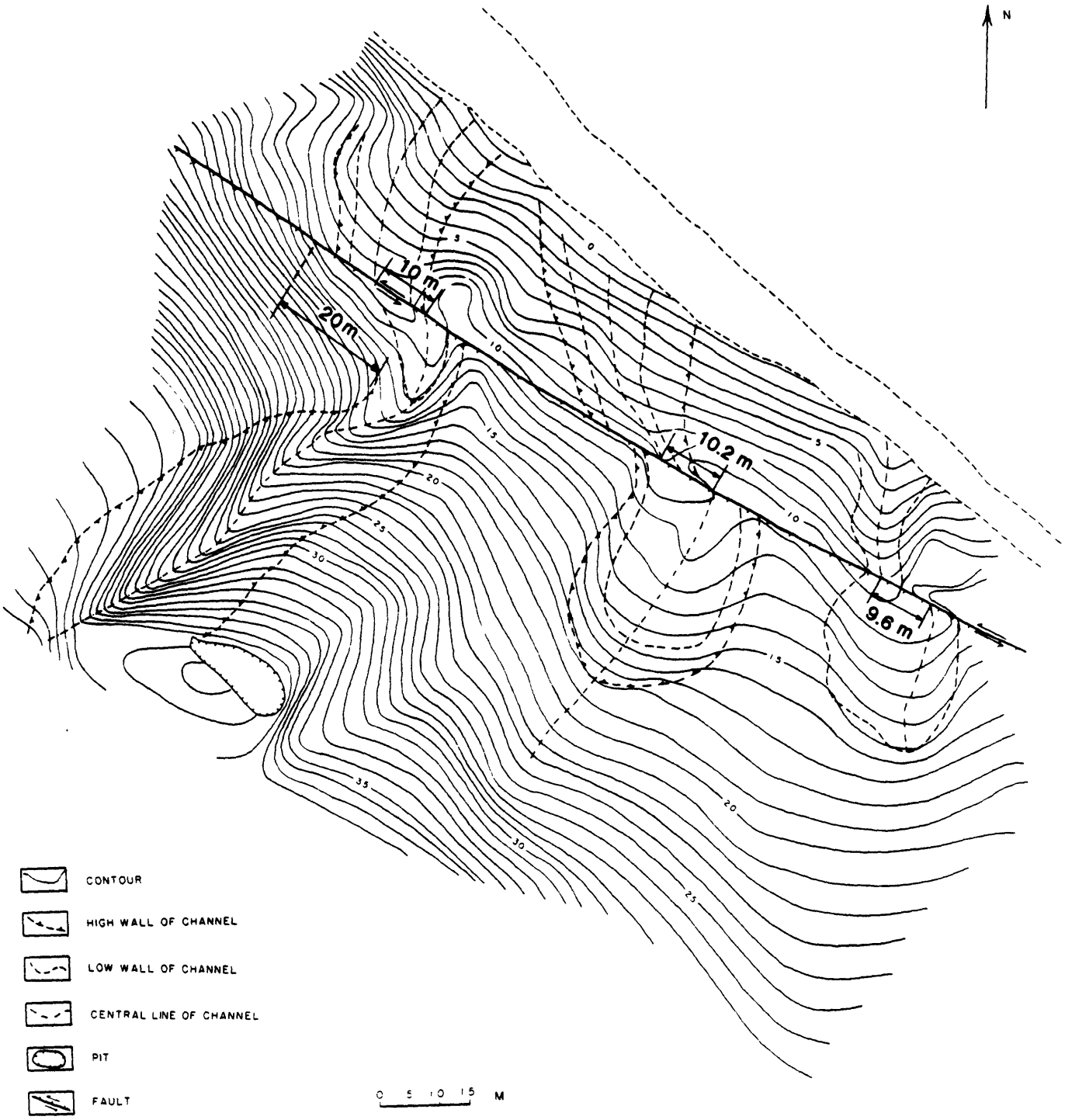
N
10 m
20m
10.2 m
9.6 m
CONTOUR
HIGH WALL OF CHANNEL
LOW WALL OF CHANNEL
CENTRAL LINE OF CHANNEL
PIT
FAULT
0 5 10 15 M

Figure 7

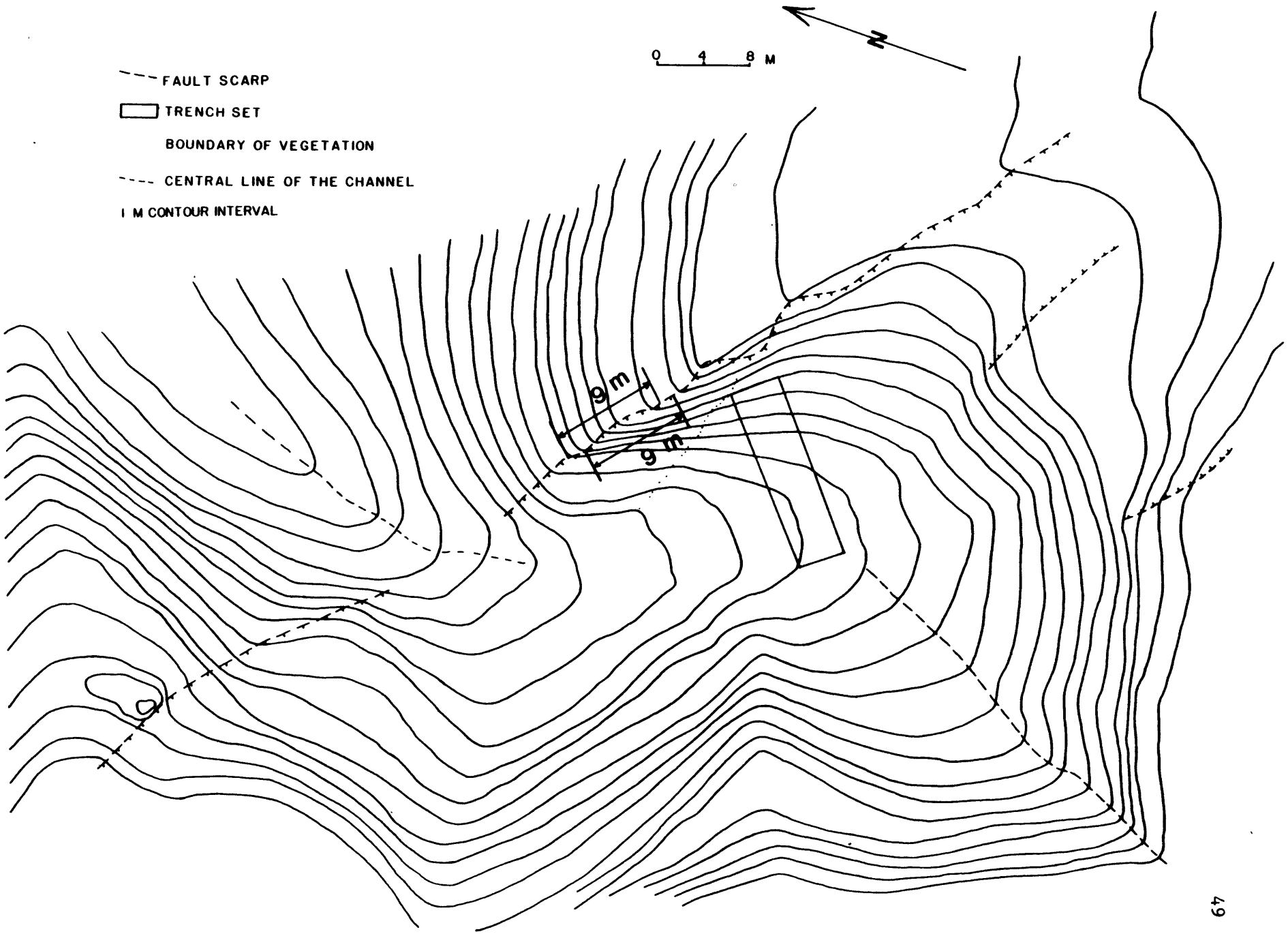
FAULT SCARP
TRENCH SET
BOUNDARY OF VEGETATION
CENTRAL LINE OF THE CHANNEL
1 M CONTOUR INTERVAL
0 4 8 M
N
9 m
9 m

Figure 8

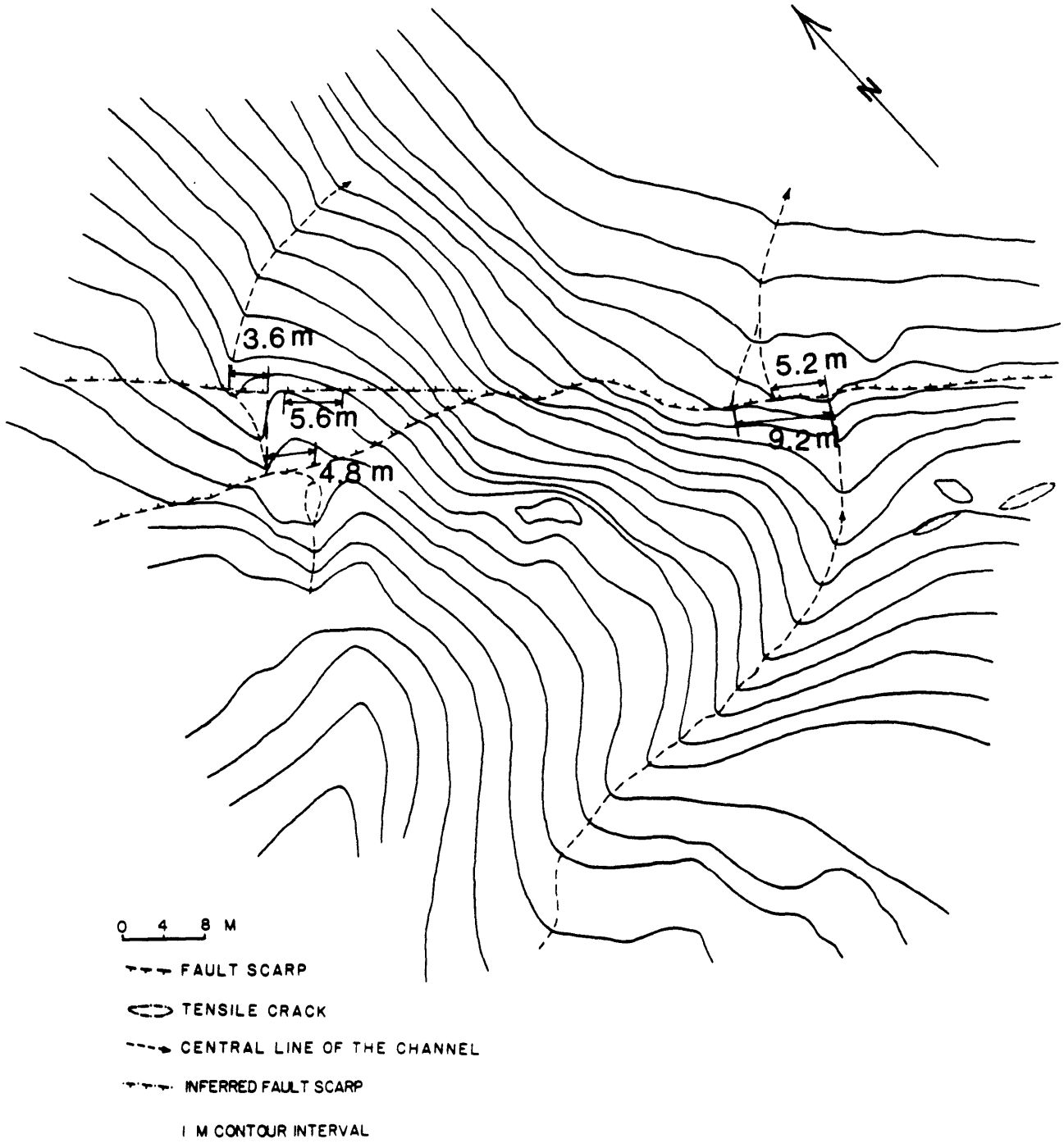
N
3.6 m
5.6m
4.8 m
5.2 m
9.2m
0 4 8 M
FAULT SCARP
TENSILE CRACK
CENTRAL LINE OF THE CHANNEL
INFERRED FAULT SCARP
1 M CONTOUR INTERVAL

Figure 9

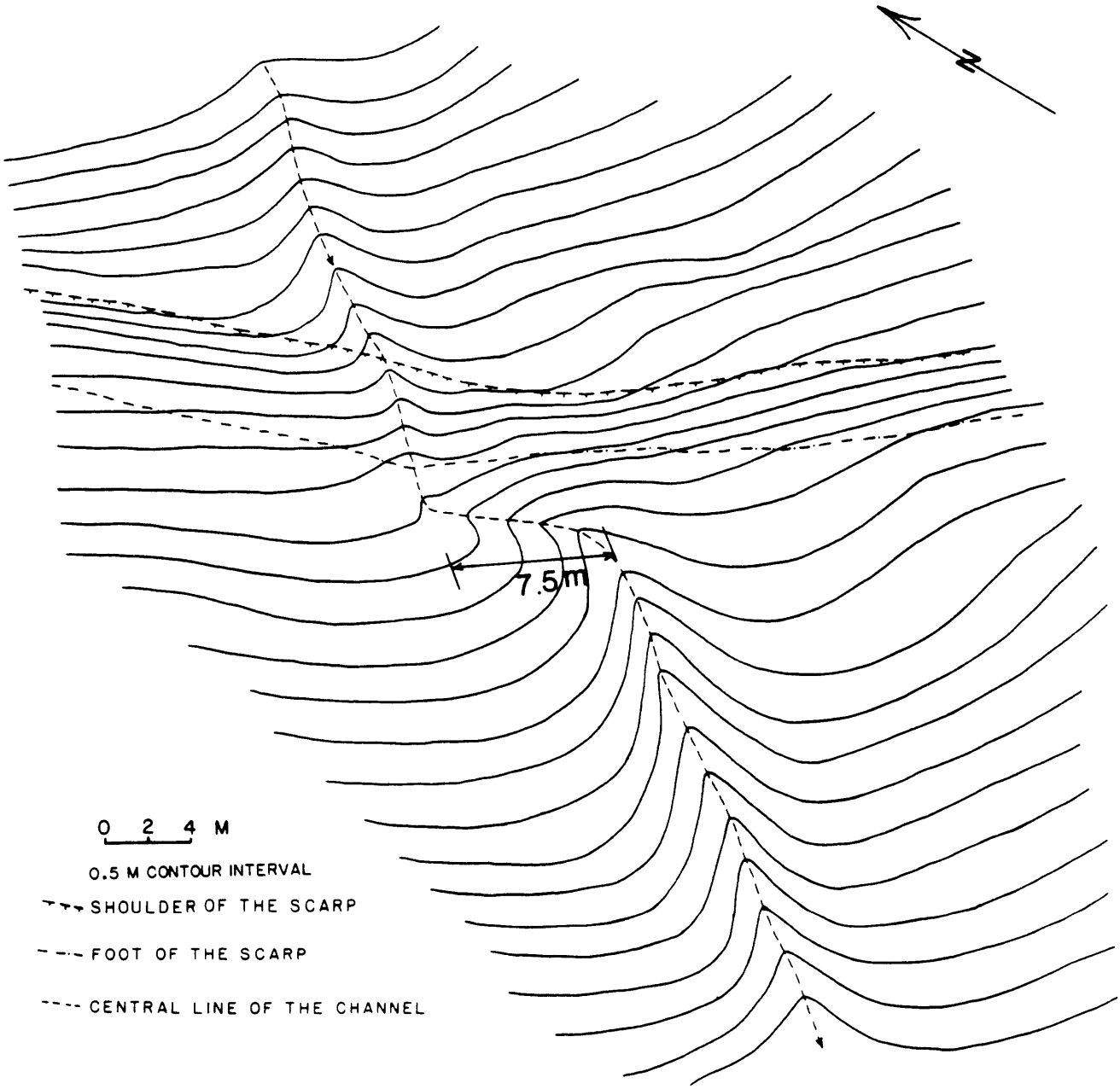
N
7.5m
0 2 4 M
0.5 M CONTOUR INTERVAL
SHOULDER OF THE SCARP
FOOT OF THE SCARP
CENTRAL LINE OF THE CHANNEL

Figure 10

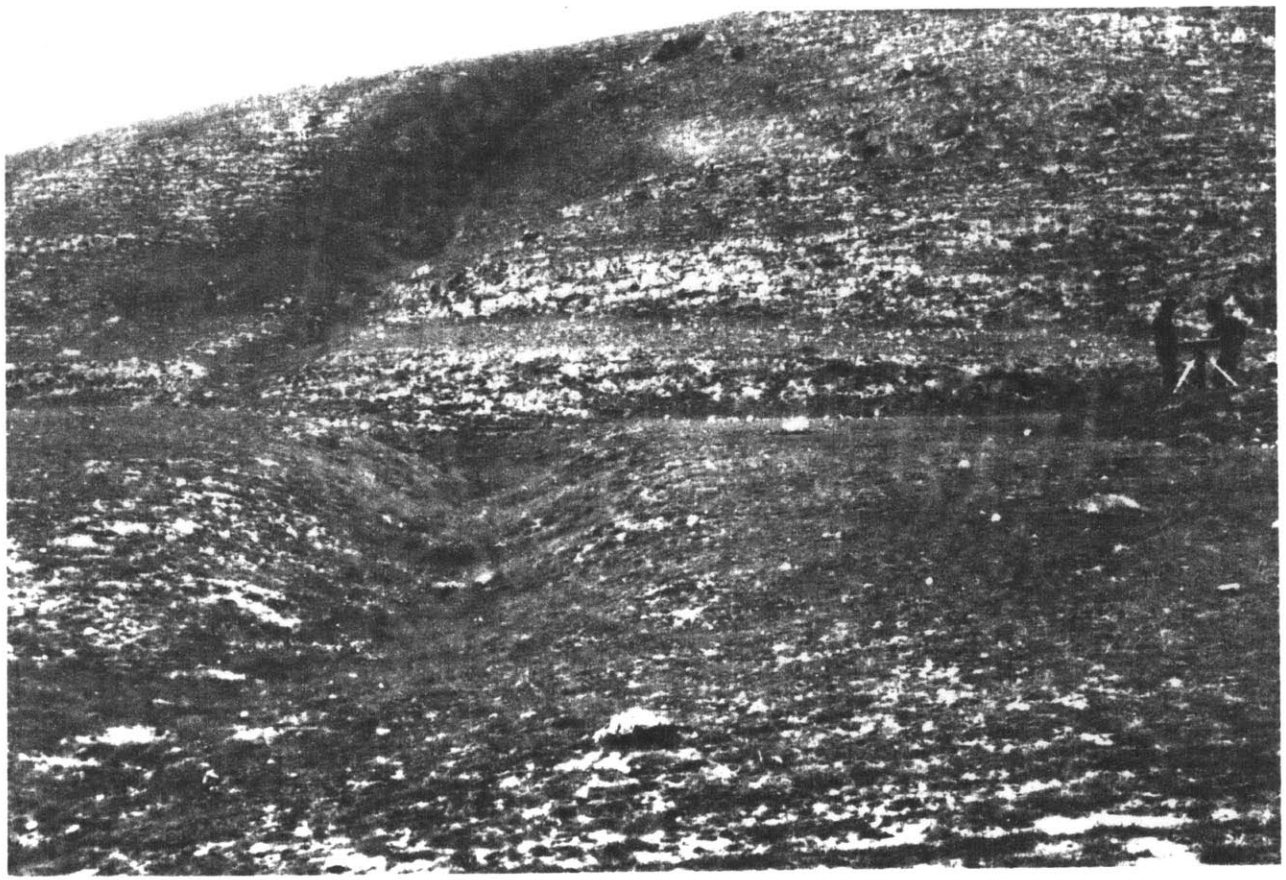

Figure 11

Chapter III

BOUNDS ON THE HOLOCENE SLIP RATE OF THE HAIYUAN FAULT, NORTH-CENTRAL CHINA

Zhang Peizhen, Peter Molnar, B. C. Burchfiel and L. Royden
Department of Earth, Atmospheric and Planetary Sciences
Massachusetts Institute of Technology
Cambridge, Massachusetts 02139

Wang Yipeng, Deng Qidong and Song Fangmin
Institute of Geology
State Seismological Bureau
Beijing, China

Zhang Weiqi and Jiao Decheng
Ningxia Seismological Bureau
Ningxia-Hui Autonomous Region
Yinchuan, China

ABSTRACT

We measured the offsets of six streams, of 30 to 90 m, along the northwest-southeast trending, left-lateral strike-slip Haiyuan fault, in north-central China, and we determined minimum ages of these offsets along the Haiyuan fault to obtain lower bounds for the Holocene slip rate. The most reliable bounds are 7.6 ± 1.0 and 6.7 ± 0.8 mm/yr, with three of the other lying between 3.5 ± 0.8 and 4.0 ± 0.4 mm/yr. Thus the average Holocene slip rate of the Haiyuan fault is larger than 6 mm/yr and probably larger than 7 mm/yr. If the average slip rate for the Quaternary period is applicable to Holocene time, the rate is 8 ± 2 mm/yr.

INTRODUCTION

Most major earthquakes occur on demonstrably active faults. In order to predict these earthquakes, and therefore to evaluate the hazards associated with them, we must know the kinematic history, especially for the Quaternary or Holocene period, of the faults along which large earthquakes occur. The geological record of the recent past provides the best opportunities for studying the recurrence intervals and average slip rates of active faults. Determinations of displacements and recurrence intervals for earthquakes associated with surface faulting along the Wasatch fault zone in Utah, for instance, suggest that most of the slip has occurred during earthquakes of essentially the same size and therefore with a relatively narrow range of magnitudes (Schwartz et al., 1980; Schwartz and Coppersmith, 1984). The studies of displacements of historical earthquake and earthquake recurrence intervals along the San Andreas fault zone, however, suggest that the displacements during one earthquake may differ from one segment to another along the fault zone, and that the different segments rupture with earthquake of different sizes, but that each segment tends to rupture with earthquakes of the same magnitude (Sieh, 1978a, 1978b, 1984; Sieh and Jahns, 1984). Therefore in so far as displacements on other faults also occur in repeatable amounts, in association with earthquakes of roughly the same magnitude, knowledge of the average slip rates and of the amounts of slip during past earthquakes should allow us to estimate the average recurrence intervals of large earthquakes. A

knowledge of when the last earthquake occurred should then allow us to predict approximately when the next earthquake will occur.

The Haiyuan earthquake (M=8.7) of December 16, 1920 in north-central China was associated with left-lateral displacement along a surface rupture zone 220 km long, and it was responsible for 220,000 deaths and the destruction of thousands of towns and villages (Lanzhou Institute of Seismology and Ningxia Seismological bureau, 1980). In 1927 another earthquake of M=8.0 occurred along the Haiyuan fault zone about 400 km west of the epicenter of the 1920 Haiyuan earthquake. It is likely that when averaged over a long term (thousands years), this fault poses the most serious seismic hazard to the inhabitants of this region, and therefore the slip rate and the earthquake recurrence interval along the Haiyuan fault have long been topics of great interest to seismologists in China. A knowledge of these quantities should contribute meaningful information both for earthquake prediction in this region and for the quantitative understanding of intracontinental strike-slip faulting in Asia.

In earlier papers (Deng et al., 1984, 1986; Song et al.,1983; Burchfiel et al., 1987; Zhang et al., 1987) we described the basic tectonics, the surface rupture and the displacements associated with the 1920 earthquake, and the geological evolution of the Haiyuan fault. In this paper we will addresses the Holocene slip rate and its relation to the earthquake recurrence interval along the Haiyuan fault.

METHOD

The key to determining the Holocene slip rate of a fault is to

relate the landforms and deposits near it to the slip on the fault. Large offsets of small stream channels provide the clearest relations between faulting and deposition. The fluctuations of a stream between periods of deposition and of erosion yield both landforms that are offset by the fault and deposits that contain organic material needed to date the landforms. In general, offset ridges are not good features for determining slip rates because the ridges do not contain organic material needed to date the offset.

In one of the best examples, Sieh and Jahns (1984) estimated the average slip rate along the San Andreas fault at Wallace Creek for two different intervals, in the Holocene and late Quaternary periods, by measuring and dating the offset of a stream channel and the offset of a alluvial fan from its source, respectively. By dating stream deposits with different ages and offset different amounts, Weldon and Sieh (1985) were able to determine the average slip rate along the southern San Andreas fault at Cajon Pass. Similar measurements have not been reported for the Haiyuan fault.

We have estimated the average slip rate for the Quaternary period. A number of geological features have been offset from several km to as much as 14 km along the Haiyuan fault (Deng et al., 1986; Burchfiel et al., 1987). Although we have not been able to date most of them accurately, by dividing the total Quaternary displacement by the duration of Quaternary period, we found the average slip rate to be 5 to 10 mm/year (Burchfiel et al., 1987). For the present study we measured stream offsets of 10's of meters and collected samples of organic material deposited in older depositional terraces (all the terraces

metioned in this paper are depositional terrace) and margins of the offset stream channels at different places along the fault. We used them to determine upper and lower bounds of the Holocene slip rate.

To estimate the offset, we measured the component of the distance parallel to the fault between the offset upstream and downstream channels. In some cases, the present stream, where it crosses the fault, does not flow parallel to the fault, presumably because of continuing incision concurrently with slip on the fault. For such cases, we measured the orientation of the stream at the offset and then calculated the component of displacement parallel to the fault from the measured distance between the upstream and downstream channels (figure 1). Because the measured offsets include the contribution of displacement associated with 1920 earthquake, the average offset of 8 m associated with that earthquake was subtracted from the measured offsets to obtain the offset that occurred since the stream channel was incised but before 1920. Then to determine a lower bound on the rate of slip, we divided these corrected offsets by the age that the organic material had in 1920, so that we ignore the large recent amount of slip associated with the 1920 earthquake.

RADIOCARBON DATING

All of our samples of organic material were dated by Beta Analytic Inc. in Coral Gables, Florida. Roots and rocks were removed before we sent the samples to be dated. Then they were given additional pretreatment before being burned. Using the traditional half-life of 5568 years, Beta Analytic calculated and reported an age before 1950 A.

D. and its uncertainty, one standard deviation. We then corrected these ages both for a revised half-life of carbon-14 of 5730 years and for variations in the rate of formation of carbon-14 in the atmosphere with time (Klein et al., 1982). Carbon-14 dating of tree rings of known ages has yielded a relation between the measured carbon-14 ages and corrected ages calibrated to the tree ring chronology for past 8000 years. All of our ages in that interval have been corrected based on scale calibrations. For radiocarbon ages older than 2000 years, but younger than 8000 years, the corrected ages and uncertainties with two standard deviations were taken from Klein et al. (1982). For ages younger than 2000 years, the corrections were taken from Stuiver (1982). For ages older than 8000 years, we simply recalculated ages using a carbon-14 half life of 5730 years, and the errors were taken to be 1000 years or more, as suggested by Klein et al. (1982). We ignore the possibility that charcoal was derived from wood that had lived and died long before it burned. Organic soil containing decayed grass may yield ages that are better than those from charcoal if the grass lived for a relatively short time and was accommodated directly into the organic material. In any case, since we are dealing with ages from 5000 years to 17,000 years, we treat the ages of charcoal and organic soil the same throughout our study.

HOLOCENE SLIP RATE OF THE HAIYUAN FAULT

FANGJIAHE. The westernmost place from which we collected organic material for dating the stream offset is near the village of Fangjiahe (figure 2). The amount of offset was measured to be about 70 ± 15 m. The

stream is aligned perpendicular to the trend of the fault, and its deflection occurs where the stream crosses the geologically mapped fault. The width of the fault zone itself is about 15 m. Thus we are confident that the deflection of the stream is due to faulting.

On the downstream (north) side of the fault, the stream has incised a deep valley, with some colluvial deposits adjacent to it, but with no clear depositional terraces. The deposits have been further modified by farming, and a relationship between these deposits to the evolution of the valley is not likely to be simple. Thus we did not use material from this side of the fault.

The upstream channel lies in a broad valley, but the present channel has cut into the valley by later incision. The upstream channel of Fangjiahe has a well-developed terrace on its southeastern side, and the terrace clearly was deposited before the present channel was incised. Because the present stream channel is very straight until it reaches the fault but the broad valley in which it flows lies mostly to the southeast of this channel, we presume that the 70 m offset occurred after the terrace was deposited. Unfortunately we found no organic material in these terrace deposits.

On its northwestern side, the upstream channel has incised deeply into colluvial gravel at the foot of the steep fill near the fault and into bed rock somewhat farther from the fault; there is no terrace on this side of the stream. Approximately 20 m south of the fault on the northwest side of the stream we found organic material, consisting of small pieces of charcoal, within a gravel layer. The sample was taken from about 2 m above the present stream channel and from 6 to 8 m below

the top of this gravel layer. The gravel appears to have been deposited within the colluvial apron at the foot of the hills. From the elevation of these deposits, which is lower than the top of the terrace on the southeastern side of the stream, we infer that the organic material was deposited before the top of the terrace on the southeastern side formed. Therefore this material predates both the present incision of the stream into the terrace and the 70 m offset.

The age of the organic material should give a minimum age of the stream offset at Fangjiahe. Using the corrected age of 17,690 ± 1000 years before 1920 (table 1), the resulting slip rate must be at least 3.5 ± 0.8 mm/year.

SHAOMAYIN. Shaomayin is a small village that straddles the Haiyuan fault about 3 km southeast of Fangjiahe (figure 2). There is a large stream flowing from southeast to northwest through Shaomayin, nearly parallel to the Haiyuan fault and with a relatively wide, high, flat terrace on both sides of the stream channel. To the south and west of Shaomayin, the high terrace grades into the erosion surface on the northern slope of the adjacent mountain (figure 3). At the northwest end of this terrace, a small stream flows northeast from the Xihua Shan across both the terrace and the Haiyuan fault. The small stream channel has incised about 4 m into both the high terrace and the erosion surface, and its valley shows a clear V-shaped cross-section. At the fault this small valley is offset 48 m, which was measured by matching the axes of the channel. We take the 4 m width of the channel bottom as the uncertainty of the offset.

Because the small stream channel was entrenched only after both the

surface of the high terrace and the erosion surface formed, a lower bound for the age of initial incision of the small stream can be estimated from the date of the erosion surface or the high terrace of the Shaomayin stream.The stratigraphy of the high terrace in the place excavated by the small stream is very simple. A thick sequence of coarse-grained sands and pebbles are interbedded with fine-grained reworked loess. Although we found no organic material in the sequence of sediments exposed in the deeply incised valley offset by the fault, about 100 m east of where reaches the main Shaomayin stream, we obtained organic material 1.8 m below the surface of the high terrace. The organic material consisted of peats with a few pebbles and some roots, which we removed before sending the sample to be dated. The black peats were in a lens-shaped layer with a maximum thickness of 30 cm, and about 7 to 8 m in horizontal extent. We think that it was deposited in a small depression while the sediments in the high terrace were deposited. Therefore it yields the age of a layer that once was the surface of the high terrace.

The radiocarbon age of this sample, which gives an upper bound for the age of the top surface of the high terrace, is 5290 ± 440 years before present (1950), and therefore 5260 ± 440 years before 1920. Because the amount of stream offset includes the contribution by 1920 earthquake, and the average displacement of 1920 earthquake is about 8 meters (Zhang W. et al., 1987), the pre-1920 amount of displacement should be about 40 ± 4 m. Thus the lower bound on the slip rate is 7.6 ± 1.0 mm/yr. This rate is a minimum because the age of the surface of the high terrace should be younger than the age of the material that we

sampled, and the onset of entrenchment of the small stream should be even younger than the surface of the high terrace.

EAST OF SHAOMAYIN 1. About 700 m east of Shaomayin (figure 2), a minor dry stream appears to be offset about 30 m (figure 4). Both the upstream channel on the southwestern side and the downstream channel on the northeastern side of the fault trend about N30E, almost perpendicular to the fault. The upstream and downstream channels are deeply incised into reworked loess and colluvium, and both show clear V-shaped cross-sections. There are no terraces adjacent to the upstream and the downstream channels. Where the stream reaches the fault, it turns to N60W, the general orientation of the Haiyuan fault. A well developed fault scarp forms the northern edge of the channel, and to the east it connects with the boundary fault of a small graben associated with the 1920 earthquake rupture zone (figure 4). It appears that all horizontal displacement was concentrated along the northern boundary fault of the graben. Only 0.4 to 0.5 meters of vertical displacement were measured on the flat area east of the valley. Thus the slip along this part of the fault was almost entirely strike-slip. There is very little vegetation on a fresh portion of the south face of the scarp at the western end of the dry stream valley. Its exposure was probably produced by slip during the 1920 earthquake. The horizontal distance between the northwest end of the escarpment and the edge of the vegetation to its southeast gives a displacement of 8 to 9 m (Zhang W. et al., 1987).

A trench across the fault scarp within the channel was dug in order to obtain the organic material to date the offset as well as to study

the earthquake recurrence intervals (Zhang P. et al., 1987). Organic material was found within two layers of sediment in the trench. The age of the younger layer is 5260 ± 440 years before 1920. Since this layer is clearly older than the 30 m offset (Zhang P. et al., 1987), its age yields a minimum slip rate. For 22 m of pre-1920 slip, the resulting lower bound on slip rate is 4.2 ± 0.4 mm/yr.

EAST OF SHAOMAYIN 2. About 900 m east of Shaomayin (figure 2), another stream channel has been offset about 100 m. There is a large stream flowing northeast from the Xihua Shan, and where it reaches the fault it turns to flow in a direction more or less parallel to the fault for about 250 m. After the stream crosses the fault, it turns to the northeast again. The offset channel that we studied developed within this large stream valley. The Haiyuan fault there strikes S65-60E, and the offset part of channel strikes about S40E. Thus the angle between them is only 20° to 25° (figure 5). Applying the calculation illustrated in figure 1, the offset along the fault would be from 90 m to 94 m. We take 92 m as the average offset. Because the channel is 10 to 20 m wide, and because neither the upstream nor the downstream channel is perpendicular to the fault, however, we take 30 m as the uncertainty of offset, but we consider it possible that this large value is still an underestimate of the uncertainty. Among the offsets that we measured, this is the most inaccurate.

The northerly flowing stream meanders through pre-Silurian schists, and farther north has incised into the young alluvium and loess. In its offset part, the channel is wide, and has a U-shaped cross-section with steep sides. It has incised into the old stream deposits (figure 6) that

have been preserved along the edge of the channel. The downstream channel north of the fault is deeply incised into Tertiary red beds and reworked loess.

The existence of the preserved channel deposits is an important sedimentary unit for obtaining a lower bound on the slip rate in this part of the fault because the offset stream channel has incised into these deposits. Therefore the time of onset of the approximately 90 m stream offset is younger than the formation of deposits in the preserved channel deposits. The distribution of the preserved channel deposits along the offset part of large stream channel, however, suggests that the stream had already been flowing subparallel to the fault when the 90 m offset began to develop.

In 1984 we took a sample of organic soil from about 5 m southeast of the fault in upstream channel, and about 2 m below the surface of the terrace. This sample gave an age of 6190 ± 250 years before 1920. For 82 ± 30 m pre-1920 displacement, the slip rate would be 13.4 ± 4.8 mm/year. When we obtained this age, we thought the sample might have been from a slump of the terrace, and the age might not be reliable. In 1985 we revisited this channel, and we found a very good sample of organic material with charcoal, also about 2 m below the surface, about 15 m southeast of the fault and along the same upstream channel. The age of this sample is 5120 ± 300 years before 1920. Its resultant lower bound on the slip rate would be 16.4 ± 5.9 mm/yr.

These two estimates for lower bounds on the slip rate are both much larger than the others that we obtained and larger than Burchfiel et al.'s (1987) average rate for the Quaternary period. We include

discussion of them here because they constitute a part of our work, but we doubt their reliability for two reasons. First, because the stream has been flowing roughly parallel to the fault since before the organic material was deposited, the measured offset might not be representative of the displacement since that age. Second, because the present stream flows at an angle of only 20° to 25° to the fault trace, meanderings of the stream could make the measured offset more uncertain than we had estimated which in the field.

DAGOUMEN. About 100 m south of Dagoumen (figure 2), a large stream, which we call the Dagoumen stream, flows from northwest to southeast almost parallel to the Haiyuan fault. The Dagoumen stream is the largest in this locality. A large wide, flat high terrace is well developed on southern side of the stream, and gradually grades into the erosion surface of the mountain to its southwest. The height of the terrace is about 10 m above channel bed, and its width is generally in about 60 to 80 m, The terrace is built on layers of gravel mixed with sand and reworked loess.

Several streams flow from the Xihua Shan, the mountains southwest of the fault, and cut the high terrace before reaching the Dagoumen stream. All of these stream channels have been offset as they cross the Haiyuan fault. The larger of these streams are offset more than the smaller ones. We studied the stream channel with the largest and clearest offset; it probably is the oldest of them. The upstream channel south of the fault shows a clear U-shaped cross-section and is deeply incised into the bed rock. The downstream channel, north of the fault, shows a clear V-shaped cross-section and is deeply incised into the

terrace of the Dagoumen stream. The bottoms of the upstream and downstream channels are separated about 87 ± 10 meters of the fault. The Haiyuan fault there strikes about S60E, but floor of the offset part of stream channel trends about S15E, so that the angle between the present stream bed and the fault is about 45 degrees. Therefore the amount of displacement along the fault is about 61 ± 10 m. Apparently continued incision of the stream has cut obliquely across the fault as the valley has been displaced by the slip on it.

Because the offset streams have incised into the high terrace of the Dagoumen stream and the erosion surface, the ages of the offset streams should be younger than the age of the terrace. Therefore the age of the surface of the high terrace can be used to calculate a minimum estimate for the slip rate along this part of the fault. By using the largest stream offset among them, we obtain the largest among a family of lower bounds on the slip rate. We collected a sample of organic material from 3 m below the top of the high terrace. The sample consists of many small pieces of charcoal distributed irregularly within a layer of reworked loess. The age of this sample is 15,370 ± 1000 years before 1920. For 53 ± 10 m of pre-1920 stream offset, the minimum slip rate estimated to be 3.5 ± 0.8 mm/yr.

YEHUPO. At a small village, Yehupo (figure 2), a stream flowing from the Nanhua Shan has been offset about 90 m. We use the width of 10 m of the stream channel for the uncertainty of the offset (figure 7). Adjacent to the stream channel are a high terrace, a lower terrace and a bench. The high terrace is about 3.5 m above the lower terrace and is composed of several thick gravel layers, which are interbedded with two

layers of pebbly reworked loess and coarse-grained sand. At the top of the high terrace is about 0.4 m thick layer of soil. The sample of organic soil was taken from 1.8 m below the surface of the high terrace within a layer of reworked loess and sand. This sample gives an age of 12,280 ± 1000 years before present (1950), and therefore 12,250 ± 1000 years before 1920. The lower terrace consists entirely of gravel, and only a thin layer of top soil has developed on top of it. Its height above the bench of the stream is about 1 m. The bench is less than 0.5 m above the channel bed.

Both the high and lower terrace are well developed on the northwest side of the channel upstream (southwest) from the fault, but remains of the high terrace can be found only in few places on the opposite (southeastern) side of the upstream channel. Downstream from the fault, the lower terrace is well developed on both sides, but remains of high terrace can be found only at one place on the northwestern side of the channel (figure 7). Both the high and lower terrace strike about N20E to N40E, parallel to the present stream and almost perpendicular to the fault, which strikes about N60W. At the part of channel flowing parallel to the fault, only the lower terrace is developed. The high terrace probably had already developed before the recent offset of the stream began. The pebble imbrication on the higher terrace in the upstream channel shows transport in the direction between N10W to N40E. Near the offset part of the stream channel, the pebbles in the high terrace are imbricated in the same direction as those in the upstream channel; they do not show any indication of a different direction of transport that might have existed if the stream were deflected at the fault when the

material was deposited. The pebble imbrication in the lower terrace, however, shows the transport in the direction N90W to N50W in the offset part of stream but northward in both the upstream and downstream channels. The variation in the direction of imbrication near where the stream is offset suggests that the stream flowed west or northwest when material in the lower terrace was deposited. Therefore the 90 m displacement started before the formation of the lower terrace but apparently after the formation of the higher terrace.

With a maximum age of surface of the high terrace 12,250±1000 years before 1920, and with an 82 m pre-1920 offset, the minimum average slip rate during this interval is 6.7 ± 0.8 mm/yr.

CONCLUSION

We obtained lower bounds on the slip rate at six localities along the Haiyuan fault (figure 9 and table 2). They range from 3.5 ± 0.8 to 16.4 ± 5.9 mm/yr with the five that we consider most reliable to be less than 7.6 ± 1.0 mm/yr.

Three small bounds on the slip rate are 3.5 ± 0.8, 3.5 ± 0.8 and 4.0 ± 0.4 mm/yr from Fangjiahe, East Shaomayin 1, and Dagoumen, respectively. At Fangjiahe the sample of organic material was taken from a sand lens interbedded with a piedmont gravel layer or with gravel deposited in a stream channel. This material now lies 6 to 8 m below the surface and clearly is older than the onset of 70 m stream offset. At East Shaomayin 1, a sample of organic material was collected from a clay layer interbedded with a wide-spread gravel layer in that locality,

whose age is clearly older than the initiation of the stream. In the Dagoumen region, the sample was collected from 3 meters below the large and high terrace of the Dagoumen stream that has been incised by a young offset stream. The gravel at Fangjiahe and East Shaomayin 1 as well as the large higher terrace of Dagoumen stream could be much older than the initiation of the corresponding stream offsets. Therefore the ages of these three samples could be so old that the lower bounds for average slip rate estimated from them might be misleading underestimates.

The offsets at both Shaomayin and Yehupo are clear and well-defined. The samples of organic material were collected from below high terraces along these channels. Because the offsets are clear and the organic materials are near the tops of the surfaces incised by the stream channels, we think that the rates of 7.6 ± 1.0 mm/yr and 6.7 ± 0.8 mm/yr from these two streams, especially that from Shaomayin, are the least disputable among those shown in figure 8. Thus we think that the average Holocene slip rate of the Haiyuan fault is almost surely more than 6 mm/yr and probably more that 7 mm/yr.

At East Shaomayin 2, we obtained a lower bound on the slip rate to be 16.4 ± 5.9 mm/yr. As mentioned above, this bound may not be as reliable as the others because of the uncertainty of the displacement. We assigned a large uncertainty of 30 m to the displacement, but it could be larger. In fact we do not think that the average slip rate is much greater than 10 mm/yr. If this were so, many great earthquake should have occurred in the past few thousand years, and our trenching studies (Zhang P. et al., 1987) do not reveal evidence of many events along the Haiyuan fault in that period of time. Moreover, we expect that

these great earthquakes would have been recorded in the historic documents of China, because the Haiyuan area is only about 300 km from the ancient capital city of Xian. Thus we suspect that the Holocene slip rate along the Haiyuan fault has not been much larger than about 10 mm/yr, but we cannot definitely prove this.

In any case the average Holocene slip rate of the Haiyuan fault is larger than 6 mm/yr. If it is less than 10 mm/yr, or in another form, 8 ± 2 mm/yr, then this rate is comparable to the 5 to 10 mm/yr average slip rate over Quaternary time obtained by Burchfiel et al. (1987).

Acknowledgement

This work was part of an exchange between the People's Republic of China and the United States on seismological studies of earthquake hazards and has been supported by the National Science Foundation through grant EAR-8306863 and by the State Seismological Bureau of China. We thanks the Institute of Geology, State Seismological Bureau and Ningxia Seismological Bureau of China for making the field work possible and successful, and K. Sieh for his suggestions on radiocarbon dating.

CARBON 14 AGE

SAMPLE	LOCATION	AND 1σ UNCERTAINTY		DATE (95% CONFIDENCE)		AGE (BEFORE 1950)	
HF84CY1	CAIYUAN	1610±70	B.P.	250-600	A.D.	1520±170	B.P.
HF84CY2	CAIYUAN	2510±100	B.P.	825-450	B.C.	2560±210	B.P.
HF84SMY1	SHAOMAYIN	4540±180	B.P.	3775-2890	B.C.	5290±440	B.P.
HF84SMY2	SHAOMAYIN	4780±80	B.P.	3820-3360	B.C.	5540±230	B.P.
HF84SMY3	SHAOMAYIN	4630±110	B.P.	3700-3050	B.C.	5320±320	B.P.
HF84SMY4	SHAOMAYIN	5550±100	B.P.	4650-4110	B.C.	6280±250	B.P.
HF84YHP1	YEHUPO	11930±200	B.P.			12280±1000	B.P.*
HF85FJH2	FANGJIAHE	17190±140	B.P.			17690±1000	B.P.*
HF85DGM1	DAGOUMEN	15061±130	B.P.			15400±1000	B.P.*
HF85SMY5	SHAOMAYIN	4470±95	B.P.	3495-2905	B.C.	5140±300	B.P.

* Corrected age assumes a half life of 5730 years, uncertainty estimate based on Klein et al. (1982)

LOCATION	TOTAL OFFSET (METER)	PRE-1920 OFFSET (METER)	YEARS BEFORE 1920	SLIP RATE (MM/YEAR)
FANGJIAHE	70±15	68±15	17690±1000	3.5±0.8
SHAOMAYIN	48±4	40±4	5260±440	7.6±0.9
EAST OF SHAOMAYIN 1	30±2	22±2	5510±230	4.0±0.4
EAST OF SHAOMAYIN 2	92±30	84±30	6190±250 5110±250	13.4±4.8 16.4±5.9
DAGOUMEN	61±8	53±8	15370±1000	3.5±0.8
YEHUPO	90±10	82±10	11280±1000	6.7±0.8

References

Burchfiel, B.C., Zhang P., Wang Y., Zhang W., Jiao D., Song F., Deng Q., Molnar P., and L. Royden, Geology of the Haiyuan fault zone, Ningxia Autonomous Region, China and its relation to the evolution of the northeastern margin of the Tibetan Plateau, submitted to J. Geophys. Res., 1987.

Deng Q., Song F., Zhu S., Li M., Wang T., Zhang W., Burchfiel B.C., Molnar P., and Zhang P., Active faulting and tectonics of the Ningxia-Hui Autonomous region, China, J. Geophys. Res., 89, 4427-4445, 1984.

Deng Q., Chen S., Song F., Zhu S., Wang Y., Zhang W., Jiao D., Burchfiel B.C., Molnar P., Royden L., and P. Zhang, Variation in the geometry and amount of slip on the Haiyuan fault zone , China and the surface rupture of the Haiyuan earthquake, Maurice Ewing Series 6, Amer. Geophys. Un., Washington, D.C., 169-182, 1986.

Lanzhou Institute of Seismology and the Seismological Bureau of Ningxia-Hui Autonomous Region, the Haiyuan Earthquake in 1920, (in Chinese), Seismological Publishing House, Beijing, 1980.

Klein J., J.C. Lerman, P.E. Damon, and E.K. Ralph, Calibration of radiocarbon dates: Tables based on the consensus data of the Workshop of Calibrating the Radiocarbon Time Scale, Radiocarbon, 24(2), 103-150, 1982.

Schwartz D.P. and K.J. Coppersmith, Fault behavior and characteristic

earthquakes: example from the Wasatch fault and San Andreas fault zone, J. Geophys. Res., 89, 5681-5698, 1984.

Sieh K.E.,Prehistoric large earthquakes produced by slip on the San Andreas fault at Pallett Creek, California, J. Geophys. Res., 83, 3907-3939, 1978.

Sieh K.E., Lateral offsets and revised dates of large earthquakes at Pallett Creek, California, J. Geophys. Res., 89, 7641-7670, 1984.

Sieh K.E. and R. Jahns, Holocene activity of the San Andreas fault at Wallace Creek, California, Geol. Soc. Am. Bull., 95, 883-896, 1984.

Song F., Wang Y., Deng Q., and Zhang W., The maximum horizontal displacement in the Haiyuan earthquake of 1920 and estimates of earthquake recurrence in northern marginal fault of the Nan-Xihua Shan , (in Chinese), Seismology and Geology, 4, 1983.

Stuiver M., A high-precision calibration of the AD radiocarbon time scale, Radiocarbon, 24(1), 1-26, 1982.

Weldon R.J. and K.E. Sieh, Holocene rate of slip and tentative recurrence interval for large earthquakes on the San Andreas fault, Cajon Pass, Southern California, Geol. Soc. Am. Bull., 96, 793-812,1985.

Zhang W., Jiao D., Zhang P., Molnar P., Burchfiel B.C., L. Royden, Deng Q., Wang Y., and Song F., Displacement along the Haiyuan fault associated with the great 1920 Haiyuan, China, earthquake, Bull. Seism. Soc. Am., 77, 117-131, 1987.

Zhang P., Zhang W., Deng Q., P. Molnar, Wang Y., B. C. Burchfiel, Song F., L. Royden, and Jiao D., Bounds on the recurrence intervals of major earthquakes along the Haiyuan fault in north-central China,

submitted to Quaternary Research, 1987

Figure Captions

Figure 1. Simple plan view showing how the measured stream separation (S) of segments of a stream is corrected to give the displacement (D), for cases where the offset segment of the stream is not parallel to the fault trace. Solid lines show the channel banks, dashed lines the channel bottom, and dot-dashed lines the edges of the valley.

Figure 2. Simplified topographic map of the Haiyuan area with the locations of features and villages mentioned in the text. The contour interval is 200 m.

Figure 3. left-lateral offset of about 48 meters of a small stream near Shaomayin. View is toward the south-southeast. The stream offset by the fault flows out of the Xihua Shan in the upper left, and near the bottom of the photo, it intersects the large Shaomayin stream, which flows northwest here. The large flat area in the left center of the photo is the high terrace of the Shaomayin stream. To the south and west, the high terrace grades into an erosion surface of the mountains. The sample of organic material was collected from 1.8 m below the surface of the high terrace at about 40 m to the left of the left edge of the photo on the northeastern side of the Shaomayin stream.

Figure 4. Contour map of an offset stream channel and the Haiyuan fault about 700 m east of Shaomayin. A small stream flows northeast, but is deflected at a small ridge that marks the Haiyuan fault. This channel is displaced about 30 m. East of the stream the fault scarp traverses a low saddle, and the surface rupture there has defined a small graben. The vertical component of slip is only about 0.5 m. Thus the displacement was primarily strike-slip. At the northwest end of the ridge that make a southeast facing scarp, the southwest side of the ridge is bare of vegetation. We presume that this bare region formed by left-lateral slip in 1920, and from its dimensions we estimate that 8 to 9 m of slip occurred (see Zhang W. et al., 1987). The rectangular area in the right-center shows the location of the trench discussed in the next paper (Zhang P. et al., 1987)

Figure 5. Left-lateral stream offset of approximately 92 m east of Shaomayin. View is to the east-southeast obliquely across the fault trace. A major stream enters the photo in the upper right, flows parallel to the fault, and then flows northward out the lower left corner of the photo. The dashed line delineates the trace of the Haiyuan fault. The stream channel that is marked by the thick arrow is upstream from the 92 m offset stream. The trapezoid shows the area covered by figure 7.

Figure 6. Detail of northwestern conner of the 92 m offset stream channel to the east of Shaomayin (figure 5). The view is to

the northwest. The stream, flowing northwest, enters the photo in the lower right corner, and is deflected to the left. The channel in the middle of the photo, with two men standing on it, flows parallel to the fault. Thus it follows the 92 m offset, which continues beyond the left edge of the photo. The channel in the upper right side of the photo is the downstream channel northeast of the fault. The gravel layers on the left side of the photo are the remnants of the old channel deposits.

Figure 7. Photo of 90 m offset of Yehupo stream. View is to the northwest. The Haiyuan fault trace passes through the deflected part of the stream. The large flat areas near the stream are the lower terraces, and the flat areas on the middle right of the photo, pointed by the arrows, are the high terrace.

Figure 8. Offsets vs maximum ages obtained from the 6 offset stream valleys along the Haiyuan fault. The radiocarbon ages are expressed in years before 1920, and 8 m has been subtracted from original measured offset to remove the contribution of the 1920 earthquake. Lines showing rates of 6 and 10 mm/yr are given for comparison.

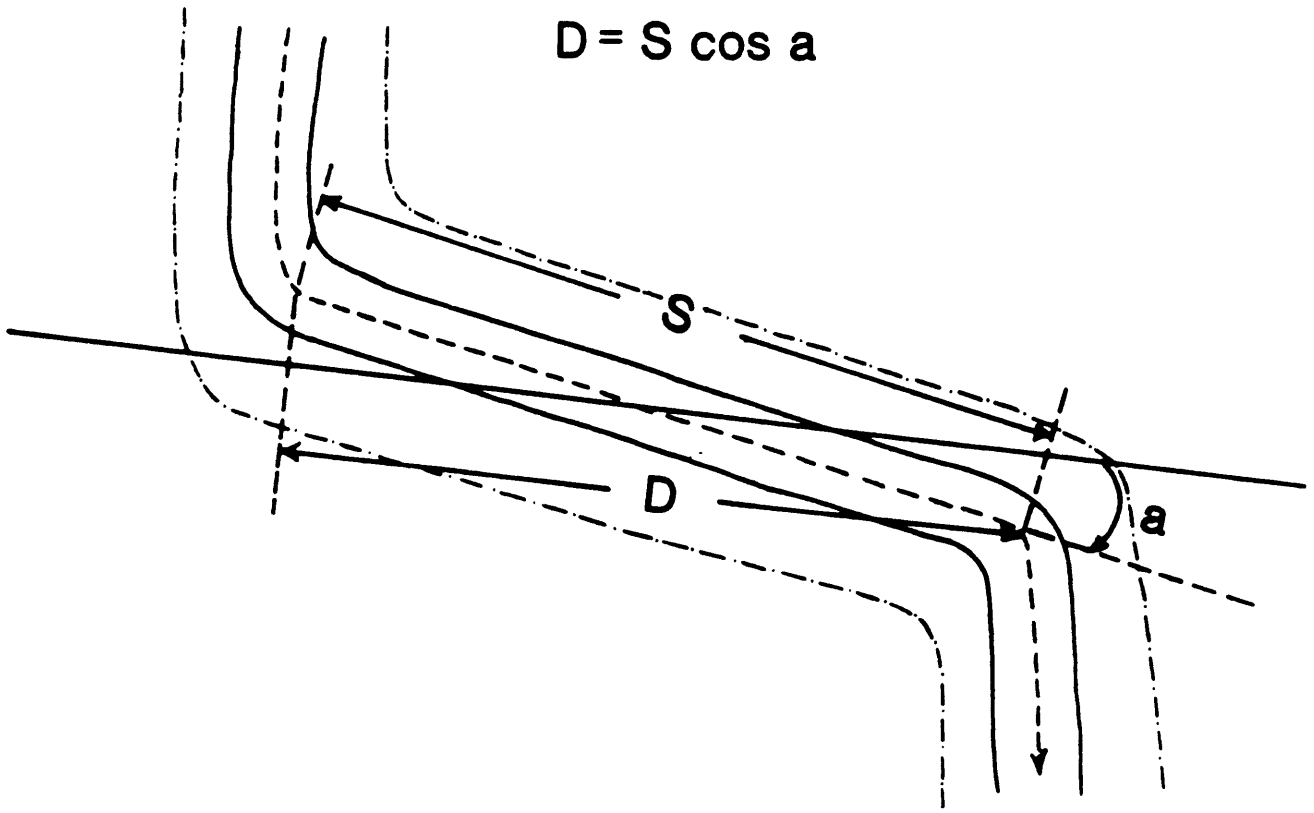

Figure 1

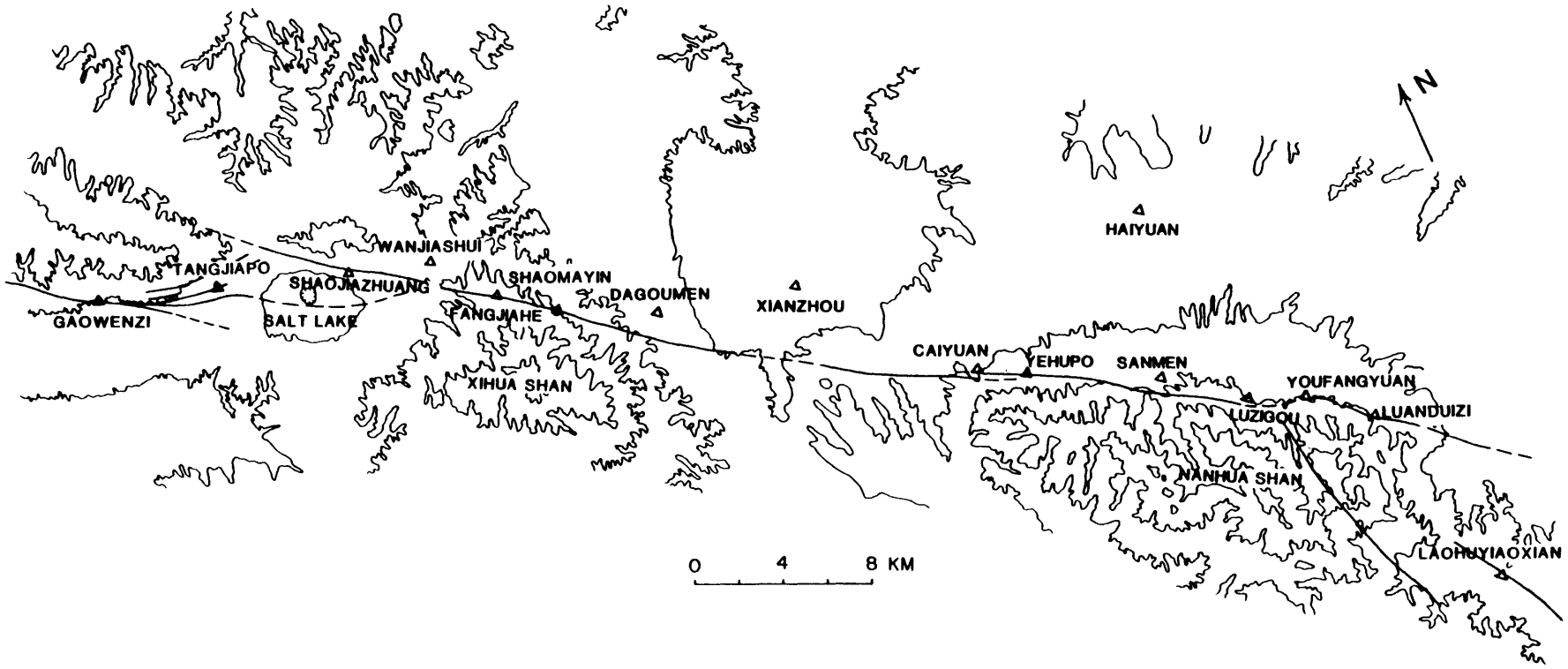
N
HAIYUAN
WANJIASHUI
TANGJIAPO
SHAOJIAZHUANG
SHAOMAYIN
DAGOUMEN
XIANZHOU
GAOWENZI
SALT LAKE
FANGJIAHE
CAIYUAN
YEHUPO
SANMEN
YOUFANGYUAN
XIHUA SHAN
LUZIGOU
LUANDUIZI
NANHUA SHAN
LAOHUYIAOXIAN
0 4 8 KM

Figure 2

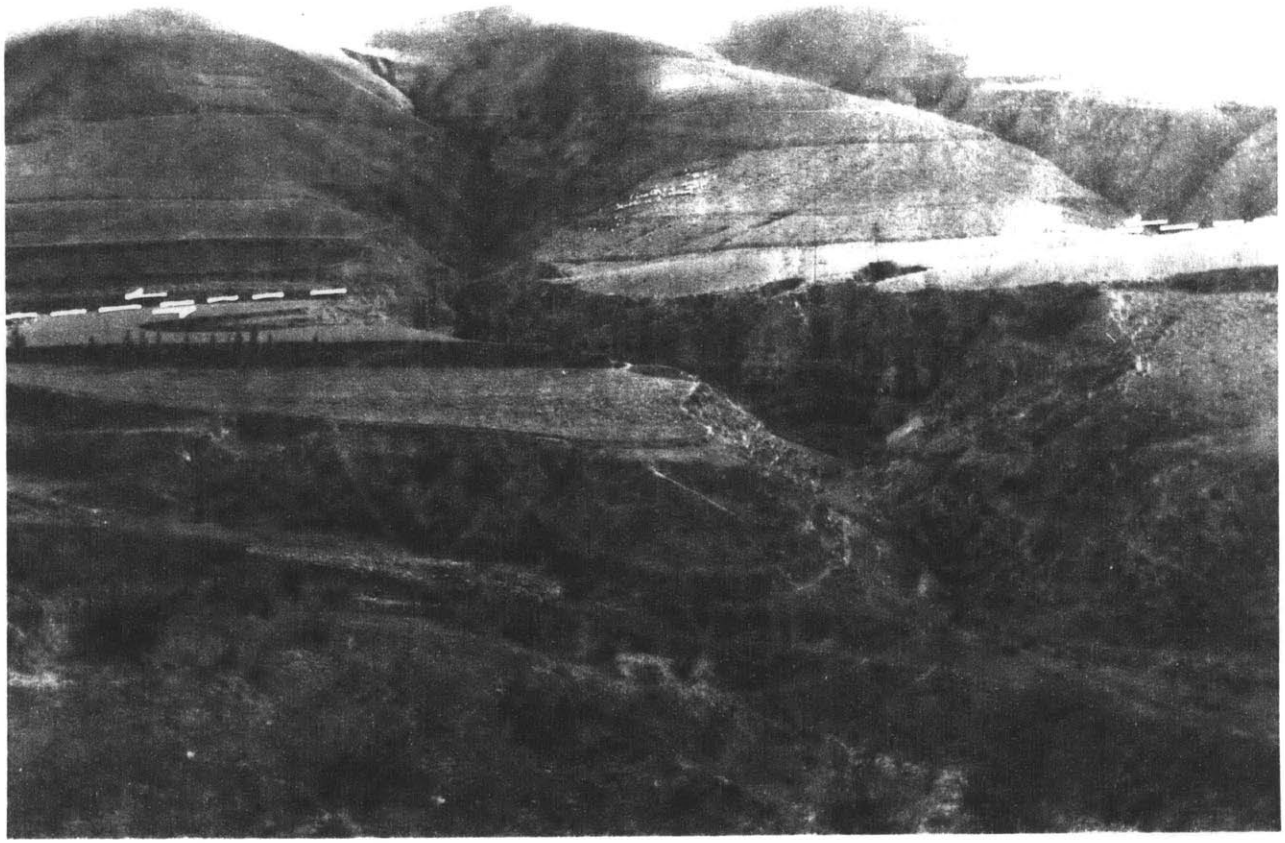

Figure 3

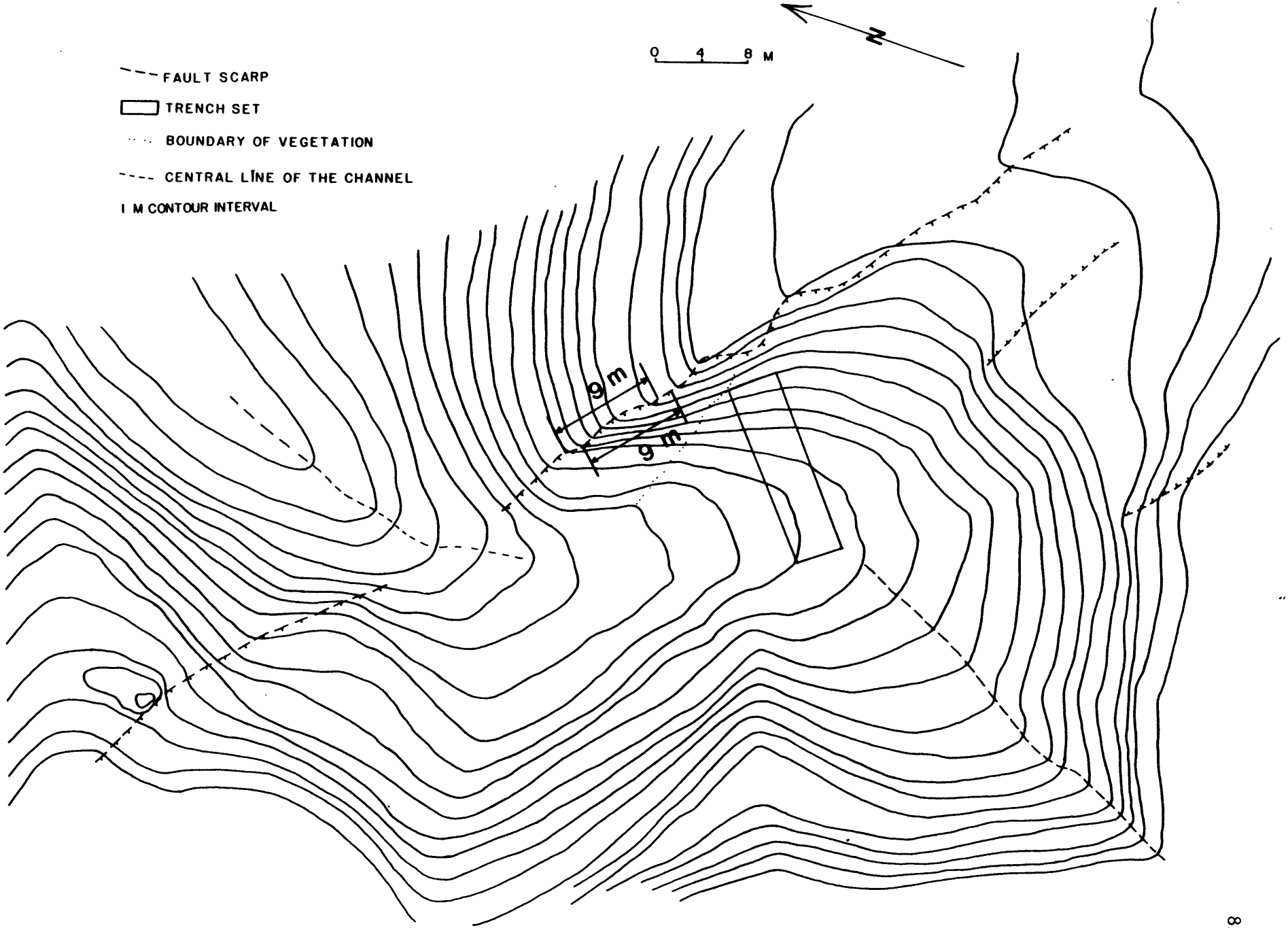
FAULT SCARP
TRENCH SET
BOUNDARY OF VEGETATION
CENTRAL LINE OF THE CHANNEL
1 M CONTOUR INTERVAL
0 4 8 M
N
9 m
9 m

Figure 4

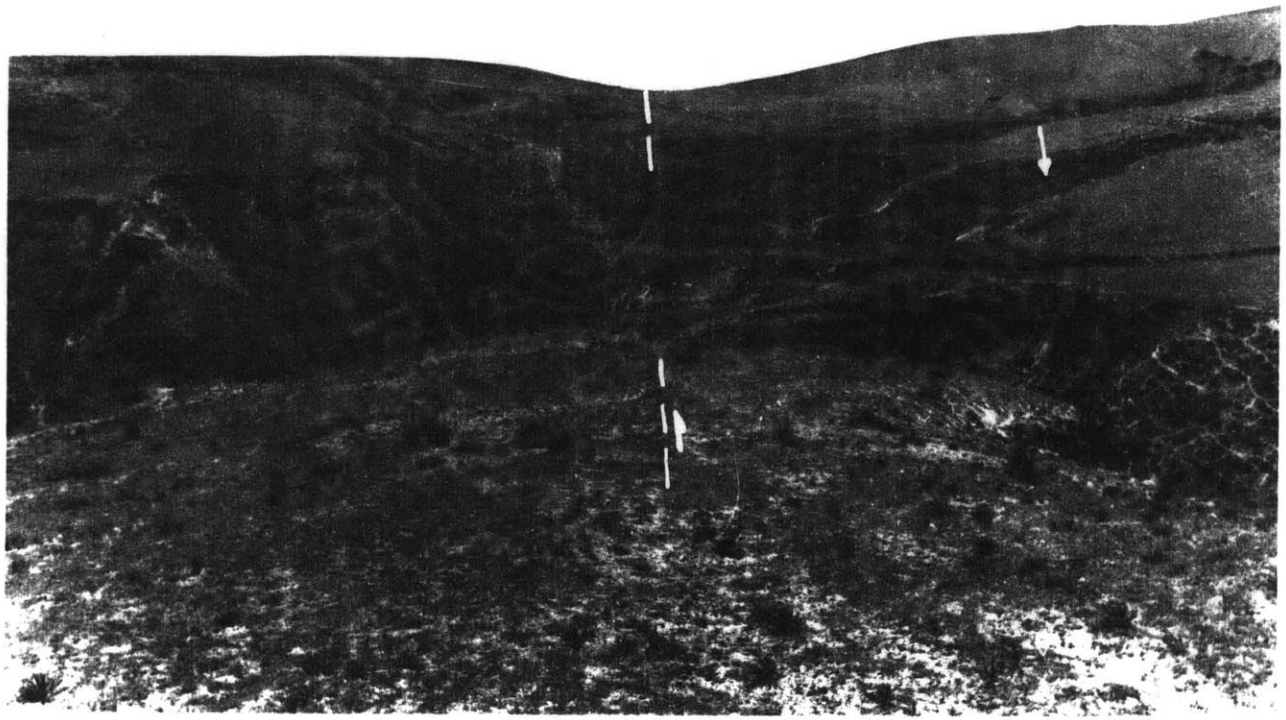

Figure 5

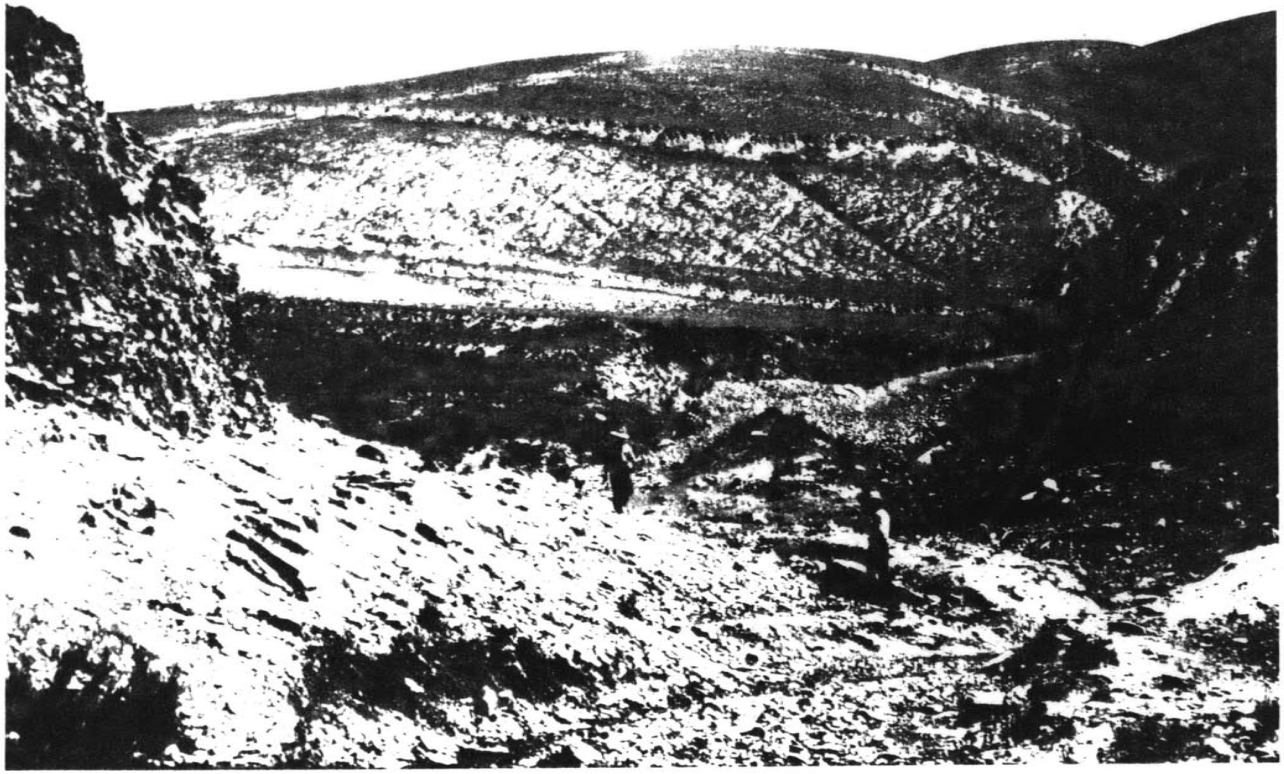

Figure 6

Figure 7

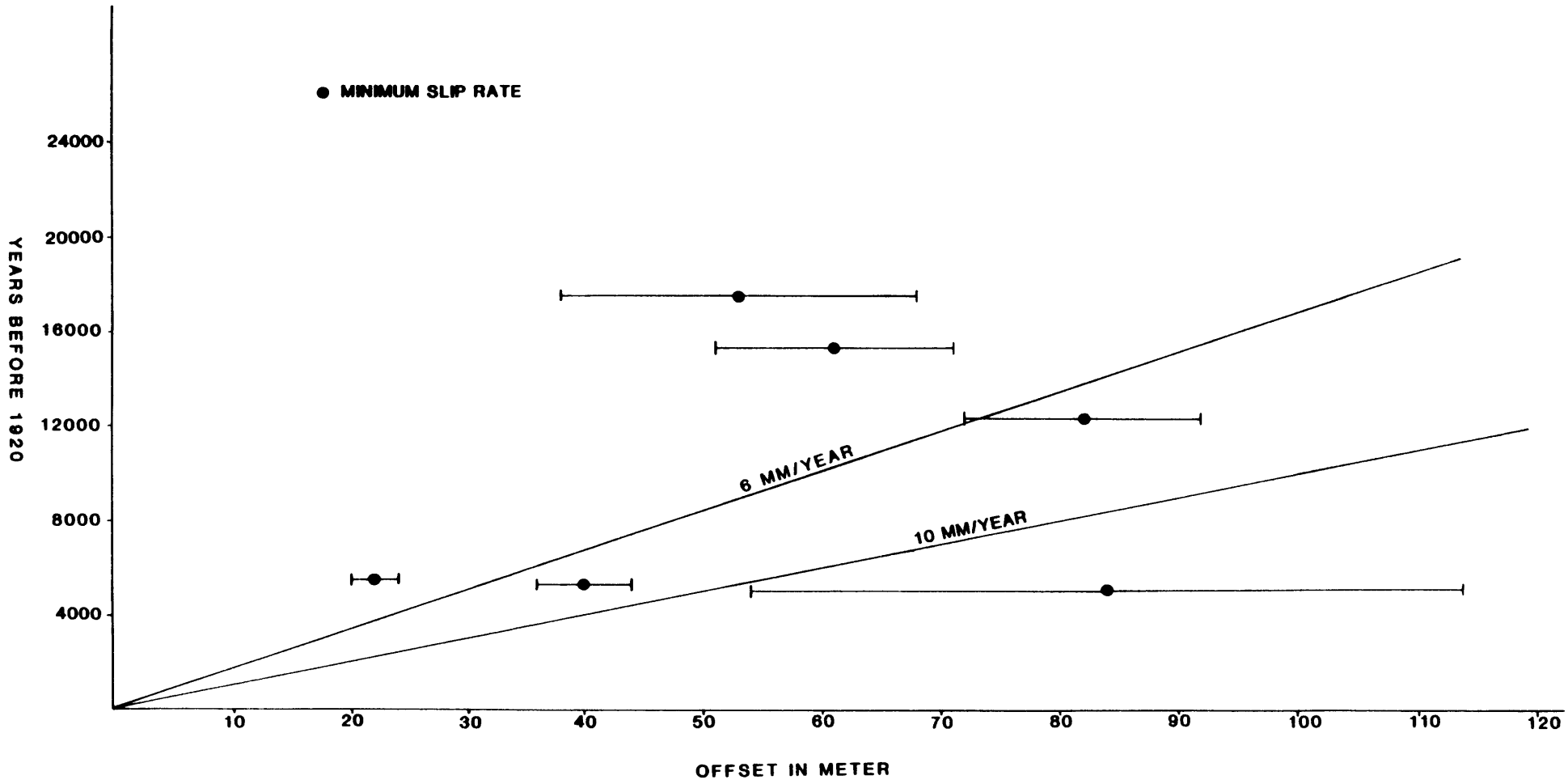
MINIMUM SLIP RATE
24000
20000
16000
12000
8000
4000
YEARS BEFORE 1920
6 MM/YEAR
10 MM/YEAR
10
20
30
40
50
60
70
80
90
100
110
120
OFFSET IN METER

Figure 8

Chapter IV

BOUNDS ON THE RECURRENCE INTERVAL OF MAJOR EARTHQUAKES ALONG THE HAIYUAN FAULT IN NORTH-CENTRAL CHINA

Zhang Peizhen[1], Peter Molnar[1], Zhang Weiqi[2], Deng Qidong[3], Wang Yipeng[3], B. C. Burchfiel[1], Song Fangmin[3], L. Royden[1] and Jiao Decheng[2]

1, Department of Earth, Atmospheric and Planetary Sciences, Massachusetts Institute of Technology, Cambridge, Mass. 02139

2, Institute of Geology, State Seismological Bureau, Beijing, China

3, Ningxia Seismological Bureau, Ningxia-Hui Autonomous Region, Yinchuan, China

ABSTRACT

Evidence of surface rupture prior to 1920 has been found in trenches near Caiyuan and Shaomayin, but neither provides tight constraints on the age of previous earthquakes. We are quite sure that there was one event since 2560 ± 210 years ago in Caiyuan, and there probably was another event since 1490 ± 175 years ago, but before 1920. Fault-related, scarp-derived colluvial wedges in the Shaomayin trench appear to record the occurrence of two pre-1920 events in the last 5000 years, but there could have been three or more events. Using the inferred slip rate for this fault to date the incision of the stream, we infer that these two events occurred since 3700 years ago, and perhaps since 2200 years ago. It seems likely that the earthquake recurrence interval along the Haiyuan fault is not less than 800 years, for the 1920 Haiyuan earthquake is the only major event to have been reported in this area as many years of recorded history. If we take the Holocene slip rate along this fault of 8 ± 2 mm/yr, and 8 m as the average amount of offset associated with past events, the resultant earthquake recurrence intervals would be from 800 to 1400 years. The results from our trenches and the historic record are consistent with this range.

INTRODUCTION

One of the most destructive great earthquakes of this century occurred near Haiyuan in north-central China on December 16, 1920. The magnitude was 8.7, and the mainshock was followed by an aftershock of magnitude of 7.3. More than 220,000 people were killed and thousands of towns and villages were destroyed during this earthquake (Lanzhou Institute of Seismology and Ningxia Seismological Bureau,1980). Four earthquakes of magnitude more than 5, but none with larger magnitude, have occurred in this area since the 1920 great earthquake (Li,1960). An important question, therefore, is when will the next great earthquake like the one in 1920 occur.

To answer this question we should know the earthquake history of the Haiyuan region. Because intracontinental earthquakes often have relatively long recurrence intervals, however, the documented history in general is too short to answer that question even for China, which has more than 1000 years of documented earthquake history. It is well known that most major earthquakes occur on major faults, and most earthquakes are associated with dislocations along active faults. The geological record of the recent past provides the best opportunity to study the long-term behavior of active faults. Thus we can learn the earthquake history by studying the kinematic history of the active faults and by studying the relationships between offsets along active faults and unconformities in the stratigraphic record along the fault traces. By dating both the sediments that were offset by slip on the fault in past

events and the continuous layers of sediments that overlie faults on which lower horizons were displaced, Clark (1972), Sieh (1978,1984), Weldon and Sieh (1986), and others have obtained bounds on when previous earthquakes occurred and on their recurrence intervals. To study such relationships between sediments and faulting, trenches are usually dug across or near active faults in order to expose these relationships.

In a previous paper (Zhang P. et al., 1987), the Holocene slip rate along the Haiyuan fault was estimated. In the present paper we address the recurrence interval of great earthquakes along the Haiyuan fault. During our studies of the Haiyuan fault, we dug several trenches across the fault, but only two of them provided useful information on the past surface ruptures. We describe the analysis of these two trenches here.

The ages of the offset sediments were determined by carbon-14 dating of organic material deposited in the sediments exposed by the trenches. In the previous paper (Zhang P. et al., 1987), we described the procedures that we followed, including corrections to the measured ages.

TRENCH IN CAIYUAN

One of the places that we selected for trenches is located along the Haiyuan fault at the small village of Caiyuan (figure 1). Two strands of the Haiyuan fault overlap each other at Caiyuan so that a small pull-apart basin, about 700 m in length and 300 m in width, has formed (figure 2). Both of these strands were activated during the 1920 earthquake; fault scarps associated with the 1920 earthquake can still be seen on the northern strand. Between these two major strands that

bound the pull-apart basin, another short fault strand developed almost parallel to the overall trend of the main fault. Slip on this strand was manifested by a series of mole tracks and tension cracks.

Although each of the three strands in the Caiyuan area may not have ruptured during all events that occurred in the past along this fault, the advantage of trenching in this area was that we found organic material needed to date the sediments displaced by past events. We dug two trenches across the zone of mole tracks in the middle of the pull-apart basin. In one of these two trenches, the fault was clear, but almost all sediments were found to be black mud. The lack of any detectable stratigraphy made it impossible to detect previous offsets. In the other, which clearly crosses a large mole track, we could not recognize the fault trace in the layers of cobbles. The only useful trench was dug adjacent to the northern strand. The Quaternary deposits exposed in that trench consist of old alluvium, colluvium, fine-grained sand and silt deposits, reworked loess, and stream channel deposits. The major lithological units identified in the trench are described below and are shown on the trench log (figure 3).

OLD COLLUVIUM (Unit A). The oldest deposits exposed in the trench are colluvial deposits. They consist of poorly sorted, bouldery gravel. Most of the boulders and detritus are schist of the pre-Silurian Haiyuan group exposed in Nanhua Shan, but some of them are granites from east of the pull-apart basin (see Burchfiel and others, 1987, for the Quaternary geology of this area). There are some irregular masses or blocks (A2) of reworked loess within the gravel. Some of this reworked loess seems to have been dragged down along what appear to be faults (such as the lower

parts of fault F3 and F4 in figure 3).

REWORKED LOESS (Unit B). Above the colluvium there is a layer of reworked loess that covers all the units beneath it. The loess is not homogeneous; numerous angular pebbles are present in some parts of it but absent in others, which may be separated from one another by faults. The sizes of the pebbles are commonly 1 or 2 cm in diameter. In parts of the trench fine-grained and well-layered sand and silt disconformably overlie the reworked loess.

FINE-GRAINED SAND AND SILT (UNIT C). At the base of southern part of the trench a sequence of well-laminated silt, sand, and clay directly overlie the reworked loess layer. There are some coarse-grained sand and pebble layers or zones in this sequence, and the sequence itself becomes coarser northward in the trench. The laminated sequence is interpreted as having been deposited in a large, wide stream. We collected organic material from a layer of black soil about 0.4 m above bottom of the trench. The age of the sample is 2560 ± 210 years before present (1950), and therefore 2530 ± 210 years before 1920.

STREAM CHANNEL DEPOSITS (Unit D). Adjacent to the fault F2, a channel was excavated in the fine-grained sand and silt, and later filled with coarse pebbles and sand (D1 + D2). The breadth of the channel is about 1.5 m and the thickness is less than 0.5 m. The stream channel sediments are well sorted. Cobbles with diameters of about 5-10 cm lie at the base of the channel deposits. The sizes of the cobbles decrease upward, until the pebbly gravel becomes coarse-grained sand. These sediments are clearly tilted down to the south.

YOUNG ALLUVIUM OR COLLUVIUM (Unit E). These deposits rest

unconformably on the fine-grained sand and silt and on the stream channel deposits. They consist of poorly sorted cobbles, gravel, and coarse-grained sand. Some fine-grained sand layers are also present within the gravel. The irregularity of the upper surface of the deposit may reflect deep (0.5 m) erosion after the deposition of this unit.

DARK SOIL (Unit F). A layer of dark soil was deposited above Unit E. The dark soil is composed mainly of loess and silt. Some pebbles are mixed within the soil, but their sizes are much less, and the number of them is much fewer than in the alluvium underneath it. The soil is not an altered zone of Unit E; its composition is different, and the contact between the layers is quite sharp. In some places there is no dark soil above Unit E, and in others the soil layer seems to fill eroded channels in the underlying deposits. A sample of organic material collected from the dark soil gave an age of about 1520 ± 175 year before present (1950), or 1490 ± 175 years before 1920.

REWORKED LOESS AND TOP SOIL (Unit G). Almost the entire ground surface of the Caiyuan pull-apart basin is underlain by a layer of reworked loess that has a variable thicknesses in different parts of the basin. The reworked loess is relatively pure and contains few, small pebbles.

FAULTS. Several faults, which we labeled from F1 to F5, were revealed in the trench exposure, but most of them probably did not rupture during the 1920 earthquake. The surface rupture of 1920 earthquake is not clear in the trench exposure. In the field we discussed the possibility of the rupture occurring along faults F3 and F4 (figure 3). There seems to have been drag of the loess blocks A2 and

of layer B along these faults, and these faults can also be correlated with two scarps present at the surface. It is also possible that the surface rupture of the 1920 earthquake, or part of it, is located about one meter north of our trench, and if so the trench did not excavate the fault scarp of the 1920 earthquake rupture zone (figure 4). We did not have permission to dig out the road just north of the trench. The curved trace of scarps and their multiplicity made defining the actual fault break of 1920 in this area difficult in 1982 to 1985.

Both faults F1 and F2 can be recognized by the juxtaposition of the old reworked loess and other younger sediments. The upper surface of reworked loess had clearly been offset. The separation of layer B on fault F1 in the plane of the trench wall is about 30 cm, and the same surface is separated about 70 cm at fault F2. It is clear that the stream channel deposits D2 are separated by only about 20 cm along fault F2 (figure 5). All of these separations could be due to strike-slip displacements along the faults, and the different amounts for different layers should not be taken as evidence of multiple offsets.

Since the reworked loess (Unit B) is juxtaposed against the fine-grained sand and silt (Unit C), slip must have occurred after the formation of Unit C, and therefore more recently than 2530 ± 210 years before 1920. It appears that the ground surface was not offset or affected by faults F1 and F2 in association with the 1920 earthquake. Unfortunately, however, we can not be certain that faults F1 and F2 did not rupture in 1920 because the fault could pass through the pebbly layer beneath the dark soil and into dark soil without our being able to recognize it. Unit E and the dark soil (Unit F) may have been affected

by faults F1 and F2, but this also cannot be proved from what we saw on this side of the trench. If this were the case, the slip along faults F1 and F2 would have occurred after the formation of the dark soil F but before the formation of the surface reworked loess G. If this were so, faulting could be constrained to have occurred before 1920 and since 1490 ± 175 years before 1920. In any case, we can be certain that slip occurred along these faults since 2530± 210 years, and we think that it probably occurred since 1490 ± 175 years before 1920 and but not in 1920.

The southern wall of the trench was similar to the northern wall, but in it we found some additional evidence that bears on when faults F1 and F2 were active (figure 6). The dark loess soil in figure 6 corresponds to layer F, and the gravel layer corresponds to layer D in figure 3. There are several layers of clean sand that are interbedded with small pebbly layers (figure 6). These sandy layers are clearly offset by a fault that we correlate with fault F1 in figure 3. Upward along fault F1 there is a large cobble. When we removed the cobble, it was clear that fault F1 did offset the gravel layer. Fault F1 can also be traced to the steep boundary of the gravel layer with the dark soil (figure 6), but we do not know whether or not fault F1 offsets the dark soil because of the absence of reference features within the dark loess.

A second strand seems to correlate with fault F2, and it also displaces some of these layers beneath the gravel layer. The gravel and possibly the dark loess seem to be affected by fault F1 and F2; if we extend faults F1 and F2 upward parallel to their dip, both of them intersect irregularities in the upper surface of the gravel layer, which

might reflect offset of the gravel with the dark loess. Thus we think that offset along faults F1 and F2 probably occurred after the formation of at least lower part of dark loess. Otherwise if the scarp-shaped features on the upper surface of the gravel layer had formed before the deposition of the dark loess, they would have been eroded. We also think that faults F1 and F2 did not slip in 1920. If the faults F1 and F2 are projected upward parallel to their dips, there are no fault scarps or otherwise localized disruption where they intersect the present ground surface. All of the fault scarps associated with 1920 earthquake appear to be either at northern edge of the trench or north of it altogether, several meters north of where faults F1 and F2 are seen. Thus slip on faults F1 and F2 probably did not occur in 1920 but did occur after the formation of the dark loess that was deposited 1490 ± 175 years before 1920.

There is another strand between faults F1 and F2 that we labeled as fault F5 (figure 6). This fault displaces a clean sand layer underneath the gravel, but it clearly does not offset the gravel. Both the gritty layer and a silty lens that overlie fault F5 have not been offset. If offset along fault F5 occurred during a major earthquake, it occurred after the formation of the pebbly loess but before the formation of the gravel layer, and therefore between 2500 and 1500 years ago.

Finally, note that all of these sand and gravel layers are tilted down to the south. This tilting cannot be assigned to the faulting events that occurred on fault F5 because layers unconformably overlying it are also tilted. Moreover the tilting is localized to the between faults F1 and F2 (see figure 3). The tilting does not appear to have

occurred in 1920, because there is no clear surface deformation above this localized tilting. Consequently, this deformation seems to have occurred since fault F5 slipped last, but before 1920; it probably occurred when slip on faults F1 and F2 last occurred and since 1500 years ago.

For this trench we are sure that there was faulting since 2530 ± 210 years ago, but before 1520 ± 175 years ago. There probably also was faulting since 1520 ± 175 years ago, but before 1920, and there seems to have been tilting since the earlier faulting event occurred. Faulting in this more recent interval of time is strongly suggested, but cannot be definitely proved. If these faulting and tilting events were associated with major earthquakes, than there definitely was one major earthquake since 2500 years ago, and probably two, with the second occurring since 1500 years ago, but before 1920.

TRENCH IN SHAOMAYIN

Another trench was dug about 700 m east of Shaomayin (figure 1). The surface rupture associated with the 1920 earthquake includes a small graben, about 30 m wide, but the slip was mostly strike-slip (see figure 4 of Zhang P. et al., 1987). There is a dry stream channel that has been offset left-laterally about 30 m where it crosses the main fault scarp of the graben. We described and discussed the offset of this stream offset in a previous paper (Zhang et al., 1987). Our trench is across the fault scarp within this channel (figure 7; Zhang P. et al., 1987, figure 4), and the trench log is presented in figure 8.

The fault breccia (unit A) exposed in northeastern part of the trench is mixed with fault gouge. Some bodies within it could be colluvium (A1, A3) and some seem to consist of pebbly sand and silt (A2). Several faults (F2, F3 and F4) could be recognized within the breccia.

Colluvial gravel (B) is the main lithological unit in southwestern part of the trench (figure 8). The gravel consists of boulders, cobbles, and pebbles, mostly of mica schist from the bed rock south of the fault. Several clay beds (B1) interbedded with the gravel indicate that unit B formed by sedimentary deposition, so that it is obviously different from the fault breccia in the northeastern part of the trench. Organic material from one of the clay layers are an age of 5510 ± 230 years before 1920.

Above the gravel in the southwestern part of the trench, there is a clayey silt layer (unit C in figure 8) in which some organic material is present. A sample of it gave an age of this silt layer of 5260 ± 440 year before 1920.

A layer of relatively pure sandy silt (unit D in figure 8) covered both layer B and C. This layer can be easily recognized by the relatively purity of the sand and the almost complete absence of pebbles. In the northeastern part of the trench a layer of similar composition is tilted, and if it is a continuation of layer D on the southwestern side, only a piece of that layer still remains in the trench. In the middle part of the trench this layer does not exist between the fault F1 and F4. Its absence may be due to erosion after uplift associated with surface faulting in the past.

Layer F is the surface soil, and is made of reworked loess. Almost the entire surface of the dry stream channel is covered by this layer.

There are two wedge-shaped sedimentary assemblages (unit E and G) in the trench. They are localized near the fault scarp F5, and their thicknesses gradually decrease away from the fault. The lower part of this assemblage consists of reworked loess with angular pebbles and cobbles mixed within it, and the upper part of this assemblage is composed of angular cobbles and pebbles in a matrix of sand and reworked loess (figure 9). We interpret these assemblages as colluvial wedges derived from erosion of the fault scarp to their north.

The fault scarp exposed at the northeast of the trench is the upward extension of fault F5. This fault ruptured in 1920. The sediments exposed by the fault scarp consist of reworked loess overlying angular cobbles and pebbles mixed with sand and reworked loess. Apparently when the free surface of the fault scarp formed, the loess that lay on the top of the gravel along the scarp became unstable and slumped first to form the base of the wedge; after the loess was eroded away from the top of the scarp, the gravel slumped on the loess to form the upper part of the wedge.

Swan et al. (1980) and Schwartz and Coppersmith (1984) recognized this kind of wedge-shaped colluvial deposit along the Wasatch fault zone, and suggested that each of these wedges represents a surface faulting event along an adjacent normal fault. For strike-slip faults, surface faulting does not always cause scarps and associated colluvial wedges, because vertical separation of the surface does not occur everywhere along the fault. In our trench the colluvial wedge G is

present only on the eastern wall of the trench, but not yet on the western wall, which is 4 m from the eastern wall. Furthermore, an older colluvial wedge can be deformed or destroyed by motions associated with the subsequent strike-slip faulting events. Therefore the number of such colluvial wedges is likely to represent a minimum number of surface faulting events for a strike-slip fault.

We associate the colluvial wedge G along the fault F5 with 1920 earthquake, because it overlies the surface layer F and is adjacent to the present free surface of the fault scarp formed during that earthquake. The colluvial wedge E along fault F5 is covered by layer F and overlies layer D and breccia A. The height of this wedge is about 2 meters. It could be associated with a surface faulting event before 1920. The wedge E itself is tilted down to the northeast, but it still retains a wedge shape. This tilting must have occurred after the event that formed the wedge, and probably before 1920, because the surface layer F above the wedge E does not seem to be tilted by that event. If the event that cause the tilting of wedge E were the 1920 earthquake, the layer F above the wedge should have been disrupted or tilted synchronously with the wedge.

If the thin wedge of sandy silt (layer D) on the northeastern side of the trench is the same age or younger than the unit D on the southwestern side, then these events occurred since 5200 years ago. We can use the Holocene slip rate to place a tighter constraint on the age of these events. The movement of the Haiyuan fault here is mainly strike-slip (Zhang W. et al., 1987). The colluvial wedges could have formed only after the free surface of the fault scarp had been

juxtaposed against the dry stream channel north of the fault. If there had been no stream channel, colluvial wedges would not have formed because there would have been no fault scarp with a free surface high enough to provide the scarp-derived colluvium. This means that the ages of these colluvial wedges probably are younger than the entrenchment of the stream channel. By using the average slip rate during Holocene time, the initiation of the stream channel can be estimated. In a previous paper (Zhang P. et al., 1987), we inferred a slip rate during Holocene time to be 8 ± 2 mm/year. For 22 m of pre-1920 displacement, the initiation of this channel could be 3700, 2750 and 2200 years before 1920 for slip rates of 6, 8 and 10 mm/yr, respectively. Thus the creation of wedge E and the tilting of it, which we assume to be associated with two pre-1920 surface faulting events, probably occurred since 3700 years and possibly since 2200 years ago.

In this trench we also found evidence of surface faulting between units A and B, associated with pre-1920 events. There are many faults exposed on the wall of the trench, but only fault F5, which ruptured in 1920, cuts the surface layer (unit F). The breccia (unit A) on the northeastern side of fault F1 had been juxtaposed against the gravel (unit B) and sandy silt (unit D). The age of the faulting that juxtaposed these units can only be constrained to be before the formation of layer F and after the formation of layer D, which is 5260 ± 440 years before 1920. Since the sediments on opposite of fault F1 are completely different, the separation along fault F1 is probably quite large. Thus probably more than one event occurred along fault F1, but we have no evidence to deduce how many more events did occur.

In this trench we probably can define three pre-1920 surface faulting events. Two of them occurred along fault F5, with one associated with the formation of the colluvial wedge, and with the other associated with the disruption and tilting of it. At least one event must be responsible for the slip on fault F1, but we do not know the relation between that event and the other events. Slip on fault F5 could have occurred simultaneously with that along fault F1. Moreover, the ages of these events are poorly known, but all of them must have occurred before 1920. At least one event occurred on fault F1 between 5200 years ago and 1920, and both events on fault F5 seem to have occurred between 3700 to 2200 years ago and 1920. Take together these results require a recurrence interval less than 2600 years, they imply recurrence intervals of 1100 to 1700 years, and they allow shorter recurrence intervals.

DISCUSSION

In an earlier paper (Zhang W. et al., 1986) we demonstrated that the maximum left-lateral displacement during 1920 earthquake was 10.2 m, and the average amount was about 8 m. Let us assume that the average displacement associated with pre-1920 event was also 8 m. The Holocene slip rate is at least 6 mm/yr (Zhang P. et al., 1987) and the average rate over Quaternary time obtained by Burchfiel et al., (1987) is less than 10 mm/yr. Thus for a slip rate of 8 $\pm$ 2 mm/yr, the resulting average recurrence interval for earthquake with slip of 8 m would be from 800 years to 1400 years.

Evidence of surface rupture prior to 1920 has been found in

trenches near Caiyuan and near Shaomayin, but neither provides tight constraints on the age of previous earthquakes. We are quite sure that faulting occurred since 2560 ± 210 years ago at Caiyuan, and there probably was another faulting event that occurred since 1520 ± 175 year ago, but before 1920.

Fault-related, scarp-derived colluvial wedges in the Shaomayin trench indicate a minimum number of two events prior to the 1920 earthquake and probably since 2200 to 3700 years ago. The juxtaposition of breccia with depositional gravel on opposite side of fault F1 in that trench also represents at least one event prior to the 1920 surface faulting event. The age of this event also can be constrained only to be between 1920 and about 5000 years ago. We do not know the relation between the events along fault F1 and those represented by colluvial wedges. Therefore during the period between 1920 and since 5280 ± 440 years before 1920 apparently at least two events occurred, and there could have been three or more events. The results from both trenches implies that the recurrence interval is less than 2500 years, probably is less than 1500 years, and could be smaller. Thus they are consistent with recurrence interval inferred from the slip rate, but they do not offer a tighter constraint on it.

The earthquake history in the Haiyuan area can be traced back to 1219, and the only large earthquake in this area with magnitude greater than 7 (Li, 1960) occurred in 1920. It is likely that no such earthquake occurred in this area 400 to 500 years before 1219, because that time corresponds to the Tang and Song Dynasties in Chinese history, during which the city of Xian was the capital and the center of culture. If

such an earthquake occurred in this area, which is only about 300 km northwest of Xian, people there are likely to have known about it and recorded it in documents. Thus the absence of such a record suggests that no significant earthquake occurred 700 years before 1920, and probably 1000 to 1200 years before 1920.

Thus the historical record suggests that the earthquake recurrence interval along the Haiyuan fault is probably not less than 800 years. The disruption of datable horizons in the two trenches suggests, but do not prove, that faulting occurred within the last 1600 years. Therefore the results from the trenches, from the historical record, and from the Holocene and Quaternary slip rate are consistent with one other.

Acknowledgements

This work was part of an exchange between the People's Republic of China and the United States on seismological studies of earthquake hazards and has been supported by the National Science Foundation through grant EAR-8306863 and by the State Seismological Bureau of China. We thank Institute of Geology, State Seismological Bureau and Ningxia Seismological Bureau of China for making the field work possible and successful, and K. Sieh for his suggestions on radiocarbon dating.

References

Burchfiel, B.C., Zhang P., Wang Y., Zhang W., Jiao D., Song F., Deng Q., P. Molnar, and L. Royden, Geology of the Haiyuan fault zone, Ningxia Autonomous Region, China and its relation to the evolution of the northeastern margin of the Tibetan Plateau, submitted to J. Geophys. Res, 1987

Clark, M.M., A. Grantz, and M. Rubin, Holocene activity of the Coyote Creek fault as recorded in sediments of Lake Cahuilla, U. S. Geol. Serv. Prof. Pap., 787, 112-130, 1973.

Deng Q., Song F., Zhu S., Li M., Wang T., Zhang W., B.C. Burchfiel, P. Molnar, and Zhang P., Active faulting and tectonics of the Ningxia-Hui Autonomous region, China, J. Geophys. Res., 89, 4427-4445, 1984.

Deng Q., Chen S., Song F., Zhu S., Wang Y., Zhang W., Jiao D., B.C. Burchfiel, P. Molnar, L. Royden, and P. Zhang, Variation in the geometry and amount of slip on the Haiyuan fault zone , China and the surface rupture of the Haiyuan earthquake, Maurice Ewing Series 6, Amer. Geophys. Un., Washington, D.C., 169-182, 1986.

Li Shanbang, A Catalogue of Earthquakes in China, (in Chinese), Science Press, Beijing, 1960.

Lanzhou Institute of Seismology and the Seismological Bureau of Ningxia-Hui Autonomous Region, The Haiyuan Earthquake in 1920, (in Chinese), Seismological Publishing House, Beijing, 1980.

Schwartz D.P. and K.J. Coppersmith, Fault behavior and characteristic

earthquakes: example from the Wasatch fault and San Andreas fault zone, J. Geophys. Res., 89, 5681-5698, 1984.

Sieh K.E.,Prehistoric large earthquakes produced by slip on the San Andreas fault at Pallett Creek, California, J. Geophys. Res., 83, 3907-3939, 1978.

Sieh K.E., Lateral offsets and revised dates of large earthquakes at Pallett Creek, California, J. Geophys. Res., 89, 7641-7670, 1984.

Sieh K.E. and R. Jahns, Holocene activity of the San Andreas fault at Wallace Creek, California, Geol. Soc. Am. Bull., 95, 883-896, 1984.

Song F., Zhu S., Wang Y., Deng Q., and Zhang W., The maximum horizontal displacement in the Haiyuan earthquake of 1920 and estimates of earthquake recurrence in northern marginal fault of the Nan-Xihua Shan , (in Chinese), Seismology and Geology, 4, 1983.

Swan, III,F.H., D.P. Schwartz, and L.S. Cluff, Recurrence of moderate to large magnitude earthquakes produces by surface faulting on the Wasatch fault zone, Utah, Bull. Seism. Soc. Am., 75, 1431-1462, 1980.

Wallace, R.E., Earthquake recurrence intervals on the San Andreas fault, Geol. Soc. Am. Bull., 81, 2875-5890, 1977.

Weldon R.J. and K.E. Sieh, Holocenc rate of slip and tentative recurrence interval for large earthquake on the San Andreas fault, Cajon Pass, southern California, Geol. Soc. Am. Bull., 96, 793-812, 1985.

Zhang W., Jiao D., Zhang P., Molnar P., Burchfiel B.C., L. Royden, Deng Q., Wang Y., and Song F., Displacement along the Haiyuan fault

associated with the great 1920 Haiyuan, China, earthquake, submitted to Bull. Seism. Soc. Am., 77, 117-131, 1987.

Zhang P., P. Molnar, B.C. Burchfiel, L. Royden, Wang Y., Deng Q., Song F., Zhang W., and Jiao D., The Holocene slip rate along the Haiyuan fault, north-central China, submitted to Quaternary Research, 1987.

Figure Captions

Figure 1. Simplified topographic map of the Haiyuan area with the locations of features and villages mentioned in the text. The contour interval is 200 m.

Figure 2. Photograph of the Caiyuan pull-apart basin . The view is to the east-southeast. The strike-slip fault on the northern side of the basin passes through the southern foot of the hill in the upper middle part of the photo, and dies out in the village in the middle left of the photo. The other fault strand is just along the foot of the mountain on the right sight side of the photo.

Figure 3. The trench log of the northwest wall of the trench in Caiyuan with a 1-meter grid.

Figure 4. Photograph of the trench site in Caiyuan. View is to the north-northwest. The scarp on the northern side of the road was associated with the 1920 Haiyuan earthquake.

Figure 5 . Photograph of the stream cobbles from the channel exposed in the northwest wall of the trench at Caiyuan. The white dashed line marks the trace of the fault F2 (see figure 3). The vertical separation of 20 cm along this fault is clear in this photo.

FIGURE 6 . Trench log on southeastern wall of the trench in Caiyuan, with 1-meter grid. The dark loess, gravel layer, and the

chaotic pebbly loess correspond to Units B, E, and F is figure 11, respectively. The faults F1 and F2 are correlated with those in figure 3.

Figure 7 . Photograph showing the 30 m stream offset 900 m east of Shaomayin, the offset associated with the 1920 earthquake, and the location of the Shaomayin trench. The view is to the east-northeast. The stream in the center of the photo and flowing north on the left side of the photo has been offset about 30 m; its upstream channel is to the right of the trench and behind the ridge in the foreground in the lower right of the photo. A fresh face of the opposite stream bank to the left of the trench marks the scarp formed during the 1920 earthquake; the offset of the surface is about 9 m. The trench, in the middle of the photo, was dug across the fault scarp. The fault scarp can also be seen receding across the flat saddle in the upper right of the photo.

Figure 8 . Trench log for the Shaomayin trench.

Figure 9 . Photo the colluvial wedge associated with the 1920 Haiyuan earthquake along the fault F5 in figure 8. The view is to the southeast. The lower part of the wedge consists of coarse grained sands and reworked loess mixed with small pebbles. The upper part of the wedge is composed mostly of pebbles and few cobbles in a matrix of sand and reworked loess.

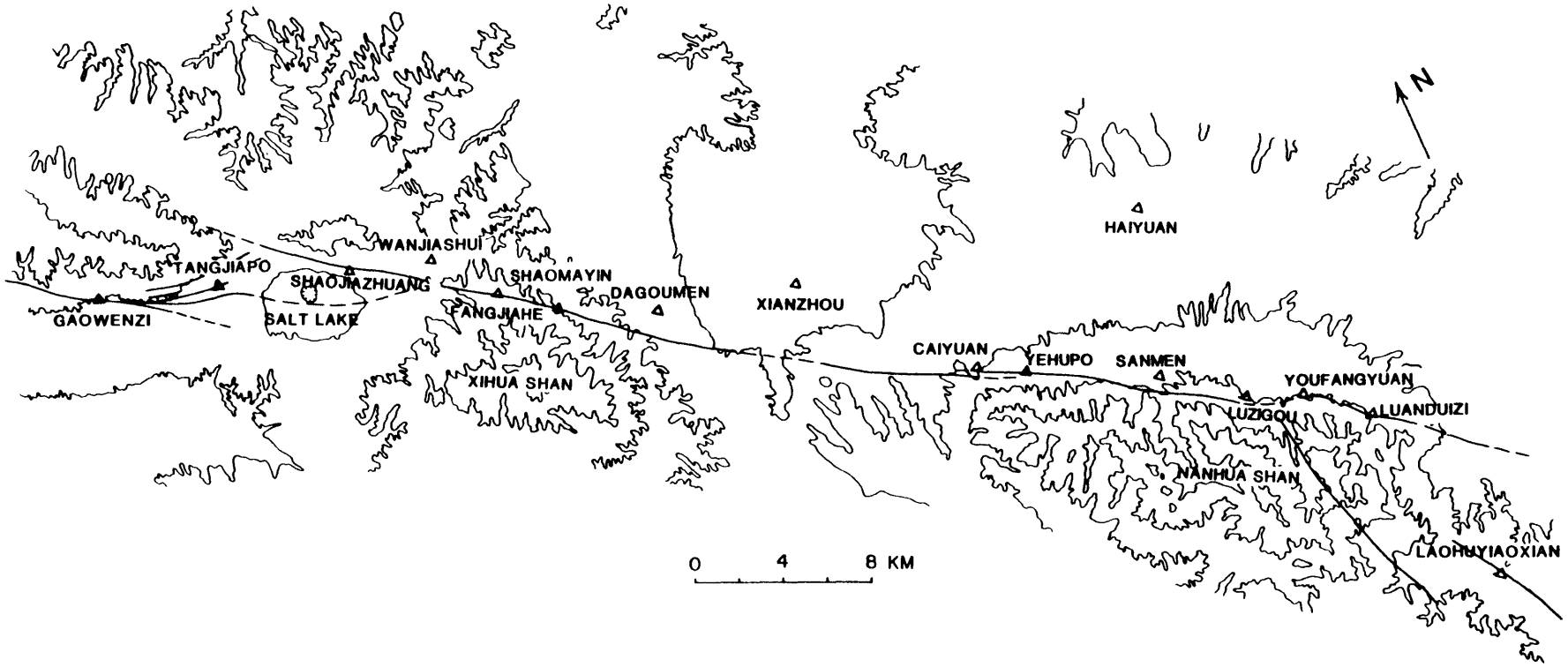
N
HAIYUAN
WANJIASHUI
TANGJIAPO
SHAOJIAZHUANG
SHAOMAYIN
DAGOUMEN
XIANZHOU
GAOWENZI
SALT LAKE
FANGJIAHE
CAIYUAN
YEHUPO
SANMEN
YOUFANGYUAN
XIHUA SHAN
LUZIGOU
LUANDUIZI
NANHUA SHAN
LAOHUYIAOXIAN
0 4 8 KM

Figure 1

Figure 2

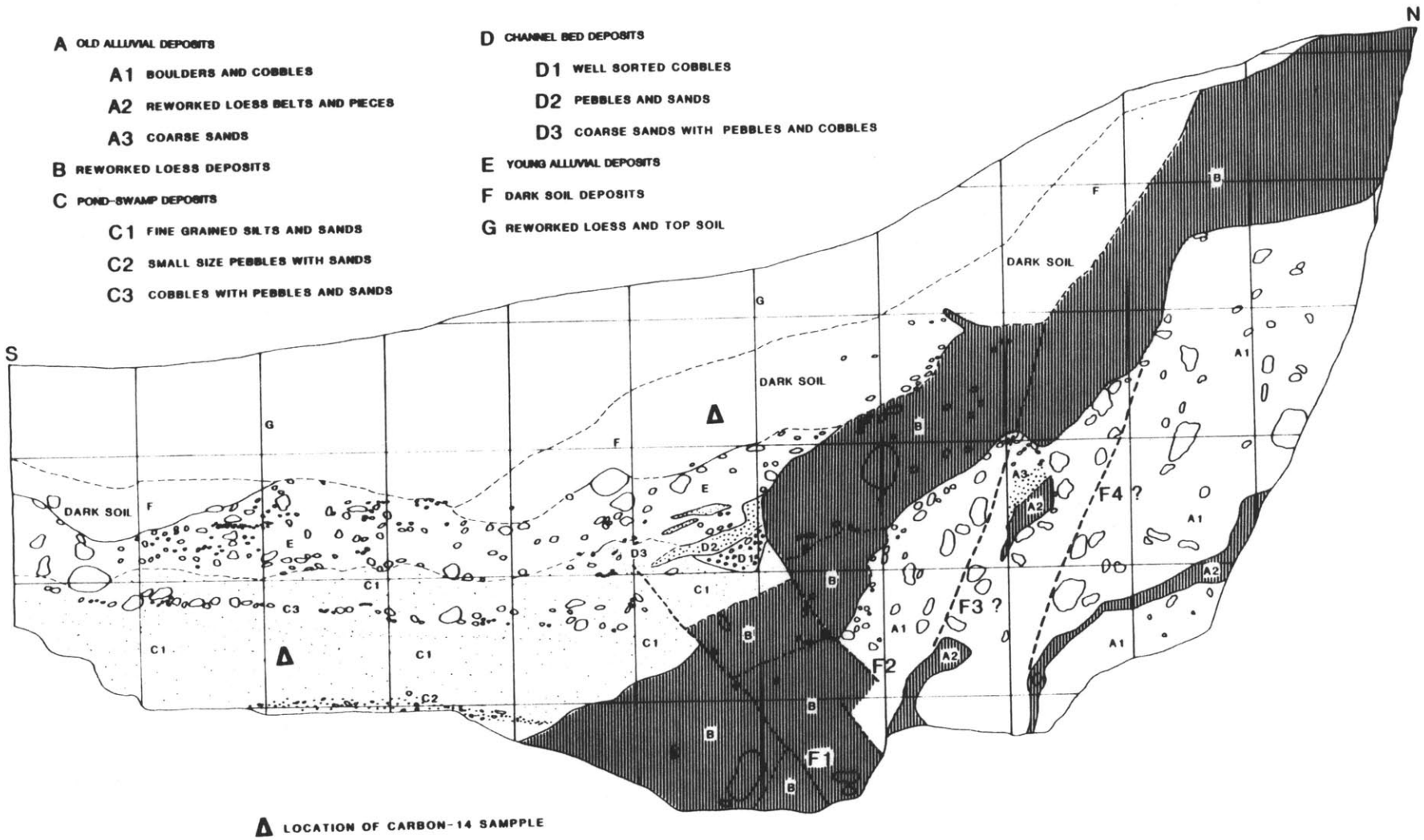
A OLD ALLUVIAL DEPOSITS
A1 BOULDERS AND COBBLES
A2 REWORKED LOESS BELTS AND PIECES
A3 COARSE SANDS
B REWORKED LOESS DEPOSITS
C POND-SWAMP DEPOSITS
C1 FINE GRAINED SILTS AND SANDS
C2 SMALL SIZE PEBBLES WITH SANDS
C3 COBBLES WITH PEBBLES AND SANDS
D CHANNEL BED DEPOSITS
D1 WELL SORTED COBBLES
D2 PEBBLES AND SANDS
D3 COARSE SANDS WITH PEBBLES AND COBBLES
E YOUNG ALLUVIAL DEPOSITS
F DARK SOIL DEPOSITS
G REWORKED LOESS AND TOP SOIL
S
N
DARK SOIL
F1
F2
F3 ?
F4 ?
Δ LOCATION OF CARBON-14 SAMPPLE

Figure 3

Figure 4

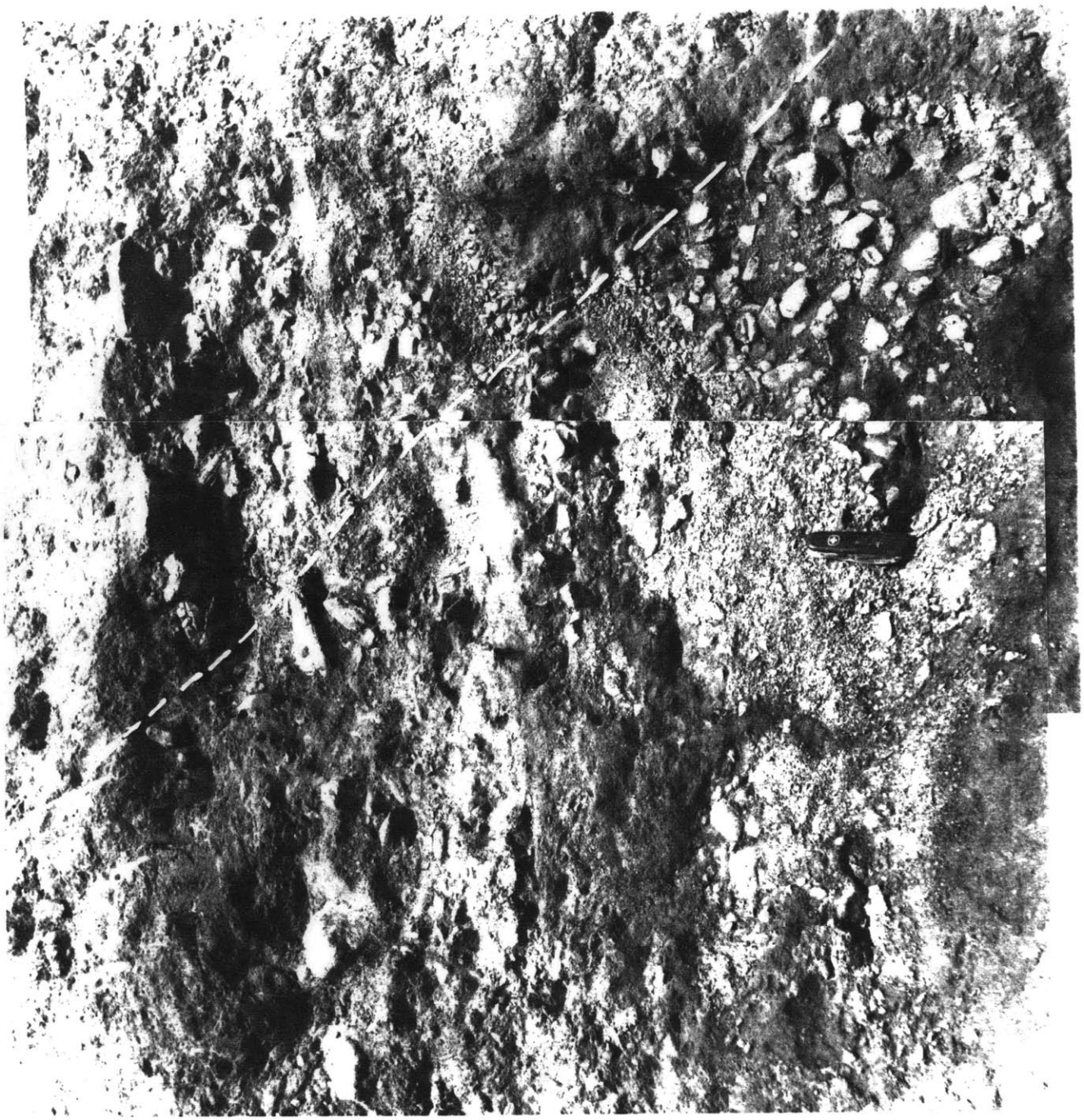

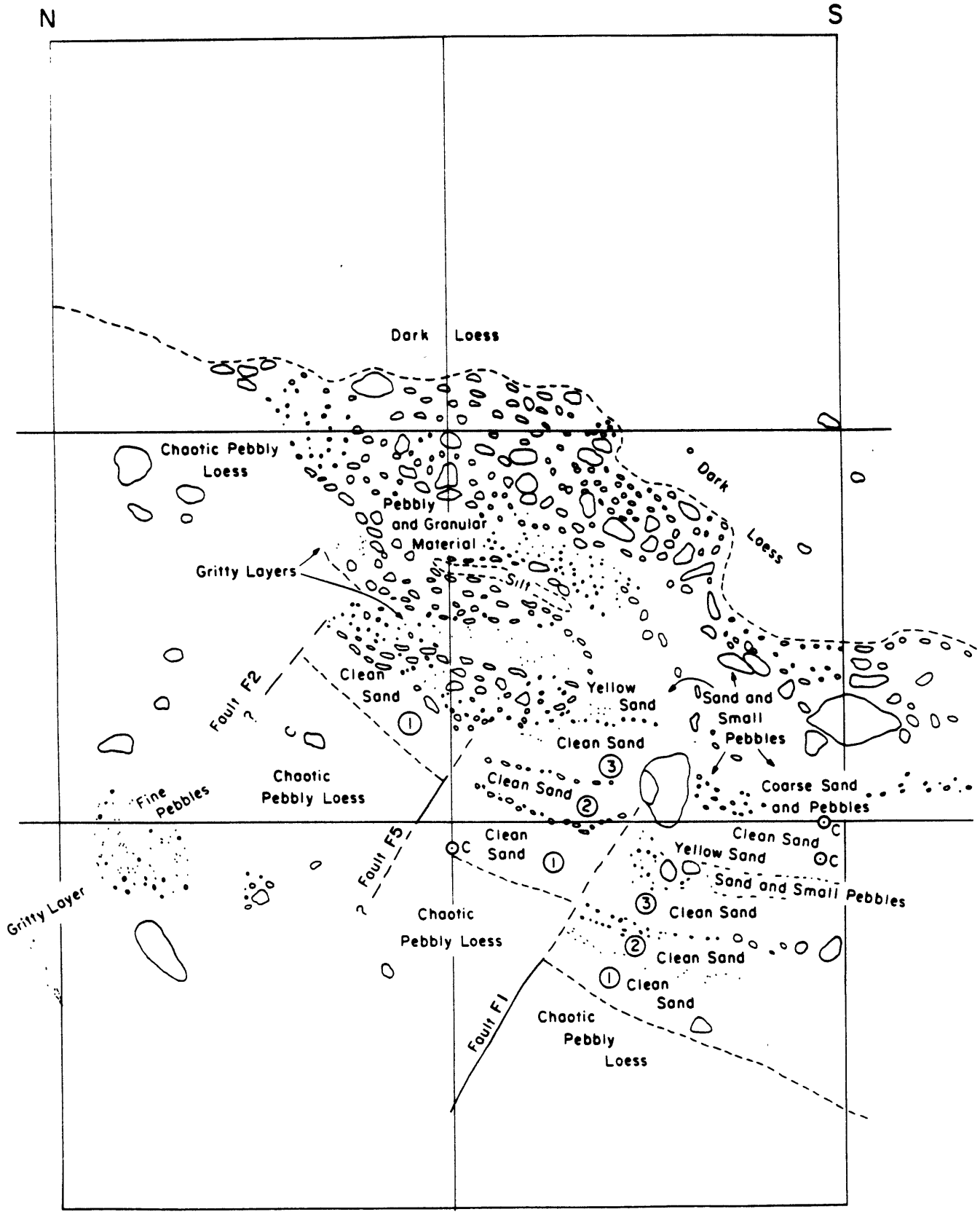
N
S
Dark Loess
Chaotic Pebbly Loess
Pebbly and Granular Material
Dark Loess
Gritty Layers
Silt
Clean Sand
Fault F2
Yellow Sand
Sand and Small Pebbles
Clean Sand
Chaotic Pebbly Loess
Fine Pebbles
Clean Sand
Coarse Sand and Pebbles
Clean Sand
Yellow Sand
Clean Sand
Sand and Small Pebbles
Fault F5
Gritty Layer
Chaotic Pebbly Loess
Clean Sand
Clean Sand
Fault F1
Chaotic Pebbly Loess

Figure 6

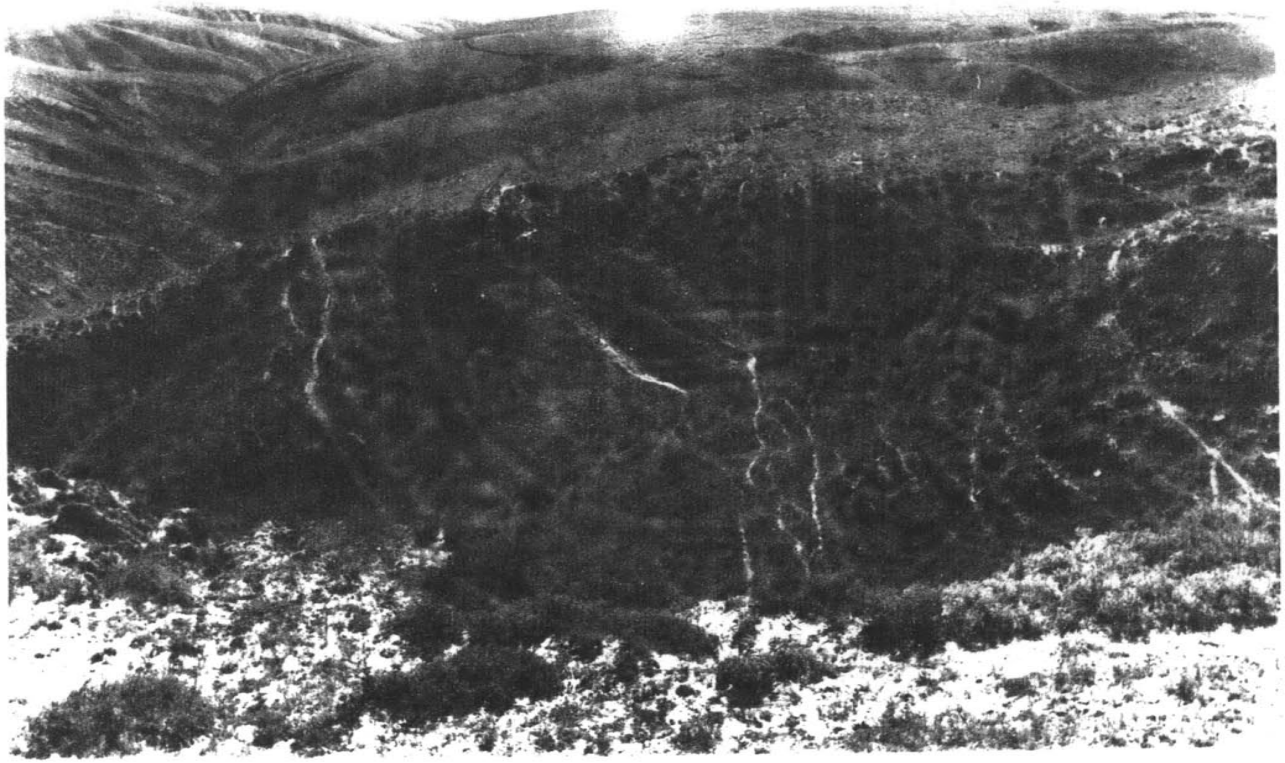

Figure 7

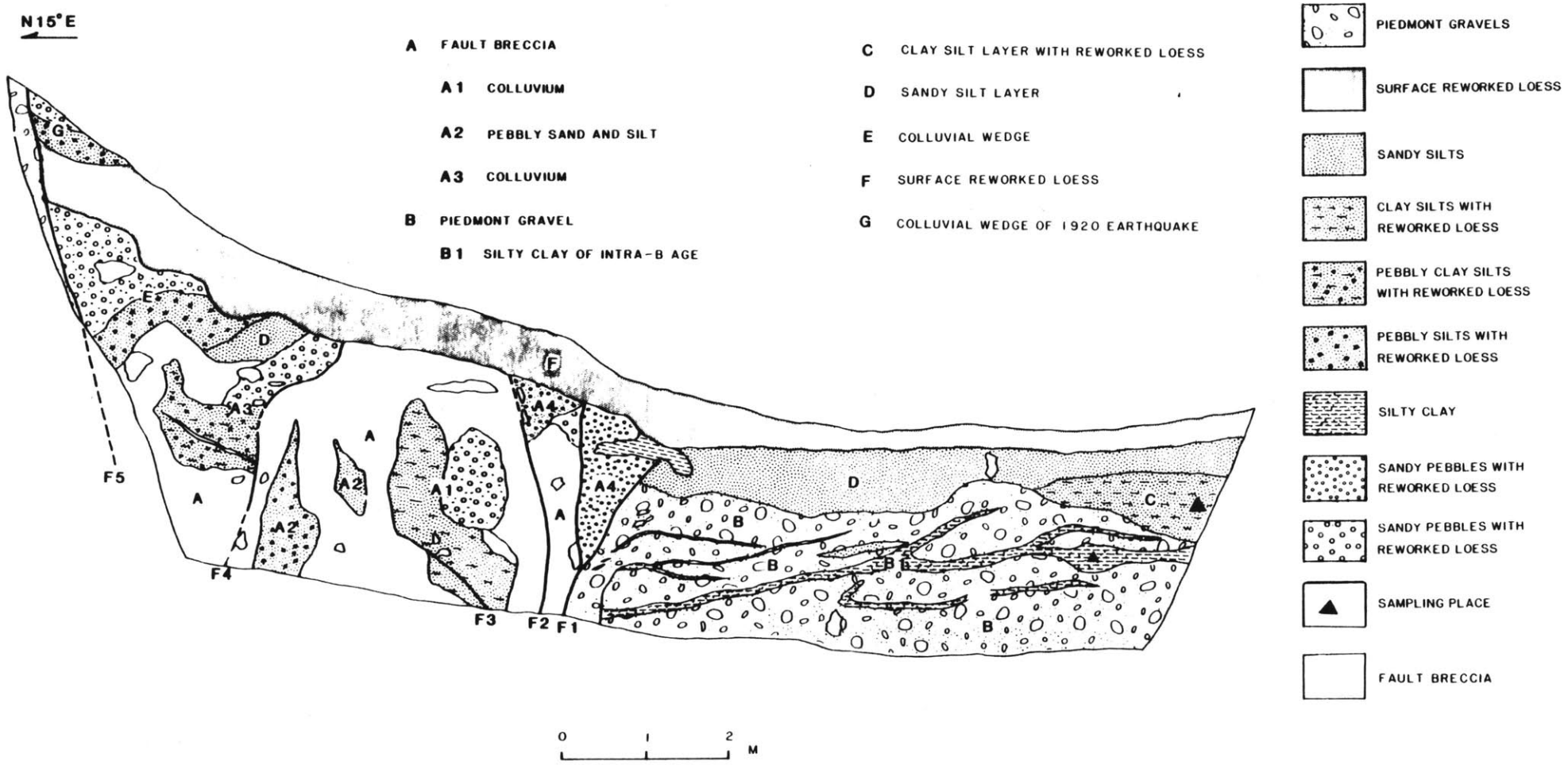
N15°E
A FAULT BRECCIA
A1 COLLUVIUM
A2 PEBBLY SAND AND SILT
A3 COLLUVIUM
B PIEDMONT GRAVEL
B1 SILTY CLAY OF INTRA-B AGE
C CLAY SILT LAYER WITH REWORKED LOESS
D SANDY SILT LAYER
E COLLUVIAL WEDGE
F SURFACE REWORKED LOESS
G COLLUVIAL WEDGE OF 1920 EARTHQUAKE
F5
F4
F3
F2
F1
0
1
2
M
PIEDMONT GRAVELS
SURFACE REWORKED LOESS
SANDY SILTS
CLAY SILTS WITH REWORKED LOESS
PEBBLY CLAY SILTS WITH REWORKED LOESS
PEBBLY SILTS WITH REWORKED LOESS
SILTY CLAY
SANDY PEBBLES WITH REWORKED LOESS
SANDY PEBBLES WITH REWORKED LOESS
SAMPLING PLACE
FAULT BRECCIA

Figure 8

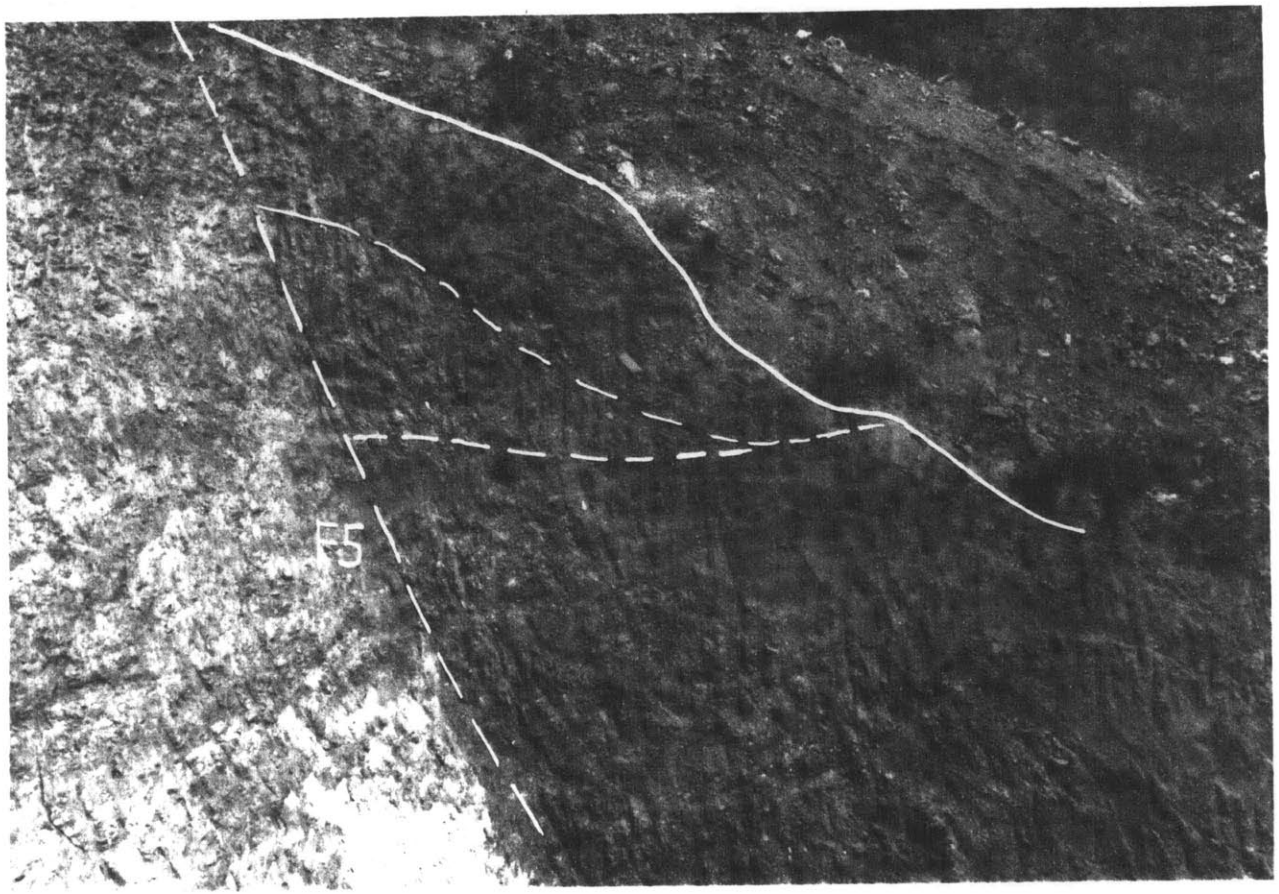

Figure 9

Chapter V

AMOUNT AND STYLE OF LATE CENOZOIC DEFORMATION IN THE LIUPAN SHAN AREA, NINGXIA AUTONOMOUS REGION, CHINA

Zhang Peizhen[1]

B. C. Burchfiel[1]

Peter Molnar[1]

Zhang Weiqi[2]

Jiao Dechen[2]

Deng Qidong[3]

Wang Yipeng[3]

Leigh Royden[1]

Song Fangmin[3]

1> Department of Earth, Atmospheric and Planetary Sciences
Massachusetts Institute of Technology
Cambridge, MA 02139

2> Seismological Bureau of Ningxia Autonomous Region
Yinchuan, China

3> Institute of Geology, State Seismological Bureau
Beijing, China

ABSTRACT

The structures of the Liupan Shan area are characterized by numerous active thrust and strike-slip faults. The structural history of this area can be divided into three phases which are parts of a single protracted deformation and are probably overlap one another in time. The oldest Cenozoic deformational phase occurred probably between late Pliocene and early Quaternary time, and produced the folds and thrust faults in the Liupan Shan and Yueliang Shan. During this phase, deformation was probably the result of approximately N50°E shortening, and the amount of shortening was about 1 km in this direction. The second phase of deformation is dominated by left-slip on the N60°W striking Haiyuan fault zone and shortening in the Liupan Shan area cause by transferring the left-slip displacement to shortening on north-south trending structures farther east. During this phase the direction of shortening in the Liupan Shan area changed to N60°W, and Madong Shan fold zone began to develop. The average amount of shortening on these north-south trending folds in the Madong Shan is about 5.7 ± 0.75 km. Most of the shortening on the Liupan Shan and Xiaoguan Shan thrust faults also occurred after slip on the Haiyuan fault began, and the amounts of shortening across them are 6.8 - 7.8 km and 5.7 - 6.9 km, respectively, in the direction of N60°W. During the third phase of deformation, about 1 - 2 km of late Pleistocene to recent left-slip occurred on the Xiaokou fault, which was transferred into oblique left-slip thrusting in the Liupan Shan. At this time deformation in the Madong Shan and Xiaoguan Shan ceased or was reduced to a very slow rate.

The present, active left-slip on the Haiyuan fault zone is accommodated by shortening in the Liupan Shan area. The total displacement along the Haiyuan fault is essentially the same as the total amount of shortening during all three phases in the Liupan Shan area. The structures in the Liupan Shan area suggest a thin-skinned deformation, and the interpretation of geology in the Liupan Shan area can be applied to the folds and thrust faults in the southern Ningxia region. Such an interpretation indicates that the northeastern margin of the Tibetan Plateau is being formed by shortening transferred from left-slip faulting farther to the west.

INTRODUCTION

One of the important questions in earth science today is the nature of intracontinental deformation and its relation to plate tectonics. In order to understand intracontinental deformational processes, we need to know the geometry, timing and magnitude of intracontinental deformation and its relation to plate boundaries. Studies of modern plate boundaries and related active intracontinental deformation is a logical approach to understand these processes. The collision of Asia by the Indian subcontinent about 40 to 55 million years ago and the continued convergence between India and Asia (for example, Molnar and Tapponnier, 1975; 1978; Tapponnier and Molnar 1976; 1977.) resulted in the development of a broad zone of intracontinental deformation that offers an excellent place to study such phenomena.

The Liupan Shan area, which includes the Liupan Shan, Xiaoguan Shan, Yueliang Shan and Madong Shan, is located along northeastern margin of the Tibetan Plateau in north-central China (Figures 1 and 2). The tectonics of the region from the Liupan Shan to the west are characterized by numerous active strike-slip and thrust faults. Slip on these faults contributes to the continuing uplift and seismic activity of the northeastern margin of the Tibetan Plateau. East of the Liupan Shan is the relative stable Ordos Plateau that tectonically belongs to the North China Block, a region that seems to share a common late Precambrian to Cenozoic geological history but that has undergone

regional extension during Cenozoic time. Thus, the Liupan Shan area forms a transition from thrust and strike-slip faulting in the west to regional extension in the east.

In earlier papers (Deng et al., 1984, 1986; Burchfiel et al., 1987; Zhang W. et al., 1987; and Zhang P. et al, 1987A, 1987B) we discussed the basic tectonics, the surface rupture and displacement associated with the 1920 Haiyuan earthquake, and the total displacement, the Holocene-slip rate, and earthquake recurrence intervals on the Haiyuan fault. In this paper, attention is focused on the geology and tectonic evolution of the Liupan Shan area, which lies east of the Haiyuan fault zone discussed in a companion paper by Burchfiel et al. (1987).

GEOLOGICAL SETTING OF THE LIUPAN SHAN AREA

The area east of the Liupan Shan forms the southwestern margin of the Ordos block. The stratigraphic sequence present in the Ordos block indicates that it is part of the larger North China Block because both blocks have had a similar depositional and tectonic evolution (Ningxia Geological Bureau, 1974; Huang, 1980). Within the southern part of the Ordos Block the oldest exposed rocks are unmetamorphosed dolomite and cherty dolomite of upper Precambrian age (assigned to the Sinian that ranged from 1950 to 800 Ma, Huang, 1980, Zhang et al., 1984). Cambrian to Middle Ordovician rocks in this area consist of shallow marine carbonate rocks with some terrigeneous interbeds. The contact between the Sinian and Cambrian rocks is not exposed in the area, but elsewhere in the North China Block it is marked by a paraconformity. Permian coal-

bearing littoral and terrestrial strata paraconformably overlie the Middle Ordovician limestone. The absence of upper Ordovician to lower Carboniferous rocks characterizes the North China Block. Lower and Middle Triassic rocks are also missing, and Upper Triassic conglomerate paraconformably overlies Permian sandstone. Jurassic coal-bearing clastic rocks overlie the Triassic rocks with a slight angular discordance. At the end of Jurassic time a major orogenic event (the Yanshanian event) occurred throughout the North China Block and almost all preexisting strata were folded and faulted. Lower Cretaceous terrestrial rocks consist of sandstone, siltstone, mudstone, and conglomerate in southwestern part of the Ordos block and unconformably overlie all older rock units. In the southwestern part of the Ordos block, middle and upper Cretaceous rocks are missing. Tertiary red beds were deposited only in graben and depressions around the boundaries of the Ordos block. Quaternary loess blankets the entire Ordos block, and other Quaternary sediments were deposited only locally.

The Liupan Shan area forms the northeastern margin of Tibetan Plateau and the eastern margin of the Paleozoic Nanshan fold belt. The complete stratigraphic sequence of the Nanshan fold belt is present about 100-150 km to the west and northwest (Li et al., 1978; Wei, 1978), but in the Liupan Shan area only part of this sequence crops out. Basement rocks for the Nanshan fold belt are poorly known although some high grade metamorphic rocks of unknown age are exposed in few places within the fold belt. The oldest sedimentary rocks deposited in the fold belt appear to be slightly metamorphosed Cambrian marine clastic rocks with some basic volcanic interbeds. The Ordovician rocks consist of

cherty limestone, granular limestone and some clastic rocks. They are slightly metamorphosed and contain a thick sequence of basic volcanic rocks to the west of the Liupan Shan area. Silurian rocks are shallow marine carbonate rocks, red sandstone, and grits. A major deformational event occurred after the deposition of Silurian rocks (Li et al., 1978; Wei, 1978). Devonian red conglomerate was deposited unconformably on all older units. West and northwest of the Liupan Shan area Carboniferous to Cretaceous rocks consist of terrigenous and terrestrial conglomerate, sandstone, siltstone, shale, mudstone, and coal-bearing strata. These rocks formed mainly in terrestrial basins and lakes, and they cannot be distinguished from those in the Ordos and North China Blocks. Farther west in the Nanshan fold belt, rocks of the same age consist of marine clastic and carbonate rocks that are completely different from those near the Liupan Shan area. During Tertiary time most of this area was the site of a large terrestrial basin that covered a large part north-central China and was filled with the Tertiary red beds. Quaternary rocks were deposited during deformation in the area and consist of locally derived deposits except for the loess that blankets the entire area.

STRATIGRAPHY OF THE LIUPAN SHAN AREA

Rock units exposed in the Liupan Shan area range from early Ordovician to Recent, but the Cretaceous and Tertiary rocks form the most extensive outcrops. The stratigraphic units used in this study have been established previously, and all the fossils mentioned in this paper were collected and dated by the Ningxia Geological Bureau (1974). Our

work has added stratigraphic detail where necessary for a more complete tectonic analysis.

LOWER ORDOVICIAN ROCKS

ORDOVICIAN LIMESTONE (Olm) The Ordovician limestone is the oldest rock unit exposed in the Liupan Shan area. It crops out only in the Xiaoguan Shan near Shanguankou (Fig. 2 and 3-see included map sheet), where it is present in the core of an anticline in the hanging wall of a west-dipping thrust fault that crops out farther east. It is truncated by a normal fault on the west, and the base of the unit is not exposed. Cretaceous rocks with a well developed basal conglomerate rest paraconformably above the limestone.

The Ordovician limestone is dark grey and weathers black. The limestone is relative pure and has been recrystallized to a coarse-grain size. It is thickly bedded, usually forming beds from 2 to 4 meters thick, and forms prominent cliffs. Rare shaly limestone interbeds are present, and they are less recrystallized than the pure limestone.

Near Shanguankou fossils collected by Ningxia Geological Bureau (1974) were identified as Helicotoma sp., Armenoceras sp., Sowerbylla sp., M. cf. magmus, and M. cf. tofargoensis. They are similar to fossils present in Lower Ordovician rocks throughout the North China Block. On this basis the thick limestone in the mapped area is assigned an early Ordovician age.

THE LIUPAN SHAN GROUP OF EARLY CRETACEOUS AGE

The lower Cretaceous rocks, here assigned to the Liupan Shan

Group, are the most widely exposed rock units in the mapped area. They form the main body of the Liupan Shan, Xiaoguan Shan, Yueliang Shan, and Madong Shan mountains (Fig. 2, 3 and 5-see included map sheet) where they have been divided into five conformable formations. The total thickness of the Liupan Shan Group is 3000 to 4000 meters.

SANQIAO FORMATION (K1s) The Sanqiao Formation forms a basal conglomerate for the Liupan Shan Group. It crops out along the Liupan Shan and the Shanguankou faults. The conglomerate is mainly grey, but its upper part is tan, brown, red and purple. Pebbles and cobbles within the conglomerate are angular, very poorly sorted, and their size varies from about 1 cm to more than 30 cm. The thickness of the Sanqiao Formation is variable: at Shanguankou, it is only about 20 m thick, but about 13 km to the west in the Liupan Shan its thickness reaches 800 m. In both the Liupan Shan and the Xiaoguan Shan (Figure 6), the clasts in the Sanqiao Formation consist of Ordovician dark grey limestone, but elsewhere granite, quartzite and some other rock types are present. The conglomerate is well cemented and often forms cliffs. The fossil Estheria sp. was reported from the conglomerate in the Liupan Shan (Ningxia Geological Bureau, 1974).

HESHANGPU FORMATION (K1h) The Heshangpu Formation gradationally overlies the Sanqiao Formation in the Liupan Shan, Xiaoguan Shan and Yueliang Shan. It is characterized by dark red sandstone, often cross bedded, with interbeds of siltstone in its lower part, and purple mudstone with light blue to gray colored siltstone, shale and marl interlayers in its upper part. The thickness of this formation is about 560 m in the Liupan Shan. The fossils cf.

Pagiophyllum sp., Otozamitas sp. have been reported in this formation near Shanguankou in the Xiaoguan Shan (Ningxia Geological Bureau, 1974).

LISANWA FORMATION (Kll) The Lisanwa Formation conformably overlies the Heshangpu Formation and is exposed in the Liupan Shan, Xiaoguan Shan and Yueliang Shan (Fig. 2 and 4). It is characterized by about 700 m of light blue and grey mudstone, silty mudstone, marl and shale interbedded with dark red and purple mudstone and shale. Fossils, such as Pagiophyllum sp., Otozamites Klipsteinii, cf. Sphenolepidium, Brachyphyllum cf. obesum, and Androstrobus nathorsti are abundant and date the Lisanwa Formation as early Cretaceous (Ningxia Geological Bureau, 1974).

MADONG SHAN FORMATION (Klm) The Madong Shan Formation is the most widely exposed Cretaceous unit in the Liupan Shan, Madong Shan, Xiaoguan Shan and Yueliang Shan (Fig. 3 and 5). Its total thickness is about 400 m and it has been subdivided into four informal subunits. They are described from the oldest to the youngest.

The white to light grey muddy limestone and marl subunit (Klmw) forms the base of the Madong Shan Formation. It contains the finest grained rocks in the Liupan Shan Group. Some oolitic limestone layers are interbedded with the limestone and marl.

The brown to grey mudstone and marl subunit (Klmb) forms steep cliffs. Muddy limestone lenses are locally present within this subunit.

The grey shale subunit (Klms) mainly consists of easily eroded grey shale, and in the Madong Shan, a valley follows the subunit that clearly outlines one of the major anticlines.

The yellow to grey mudstone subunit (Klmy), the uppermost

subunit, is well exposed in the Madong Shan and Xiaoguan Shan. It is easily distinguished from other units by its color, and often forms cliffs.

Some of the fossils reported from this formation, such as Lycoptera sp., Sphaerium sp., Frenelopsis sp., Cypridea vitimemsis, C. cf. porrecta, C. magna, Ziziphocypris cf., rugosa, Darwinula contracta, C. cf.tera, C. cf. lunata, Mongolianella cf. palmasa, date the Madong Shan Formation as early Cretaceous in age (Ningxia Geological Bureau, 1974).

NAIJIAHE FORMATION (Kln) The Naijiahe Formation is the uppermost formation in the Liupan Shan Group. The total thickness of this formation is about 630 m. It crops out mainly in the Madong Shan, Xiaoguan Shan and Yueliang Shan. The lower part of the formation consists of light blue mudstone and rare marl. The upper part of the formation becomes coarser grained upward, and it is characterized by dark red and purple mudstone and siltstone interbedded with light blue to grey mudstone and sandstone. The upper part of this formation is present only in the northwestern part of the Yueliang Shan.

Lycoptern sp., Bairdestheria guyuangensis, Kutsangkouensis, Eosestheria middendorfii, Yanjiestheria cf. proamurensis, are reported from the Naijiahe Formation and are regarded as early Cretaceous in age (Ningxia Geological Bureau, 1974).

The top of the Naijiahe formation is an unconformity. In the Liupan Shan the Naijiahe Formation is missing, and the Tertiary red beds directly overlie the Madong Shan Formation.

TERTIARY RED BEDS

Tertiary rocks crop out in the Xiaoguan Shan, Madong Shan and in the western part of the Liupan Shan. They consist of several kilometers of non-marine red and tan mudstone, siltstone, sandstone, and conglomerate, that range from probably early Oligocene to Pliocene in age and for the most part are similar to rocks in the Haiyuan area (Burchfiel et al., 1987). They have been divided into four informal formations.

SANDSTONE OF SIKOUZI (Ors) The Sandstone of Sikouzi crops out in the Liupan Shan, Xiaoguan Shan and Madong Shan. Its thickness is about 270 m. It consists of conglomerate, sandstone, and rare siltstone. Most of the beds are dark to medium red, but some are pale red, orange, and tan. Conglomerate is common in the middle and lower part of the formation. It generally consists of rounded pebbles and cobbles, clasts of resistant rock types such as quartzite, chert, vein-quartz, and more rarely Devonian red sandstone and conglomerate and medium-grained granite. Quartz-rich sand forms the matrix of the conglomerate and also forms sandstone and siltstone interbeds.

The Sandstone of Sikouzi rests unconformably on rocks of the Cretaceous Liupan Shan Group. In some places a basal conglomerate with angular fragments from the underlying rocks is present. The basal conglomerate, where present, is less than one meter thick. Some rounded pebbles of quartzite, red sandstone and other resistant rock types are also present within the basal conglomerate (Figure 7). The basal conglomerate is directly overlain by sandstone, but where the conglomerate is absent the sandstone directly overlies the underlying

rocks, and a yellow weathered surface is often present. The Sandstone of Sikouzi is considered to be either latest Eocene or early Oligocene in age, but no fossils have been found in this formation. The rocks are probably correlative with the Sandstone of Guanmen Shan in the Haiyuan area (Burchfiel et al., 1987).

RED BEDS OF SIKOUZI (Orb) On the western side of the Liupan Shan and Xiaoguan Shan, and on the eastern side of the Madong Shan, a sequence, about 700 m, of red sandstone, siltstone, and mudstone with evaporite beds, here called the Red Beds of Sikouzi, rests conformably on the Sandstone of Sikouzi. The formation consists of maroon and dark red sandstone and mudstone with beds of red quartz-rich sandstone. The sandstone and mudstone may be well bedded or massive, and both contain thin beds of green or white siltstone. Beds of gypsum 20 cm to 1 m thick are present within the lower and middle parts of the formation and become less common in its upper part. The following fossils are reported from this formation near Sikouzi: Cyprinotus formalis, Cyprinotus beljaewskyi, Eucypris longa, Baluchitherium sp., Tsaganomys altaicus, Bithynia sp., Unio sp., and Darwinula sp. (Ningxia Geological Bureau, 1974). This assemblages dates the rocks as Oligocene. These rocks are correlative with the Red Beds of Shaojiazhuang of the Haiyuan area (Burchfiel et al., 1987).

RED BEDS OF YANGJUANPU (Mrb) The Red Beds of Yangjuanpu conformably overlie the Oligocene red beds, and they consist of a thick sequence, about 963 m thick, of red to tan mudstone and siltstone with sandstone present in the upper part. The contact between the Oligocene red beds and the Red Beds of Yangjuanpu is gradational through several

tens of meters and is marked by a change in color, bedding, and grain size. The Red Beds of Yangjuanpu are red to pale red or tan. In contrast with the maroon or dark red of the underlying Oligocene rocks, bedding is generally more massive, and sometimes is impossible to identify. In the upper part of the formation, the grain size becomes coarser, and conglomerate beds are present in the upper few hundred meters of the formation. Clasts in these conglomerates are dominated by resistant rock types such as white vein quartz, quartzite, and Paleozoic red sandstone, with rare clasts of granite and schist.

The following fossils have been reported in this formation near the Sikouzi: Mastodon sp., Testudo sp., Cyprinotus sp., Limnocythere sp. (Ningxia Geological Bureau, 1974). These fossils date the formation as Miocene in age. They are correlative with the Red Beds of Wanjiashui in the Haiyuan area (Burchfiel et al., 1987).

CONGLOMERATE OF YANGJUANPU (Pcg) Resting conformably above the sandstone and conglomerate of the Red Beds of Yangjuanpu is conglomerate and sandstone mapped here as the Conglomerate of Yangjuanpu. The conglomerate is about 630 m thick and consists of pebbles, cobbles and boulders composed dominantly of white vein-quartz, fine-grained grey or white quartzite and chert, red sandstone and conglomerate, marble, schist, gneiss, and rare granite. Much of the matrix of the conglomerate is quartz, feldspar, and lithic grit, and the interbedded sandstone is generally coarser grained than the sandstone in the underlying Tertiary rocks.

Fossils reported from the eastern part of the Madong Shan are Ilyocypris cf. bradyi, Candona sp., Limnocythere luculenta, Cadoniella

sp., Cyprinotus sp., Chara sp., and Cathaica sp. (Ningxia Geological Bureau, 1974). These fossils are considered to be Pliocene in age. The Conglomerate of Yangjuanpu probably correlates with the Conglomerate of Dagoumen in the Haiyuan area (Burchfiel et al., 1987) but the clast composition of the two units is quite different.

QUATERNARY SEDIMENTARY ROCKS

Quaternary rocks of the Liupan Shan area have been mapped and assigned to local informal rock units because most of them were deposited during deformation and reflect deposition in local environments and derivation from local sources. The lack of age control on these units makes it impossible to correlate accurately these separated and locally restricted units. The relative ages of these units are estimated according to their relation to the loess, which is the most widespread Quaternary unit in the mapped area as well as in northeastern margin of Tibetan Plateau.

CONGLOMERATE OF YANGZHONGPU (Qcg) At the southeastern foot of Madong Shan, several tens of meters of conglomerate with poorly sorted pebbles and angular rock fragments was deposited conformably on the Pliocene Conglomerate of Yangjuanpu. To the southeast the conglomerate is covered by the loess. The maximum thickness of this conglomerate is unknown. The generally dark grey conglomerate contains clasts that range from 1 cm to 20 cm in diameter. All the pebbles within the conglomerate consist of grey to brown siltstone, mudstone, sandstone, marl, and limestone. They are mostly angular and are set in a sandy matrix cemented by calcium carbonate. The clasts were derived from

the local Cretaceous rocks, and because of their angular shape they probably have not been transported far. The Conglomerate of Yangzhongpu is easy to distinguish from the underlying Pliocene conglomerate, because the Pliocene conglomerate contains no fragments of the distinctive Cretaceous rocks. The age of the conglomerate of Yangzhongpu is unknown. It is younger than the underlying Pliocene conglomerate and older than the overlying loess. Thus its age can be constrained to be either the latest Pliocene or early Quaternary.

LOESS (Ql) The most widespread Quaternary unit is the loess. It consists of fine silt-to dust-sized material that blanks all older rocks except on the sides and tops of some of the high mountains. The tan loess is massive, soft, easily eroded, and subject to down-slope movement, and thus it usually forms poor outcrops. Its best exposures are along the blanks of incised streams where the loess forms nearly vertical cliffs. The thickness of the loess is highly variable but generally ranges from 10 to 30 m. It is uncertain if the loess in the map area is only late Pleistocene or older (see discussion in Burchfiel et al., 1987).

CONGLOMERATE OF THE LIUPAN SHAN (Qcl) East of the Liupan Shan is about 20 to 30 m of conglomerate that was deposited unconformably on pre-Quaternary rocks. It consists of conglomerate with interbedded sandstone and siltstone. Clasts within the conglomerate commonly range from 1 to 5 cm in diameter, but a few large clasts reach about 20 to 30 cm in diameter. The clasts are dominated by dark grey or greyish brown Cretaceous rocks that are angular and not well sorted. Conglomerate beds range from a few decimeters to about one meter thick and are interbedded

with beds of siltstone and sandstone of similar thickness. The upper part of the conglomerate is interbedded with loess or reworked loess, and the thickness of the loess beds is usually thicker than the conglomerate beds. The age of this conglomerate is unknown. No fossils have been found or reported from this formation. The conglomerate of Liupan Shan could be older than the Pliocene tan conglomerate in its lower part, and it is as young as the loess in its upper part.

REWORKED LOESS AND ALLUVIUM (Qrla) Directly overlying the Conglomerate of the Liupan Shan are thick layers of reworked loess. The loess in upper part of this unit is clearly reworked, because some gritty sand lenses and small pebbles are mixed with the loess.

POST-LOESS TERRACE DEPOSIT (Qt) Numerous terrace deposits have been mapped in the Madong Shan area. These deposits consists of pebbles interbedded with reworked loess or other fine-grained sediment. The clasts within the terrace deposits are from locally exposed rock units, and they are angular and poorly sorted.

HOLOCENE TO RECENT DEPOSITS (Qal) Holocene to Recent deposits occur mainly in present stream valleys and basins. These deposits consist of conglomerate set in a sandy matrix of the same composition. They often form the channel beds, benches, and low terraces.

STRUCTURE OF THE LIUPAN SHAN AREA

Because the pre-Cretaceous rocks are poorly exposed in the Liupan Shan area, and the major structures were formed during late Cenozoic deformation, the focus of this paper is on the Cenozoic deformational and tectonic history of the area. The geological structure in the Liupan

Shan area is dominated by thrust or reverse faults and related folds.

THE LIUPAN SHAN THRUST FAULT

The north-trending Liupan Shan thrust fault is exposed along the eastern foot of the Liupan Shan mountains, and is characterized by the eastward displacement of the Cretaceous Liupan Shan Group over the Tertiary red beds (Fig. 2, 3, and 8). The Cretaceous rocks in the hanging wall form the Liupan Shan mountains, and the footwall consists of Tertiary red beds and Quaternary sediments forming an eastward sloping lowland.

The Liupan Shan thrust fault apparently dies out at its northern end near Xiaokou, and part of the displacement along the thrust fault has been taken up by a more northwest-trending fault, the Xiaokou fault. A pull-apart structure near Xiaokou (Fig. 5) appears to mark the transition between these two faults.

The northern part of the Liupan Shan thrust fault strikes about N20W and in generally consists of two strands. The southwestern strand is located along the foot of high mountains, and the northeastern strand is usually about 200 to 300 m to the east in the low hills. The Cretaceous rocks exposed between the two strands are strongly deformed and brecciated. Numerous small faults and folds of varied orientation are present. Although the fault surface is not well exposed, it can still be inferred to dip to the southwest from its topographic trace. At Haizikou, the Liupan Shan thrust fault is exposed where it crosses a stream. Here the Cretaceous Lisanwa Formation and fault breccia are thrust on young Quaternary sediments in the bench of a stream (Fig. 9)

along a fault dipping 44° southwest.

The Main segment of the Liupan Shan thrust fault is characterized by a single fault. Different formations of the Liupan Shan Group are thrust over the Tertiary red beds and Quaternary sediments on the east. In a few places a fault surface dipping 50°-60° west is exposed, but based on its topographic trace the thrust fault should dip at a smaller angle.

The hanging wall of the Liupan Shan thrust fault consists mainly of west-dipping Cretaceous rocks of the Liupan Shan Group, with progressively older parts of the group present toward to the southeast (Figures 3 and 4). The oldest rocks exposed in the Liupan Shan, the Cretaceous basal Conglomerate of the Sanqiao Formation (K1s), is discontinuous and appears only in two places (Fig. 3). Because the conglomerate is massive, structures within it are difficult to detect. In some places it dips about 30° to west or southwest. The overlying Heshangpu Formation generally dips 15°-30° to the west, but two anticlines are present near the thrust fault in the southern part of the mapped area (Fig. 3 and 4). The exposed Lisanwa (K1l) and Madong Shan formations (K1m) dip 45°-55° to the west and are not folded. The upper part of Madong Shan Formation and the entire Naijiahe Formation (K1n) are missing in the Liupan Shan, and the Tertiary red beds overlie the lower part of the Madong Shan Formation along an irregular erosion surface. The Tertiary red sandstone (Ors) also dips to the west, at about the same angle as the Cretaceous rocks, but its dip becomes more gentle toward the west. The red siltstone and mudstone west of the sandstone dip only about 15°, and farther west it gradually becomes

almost horizontal. These relations in the hanging wall suggest the Liupan Shan thrust fault ramps generally upward to the east beneath the Liupan Shan (see below).

The major trends of rocks in the hanging wall block of the Liupan Shan thrust fault are from N20W to north-south, but near the fault, the strikes of these rocks are often deflected to N30W-N50W, and some small folds are usually present. In the north-northwest-trending part of the Liupan Shan, these folds are more common than in the north-south trending part of the Liupan Shan, where the rocks near the fault are mainly massive conglomerate. All of these folds are small, generally several hundreds meters in length, and plunge to the northwest (Fig. 3). In one place near Haijiazhuang, a syncline near the Liupan Shan fault is overturned to the northeast (Fig. 10). The normal limb (northeast) dips about 16° to the southwest, and the overturned limb (southwest) dips about 34° also to the southwest. In two places along the Liupan Shan thrust fault, near Haizikou and Yanglin, a few small folds trend northeast. In both places the Cretaceous rocks on the hanging wall strike northeast, and the folds parallel the trend of the strata.

We interpret these small scale folds to be drag features associated with early movement along the Liupan Shan thrust fault. They suggest that the early thrust displacement may have had a right-lateral component.

The foot wall of the Liupan Shan thrust fault consists of Tertiary red beds, some Quaternary sedimentary rocks, and, in the east, Cretaceous rocks that form the Xiaoguan Shan. The Tertiary red beds just below the Liupan Shan thrust fault have been folded into a foot wall

syncline whose axial trace is approximately parallel to the thrust fault (Fig. 3 and 4). The asymmetric syncline has a steep western limb that suggests a relative northeast movement on the Liupan Shan thrust fault.

Present displacement of the Liupan Shan thrust fault determined by seismological data is unclear because of the lack of well constrained fault plane solutions, but our work provides some information on the fault displacement in Holocene time. In many places along the fault a series of ridges and streams appear to be deflected left-laterally where they cross the fault (Fig. 11 and 12), but for most of them the offset cannot be measured accurately. Some of the deflections may be fortuitous due to the meandering of the streams and the irregularity of the ridges, but the presence of many consistent deflections suggests a component of left-slip along the Liupan Shan thrust fault during Late Pleistocene or Holocene time.

At Haizikou clear evidence is present for left-slip along the Liupan Shan thrust fault. The fault trends about N20W and is clearly marked by a zone of gouge about 2-4 meters wide. The gouge zone and Cretaceous rocks are thrust above Quaternary terrace deposits along a fault dipping 40° southwest (Fig. 9). Along a stream flowing from the mountains to the northeast, the upstream part of the channel is incised into the Cretaceous rocks, and its downstream part is incised into young Quaternary terrace deposits. The stream has been offset left-laterally 14 ± 3 m where it crosses the fault (Fig. 13), and the offset part of stream flows along the fault zone. There is a bench about 1 meter above the channel bed. This bench is offset about 5 to 6 meters along the fault within the 14 ± 3 meters of total stream offset (Fig. 13). The

offset seems to be very young, but unfortunately, we can not determine its age.

In summary, the geological evidence indicates the Liupan Shan thrust fault has a complex kinematic history. Generally, the hanging wall of the thrust fault moved to the east-northeast. In the early stage of thrusting a right-slip component may have been present, but in the later stage of thrusting the Liupan Shan fault had a component of left-slip.

THE XIAOGUAN SHAN FAULT

The Xiaoguan Shan fault is parallel to and lies about 14 km east of the Liupan Shan thrust fault (Fig. 2, 3, and 4). The fault dips 40°-50° to the west the Cretaceous and Ordovician rocks have moved relatively eastward over Tertiary red beds. Its hanging wall consists mainly of Cretaceous rocks from the Sanqiao Formation to the Naijiahe Formation, and Ordovician limestone is exposed near the Xiaoguan Shan fault in the core of an anticline. The anticline lies near the fault and its eastern limb is steeper than its western limb. A west-dipping high-angle normal fault cuts its western limb. The relation between the high-angle normal fault and the Xiaoguan Shan fault is unknown. West of the anticline both Cretaceous and Tertiary rocks dip generally to the west. The foot wall of the Xiaoguan Shan fault consists of Tertiary red beds, and farther to the east Cretaceous rocks are exposed.

No detailed work was done along this fault, and its evolution is unclear. Topographically the hanging wall and foot wall crop out at about the same elevation. No ridge or stream offsets were observed and

none have been reported. We interpret these data to suggest that the fault is inactive or its slip rate is very small. Most of the recent tectonic activity in this area has taken place along the Liupan Shan and Xiaokou faults.

THE XIAOKOU FAULT

The Xiaokou fault strikes about N40W (Figure 2 and 5) and can be traced from Xiaokou for about 60 km to the northwest, where it steps left through the Laohuyiaoxian basin, then crosses the Nanhua Shan, and intersects the Haiyuan fault southwest of Youfangyuan, just where the N60W-trending left-slip Haiyuan fault zone changes its character (Fig. 2) (see Burchfiel et al., 1987). East of the Xiaokou fault is the Madong Shan fold zone that trends about N20°-30°W. The Xiaokou fault apparently dies out at Xiaokou or transfers displacement to the Liupan Shan fault (see above).

The Xiaokou fault is clearly marked by the juxtaposition of the Cretaceous Naijiahe Formation to the west with Tertiary red beds to the east (Fig. 5). The light blue mudstone and marl of the Naijiahe Formation form the Yueliang Shan mountains on the southwest side of the Xiaokou fault, and the Tertiary red beds to the northeast often form basins and small hills separated by wide valleys. The difference in elevation across the fault is usually about 100 to 200 m. Only in one place, at Caixangpu, is the fault exposed. The width of the fault zone is about 60 m. The Cretaceous Naijiahe Formation has been intensively brecciated, and gypsum and other evaporites are common near the fault. The Tertiary massive mudstone is also brecciated and has been injected

into the fault zone. The dip of the Xiaokou fault is about 40° - 50° southwest, but its dip is poorly determined.

The hanging wall of the Xiaokou fault consists of Cretaceous rocks, but its structure has not been well studied. According to previous work (Ningxia Geological Bureau, 1959), the Cretaceous rocks extend about 30 km to the west from the Xiaokou fault. Devonian red conglomerate and granodiorite of unknown age are reported farther southwest of the Cretaceous outcrops. All the formations present in the Liupan Shan Group are exposed in Yueliang Shan.

The footwall block of the Xiaokou fault mainly consists of Tertiary red beds, which have been intensively folded near the southeast end of the fault (Fig. 5). The axes of these folds are approximately parallel to the fault. Along the middle segment of the fault, the Tertiary rocks are massive mudstone, and they are not folded but are gently warped. Farther to the north, the outcrops are very poor due to cover by loess and other Quaternary sediments, but gentle folds are present beneath the loess.

Near the southeastern end of the Xiaokou fault, at Xangshuigou, the Cretaceous rocks in the hanging wall adjacent to the fault have been intensely folded. These folds disappear away from the fault. The folds trend about N30-35W, parallel to the trend of the Xiaokou fault. About 15 km northwest of Xangshuigou, at Shangdazai, folds in the hanging wall adjacent to the Xiaokou fault also are parallel to the fault (Fig. 14). About 4 km northwest of Xangshuigou, folds are developed within the Tertiary red beds in the footwall and are parallel to the Xiaokou fault. The parallelism of the folds and the faults suggests that the Xiaokou

fault probably was a thrust fault or had an important component of thrusting across it in its early stage of displacement.

Late Pleistocene and Holocene features show evidence of left-slip along the Xiaokou fault. At Xangshuigou, a stream channel has been offset about 27 ± 5 m left-laterally along the Xiaokou fault (Fig. 15). Both the upstream and downstream parts of the channel are straight, and terraces are well developed on both sides of the channel. The fault is clearly marked by the juxtaposition of Cretaceous and Tertiary rocks. At the fault, the Cretaceous rocks are vertical and form a small waterfall, but the fault surface is covered by alluvium.

About 12 km northwest of Xiaokou, a series of streams have been offset left-laterally (Fig. 16). The fault surface is not exposed because alluvium covers all older rocks. The stream offsets in Fig. 17 were measured to be 380 ± 30 m. Although we have not been able to date any of these stream offsets, they indicate that the Xiaokou fault has had a significant component of left-slip during its later history.

MADONG SHAN FOLD AND FAULT ZONE

The Madong Shan is a roughly northerly trending range located northeast of the Xiaokou fault (Fig. 2, and 5). The structures in the northern part of the Madong Shan trend approximately N20°W, whereas in the wide southern part they trend about N20°E. East of the Madong Shan is the north-south-trending Qinshuihe basin (Fig. 2), which is filled with Quaternary sediments and is underlain by Tertiary conglomerate. The thickness of Quaternary sediments in the basin is generally between 100 to 200 m. The eastern boundary of the Qinshuihe basin is covered by

loess. Cretaceous rocks and Tertiary red beds are exposed east of the basin, and dip west it (Ningxia Geological Bureau, 1974). Thus the Qinshuihe basin is a buried open syncline. To the south, the Madong Shan ends near the transition between the Xiaokou fault and the Liupan Shan thrust fault. To the north, the area is covered by thick loess, but on the satellite images a linear feature extends eastward from the Haiyuan fault zone across the loess-covered area and merges with the northern end of the Madong Shan (Fig. 18).

The higher parts of the Madong Shan are formed by rocks from the lower Cretaceous Madong Shan and Naijiahe formations. The lower flanks of the mountains are composed mainly of Tertiary red beds of Oligocene to Pliocene age. All these rocks are intensely deformed into three major anticlines. From south to north they are the overturned Taozigou anticline, the box-shaped Chenzhuang box anticline, and the faulted Sikouzi anticline (Figures 5 and 19). Some small folds are developed between and adjacent to these major folds. Along the eastern side of the Madong Shan there is a scarp, but it is not clear if it is a fault scarp or an erosional feature.

THE TAOZIGOU ANTICLINE The Taozigou anticline consists of the Cretaceous Madong Shan and Naijiahe formations and Tertiary red beds (Figure 5 and section AA′, BB′ in Figure 19). The oldest rocks exposed are pink siltstone and mudstone of the Cretaceous Lisanwa Formation (Kll), that crops out at only two places in deeply incised canyons. The subunits of Madong Shan and Naijiahe formations form most of the core of the fold.

The anticline is doubly plunging and overturned to the southeast. The northwestern limb of Taozigou anticline normally dips 30°-50° to northwest. The northern part of its western limb is much wider than the southern part, and the Naijiahe Formation crops out in a wide region where it is folded on a smaller scale between the Taozigou anticline and the Chenzhuang anticline to the northwest (Fig. 5). The southeastern limb of the anticline is more complex. The Cretaceous and lower Tertiary rocks are overturned and dip 70°-80° to the northwest. The Tertiary rocks farther east are upright and dip 50°-70° to the southeast. Quaternary conglomerate (Qcg) on the eastern limb of the fold contains debris of the Cretaceous rocks and records the beginning of the deformation in the Madong Shan. The northeastern limb of fold is also overturned, and dips 70° - 80° to the southwest.

The Taozigou anticline can be divided into two segments: southern segment that trends about N20°E, and the northern segment that trends about N20°W. At its north end the fold plunges gently to the northwest, but at its south end it plunges steeply and contains several parallel folds. At its very southern end the trend of the fold is again deflected to become southeasterly.

THE CHENZHUANG ANTICLINE The Chenzhuang anticline, the middle of the three folds (Figure 5), is formed by the Cretaceous Madong Shan and Naijiahe formations, and Tertiary red beds. The anticline trends about N15°E, but like the Taozigou anticline, its northern segment trends more northwesterly than the southern segment. The Chenzhuang anticline is a doubly plunging box-type fold. The broad crest

of the anticline is about 2 km wide and has been gently warped into three small anticlines. The anticline is asymmetric: its eastern limb dips 50°-70°southeast, and its western limb dips 40°-60° northwest (section CC′ and DD′ in Fig. 19).

Toward the west, the Tertiary red beds of the western limb are covered by loess and Quaternary sediments, but a few outcrops indicate a progressively more gentle dip to the northwest, decreasing from 30°-40° in Oligocene red sandstone and red beds to 10°-20° in Miocene massive mudstone.

At its south end the Chenzhuang anticline plunges south and breaks up into a series of small folds (Fig. 5). To the northeast the extension of the anticline is deflected to the northwest, its amplitude is reduced, and some shortening has been transferred into the adjacent Sikouzi anticline. Farther to the north, the Chenzhuang anticline and the syncline west of it are probably connected with the anticline and syncline east of the Sikouzi anticline. Unfortunately, we did not complete the mapping between them, but the folds clearly project into one another.

THE SIKOUZI ANTICLINE The Sikouzi anticline (Fig. 5 and section GG′, HH′ in Fig. 19) trends about N15°-20°W and differs considerably from the main structural orientation of the Madong Shan, but its trend is similar to the northwest segments of the other two folds. To the north it plunges beneath loess and Quaternary sediments where the eastern extension of the Haiyuan fault zone traced on the satellite image (Fig. 18) ends. To the south it overlaps with the

northeast-trending northern segment of Chenzhuang anticline, and its southern end curves to trend northeast. If its southern end is projected to the southwest, it should connect with the northeast-trending anticline west of the Taozigou anticline. However, the exposure in that area is very poor. The rocks forming the anticline are the Tertiary red beds and Cretaceous Naijiahe Formation (Kln).

The Sikouzi anticline can be divided into southern and northern segments. The southern segment is cored by the Naijiahe Formation. Its eastern limb dips 40°-50° to the northeast and connects with the northern part of the Chenzhuang anticline through an open north-plunging syncline. Its western limb dips to the southwest. The Tertiary rocks (Ors and Orb) are covered by the loess. Farther west the Miocene massive mudstone is only gently warped, but does not appear to have been involved in the folding of the Madong Shan. Most of the southern segment of the Sikouzi anticline apparently is not overturned. In one well exposed cross-section near the crest of the anticline on its western limb, however, the lower unit of the Naijiahe Formation rocks dip northwest in lower part of the section, but in upper part of this section, the layer of rocks is overturned to the northeast. It is possible that the axial surface of the fold is upright at depth but becomes overturned upward, and that most of the overturned rocks have been removed by erosion.

The northern segment of the fold is more complex than the southern segment even though there is no change in strike between the two segments. The west limb of the fold is cut by an east-dipping thrust fault that trends parallel to the anticline. The fault places the lower

units of Cretaceous Naijiahe Formation rocks over the Tertiary red beds. The Cretaceous rocks in the hanging wall near the fault are overturned and dip northeast. The eastern limb of this segments dips 40°-50° to the northeast, and contains a fold whose western limb is more gentle than the eastern limb (Fig. 5 and section GG′ and HH′ in Fig. 19). West of the thrust fault the rocks are also folded. In the northern part of this segment, an overturned foot wall syncline is present below the thrust fault, and an open anticline is present farther west. West of this anticline the Miocene massive mudstone is only gently warped, and dips are less than about 10°. In southern part of this segment, a tight anticline cored by Kln rocks is developed west of the thrust fault. This anticline trends north and plunges steeply northward.

In summary, the Madong Shan fold zone has a different structural style and evolution from the structures in the Liupan Shan, Xiaoguan Shan and Yueliang Shan. The major structural pattern in the Madong Shan is formed by three anticlines with curved axial traces and other smaller parallel folds. We suggest that the Sikouzi anticline is connected with the anticline west of the Taozigou anticline to the south, and the Chenzhuang anticline is connected with the anticline east of the Sikouzi anticline to the north. The northern segments of the three anticlines are all deflected to the northwest, suggesting that they have undergone the left-lateral shear during and / or after their formation. The southern part of the Madong Shan is east vergent, whereas the northern part is west vergent. Because of the changes in vergence and the gently Z-shaped axial traces, we suggest that these folds formed with a component of left-lateral shear.

TIMING RELATIONS OF STRUCTURES IN THE LIUPAN SHAN AREA

Based on the data presented above, the structural evolution in the Liupan Shan area can be divided into 3 phases: 1> folding and thrust faulting along the Liupan Shan, and Xiaokou faults, with a possible right-lateral component of displacement along the Liupan Shan thrust fault; 2> formation of the fold zone in the Madong Shan, thrust faulting in the Xiaoguan Shan, and continued thrust faulting in the Liupan Shan; 3> left-lateral strike-slip along the Xiaokou fault and northern part of the Liupan Shan fault, and continued thrusting in the Liupan Shan. These phases should not be considered isolated events, but are interrelated and probably diachronous.

1> FOLDING AND THRUST FAULTING WITH ASSOCIATED STRIKE-SLIP MOTION The oldest Cenozoic structures recognized are the folds and thrust faults in the Liupan Shan and Yueliang Shan (Figure 20). Their ages can only be estimated on the basis of the age of the youngest sedimentary rocks that were involved in these structures. The Liupan Shan and Xiaokou faults all offset the contact between Cretaceous and Tertiary red beds, which is a paraconformity, throughout the Liupan Shan area and northeastern margin of Tibetan Plateau. Rocks above the paraconformity contain only rare fragments of underlying Cretaceous rocks, and most of the pebbles and cobbles in the early Tertiary conglomerate are quartzite, gritty red sandstone, red conglomerate and other resistant rock types. This suggests that no significant tectonic event occurred within the hiatus represented at the paraconformity. The

mapped area as well as the northeastern part of Tibetan Plateau was the site of continued deposition of fine-grained terrestrial red sediments from early Oligocene to Pliocene time (Burchfiel et al., 1987), and the evidence suggests that deformation did not begin in this area until Pliocene time. The Pliocene conglomerate contains debris from all underlying units and probably marks the onset of Cenozoic deformation in this area. Therefore the age of this deformation is probably Pliocene and younger.

During this earliest deformational event the thrust faults and related folds involved rocks as old as the Ordovician limestone. Relative displacement along thrust faults was to the east-northeast and may have been associated with right-lateral displacement in the Liupan Shan.

2> FORMATION OF THE FOLD ZONE IN THE MADONG SHAN AND THRUST FAULTING IN THE LIUPAN SHAN AND XIAOGUAN SHAN The Madong Shan fold zone consists of three major anticlines, each with a different geometry. Vergence is both to the southeast and northwest, and the axial traces of most of the folds are curved. The folds probably formed in part later than the earliest structures in the Liupan Shan, and Yueliang Shan. In eastern limb of the Taozigou anticline the Quaternary conglomerate (Qcg) has been involved in the folds. The Quaternary conglomerate conformably overlies the Pliocene conglomerate, and it contains the first abundant debris of grey, and yellow, light blue mudstone, siltstone, marl and fine-grained sandstone that were clearly eroded from the nearby Cretaceous rocks. The source for the clasts in the Quaternary

conglomerate may have been from the Cretaceous rocks in the deformed and uplifted areas such as the Yueliang Shan and Liupan Shan. The uppermost part of the folded Quaternary conglomerate is interbedded with loess, whereas the loess in the other adjacent ranges rests unconformably on older rocks. This suggests that folding in the Madong Shan began later than the folding and thrust faulting in the adjacent areas. For reasons given below we interpret that much of the thrusting in the Liupan Shan and Xiaoguan Shan was contemporaneous with folding in the Madong Shan. The younger part of the loess does not appear to be involved in the Madong Shan and Xiaoguan Shan structures.

3> LEFT-LATERAL FAULTING The youngest phase of deformation in this area is left-lateral strike-slip faulting along the Xiaokou fault and thrusting in the Liupan Shan fault with a left-slip component in its northern part. This deformation is still active. An important question is when this left-slip motion started, because development of left-slip on the Xiaokou fault has probably been responsible for ending or slowing the rate of deformation in the Madong Shan and Xiaoguan Shan, where the loess does not appear to be involved in active structures. It is difficult to determine when left-slip displacement began on the Xiaokou fault within the map area. Although a series of streams across the fault have been offset, no material was found to date them. Data produced by Burchfiel et al. (1987) has suggested that left-slip on the Xiaokou fault may have begun only about 250,000 years ago.

KINEMATICS OF THE GEOLOGICAL STRUCTURE IN THE LIUPAN SHAN AREA

Along the Xiaokou fault displacement in the earliest phase of deformation (folding and thrust faulting) appears to be convergence from southwest to northeast, as suggested by the drag folds on the hanging wall block of the fault near the Xangshuigou and Shangdazai (Figure 5 and 14) without lateral motion. Along the Liupan Shan fault, a series of folds adjacent to the fault are also present, but the axes of these folds are oblique to the fault and intersect it at an acute angle, suggesting a component of right-lateral displacement along the Liupan Shan fault during an earliest phase of folding and thrust faulting.

From late Pliocene and Quaternary time, the depositional pattern of Cenozoic rocks changed from a large basin filled with fine-grained sediments to local tectonically related sequences dominated by conglomerate. This was accompanied by deformation and elevation along several mountain ranges. Folds and thrust faults developed at this time along the ranges in southern Ningxia (Figure 2). The youngest rocks involved in these folds and thrust faults are the Pliocene tan conglomerate and its correlatives, and Quaternary rocks overlie the structures but remain unfolded except in the Madong Shan area. Thus, all these folds and thrust faults were formed probably during the same deformational phase. The folds and thrust faults strike N30° to 40°W adjacent to the Haiyuan fault in Nanhua Shan, Xihua Shan and Huangjiawa Shan (Burchfiel et al., 1987). In the Tianjin Shan, Mibo Shan, Yanton Shan, Dalou Shan, and Xiaolou Shan areas, the folds and thrust faults also trend about between N30°-40°W (Figure 2), which is also the trend of the Xiaokou fault. On the basis of the orientation of these folds and

thrust faults it is reasonable to conclude that the direction of the convergence in southern Ningxia was about N50°-60°E during the earliest phase of deformation.

It is clear that the Liupan Shan fault is oblique to the direction of convergence that we inferred from the trend of folds and thrust faults in southern Ningxia. The angle between the strike of Liupan Shan fault and the direction of regional convergence is about 20° to 30°. This trend is appropriate to contain a component of right-lateral displacement on the Liupan Shan fault. Thus the Liupan Shan fault is interpreted as thrust fault with right-lateral displacement, and the Xiaokou fault as a thrust fault.

The work on the Haiyuan fault zone indicates that left-slip displacement on the fault zone followed the development of the folds and thrust faults. After the left-slip began, all or most of the succeeding deformation was taken up by left-slip (Burchfiel et al., 1987). The formation of the left-slip Haiyuan fault zone probably caused a significant change in tectonics of southern Ningxia, especially in the area near southeastern end of the fault zone, and this change also probably affected the tectonics in the Liupan Shan area. We suggest that the Liupan Shan thrust fault zone has been affected. The southern block of the Haiyuan fault zone began to move to the southeast with respect to its northern block, and thus the direction of convergence in the Liupan Shan area changed to southeast-northwest. As a result, the right-lateral displacement associated with thrust faulting on the Liupan Shan fault would have stopped and changed to left-slip, and most of shortening on the Liupan Shan thrust fault would have occurred during left-slip

movement along the Haiyuan fault and was contemporaneous with the folding in the Madong Shan (see below).

Left-slip on the Haiyuan fault also appears to have affected the structures in the Madong Shan. As described above, the Haiyuan fault projects into the northern end of the Madong Shan, and left-slip on it may have been transformed into convergence in the Madong Shan. If this is so, both the structural pattern and history of the area should be comparable with the left-slip on the Haiyuan fault. As shown in Figure 21, the overall pattern of the fold zone, the northwest-deflection of northern ends of the anticlines and the southern end of the Taozigou anticline, and the different directions of convergence all reflect the combination of compression and left-lateral shear in the Madong Shan mountain. However, the left-lateral shear component in the Madong Shan cannot be due to regional northeast convergence that we inferred from the trends of folds and thrust faults in southern Ningxia, because the N20W-trending fold zone should possess a right-lateral shear component in the displacement field produced by that regional convergence in southern Ningxia. The movement of southwestern block of the left-slip Haiyuan fault with respect to its northeastern block to the southeast would produce a southeast convergence direction in the Madong Shan area; as a result, the N20°W-trending Madong Shan fold zone in this displacement field would possess convergence with a left-lateral shear component.

The above suggestion is also supported by the age of deformation in Madong Shan area. The Quaternary conglomerate consisting of angular debris from the Cretaceous rocks conformably overlies the Pliocene tan

conglomerate only in the Madong Shan area; elsewhere in southern Ningxia the contact is an angular unconformity. This implies that when surrounding areas, such as the Liupan Shan and Yueliang Shan, were subjected to deformation and uplift, the Madong Shan area continued to be a site of deposition. Later, the Madong Shan area began to be folded and faulted, and involved the Quaternary conglomerate (Qcg). The deformation in Madong Shan is obviously later than the folding and thrust faulting in some other mountain ranges, and its deformation probably began at the time when left-slip on the Haiyuan fault started.

The left-lateral deflection of Madong Shan fold zone suggests that there must be structures east of it to accommodate the continued displacement after its formation, represented by the left deflection of the folds (Figure 20B). The Xiaoguan Shan thrust fault is the only candidate structure east of the Madong Shan. For the thrust fault in the Xiaoguan Shan to take up shortening related to movement southeast of the Haiyuan fault zone requires that the Haiyuan fault continued southeast from the northern end of the Madong Shan to the northern end of the Xiaoguan Shan (Figure 20B). Presently there is no evidence for the fault between the Madong Shan and Xiaoguan Shan. The fault would cross the Qinshuihe river valley. The valley is located along the axis of a broad north-plunging syncline that can be traced northward to Zhongning. This syncline is one of several synclines that form topographic low areas of active uplift in adjacent ranges. The Qinshuihe basin was thus a topographically low area that has been filled with loess and other sediments. If the southeastern extension of the Haiyuan fault became inactive during late Pleistocene time, when movement began on the

Xiaokou fault, the trace of the Haiyuan fault in the Qinshuihe basin would have been concealed beneath these young sediments (Figure 20C). We infer that the Haiyuan fault did continue to the Xiaoguan Shan, because the only structures present to accommodate the shortening transferred from the Haiyuan fault zone in this region are the structures in the Liupan Shan, Madong Shan and Xiaoguan Shan. We consider it no coincidence that by assuming the shortening in these two structural zones in the direction of the Haiyuan fault zone yields a magnitude equal to the left-slip displacement on the Haiyuan fault zone. The Z-shaped trace of the Madong Shan folds clearly record the left-slip strain.

The left-slip along the Haiyuan fault has continued to the present. The slip rates over Quaternary time and Holocene time are 5 to 10 mm/yr and 8 ± 2 mm/yr, respectively (Burchfiel et al., 1987; Zhang et al., 1987). However, at the eastern end of the Haiyuan fault, the structures in Madong Shan area do not appear to be active. The surface ruptures associated with the 1920 Haiyuan earthquake developed along the Xiaokou fault rather than the Madong Shan fold and fault zone. In the satellite image (Figure 18), a lineation can still be seen from southeastern extension of the Haiyuan fault to the Madong Shan, but it is impossible to trace it in the field because of the loess cover. These observations suggest that the Madong Shan fold zone no longer absorbs displacement, despite the continued left-slip displacement on the Haiyuan fault.

The Xiaokou fault trends about N30°-40°W, and intersects the Haiyuan fault southwest of Youfangyuan just where the Haiyuan fault

becomes more obscure (Burchfiel et al., 1987). Tectonic activity in the Madong Shan has ceased because the displacement along the Haiyuan fault has been taken up by the Xiaokou fault. Displacement along a fault was probably easier to absorb by continued slip rather than by being absorbed by convergence in the fold and thrust fault zone. These could be part of the reason why deformation at the eastern end of the Haiyuan fault shifted to the Xiaokou fault from the Madong Shan fold zone. At present, the left-slip along the Haiyuan fault has been absorbed by left-slip and probable convergence on the Xiaokou fault, and farther to the southeast, finally by left-slip and convergence along the Liupan Shan fault.

SHORTENING ACROSS THE LIUPAN SHAN AND XIAOGUAN SHAN

In the Liupan Shan area shortening occurred mainly along the major thrust faults, and its magnitude can be estimated. The shortening on the Xiaokou fault will not be discussed here because we did not study its poorly exposed hanging wall.

The geometry of the Liupan Shan fault and its hanging-wall ramp are shown in Figure 4. The minimum east-west displacement on the Liupan Shan fault appears to be 5.5 - 6.5 km. If we unfold the anticline in the hanging wall and syncline on the foot wall, another 2 km shortening is obtained. Thus the total apparent east-west shortening is estimated to be 7.5 - 8.5 km. This is certainly a minimum. The net slip along the Liupan Shan fault could be much larger. Movement on the fault was probably mostly parallel to the trend of the Haiyuan fault, which is N60W, and the shortening in that direction would be 8.6 - 9.8 km.

The total shortening along the Xiaoguan Shan fault is also difficult to estimate. The Xiaoguan Shan fault dips to the west, and the Ordovician rocks were thrust over the Tertiary red beds, but no Ordovician rocks are exposed in the foot wall and no drill hole or other geophysical data are available in this area, so no reasonable correlate of units on both sides of the fault can be made. Unfolding the rocks in the hanging wall of the fault, and projecting units, now eroded, into the hanging wall, yields a minimum east-west displacement of at least 5 to 6 km.

To summarize, we obtained a minimum of about 12.5 - 14.5 of shortening in east-west direction across the Liupan Shan and Xiaoguan Shan, but the true amount of crustal shortening could be larger.

SHORTENING IN THE MADONG SHAN

As we described above, the direction of tectonic transport in southern Ningxia region is about N50E during the time when the major structures, such as the Liupan Shan thrust fault, the Xiaokou fault, and the Haiyuan fault were formed. The deformation in the Madong Shan has resulted from left-slip on the Haiyuan fault zone, and if so, the amount of shortening should be comparable with the displacement along the Haiyuan fault. Burchfiel et. al. (1987) demonstrated that the total left-lateral displacement on the Haiyuan fault is from 10.5 to 15.5 km. The left-slip on the Xiaokou fault is about 1 to 2 km based on the evidence from the Laohuyiaoxian pull-apart basin. There is a thrust component associated with the left-slip on the Xiaokou fault, but the amount of shortening is probably no more than about 1 km. Thus, about 2

km of the displacement on the Haiyuan fault is taken up on the Xiaokou fault, and about 8.5 - 13.5 km of displacement on the Haiyuan fault should be accommodated by the shortening in the Madong Shan and the area east of it.

The total shortening in the Madong Shan cannot be measured by the same method applied to the Liupan Shan and Xiaoguan Shan, because the deformation is due to both compression and left-lateral shear. The trend of the folded zone is neither perpendicular to the strike of the Haiyuan fault, nor to the inferred direction of crustal shortening in southern Ningxia. Calculations made by unfolding the cross-section normal to the folded zone do not yield the amount of total shortening required to absorb the displacement from the Haiyuan fault zone. The total shortening should be measured parallel to the direction of tectonic transport in the folded zone (eg. see Woodward et al., 1985). The folds in the Madong Shan have curved axial traces, and it is unknown if the shortening along a specified direction across the Madong Shan would be representative of the entire fold zone. The shortening can be measured perpendicular to each segment of the fold zone where the folds within it parallel each other, and then compared to the amount of shortening for each segment; if the volumes in each segment are similar, it would be reasonable to conclude that this value represents the total shortening in the Madong Shan.

There are 8 cross-sections across the Madong Shan (Figure 19). The measured shortening along each section is shown in table 1. Section AA′ crosses southern end of the Madong Shan and is perpendicular to the Taozigou anticline. The measured crustal shortening along it is 5.4 ±

0.5 km. Section BB′ is across and perpendicular to both the Taozigou anticline and the anticline west of it. The measured crustal shortening is 6.2 ± 0.5 km. Section CC′ crosses northern end, deflected segment of the Taozigou anticline and undeflected segments of the Chenzhuang anticline and the Sikouzi anticline. The measured shortening is about 5.9 km. This section is not perpendicular to the major anticlines; the deviation is 10° to 20°. According to the suggestion by Price (1981) that no major error (15%) in calculating the amount of shortening results if a section line is within 30° of the tectonic transport direction, the 5.9 ± 0.8 km amount of shortening along the section CC′ is probably reasonable. Section DD′ crosses the area between the Taozigou and the Chenzhuang anticlines. The shortening across it is 5.8 ± 0.5 km. Section EE′ crosses deflected segments of all three major anticlines, and the amount of shortening along it is 5.7 km. It is again not perpendicular to those folds. The deviation is more than 30°. The resultant error in shortening could be larger than 15 %, thus an uncertainty of 1.5 km was placed on this measurement. The purpose of drawing section FF′ was to show the geometry of the Chenzhuang anticline. We did not measure the shortening along it because it does not cross the Taozigou anticline. Both sections GG′ and HH′ cross the Sikouzi anticline and the anticline east of it as well as the east-dipping thrust fault west of Sikouzi. The shortening across the thrust fault is 1.07 km along the section GG′ and 1.3 km along the section HH′. The shortenings by folding are 4.4 and 4.5 km along sections GG′ and HH′ respectively. The total shortening across these two sections is 5.4 ± 0.5 and 5.8 ± 0.5 km respectively. The calculated shortening in all 8

sections across the Madong Shan, is similar, and an average of 5.7 ± 0.75 km is representative of the total shortening across the Madong Shan.

The relatively constant amounts of crustal shortening across different segments of the Madong Shan fold zone suggest that the left-lateral deflection of northeastern ends of the major folds occurred mostly after their formation, because if the deflection occurred during their formation, the amount of crustal shortening might be considerably different between the deflected and undeflected segments of the fold zone, and the amount of shortening across the undeflected segment would be equal to the amount of shortening and the amount of deflection across the deflected segment. The structural pattern of the deflected segments of major anticlines approximately parallel one another, and the angles between them and their central original trend are all between 30° to 40°. If we rotate back the deflected segments of each of the folds to their original trend before deflection, the amount of left-lateral displacement on the Sikouzi, Chenzhuang and Taozigou anticlines would be 5.0, 5.2 and 4.7 km, respectively (Figure 21). Thus, it appears that the Madong Shan fold fold zone has been subjected to about 5.0 ± 1.0 km left-lateral displacement after its formation.

The total shortening in the Madong Shan is 5.7 ± 0.75 km, and the left-deflection is 5.0 ± 1.0 km, and the total amount of shortening, 10.7 ± 0.9 km, is well comparable to 8.5 - 13.5 km of displacement that should be accommodated in the Madong Shan fold zone from the left slip on the Haiyuan fault zone.

DISPLACEMENT AND STRAIN EVOLUTION IN THE LIUPAN SHAN AREA

From the descriptive geology and timing constraints presented above, a displacement and strain evolution of the Liupan Shan area has been developed. This evolution must be related to the evolution of adjacent areas in southern Ningxia, particularly the Haiyuan area. Furthermore, most of the magnitude of the deformation in the Liupan Shan area can be shown quantitatively to have been the result of the left-slip displacements on the Haiyuan fault zone. The first structures to form were the thrust faults and related folds in the Yueliang Shan (Xiaokou fault) and Liupan Shan. The magnitude of this shortening is difficult to determine. Cross sections of the Xiaokou fault indicate a total thrust displacement of about 2 km (or horizontal shortening of 1.4 km), plus unfolding the folds in both hanging wall and foot wall, 1.6 - 1.8 km horizontal shortening may be obtained. But not all of this displacement need to have occurred during this early deformation. If some of the shortening is related to oblique strike-slip during the youngest events (see below) then about 0.8 km of horizontal shortening could have occurred in this earliest event. Such a magnitude of shortening is reasonable to have formed the earliest structures in the Haiyuan area. We infer that perhaps about 1 km of horizontal shortening would have occurred at this time on the Liupan Shan thrust fault Figure 20A).

Following formation of these early structures movement on the Haiyuan fault took place and changed the kinematic evolution in the Liupan Shan area from early Quaternary time to the present. Total displacement on the Haiyuan fault zone, the dominant structure in the

southern Ningxia area, is between 10.5 to 15.5 km (Burchfiel et al., 1987). The greatest magnitude of shortening in the Liupan Shan area is present in the folds and thrust faults in the Madong Shan, Liupan Shan and Xiaoguan Shan.

The average shortening for the Madong Shan fold zone is 5.7 ± 0.75 km. Horizontal shortening across the Liupan Shan thrust fault is measured to be 7.5 - 8.5 km (Figure 4). The shortening calculated parallel to the Haiyuan fault is 8.6 - 9.8 km. About 1 km of this displacement may have occurred during the earliest phase of deformation and another 1 - 2 km in the youngest phase (see below); thus during the folding in the Madong Shan about 6.8 to 7.8 km of shortening occurred on the Liupan Shan thrust fault (Figure 20B). Since this amount is close to that obtained from the Madong Shan (5.7 ± 0.75 km) we infer that this shortening was contemporaneous in this two areas.

Structures in the two areas are not continuous. Structure in the Liupan Shan is dominated by thrust faults, whereas the Madong Shan is dominated by folds. The folds at the southern end of the Madong Shan plunge steeply south and are not aligned with the Liupan Shan thrust fault. We interpret these relation, to result from early deformation, possibly thrust faulting in the Liupan Shan that was not present in the Madong Shan. Later, when both areas were deformed, shortening continued by thrust faulting in the Liupan Shan, but occurred by folding in the Madong Shan. A zone of accommodation between these two structural styles, with a possible left-slip component, occurred between Xiaokou and Yangzhongpu where structures form both mountain ranges show a left-handed deflection.

Displacement on the Xiaoguan Shan thrust fault east of the Liupan Shan is estimated to be 5 - 6 km in east-west direction or in a N60°W direction 5.7 - 6.9 km.

Thus before the youngest event structures in the Madong Shan and Liupan Shan would account for 5.7 ± 0.75 and 6.8 - 7.8 km of shortening respectively; when combined with shortening in the Xiaoguan Shan (5.7 - 6.9 km) this yields a total shortening of 11.4 to 14.7 km in the direction of the Haiyuan fault zone. The youngest event, left-slip on the Xiaokou fault, would add 1 - 2 km to the horizontal shortening on the Liupan Shan thrust fault (parallel to N30°W), and perhaps 0.6 - 0.8 km on the shortening at the latitude of the Madong Shan. Added to the earliest displacements it would yield a total shortening in the Liupan Shan area of 12.4 - 16.7 km parallel to the Haiyuan fault zone.

DEPTH OF DEFORMATION BENEATH THE LIUPAN SHAN AREA

Shortening deformation in the Liupan Shan area consists of thrust faults and flexural-slip folds that suggest a thin-skinned style of deformation. Constructing a cross section on the Liupan Shan and Xiaoguan Shan thrust faults based on a thin-skinned geometry indicates the depth to the detachment would be at about 6 km. This would place the decollement zone below the Cretaceous rocks exposed in the area.

For the Madong Shan folds, the method used by Laubscher (1965), Dahlstrom (1969), and later expended by Hossach (1979), Suppe (1985) and Woodward et al. (1985), can be applied. It is based on the principle of conservation of volume. By assuming plane strain, the volume conservation is reduced to area conservation. If the section above the

detachment is shortened by folding, the left side of the section will move forward by the amount of shortening. If the right side of the section is fixed, the area generated by the translated rear of the right end will equal the area of resulting fold above the unfolded datum. Because the amount of shortening is a known constant, if the area of the resulting fold can be measured, the area divided by the amount of shortening will yield the depth to the detachment. To measure the shortening area of a cross-section, we arbitrarily select a bedding and trace it downward, parallel to the stratigraphic units above it, till it becomes horizontal. The area enveloped by the bedding and the horizontal line at its bottom would be the shortening area. If there is no fault underneath the section and above the detachment, the down-tracing bedding toward both sides of the section would become horizontal in the same level; otherwise there would be a fault underneath the section and above the detachment.

By measuring the area beneath the folds for 7 cross sections (Figure 22, excluding section F-F′ in Figure 19), the average depth to decollement is about 4.5 ± 0.7 km and ranges from 3.5 km along section A-A′ to 5.2 km along section E-E′. This depth again requires the decollement to be well below the Cretaceous rocks that are exposed in the cores of the folds, and the depth is comparable to that for the thrust faults in the area.

The geometry of the folds indicates complication at depth: the western limb of the fold zone is consistently 1.5 to 2 km shallower than the eastern limb. This is interpreted to be the result of west-dipping blind thrust faults beneath the fold.

The thin-skinned geometry of the structures in the Liupan Shan area might be applied to the folds and thrust faults in the southern Ningxia region. Folds and thrust faults in the region expose rocks as old as Cambrian metasedimentary rocks or pre-Silurian metamorphic rocks. This suggests that if there is a decollement zone beneath these structures it cuts through structurally complex pre-Cenozoic rocks and structures in the region, and that much of the Pliocene - Quaternary structural development in southern Ningxia has a style similar to that of the Haiyuan - Liupan Shan area where left-lateral strike-slip displacement is transferred to a north or northwest trending zone of shortening.

CONCLUSION

The oldest rocks exposed in the Liupan Shan area are Ordovician limestone, but they only crop out locally. The most widely exposed rocks in the area are the lower Cretaceous Liupan Shan Group and Tertiary red beds. The contact between Cretaceous rocks and Ordovician limestone is a paraconformity, and the contact between Tertiary red beds and Cretaceous rocks is also a paraconformity. Quaternary rocks unconformably overlie the older rock units except in the Madong Shan, and most of them were deposited in local environments from local sources except the widespread eolian loess.

The Liupan Shan thrust fault trends generally north-south, except in its northern part where it trends north-northwest. It is characterized by the eastward displacement of Cretaceous Liupan Shan Group above the Tertiary red beds. The hanging wall has been folded into

an anticline near the thrust fault, but to the west the rocks dip gently west, and farther west they become horizontal. This relation suggests that the Liupan Shan thrust fault is a decollement-style thrust fault that ramps gently upward to the east and that the folds were developed only near the thrust fault. A series of small folds are present in the hanging wall west of the fault; these trend obliquely to the Liupan Shan fault, and intersect it at an acute angle facing to the southeast. These relations suggest that the early thrust displacement may have been associated with a component of right-slip. Along the northern part of the Liupan Shan thrust fault, several left-lateral stream offsets are present. The clearest left-lateral offset was 14 ± 3 m, and the bench within the same stream was offset about 5 m. Thus, the younger stage of thrusting on the Liupan Shan thrust fault has had a component of left-slip.

The Xiaoguan Shan fault is parallel to the Liupan Shan thrust fault. The Cretaceous and Ordovician rocks in its hanging wall have moved relatively eastward over Tertiary red beds. No detailed work was done on this fault, and its evolution is poorly known.

The Xiaokou fault trends about N40°W and lies north of the Liupan Shan thrust fault. Cretaceous rocks are thrust eastward over Tertiary red beds. Small folds parallel to the Xiaokou fault in both hanging wall and foot wall suggest that no lateral displacement was associated with the thrust faulting in its early stage of deformation. A series of ridges and streams that cross the fault have been offset left-laterally in Pleistocene and Holocene time, and a stream offset of 380 ± 30 m was measured at one place.

The Madong Shan fold zone is located east of the Xiaokou fault. It trends about N20°W, and consists of three anticlines with Z-shaped axial traces. Each of the anticlines in the zone has a different geometric style. The Taozigou anticline is overturned to the southeast, the Chenzhuang anticline is box-shaped, and the Sikouzi anticline is cut by an east-dipping thrust fault. The southern part of the fold zone is east vergent, whereas the northern part is west vergent.

The tectonic history of the Liupan Shan area can be divided into three interrelated events. During the first event folds and thrust faults along north-northwest strands were associated with left-slip motion. This event occurred probably between late Pliocene and early Quaternary time, because the Pliocene conglomerate has been involved in the folds and thrust faults, but Quaternary rocks unconformably overlie the folds. Structures were formed in the Xiaoguan Shan, Liupan Shan and Yueliang Shan. Shortening during this event was about 1 km in a N50°-60°E direction. During the second event, folding began in the Madong Shan and thrust faulting continued in the Xiaoguan Shan and Liupan Shan. In the folds of the Madong Shan, the Quaternary conglomerate (Qcg) conformably overlies the Pliocene conglomerate and contains detritus from Cretaceous rocks indicating the Madong Shan folds are probably younger than the initial deformation in the Yueliang Shan and Liupan Shan. Most of the shortening in the Liupan Shan area occurred at this time. During the third event, about 1 - 1.5 km of late Pleistocene to Recent left-slip occurred on the Xiaokou fault, which was transferred into left-slip thrusting on the Liupan Shan. Deformation ceased or was reduced to a very slow rate in the Madong Shan and Xiaoguan Shan.

Left-slip on the N60°W striking Haiyuan fault zone has been transferred into shortening on the generally north-trending structures in the Liupan Shan area. The 10.5 to 15.5 km of left-slip on the Haiyuan fault zone is balanced by 12.4 - 16.7 km of shortening in the Liupan Shan structures. The structures in the Liupan Shan area are probably thin-skinned, and the depth to the decollement zone is 4 - 6 km, a depth that places the decollement within a varied complex of pre-Cretaceous rocks.

Interpretations of the geology in the Liupan Shan area can be extended to the folds and thrust faults in southern Ningxia that form the developing northeastern margin of the Tibetan Plateau. The structural pattern in this region suggests that left-slip faulting is transferred into northeast and east - west shortening along folds and thrust faults that are detached within the upper crust.

Table 1

SECTION	SHORTENING (KM)	SHORTENING AREA (KM^2)	DEPTH (KM)	SEPARATION (KM)
AA′	5.4 ± 0.5	19.0	3.5	1.34
BB′	6.2 ± 0.5	29.5	4.8	1.25
CC′	5.9 ± 0.8	30.0	5.1	1.06
DD′	5.8 ± 0.5	26.5	4.7	0.76
EE′	5.7 ± 1.5	29.5	5.2	1.45
FF′				
GG′	4.4 ± 0.5 (folding)	21.0	4.6	1.80
	1.0 ± 0.3 (faulting)			
HH′	4.5 ± 0.5 (folding)	19.5	4.3	1.75
	1.3 ± 0.3 (faulting)			
	AVERAGE AMOUNT OF SHORTENING	5.7 ± 0.75 KM		

REFERENCES

Burchfiel, B. C., Zhang, P., Wang, Y., Zhang, W., Jiao, D., Song, F., Deng, Q., Molnar, P., and L. Royden, Geology of the Haiyuan fault zone, Ningxia Autonomous Region, China and its relation to the evolution of the Northeastern margin of the Tibetan Plateau, submitted to J. Geophys. Res., 1987.

Dahlstrom, C. D. A., Balanced cross sections, Can. Jour. Earth Sci.,6, 743-754, 1969.

Deng, Q., Song, F., Zhu, S., Li, M., Wang, T., Zhang, W., Burchfiel, B. C., Molnar, P., and P. Zhang, Active faulting and tectonics of the Ningxia-Hui Autonomous Region, China, J. Geophys. Res., 89, 4427-4445, 1984.

Deng, Q., Chen, S., Zhu, S., Wang, Y., Zhang, W., Jiao, D., Burchfiel, B.C., Molnar, P., Royden, L., and P. Zhang, Variation in the geometry and amount of slip on the Haiyuan fault zone, China, and the surface rupture of the 1920 Haiyuan earthquake, Maurice Ewing Series 6, Amer. Geophys. Un., Washington D.C., 169-182, 1986.

Hossack, J. R., The use of balanced cross-sections in the calculation of orogenic contraction: a review, Jour. Geol. Soc. Lond., 136, 705-711, 1979.

Huang, T. K., An outline of the tectonic characteristics of China, Continental Tectonics, National Academic Press, 184-197, 1980.

Laubscher, H. P., Ein kinematisches Modell der Jurafaltung: Ecolgae Geol. Helvetiae, v. 54, p. 231 - 318.

Li, C., Liu, Y., Zhu, B., Feng, Y., and H. Wu, Structural evolution of Qinling and Qilian, in Scientific papers on geology for international exchange, Beijing, China, Publishing House of Geology, 174-189, (in Chinese), 1978.

Molnar, P. and P. Tapponnier, Cenozoic tectonics of Asia: Effects of a continental collision, Science, 189, 419-426, 1975.

Molnar, P. and P. Tapponnier, Active tectonics of Tibet, J. Geophys. Res., 83, 5361-5374, 1978.

Ningxia Geological Bureau, Geological map of the Pingliang area (1/200,000), Geological Press, 1974.

Ningxia Geological Bureau, Geological map of the Zhongwei area (1/200,000), Geological Press, 1976.

Price, R. A., The Cordilleran foreland thrust and fold belt in the Southern Canadian Rocky Mountains, Thrust and Nappe Tectonics, Coward, M. P. and McClay, K. R. eds., Geol. Soc. London Spec. Pub., No. 9, 427-448, 1981.

Suppe, J., Principles of Structural Geology, Prenctics-Hall, Inc. Englewood Cliffs, N. J., 65-70, 1985.

Tapponnier, P. and P. Molnar, Slip-line field theory and large scale continental tectonics, Nature, 264, 319-324, 1976.

Tapponnie r, P. and P. Molnar, Active faulting and Cenozoic tectonics of China, J. Geophys. Res., 82, 2905-2930, 1977.

Wang, Y., Song, F., Liao, Y., Zhang, W., Kuei, F., and P. Liu, Some characteristics of seismotectonics in North Ningxia, and the effects of uplifting of Tibetan Plateau to North China Block, Recent Crustal Movement, (in Chinese), 1985.

Wei C., Geological characteristics of the Qilian Mountain, China, Acta. Geologica Sinica, 53, (in Chinese), 1978.

Woodward, C. B., Boyer, S. E., and J. Suppe, An outline of balanced cross-section, Short course on balanced sections sponsored by the Structural Geology and Tectonics Division of the Geological Society of America meeting held at Orlando, Florida, 1985.

Zhang, P., Molnar, P., Burchfiel, B. C., Royden, L., Wang, Y., Deng, Q., Song, F., Zhang, W., and D. Jiao, A, Bounds on the Holocene slip rate of the Haiyuan fault, North-Central China, submitted to Quaternary Research, 1987.

Zhang, P., Molnar, P., Zhang, W., Deng, Q., Wang, Y., Burchfiel, B. C., Royden, L., and D. Jiao, B, Bounds on the recurrence interval of major earthquakes along the Haiyuan fault in North-Central China, submitted to Quaternary Research, 1987.

Zhang, W., Jiao, D., Zhang, P., Molnar, P., Burchfiel, B. C., Deng, Q., Wang, Y., and Song, F., Displacement along the Haiyuan fault associated with the great 1920 Haiyuan earthquake, Bull. Seism. Soc. Am., 77, 117-131, 1987.

Zhang, Z., Liou, J. G., and R. G. Coleman, An outline of the plate tectonics of China, Geol. Soc. Am. Bull., 95, 295-312, 1984.

FIGURE CAPTIONS

Figure 1, Regional tectonic map of north-central China. Three major crustal blocks are shown in this map. The Nanshan fold belt tectonically belongs to the Tibetan Plateau, and the Ordos block belongs to the North China Block. Only major active faults are shown in this map by thick lines. Thick lines with arrows are strike-slip faults, thick lines with ticks are normal faults, and thick lines with solid triangles are thrust faults.

Figure 2, Cenozoic geological structures in southern Ningxia.

Figure 3, Geological map along the Liupan Shan thrust fault and its vicinity.

Figure 4, Geological cross-section across the Liupan Shan thrust fault and Xiaoguan Shan fault. The location of this section is shown in figure 2.

Figure 5, Geological map of the Madong Shan area. The thrust fault south of Xiaokou is the north continuation of the Liupan Shan thrust fault in Figure 3.

Figure 6, Basal conglomerate of Sanqiao Formation, Liupan Shan Group of Cretaceous in age. The dark grey pebbles and cobbles are fragments from the underlaying basement rocks of Ordovician thick limestone. These clasts are angular and very poor sorted, and they are cemented by fine-grained material whose composition is the same as the clasts.

Figure 7, Basal conglomerate above the paraconformity between the

Cretaceous rocks and Tertiary red beds. The clasts within the conglomerate are well rounded resistant rock types, such as quarzite, chart, vein-quartz, and Devonian red sandstone and conglomerate. Quartz-rich sand of the same material forms the matrix of this conglomerate. The thickness of this conglomerate is about two meters.

Figure 8, Topographic feature along the Liupan Shan thrust fault. View is to the north-northwest. The fault is along the break in slope between the mountains and the basin. The mountains on the west consist of Cretaceous rocks thrusted onto the Tertiary red beds and Quaternary sediments on the east. The fault dips to the west.

Figure 9, The exposed fault surface of the Liupan Shan fault at Haizikou. Along the stream channel in the front part of the photo are flat chennal benches. The horizontal flat surface above the cliff in front of the mountain is a high terrace of the stream. The fault crosses the stream channel as shown by the dashed line with double arrows. The black material near the lower left corner is fault gouge and breccia that has been thrust onto the stream deposits in the channel. The single arrow points to the fault surface that dips to the northwest at about 44°.

Figure 10, One of the overturned synclines among the drag folds adjacent to the Liupan Shan fault at Haijiazhuang. The view is approximately to the north. The Liupan Shan fault is about 40 m to the east of the photo. This overturned syncline is developed

in Cretaceous Lisanwa Formation (K11) in the hanging wall of the Liupan Shan thrust fault. About 50 m west of the western margin of the photo rocks dip normally to the southwest through an overturned anticline.

Figure 11, Left-lateral deflection of a stream across the Liupan Shan fault about 1.5 km north of Haizikou. The view is to the northeast. The stream flows from southwest to northeast, and is deflected where it crosses the fault. The fault surface has not been identified at the stream deflection. But according to other geological features nearby, one can infer that the fault zone should project through this deflection as shown by the dashed line with arrows.

Figure 12, Left-lateral deflection of a stream along the Liupan Shan thrust fault about 2 km south of the Haizikou. The view is to the west. The dashed line with arrows shows the location of the Liupan Shan thrust fault. The Cretaceous rocks crop out to the west of the fault, but no Cretaceous rocks crop out east of the fault. The stream has been deflected left-laterally where it crosses the fault.

Figure 13, Plane-table map of the stream offset along the Liupan Shan thrust fault at Haizikou. The thick lines show boundaries of the fault zone. The stream flows from southwest to northeast, and is offset where it crosses the fault. The measured offset is about 13 ± 2 m. A channel bench is present along the stream. The fault also offsets this bench 5 to 6 m.

Figure 14, An overturned anticline adjacent to the Xiaokou fault near

Shangdazai. The view is to the northwest. The Xiaokou fault is along the foot of the mountains as shown by the dashed line with arrows. There is an anticline on the hanging-wall block of the Xiaokou fault with its eastern limb overturned. The axis of this anticline is parallel to the fault. It is interpreted to be a hanging-wall anticline for the Xiaokou fault.

Figure 15, The left-lateral stream offset along the Xiaokou fault at Xangshuigou. The view is to the northeast. The stream flows from southwest to northeast, and is offset where it crosses the fault. the measured offset is about 27 ± 4 m. The fault is marked by the juxtaposition of Cretaceous rocks and Tertiary red beds, but the fault surface is not well exposed.

Figure 16, Topographic map showing stream offsets along the Xiaokou fault at Shangdazia. The dashed lines delineate the streams, and the arrows show the direction of stream flow. The thick line is the left-slip Xiaokou fault.

Figure 17, The left-lateral stream offset along the Xiaokou fault about 2 km southeast of Shangdazai. The view is to the southwest. The stream flows from the mountains and has been offset where it crosses the fault. The measured offset is about 380 m. The terrace of the stream is also offset, but we have not been able to date this offset. To both northwest and southeast, a series of ridges and streams are also offset.

Figure 18, Satellite photo of the Haiyuan and Liupan Shan areas, and generalized map showing the major structures mapped on the ground.

Figure 19, Cross-sections from the Madong Shan mountains. The locations of the cross-sections are shown in figure 5.

Figure 20, Diagram of the three phases of the tectonic history and amounts of shortening in the Liupan Shan area.

Figure 21 Simplified map of the Madong Shan area. The shaded area shows Cretaceous rocks in the Madong Shan area. Deflections of the Sikouzi, Chengzhuang, and Taozigou anticlines are 5.0, 5.2, and 4.7 km respectively.

Figure 22, Cross-sections showing the excess area beneath the folds along each of the sections in figure 21. The diferrence between horizontal level underneath eastern and western sides of each sections suggests that there is a fault underneath the Madong Shan fold belt or that three folds have been warped by young shortening related to the formation of the Qinshuihe basin farther east.

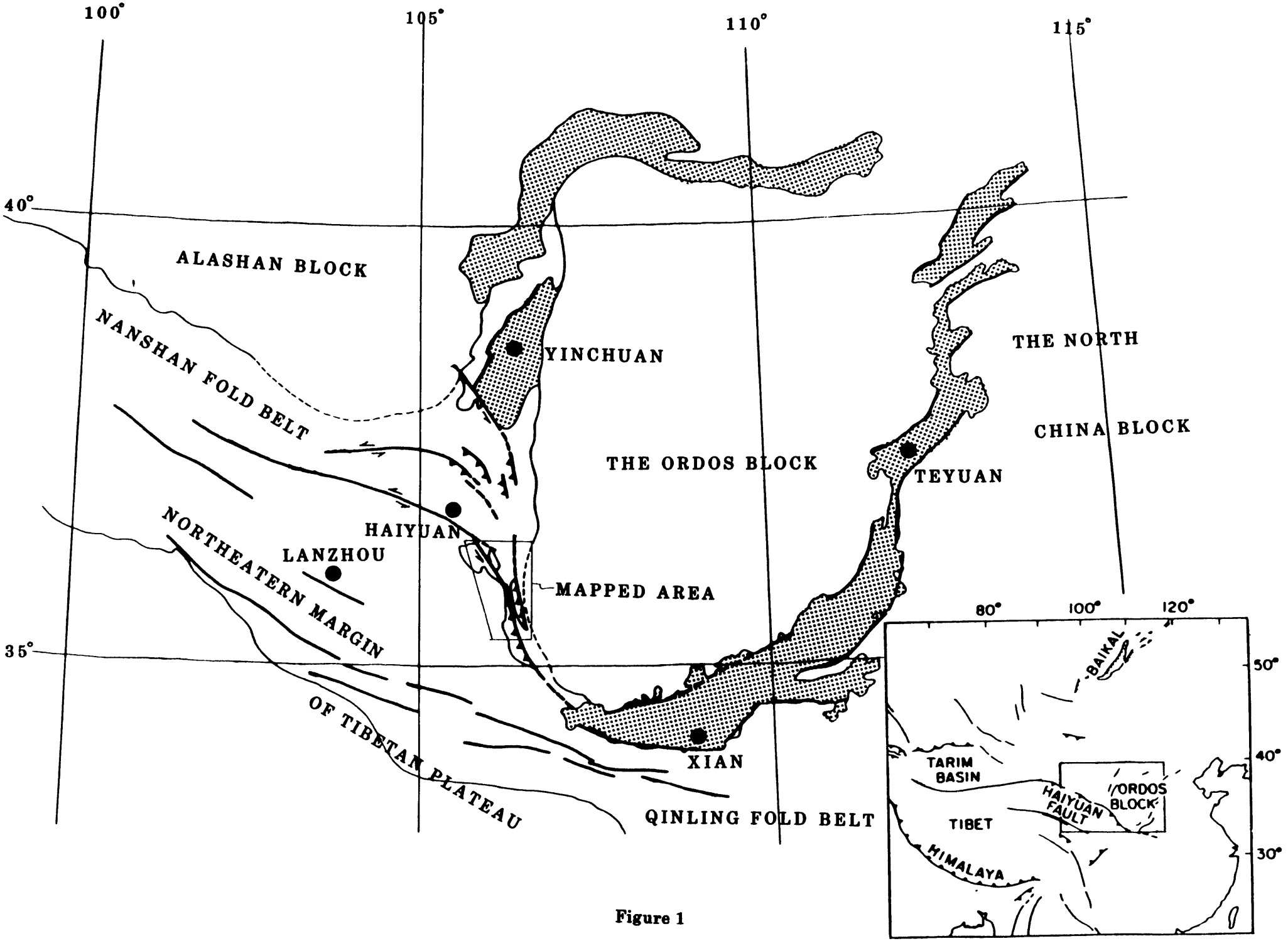
100°
105°
110°
115°
40°
35°
ALASHAN BLOCK
NANSHAN FOLD BELT
YINCHUAN
THE NORTH
CHINA BLOCK
THE ORDOS BLOCK
TEYUAN
HAIYUAN
LANZHOU
NORTHEATERN MARGIN
MAPPED AREA
OF TIBETAN PLATEAU
XIAN
QINLING FOLD BELT
80°
100°
120°
50°
40°
30°
BAIKAL
TARIM BASIN
HAIYUAN FAULT
ORDOS BLOCK
TIBET
HIMALAYA

Figure 1

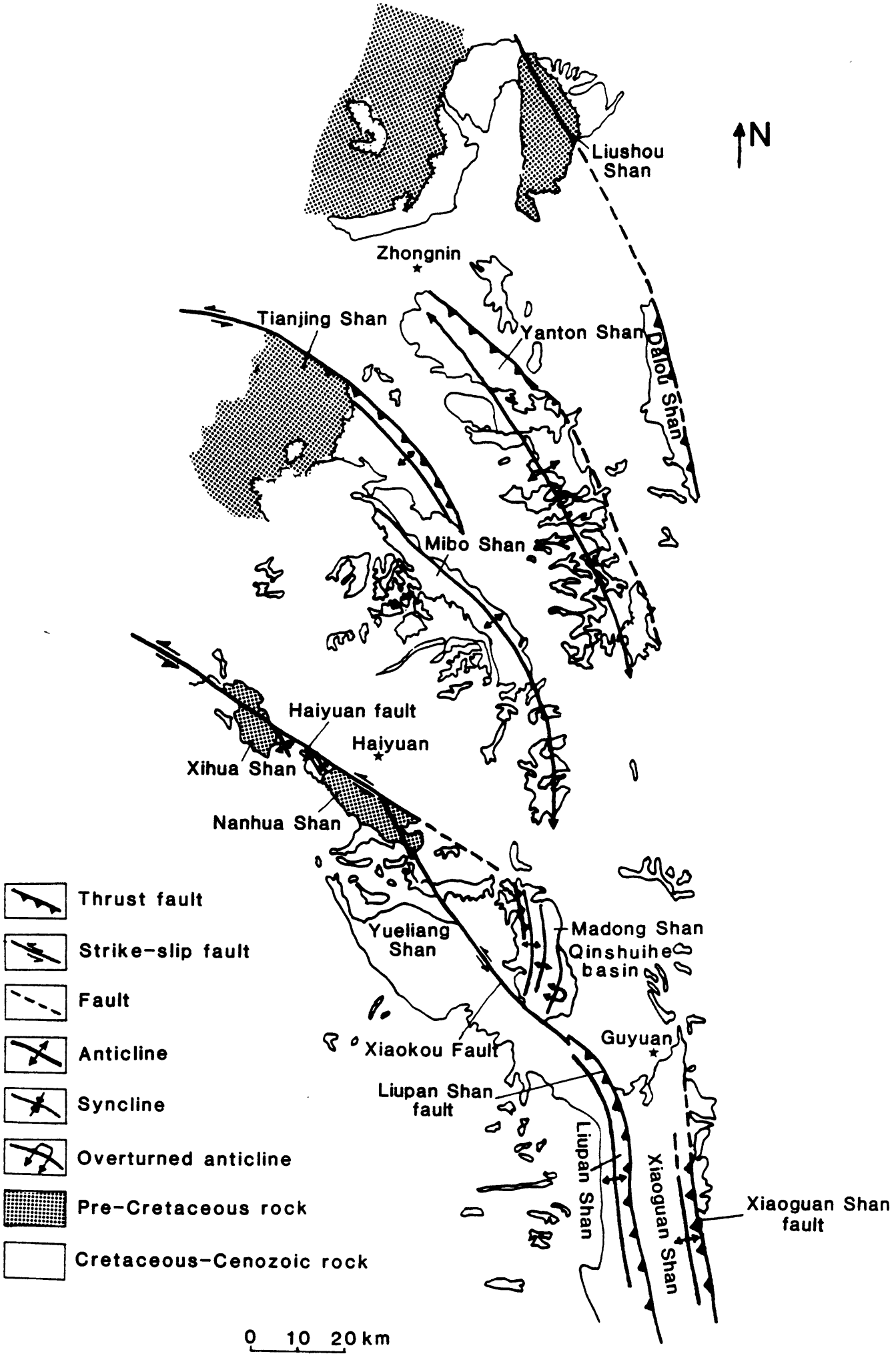
N
Liushou Shan
Zhongnin
Tianjing Shan
Yanton Shan
Dalou Shan
Mibo Shan
Haiyuan fault
Haiyuan
Xihua Shan
Nanhua Shan
Yueliang Shan
Madong Shan
Qinshuihe basin
Xiaokou Fault
Guyuan
Liupan Shan fault
Liupan Shan
Xiaoguan Shan
Xiaoguan Shan fault
Thrust fault
Strike-slip fault
Fault
Anticline
Syncline
Overturned anticline
Pre-Cretaceous rock
Cretaceous-Cenozoic rock
0 10 20 km

Figure 2

FIGURE 3

SEE THE FOLDED MAP SHEET

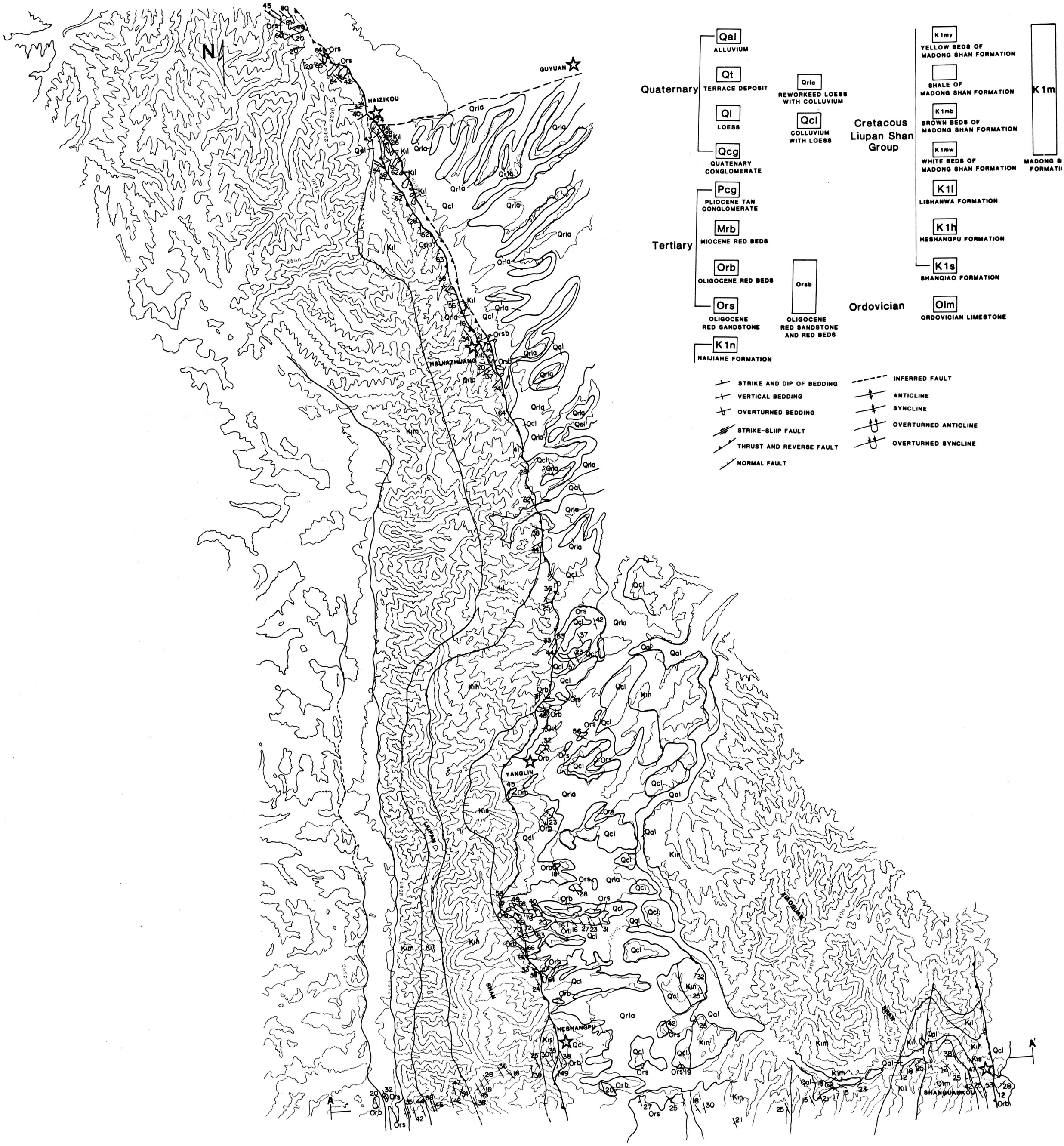

Figure 3 of Chapter V

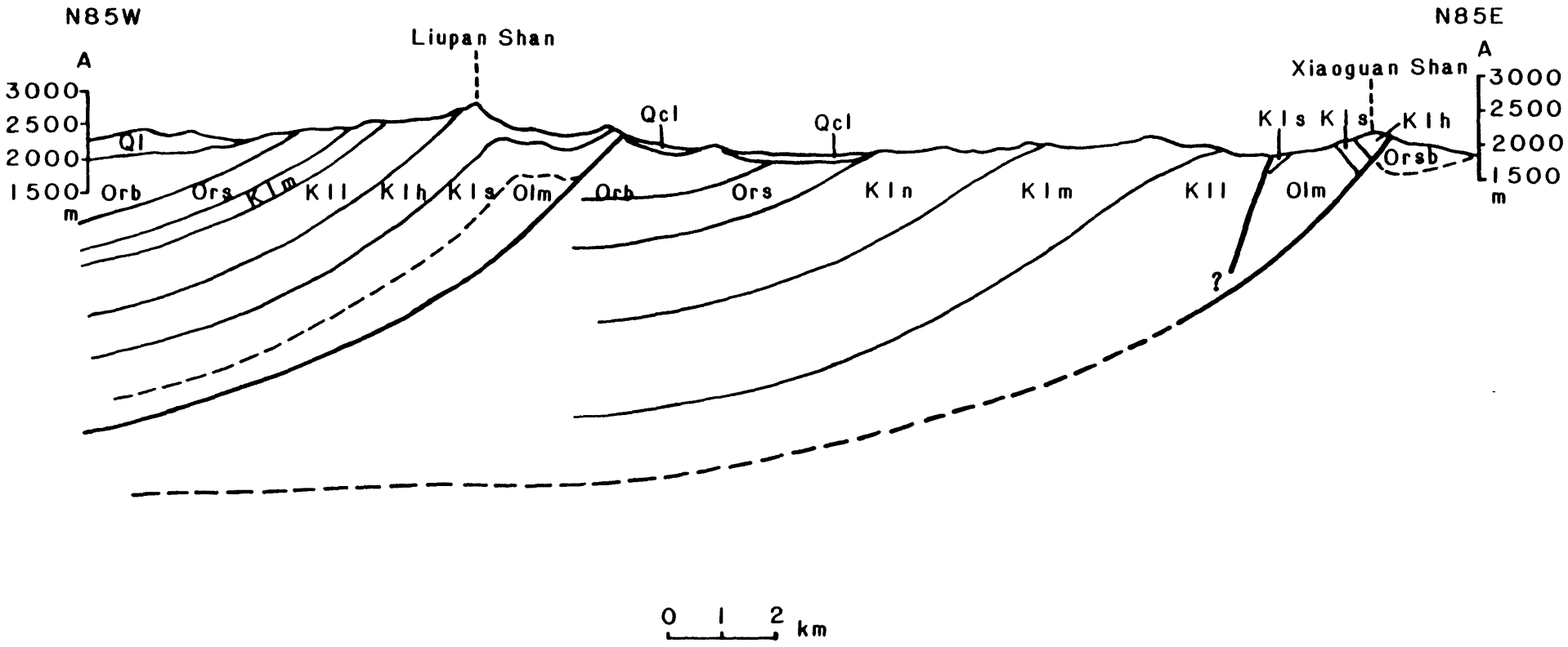
N85W
A
3000
2500
2000
1500
m
Liupan Shan
Ql
Orb
Ors
K l m
K l l
K l h
K l s
Olm
Qcl
Qcl
Orb
Ors
K l n
K l m
K l l
?
Xiaoguan Shan
K l s
K l s
K l h
Orsb
Olm
N85E
A
3000
2500
2000
1500
m
0 1 2 km

Figure 4

FIGURE 5

SEE THE FOLDED MAP SHEET

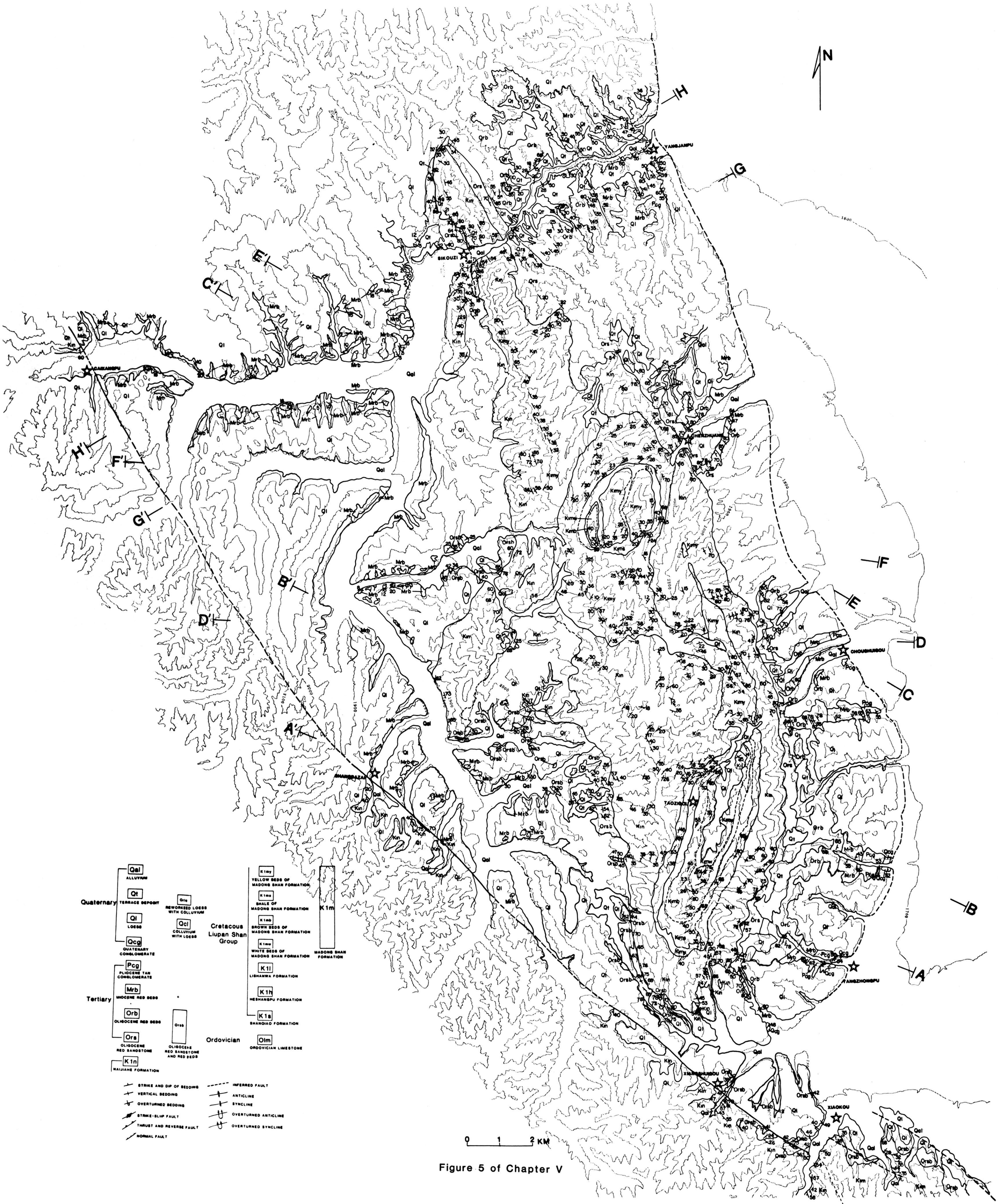

Figure 5 of Chapter V

Figure 6

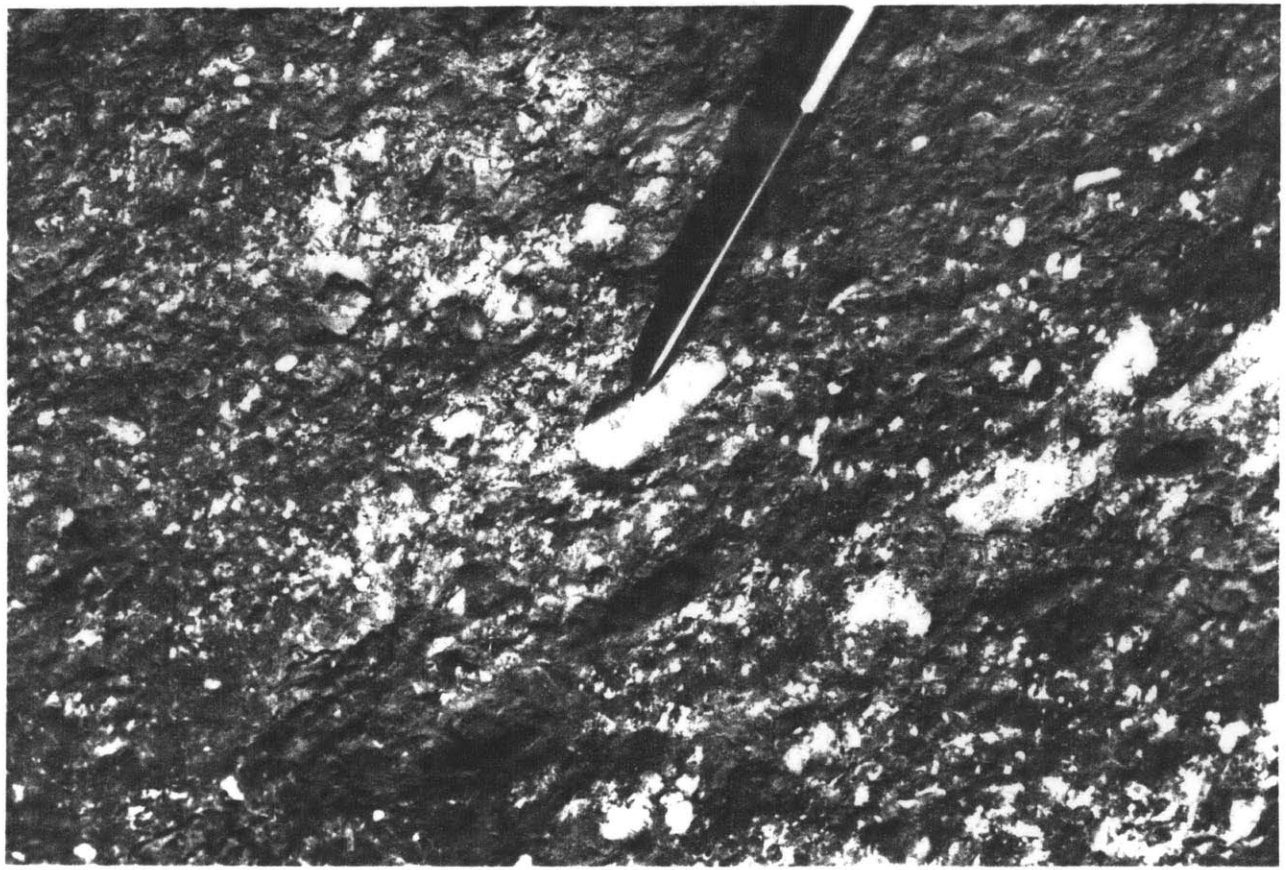

Figure 7

Figure 8

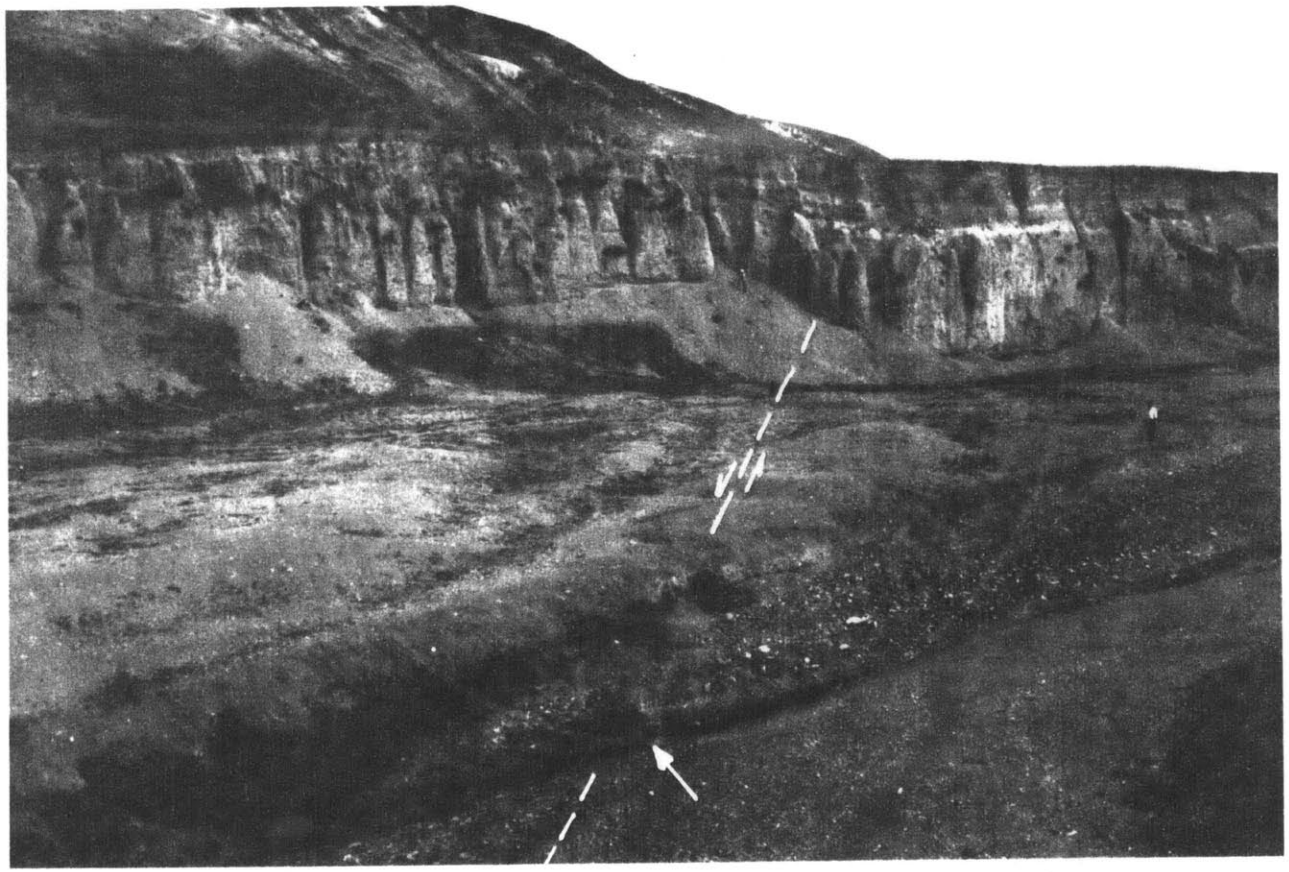

Figure 9

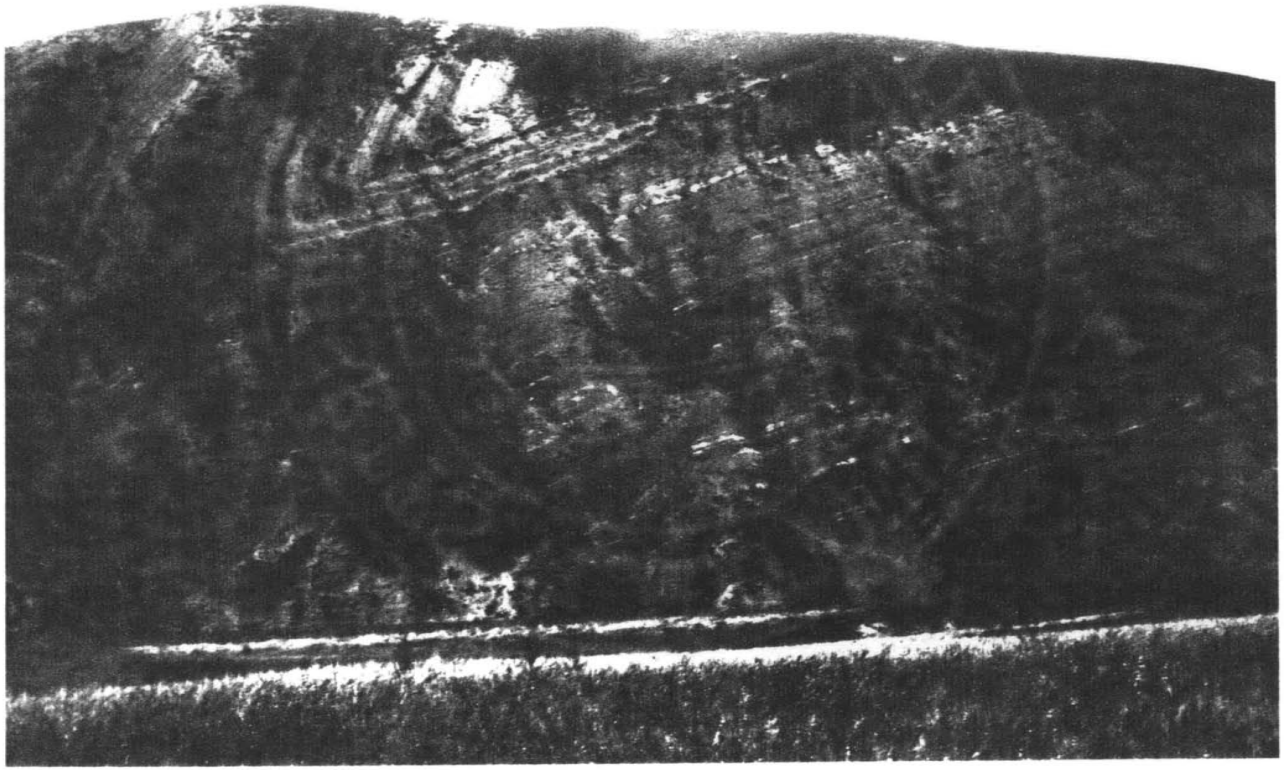

Figure 10

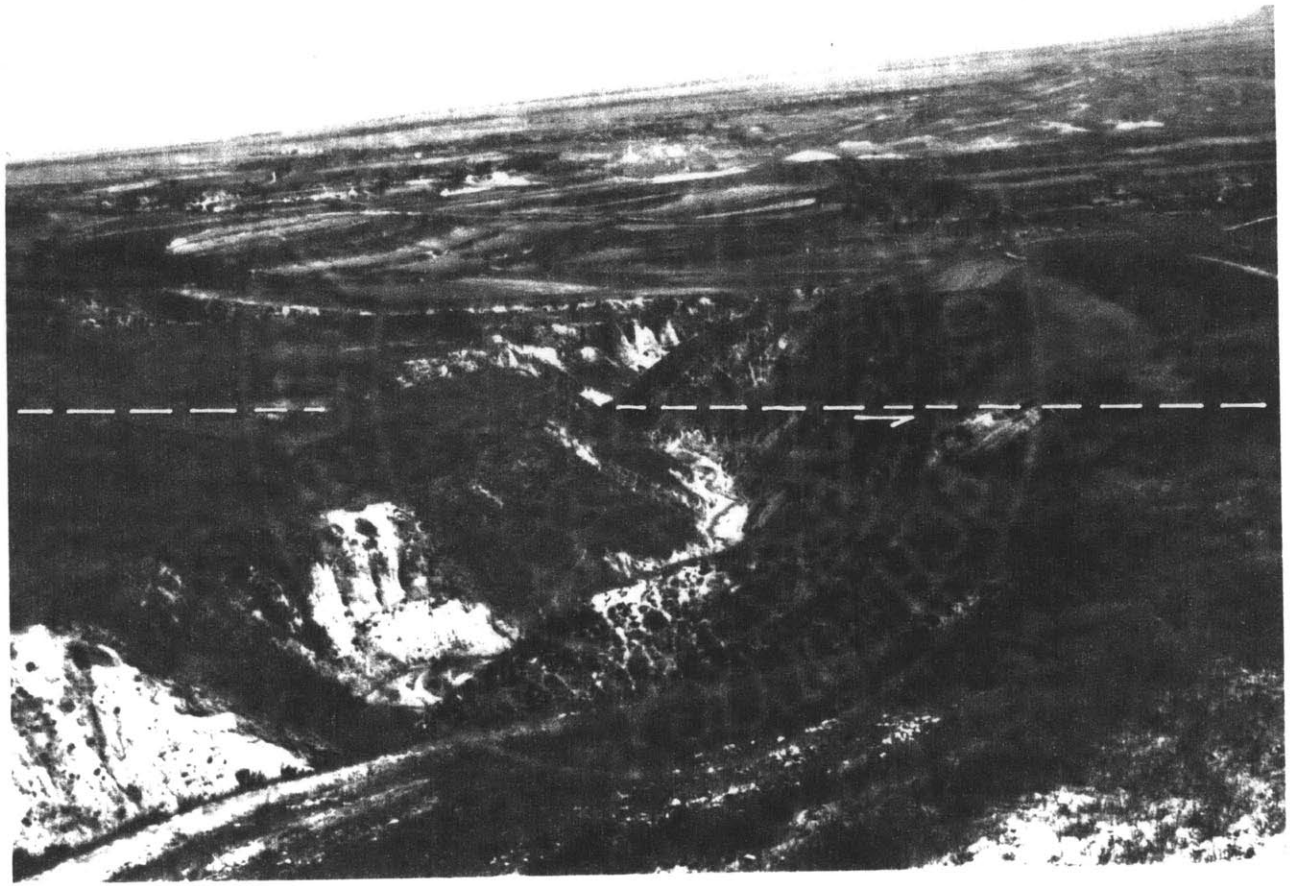

Figure 11

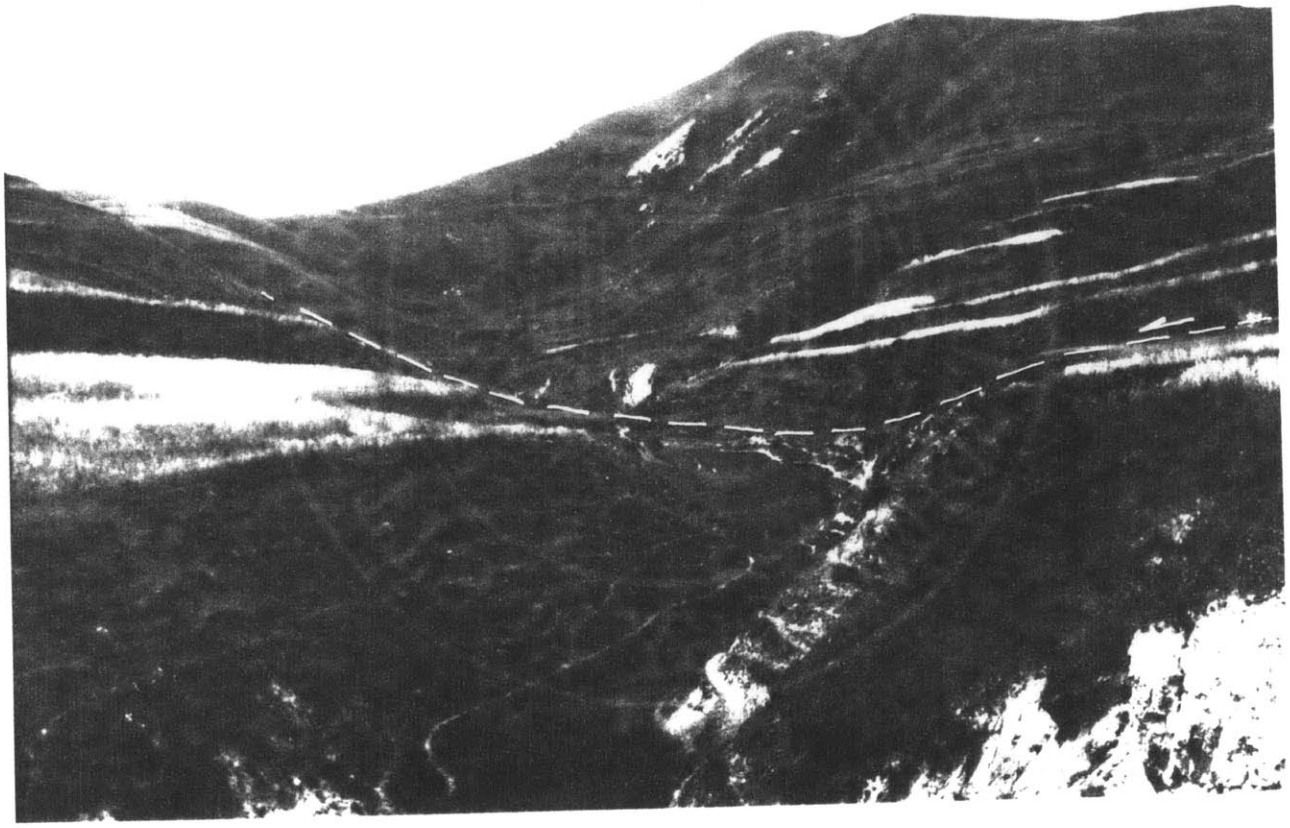

Figure 12

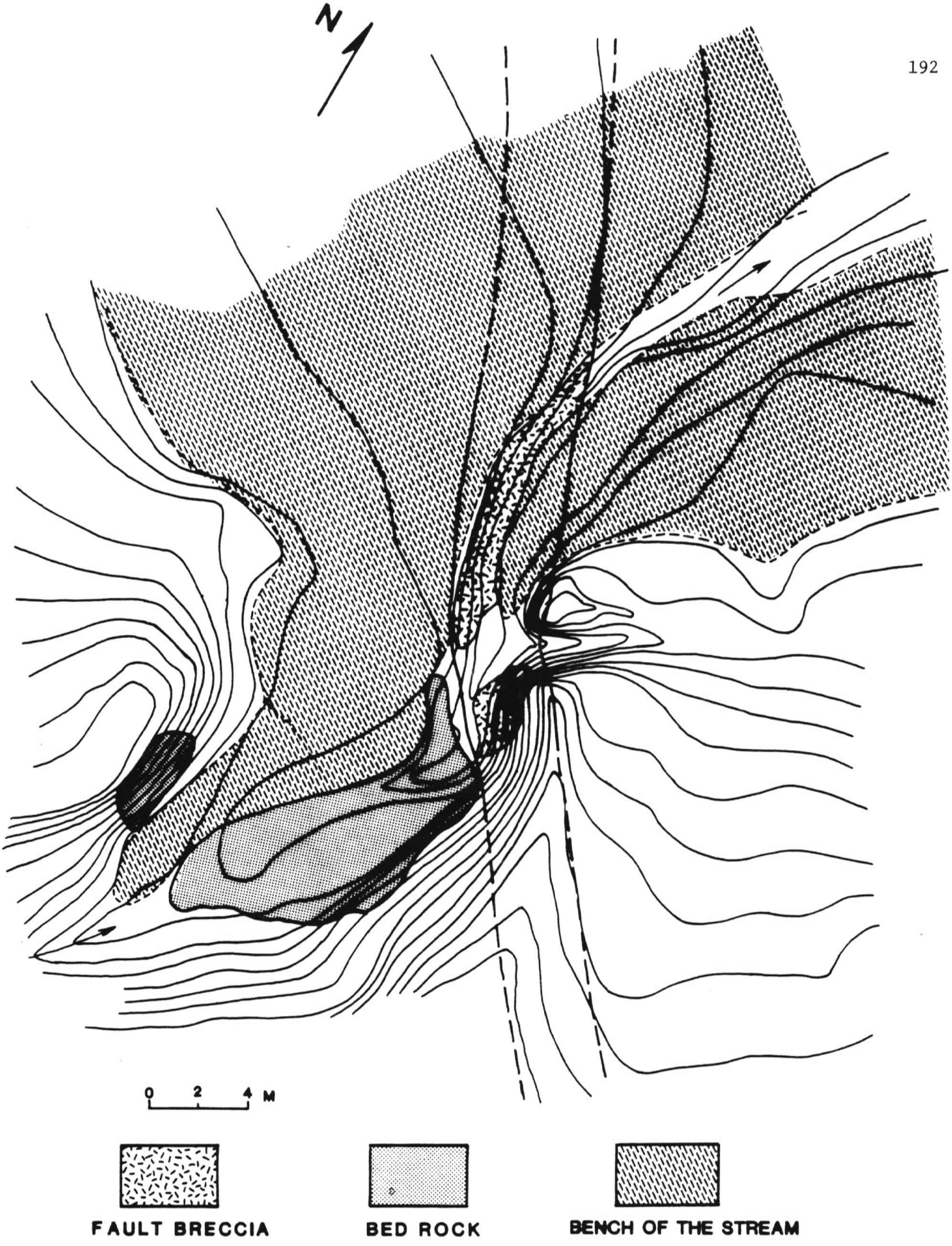

Figure 13

Figure 14

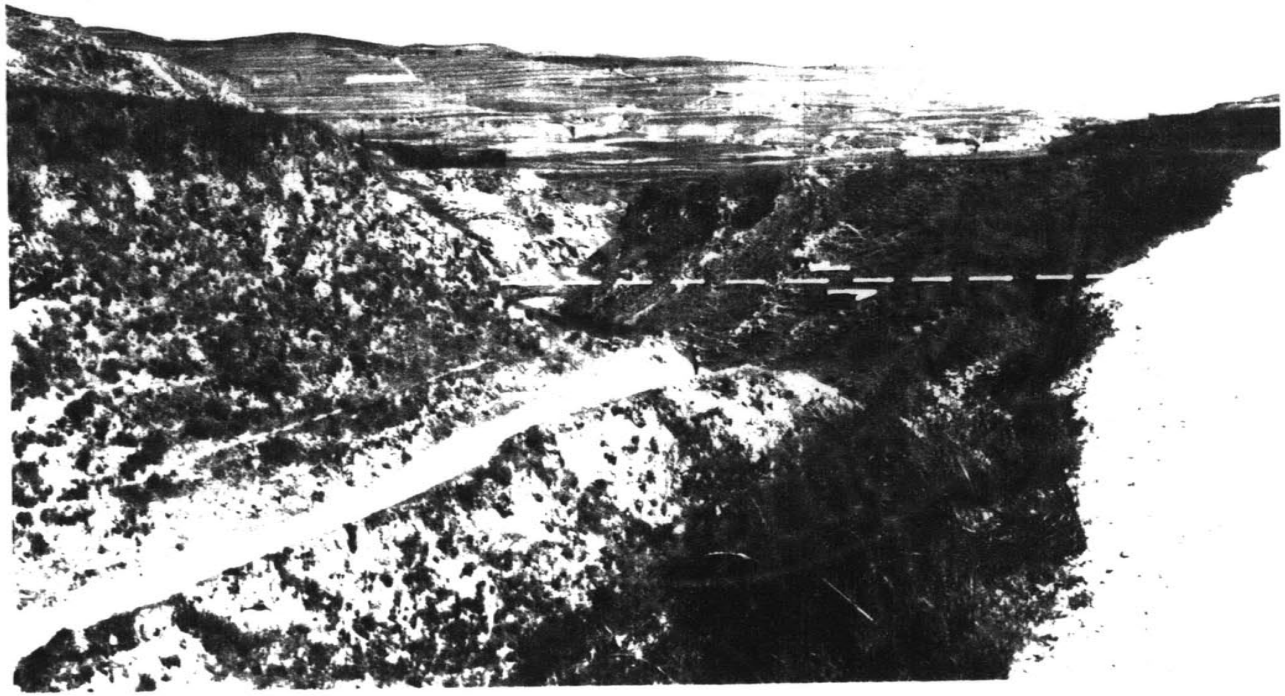

Figure 15

Figure 16

Figure 17

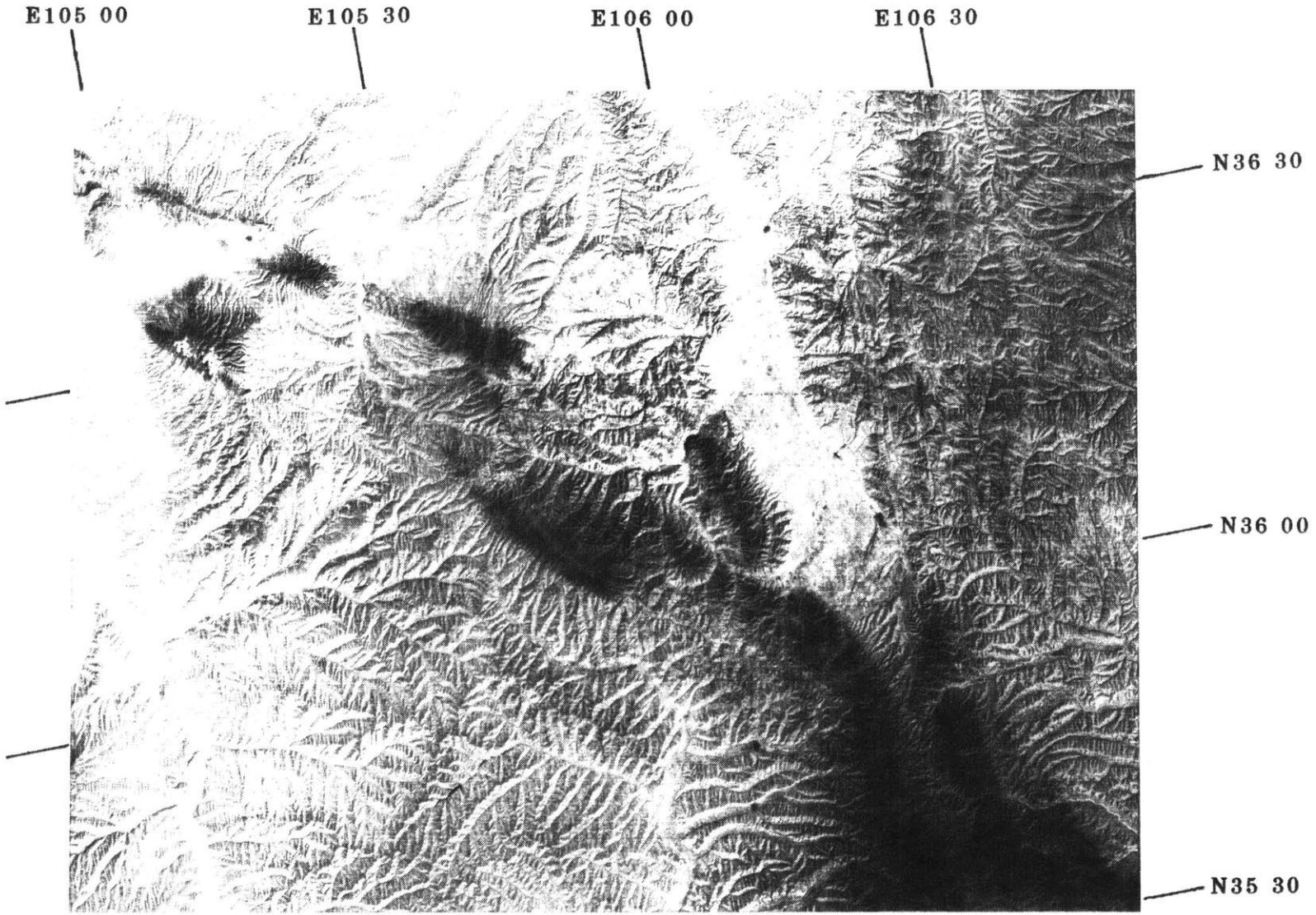

Figure 18A

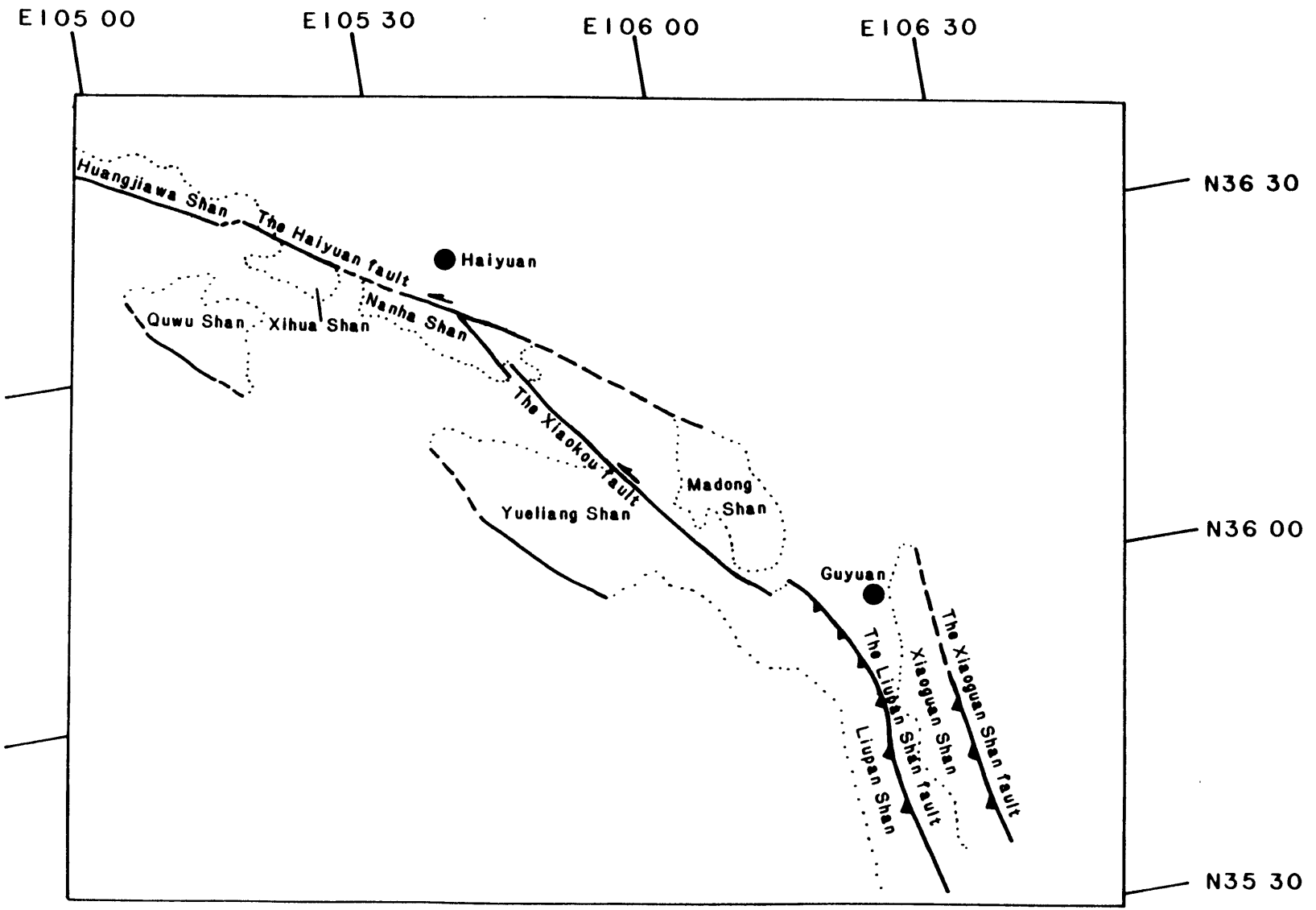
E105 00
E105 30
E106 00
E106 30
N36 30
N36 00
N35 30
Huangjiawa Shan
The Haiyuan fault
Haiyuan
Quwu Shan
Xihua Shan
Nanhe Shan
The Xiaokou fault
Madong Shan
Yueliang Shan
Guyuan
The Liupan Shan fault
Xiaoguan Shan
The Xiaoguan Shan fault
Liupan Shan

Figure 18B

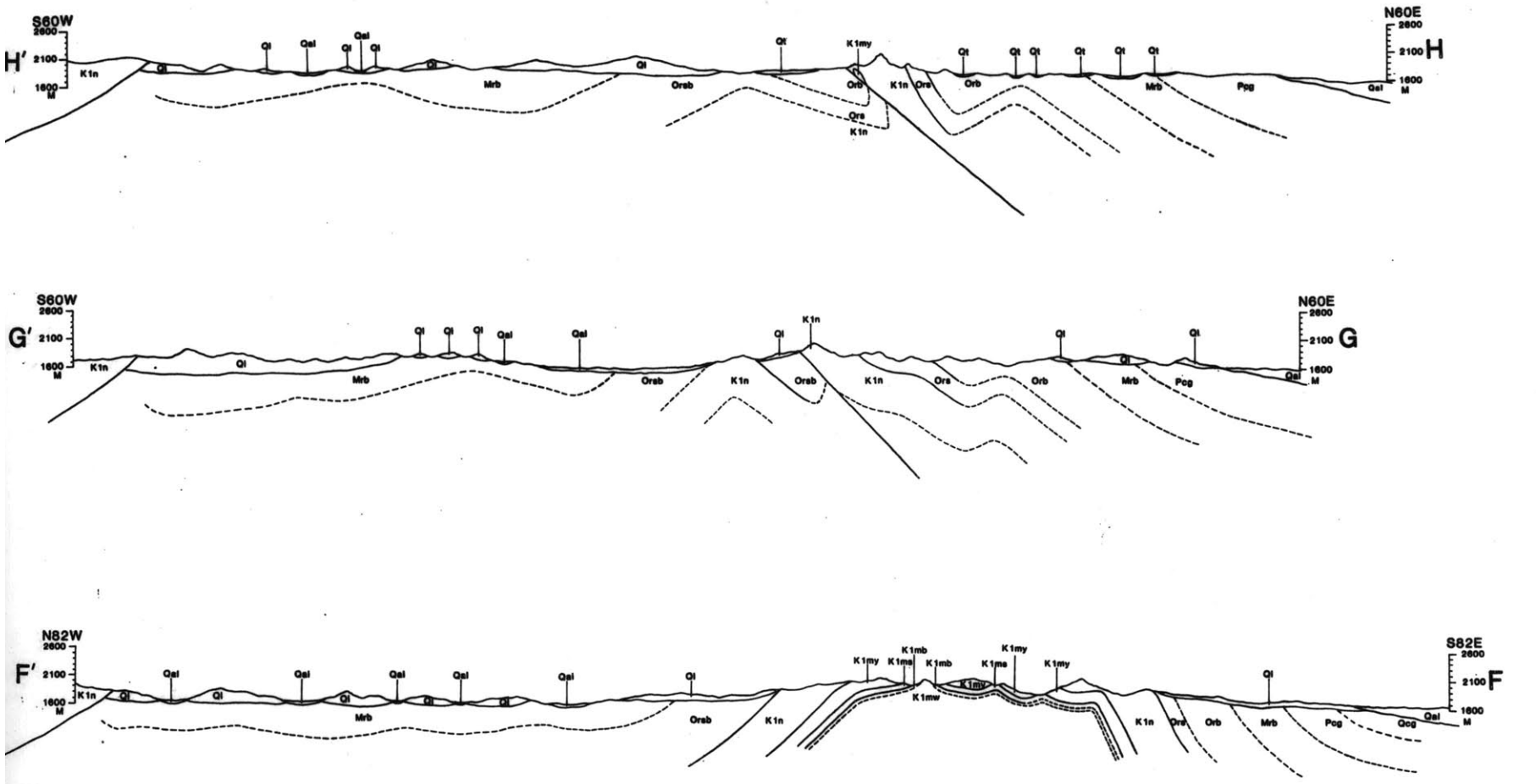

Figure 19 of Chapter V

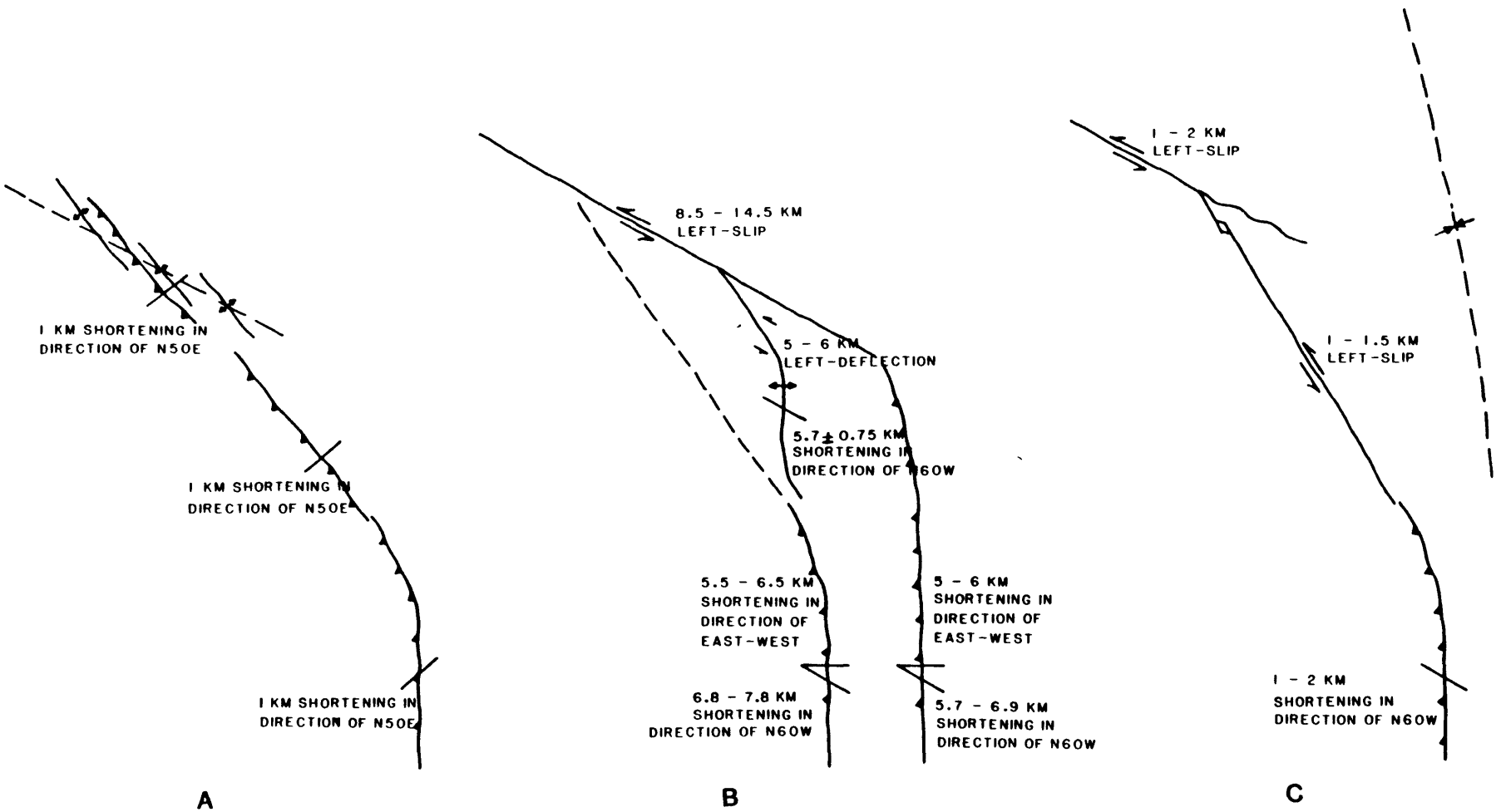
1 KM SHORTENING IN
DIRECTION OF N50E
1 KM SHORTENING IN
DIRECTION OF N50E
1 KM SHORTENING IN
DIRECTION OF N50E
A
8.5 - 14.5 KM
LEFT-SLIP
5 - 6 KM
LEFT-DEFLECTION
5.7 ± 0.75 KM
SHORTENING IN
DIRECTION OF N60W
5.5 - 6.5 KM
SHORTENING IN
DIRECTION OF
EAST-WEST
6.8 - 7.8 KM
SHORTENING IN
DIRECTION OF N60W
5 - 6 KM
SHORTENING IN
DIRECTION OF
EAST-WEST
5.7 - 6.9 KM
SHORTENING IN
DIRECTION OF N60W
B
1 - 2 KM
LEFT-SLIP
1 - 1.5 KM
LEFT-SLIP
1 - 2 KM
SHORTENING IN
DIRECTION OF N60W
C

Figure 20

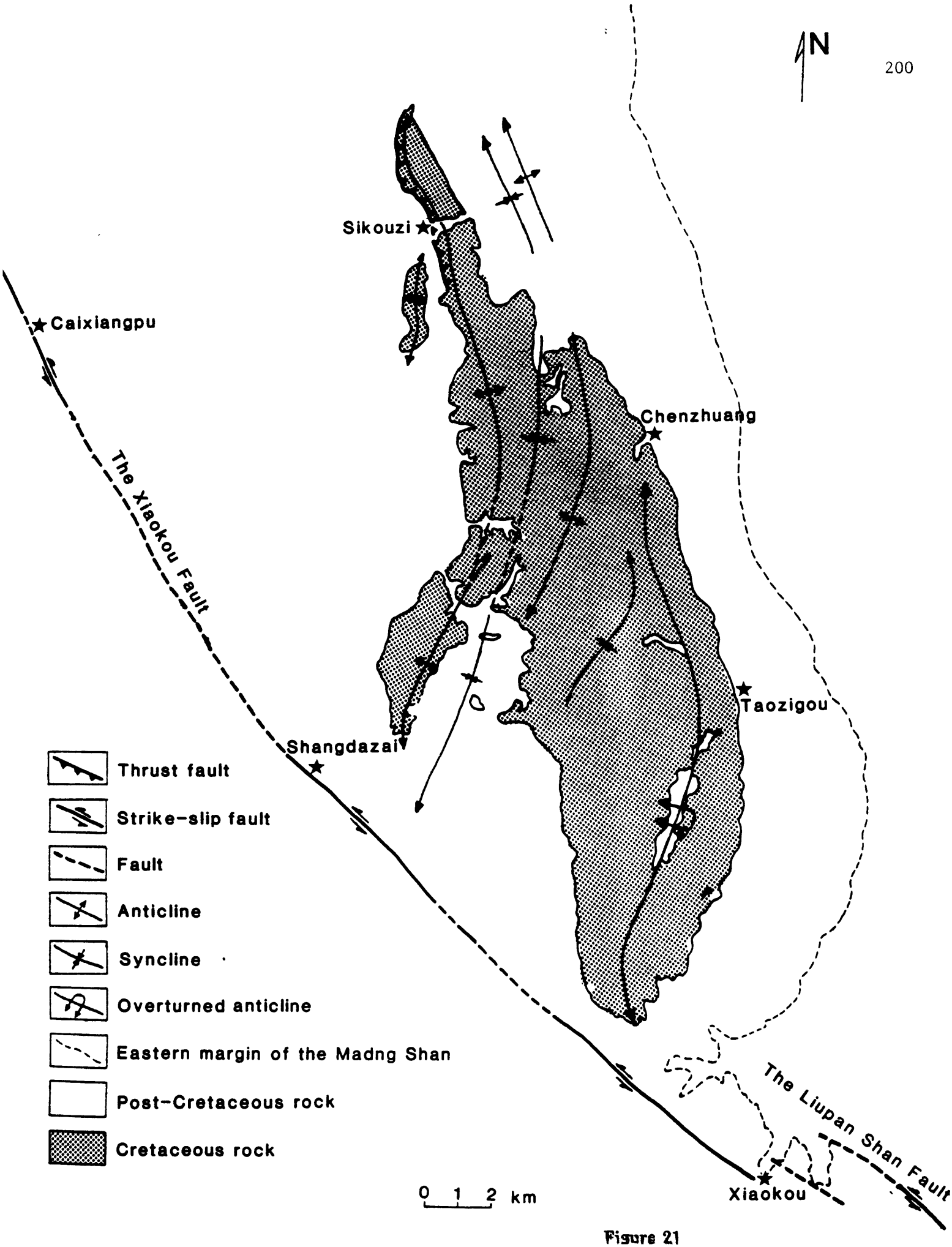
N
200
Sikouzi
Caixiangpu
Chenzhuang
The Xiaokou Fault
Taozigou
Shangdazai
Thrust fault
Strike-slip fault
Fault
Anticline
Syncline
Overturned anticline
Eastern margin of the Madng Shan
Post-Cretaceous rock
Cretaceous rock
0 1 2 km
The Liupan Shan Fault
Xiaokou

Figure 21

FIGURE 22

SEE THE FOLDED MAP SHEET

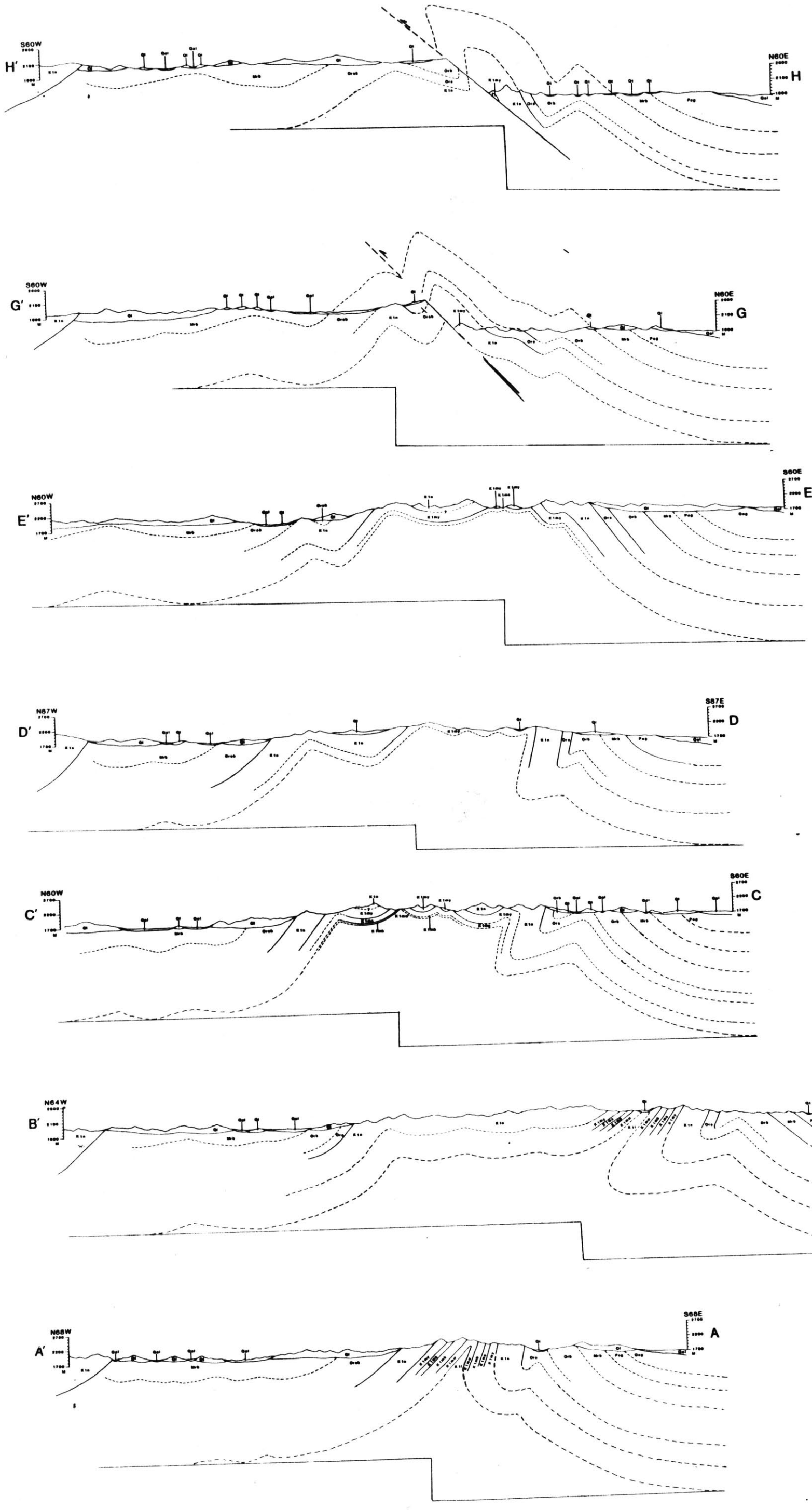

Figure 22 of Chapter V

Chapter VI

LATE CENOZOIC TECTONIC EVOLUTION OF NINGXIA AUTONOMOUS REGION, CHINA

Zhang Peizhen[1]

B. C. Burchfiel[1]

Peter Molnar[1]

Zhang Weiqi[2]

Jiao Decheng[2]

Deng Qidong[3]

Wang Yipeng[3]

Leigh Royden[1]

Song Fangmin[3]

1> Department of Earth, Atmospheric and Planetary Sciences
Massachusetts Institute of Technology
Cambridge, MA 02139

2> Seismological Bureau of Ningxia Autonomous Region
Yinchuan, China

3> Institute of Geology, State Seismological Bureau
Beijing, China

ABSTRACT

The Ningxia Autonomous region spans part of the transition from active crustal shortening and strike-slip faulting in northwestern China to active extension in northeastern China. The structures in southern Ningxia are dominated by four arcuate zones of both strike-slip faults and thrust faults with associated ramp anticlines. Deformation in these zones indicates a component of left-lateral displacement that was preceded by northeast-southwest crustal shortening. The left-slip displacement is transferred into crustal shortening on the north-south trending structural zones. The average Quaternary slip rate along the Haiyuan - Liupan Shan fault zone is 5 - 10 mm/yr, and that along the Tianjin Shan - Mibo Shan fault zone is about 1.5 - 2.7 mm/yr. The amount of offset and rate of slip along the Yanton Shan and the Niushou Shan - Dalou Shan fault zones are unknown, but the topography of the mountains suggests that the rates of slip along these zones is lower than that of the Haiyuan - Liupan Shan fault zone. The deformation in the northern Ningxia is dominated by normal faulting and extension. The Yinchuan graben has been filled by about 6000 to 7000 m of Cenozoic sediments, and the Helan Shan mountain is about 2000 m above the Yinchuan basin. The average rate of vertical separation in Quaternary time along the East Helan Shan fault is estimated to be at least 2.0 mm/yr. The opening of the Yinchuan graben is probably in partly related to left-lateral slip on the Niushou Shan and Dalou Shan fault zone. The northeastern margin of Tibetan Plateau is probably being elevated by the irregular growth of convergent and left-slip structural zones. The evolution of

deformation along the Haiyuan - Liupan Shan structural zone probably foreshadows the future deformation in the ranges north of it.

INTRODUCTION

The geology of western China differs from that of northeastern China in both geological history and present seismotectonics (Huang, 1980; Zhang et al., 1984; Deng et al., 1979; Wang et al., 1985). The Cenozoic tectonics of western China, which includes of Tibetan Plateau and the area north of it, is dominated by thrust and strike-slip faulting, but in northeastern China, extension appears to be the dominant tectonic process. The Ordos block is surrounded by normal faults except along its southwestern side. The Ningxia Autonomous Region spans part of the transition from active crustal shortening and strike-slip faulting in western China to active crustal extension in northeastern China (Figure 1).

The neotectonics of southern Ningxia is dominated by strike-slip faulting and crustal shortening. The structures in southern Ningxia consist of four arcuate zones of both strike-slip faults and thrust faults with associated ramp anticlines (Figure 2). These structures form an arcuate structural system along the northeastern margin of the Tibetan Plateau that has created the topographic features of southern Ningxia (Figure 2 and 3). From south to north the individual structures that comprise this arcuate system are: the Haiyuan - Liupan Shan fault zone; the Tianjin Shan - Mibo Shan fault zone; the Yanton Shan fault zone; and the Niushou Shan - Dalou Shan fault zone. Each of these fault zones consists of west-northwest trending faults with major left-slip components and north-northwest trending thrust faults or folds with minor strike-slip components. North of the Niushou Shan - Dalou Shan

fault zone, the structures are dominated by normal faults, which have formed along both the east and west sides of the Helan Shan. The subsidence of the Yinchuan graben, which is bounded on both sides by normal faults, is the site of more than 6000 m of latest Eocene or early Oligocene to present sediments.

In a previous paper (Deng et al., 1984), we briefly described the active tectonics of the Ningxia region and adjacent areas based on our reconnaissance work and studies of Landsat imagery. We also studied geological evolution, kinematic history, and amount, rate and style of deformation in the Haiyuan and Liupan Shan area (Burchfiel et al., 1987; Zhang et al., 1987c), which is the southernmost arcuate structural zone in southern Ningxia (Figure 2). In this paper we describe our field geological mapping and investigation on the Tianjin Shan - Mibo Shan zone, Niushou Shan - Dalou Shan fault zone and the Helan Shan and Yinchuan graben, in order to understand when and how deformation occurred in different parts of the Ningxia region and its relation to the development of the northeastern margin of Tibetan Plateau.

TERTIARY RED BEDS IN NINGXIA REGION

The ages of rocks exposed in southern Ningxia range from Cambrian or pre-Silurian to Quaternary. Paleozoic and Mesozoic rocks have been folded and faulted during pre-Cenozoic deformation. Petrological and structural features show that during Paleozoic and perhaps part of Mesozoic time, southern and northern Ningxia had different stratigraphic and tectonic histories (Zhang et al., 1987C). A fault zone through the Niushou Shan - Dalou Shan region separates these

geological units (Wang et al., 1985; Huang, 1980), but the detailed geological history and kinematic features along this zone are poorly known.

After the deposition of lower Cretaceous rocks, the entire Ningxia region appears to have been uplifted and subject to erosion, as Upper Cretaceous rocks are missing from this area. A large Tertiary basin was formed in late Eocene or Oligocene time in what is now the northeastern margin of the Tibetan Plateau and included much of Ningxia region (Figure 4). From Oligocene to Pliocene time, this large Tertiary basin received 3 to 4 km of red mudstone, siltstone, sandstone, and conglomerate. There are no unconformities between stratigraphic units, and the transition from one formation to another is gradual.

Most of the Quaternary sediments were formed during deformation and reflect deposition in local environments from local sources. They unconformably overlie all preexisting rocks and structures (Burchfiel et al., 1987; Zhang et al., 1987c). We will not describe in detail the Quaternary units in Ningxia area, because the lack of age control on these units makes it impossible to correlate accurately the separate and locally restricted units. The similar lithological features and abundant fossils within most of the Tertiary formations enable us to correlate these formations in different areas, however, so that the time of initiation Cenozoic deformation can be constrained, but it is much more difficult to correlate events within the Quaternary. All the fossils mentioned in the following sections are collected and dated by the Ningxia Geological Bureau (1974, 1976, 1980). In the following we describe the Tertiary formations, and use fossil evidence to correlate

them throughout the Ningxia region.

SIKOUZI FORMATION (Ors) The oldest formation in the Cenozoic rock sequence, the Sikouzi Formation, consists of red conglomerate and red sandstone (Ningxia Geological Bureau, 1974). In the Liupan Shan and Haiyuan area quartz-rich sand forms sandstone and also the matrix of the conglomerate layers in the Sikouzi Formation. The conglomerate generally consists of rounded pebbles and cobbles of resistant rock types such as quartzite, chert, vein-quartz, and rarely Devonian sandstone (Burchfiel et al., 1987; Zhang et al., 1987c). Its thickness varies from about 60 m to 350 m. In the Tianjin Shan, Mibo Shan and adjacent areas, the Sikouzi Formation consists mainly of dark to medium red conglomerate in its lower part and red sandstone and siltstone layers interbedded with the conglomerate in its upper part. Most of the cobbles and pebbles are derived from resistant Devonian red sandstone. Most of the clasts are angular and very poorly sorted, and range from 2 to 20 cm in diameter. The pebble imbrication south of Xiao Hong Gou (Figure 3) indicates that they were derived from northeast. The thickness of the Sikouzi Formation in Tianjin Shan is more than 1000 meters. In the Helan Shan and Yinchuan graben area, the Sikouzi Formation also consists of about 700 m of red conglomerate with sandstone and mudstone interbeds. Most cobbles within the conglomerate are angular and very poorly sorted, and they are composed of slate, limestone, and sandstone from local Paleozoic rocks. The colors of the cobbles are mainly grey, yellow and orange, but the matrix is red mud and sand. There are no fossils from the Sikouzi Formation, and its thickness and composition change from place to place. We regard it as a basal conglomerate of probable Oligocene age. The age

and correlation of this formation is based on its relation to units of known age. It unconformably overlies early Cretaceous rocks and it conformably underlies dated Oligocene red beds. Its age could be late Cretaceous or early Tertiary, but because it forms a gradational contact with Oligocene red beds we consider it to be latest Eocene or early Oligocene in age.

QINSHUIYIN FORMATION (Orb) The Qinshuiyin Formation consists of red sandstone, siltstone, and mudstone with evaporite beds. The thickness of the Qinshuiyin formation ranges from 700 to 1070 m. It crops out throughout the Ningxia region, and rests conformably on the Sikouzi Formation. The Qinshuiyin Formation consists mainly of maroon and dark red, well bedded to massive sandstone and mudstone with beds of red quartz-rich sandstone and thin beds of green or white siltstone and evaporite deposits. Beds of gypsum 20 cm to 1 m thick are present within the lower and middle parts of this formation and become less common in its upper part. This formation can be easily distinguished from other units by the presence of evaporite beds. The abundance of fossils within the formation allows us to correlate the outcrops in different places. In the Liupan Shan and Haiyuan area, the following fossils are reported: Cyprinotus formalis, Cyprinotus beljaewskyi, Eucypris longa, Baluchitherium sp., Tsaganomys altaicus, Bithynia sp., Unio sp., and Darwinula sp.. In the Tianjin Shan and Mibo Shan area, the following fossils are found: Cyprinotus formalis, Eucypris longa, Cyprinotus beljaewskyi, and Baluchitherium sp.. In the Helan Shan area, Baluchitherium grangeri, and Chilotherium sp. have been reported in this formation. All the fossils have been collected and identified by the

Ningxia Geological Bureau (1959, 1974, 1976, 1980). They date this formation as Oligocene in age.

HONGLIUGOU FORMATION (Mrb) The Hongliugou Formation conformably overlies the Oligocene Qinshuiyin Formation, and consists of a 280 m to 960 m sequence of red to tan mudstone with sandstone present in its upper part. The contact between the Hongliugou and Qinshuiyin formations is gradational through several tens of meters and is marked by a change in color, bedding, and grain size. The rocks of Hongliugou Formation are generally more massive, and in many places bedding is impossible to identify. In the upper part of the formation, the grain size becomes coarser and the bedding becomes better developed. A few thin conglomerate beds are present in the upper few tens of meters of this formation. Clasts in the conglomerate are dominated by resistant rock types such as white vein-quartz, quartzite, and Paleozoic red sandstone, with rare clasts of granite and schist.

The bedding characteristics, color, and grain size are used for a lithological correlation of the outcrops throughout the Ningxia region. The fossils from different places provide the age control on the Hongliugou Formation. In Haiyuan and Liupan Shan area, the following fossils have been reported: Mastodon sp., Testudo sp., and Limnocythere sp. In the Tianjin Shan and Mibo Shan area, Limnocythere Cinctura, C. Kirgizica, Condona cf. subita, limnocythere sp., Platybelodon sp., Gomphotheriidate indet., Amyda sp., Stephanocemas sp., and Cervidae have been reported. No fossils have been reported from the Helan Shan area, and the correlation of rocks to the Hongliugou Formation is based solely on lithology. All the fossils have been collected and identified by the

Ningxia Geological Bureau (1959, 1974, 1976, 1980). They date the Hongliugou Formation as Miocene in age.

GANHEGOU FORMATION (Pcg) Lying conformably above the Hongliugou Formation is 240 m to 800 m of conglomerate and sandstone of the Ganhegou Formation. The conglomerate consists of pebbles, cobbles, and boulders composed dominantly of white vein-quartz, fine-grained grey or white quartzite and chert, red sandstone and conglomerate, marble, schist, gneiss, and rare granite. Much of the matrix of the conglomerate is quartz, feldspar, and lithic grit, and the interbedded sandstone is generally coarser grained than the sandstone in the underlying Oligocene and Miocene rocks. This coarse conglomerate contains material denuded from all the older rocks, and their deposition marks the onset of Cenozoic deformation.

Fossils reported from the Haiyuan and Liupan Shan area are Ilyocypris cf bradyi, Candona sp., Limnocythere luculenta, Cadoniella sp., Cyprinotus sp., Chara sp., and Cathaica sp.. In the Tianjin Shan and Mibo Shan area, Paracondona sp., Hipparion sp., Rhinoceros sp., Bovinae, Elasmotheriidae indet., and Rhinocerotidae indet. have been reported. In the Helan Shan area this formation is missing. All the fossils date the Ganhegou Formation as Pliocene in age (Ningxia Geological Bureau, 1959, 1974, 1976, 1980).

STRUCTURE OF THE NINGXIA REGION

We have mapped in detail two large areas within the southern Ningxia region: one along the Haiyuan fault zone (Burchfiel et al., 1987) and the second in the Liupan Shan area (Zhang et al., 1987c). In

addition, we have mapped small areas along the Tianjin Shan - Mibo Shan fault zone (Figure 3), and we have visited all the other structural zones in the Ningxia region (Deng et al., 1984). These data serve as a basis for understanding the structural development of these fault zones and their relation to the growth and evolution of the northeastern margin of the Tibetan Plateau.

THE HAIYUAN - LIUPAN SHAN FAULT ZONE

The Haiyuan fault zone is located in southern Ningxia along the northern foot of the Nanhua Shan and Xihua Shan mountains (Figure 2). The strike of the fault zone is generally N60° - 65°W. Slip on this fault is mainly left-slip (Deng et al., 1984; Burchfiel et al., 1987). At the eastern end of the Haiyuan fault zone is the Liupan Shan area, where the tectonics is dominated by crustal shortening (Zhang et al., 1987c). The left-slip on the Haiyuan fault has probably been transferred into crustal shortening in the Liupan Shan area.

The oldest Cenozoic structures in the Haiyuan area consist of folds and thrust faults that generally strike N30°-45°W and involve mostly pre-Quaternary rocks. These structures are characterized by brittle thrust faults in the metamorphic basement rocks and folds in the overlying sediment cover. Because Quaternary rocks are not involved in these folds and thrust faults, the deformation probably occurred in latest Pliocene time. The left-slip faults, including the N60°W trending Haiyuan fault, may have begun to develop during the late stage of this folding and thrust faulting, but the major left-lateral displacement on the strike-slip faults that trend west-northwest to west followed the

formation of the folds and thrust faults (Burchfiel et al., 1987).

By matching offset geological units, unconformities, and structures on both sides of the fault, the total left-lateral displacement along the Haiyuan fault zone is measured to be between 10.5 km and 15.5 km (Burchfiel et al., 1987). If left-slip faulting began near the end of Pliocene time or in Quaternary times, the average slip rate over Quaternary time is between 5 to 10 mm/yr (Burchfiel et al., 1987). The Holocene slip rate, determined by dating stream offsets, is 8 ± 2 mm/yr and is consistent with the average Quaternary slip rate (Zhang et al., 1987a, b).

In the east the Haiyuan fault ends in the Liupan Shan area, which structurally includes the Xiaokou fault, Liupan Shan thrust fault, Xiaoguan Shan fault, and Madong Shan fold zone (Zhang et al., 1987c). The earliest Cenozoic structures in the Liupan Shan area are thrust faults and folds in the Liupan Shan and Yueliang Shan. The youngest rocks involved in the folds and thrust faults are a Pliocene tan conglomerate probably equivalent to the Ganhegou Formation. Quaternary rocks unconformably overlie these structures. The direction of shortening during this phase was N50°-60°E, and the amount of shortening is about 1 km. It is contemporaneous with the early folds and thrust faults in the Haiyuan area (see Burchfiel et al., 1987; Zhang. et al., 1987C).

Following the formation of these structures, left-slip on the N60°W-trending Haiyuan fault zone was initiated and changed the kinematic evolution of the Liupan Shan area. The geometry and timing relations indicate that the structures in the two areas are related, and

left-slip on the Haiyuan fault zone is transferred into shortening by the folding and thrust faulting in the Liupan Shan area (Zhang et al., 1987c). Stratigraphic relations show that shortening in the Madong Shan followed the development of the earliest Cenozoic structures in the Liupan Shan area, and it was probably contemporaneous with the left-slip on the Haiyuan fault zone. The average amount of shortening across the Madong Shan is 5.7 ± 0.7 km. Most of the shortening in the Liupan Shan and Xiaoguan Shan were contemporaneous with the folding in the Madong Shan. The magnitude of horizontal shortening across the Liupan Shan and Xiaoguan Shan thrust faults is 6.8 to 7.8 km and 5.7 to 6.9 km respectively in the direction parallel to the Haiyuan fault (Zhang et al., 1987c).

Since late Pleistocene time left-slip on the Haiyuan fault has been taken up by the slip on the Xiaokou fault. As a result, the deformation in the Madong Shan and Xiaoguan Shan either has ceased or has proceeded at a very slow rate, and the thrust faulting in the Liupan Shan has continued with a left-slip component (Zhang et al., 1987c). The 1 - 1.5 km left-slip along the Xiaokou fault probably requires that shortening to the Liupan Shan thrust fault is 1 - 2 km more than that in the Madong Shan region (Figure 2). Thus, the total shortening, parallel to the Haiyuan fault, during these three phases of deformation in the Liupan Shan, Madong Shan and Xiaoguan Shan areas is 12.4 - 16.7 km, and this total is comparable to the 10.5 - 15.5 km of left-slip on the Haiyuan fault zone.

The structures in the Liupan Shan area indicate a thin-skinned style of deformation. The average depth to the decollement is about 4.5

± 0.7 km, which suggests that the decollement is well below the Cretaceous rocks that are exposed in the core of the folds and along the thrust faults. This thin-skinned geometry of structures probably can be extended to include the other zone of folds and thrust faults in southern Ningxia region.

THE TIANJIN SHAN - MIBO SHAN REVERSE FAULT AND FOLD ZONE

About 40 - 50 km northeast of the Haiyuan fault zone is the Tianjin Shan - Mibo Shan arcuate zone of folds and reverse faults (Figure 2). The area between these two zones is covered by almost horizontal or gently warped Cenozoic continental sedimentary rocks that form a broad syncline or structural basin. Tectonic activity within this area is generally mild in comparison with that in the surrounding structural zones, and most of the deformation has occurred within the arcuate mountain ranges, where folds and thrust or reverse faults are well developed. We mapped several segments along the Tianjin Shan and Mibo Shan fold and thrust zone (Figure 3), where late Cenozoic deformation is similar to that of the Haiyuan and Liupan Shan zone.

HONG GOU LIANG In the western part of Tianjin Shan (Figure 2 and 3), the structure is dominated by east-west or northwest-trending thrust or reverse faults. Paleozoic formations have been thrust over one another and over Tertiary red beds. Near Hong Gou Liang, 4 or 5 thrust faults are present (Figure 5).

The southernmost fault strand is a thrust fault that dips about 45° to the southwest. The hanging wall of this thrust fault consists of light green metamorphosed phyllite, sandstone and slate with some

marble, cherty limestone, and siliceous dolomite interbeds. Abundant trilobites are reported from this formation in the Tianjin Shan (Ningxia Geological Bureau, 1976) and they include Inouyia capax, Metagrulos sp., Porilorenzella sp., Wuania sp., and Proasaphiscus sp. These fossils date the formation as early Middle Cambrian. The Cambrian rocks have been thrust over thick limestone in the footwall. The dark gray limestone contains cherts and cherty layers in the lowest outcrops of this formation. Fossils in the limestone are are abundant and, include trilobites, such as Geragnostus cf. wimani, Bathyuriscops kantsingensis, Asaphus sp., Basiliella sp., and Pleiomgalaspis sp. as well as cephalopoda Anthoceras sp. and Notocycloceras sp., which date the limestone as early Ordovician in age (Ningxia Geological Bureau, 1976). This fault appears to be one of the major strands in the Tianjin Shan fault zone. At the west end of our map, the thrust fault places the Cambrian rocks above the Carboniferous rocks. Farther west, it trends almost east-west, and the Cambrian phyllites have been thrust directly over the Tertiary red beds (Figure 5).

The next fault to the north at Hong Gou Liang crops out as a high angle (about 70°) reverse fault along which the Ordovician limestone is faulted against Devonian red beds (Figure 5). The red beds consist mostly of red quartz-rich sandstone. The fossils Antiarchi, Bothriolepis sp., and Actinolepidoe date the red beds as late Devonian in age (Ningxia Geological Bureau, 1976). About 20 m to the north is another southwest-dipping, high- angle reverse fault. The Devonian red beds in the hanging wall are juxtaposed against black shale and siltstone in the footwall. The shale and siltstone are characterized by

abundant coal beds and white sandstone interlayers. Many fossils have been reported from these rocks: such as Rhodea hsianghsiangensis, Triphyllopteris collumbiana, Sunlepidodendron mirabile, Sphnophyllum lungtanense, Lepidoden dron kirghizicum, Cardiopteridium spetsbergense, Athyris sp., Theodossia sp., Schuchertella cf rornensis, Cancrinella Tenuistriatus, and Streptorhynchus sp. (Ningxia Geological Bureau, 1976). The fossils date the black shale and siltstone as early Carboniferous in age. The displacements on this fault and on the one 20 m to the south are small, and both faults are cut at both ends by the large thrust fault south of them (Figure 5).

To the north, Carboniferous rocks have been thrust over Permian sandstone and shale. To the east and west along the same fault the Carboniferous rocks are thrust over Tertiary red beds (Figure 5). The Tertiary red beds consist of Oligocene red mudstone and siltstone with gypsum layers and belong to the Qinshuiyin Formation. They unconformably overlie the Permian rocks, but in some places there are minor faults present at the contact between them. Farther to the north, both the Tertiary red beds and Permian rocks are covered by loess and Quaternary alluvium. We infer the presence of another reverse or thrust fault, which lies underneath the cover at the front of the Tianjin Shan, because west of Hong Gou Liang the Tertiary red beds dip to the south at an angle of more than 80°.

There are several stream channels that appear to be offset across the fault that thrusts the Carboniferous rocks over Tertiary red beds and Permian sandstone. At one place near Hong Gou Liang about 5 to 6 m wide has been offset about 30 m left-laterally. Two adjacent small

streams are both offset 6 ± 2 m (Figure 6 and 7), and the fault surface is exposed at the stream offset. Along this part of the fault, black Carboniferous rocks crop out on the south side of the fault and red Tertiary rocks crop out on the northern side. Several ridges are also offset, but they have irregular morphology and the amount of offset cannot be measured accurately.

West of the area that we mapped, there is an offset within the Cambrian rocks (Figure 2) recently studied by two of us (Zhang Weiqi and Jiao Decheng). The unconformity between the Cambrian rocks and the Tertiary red beds has been offset left-laterally 3.6 ± 1 km (see point A, Figure 5). Also, another series of small stream channels in this area have been offset left-laterally 4 to 6 m.

East of Hong Gou Liang, the major thrust fault splays into several strands. All of the faults dip about 70° to 80° to the south. The dips of Paleozoic rocks between these faults also dip very steeply. Along the foot of the mountains, Tertiary red beds unconformably overlie Devonian red beds. There are low hills north of the main mountain front (Figure 8) that are underlain by Tertiary red beds that are unconformably overlain by loess. The Tertiary red beds are folded into a syncline (Figure 5). Near the northern edge of these hills, the Tertiary red beds are tilted and dip southward toward the mountains, with steeper dips toward the north. This suggests that there may be a thrust fault or blind thrust underneath the low hills of Tertiary rocks. The modern alluvial fans that spread northward south of the low hills are deflected and end against the northern most ridge of Tertiary rocks, indicating the very young age of the folding and faulting.

QINGEDA About 20 km southeast of Hong Gou Liang, near Qingeda, the trends of both the mountain front and the structures are N30°-40°W (Figures 3 and 9). The high mountains west of Qingeda consist mainly of thick, dark grey Ordovician limestone (Ningxia Geological Bureau, 1976). Tertiary red conglomerate, probably equivalent to the Sikouzi Formation, unconformably overlies the Ordovician limestone (Figure 9). A basal conglomerate, which contains angular boulders of dark grey limestone from the underlying rocks, is clearly present near the contact. Farther from the contact, roughly 50 meters above it, most of the cobbles and pebbles within the conglomerate are Devonian red sandstone and siltstone.

Near Qingeda is a N45°W trending high-angle fault that dips steeply to the west. The hanging wall of the fault consists of Tertiary red conglomerate (Sikouzi Formation) that, near the fault, dips steeply to the west and forms a hanging-wall syncline. The geometry of the syncline and the fault suggests that western side of the fault moved down, and therefore that the fault is a high-angle normal fault. The east side of the fault consists of Ordovician to Carboniferous rocks that strike roughly east-west to west-northwest and are repeated several times. Their relation to the west-dipping fault and their structural evolution, however, are not clear due to insufficient mapping of this area. The west-dipping fault, which does not make range front, appears to be inactive.

The area east of Qingeda is mostly covered by loess and Quaternary alluvial fans. About 5 km northeast of Qingeda, some Tertiary conglomerate and Devonian red beds crop out (Figure 9). Tertiary tan

conglomerate, mapped as the Sikouzi Formation) west of the Devonian red beds, dips to the west, but the relation between the two formations is unknown because of Quaternary loess cover. The Devonian rocks have been folded; a syncline and an overturned anticline are present in the Devonian outcrop (Figure 10). East of the Devonian outcrop is a valley covered by Quaternary sediment, and Tertiary conglomerate crops out east of the valley. The conglomerate dips 62° to the northeast at the western front of the outcrop, but about 20 m to the east it dips only 15° to the northeast. From these relations we infer a thrust fault or blind thrust east or between the easternmost outcrops of the Tertiary conglomerate and probably another thrust fault west of these rocks.

XIAO HONG GOU Xiao Hong Gou is located only about 4 km southeast of Qingeda along the same mountain front (Figure 3), but the structural pattern is very different from that in the Qingeda. About 2 km northwest of Xiao Hong Gou, Quaternary alluvium directly overlies Carboniferous rocks. At one place, it appears that Carboniferous rocks have been thrust over Quaternary sediments, but in most places the fault is not clear. About 0.5 to 1 km northwest of Xiao Hong Gou, red beds of Oligocene, Miocene, and Pliocene age overlie the Carboniferous rocks, and the Quaternary sediments unconformably overlie all of them. The Tertiary rocks have been folded into a syncline and an overturned anticline within the Tertiary red mudstone of the Hongliugou Formation (Figure 11).

South of Xiao Hong Gou, the Carboniferous black shale and siltstone are unconformably overlain by Tertiary rocks both to the north and south. Along the western side, Permian sandstone and siltstone are

faulted against the Carboniferous rocks (Figure 11). A sequence of thick-bedded red conglomerate (Ocg in Figure 11), which consists of cobbles mostly from Devonian red beds, unconformably overlies the Permian sandstone. The age of this conglomerate is unknown. This conglomerate has been cut by a west-dipping high-angle fault and is juxtaposed against a very thick (at least several hundred meters) sequence of Tertiary red conglomerate that consists of cobbles and pebbles from both Devonian red beds and Permian sandstone. This thick conglomerate is tentatively correlated with the Sikouzi Formation. Only in one place west of Xiao Hong Gou does the young Tertiary red conglomerate (Ors) unconformably overlie the older conglomerate (Ocg). The structures within the nearly vertical Carboniferous rocks southeast of Xiao Hong Gou are very complex. The black shales have been folded and sheared, and the overall structural pattern within them is unknown. Because these rocks are much more intensely deformed than the Cenozoic rocks, the structures are probably pre-Cenozoic in age.

The overall structure near Xiao Hong Gou is dominated by the frontal anticline, which is probably cored by Carboniferous rocks near Xiao Hong Gou. Beginning 1.5 km southeast of Xiao Hong Gou, only the Tertiary red conglomerate crops out, but the frontal anticline is clearly present, and its axis is parallel to the mountain front (Figure 11). Its eastern limb generally dips more steeply than its western limb. This frontal anticline can be traced all the way to the south end of the Tianjin Shan. We infer that it is formed above a blind thrust fault at depth.

The late Cenozoic rocks 0.5 km south of Xiao Hong Gou in a

profile well exposed along the south side of the river show well the progressive development of the structure (Figure 12). Oligocene and Miocene red beds dip steeply northeast, and all are overlain by tan conglomerate of probably Pliocene age. The Pliocene conglomerate is unconformably overlain by more gently north-dipping tan conglomerate and sandstone that might be late Pliocene or early Quaternary in age. To the north light-brown conglomerate interbedded with loess rests unconformably on the tan conglomerate, and these two units are folded into a syncline - anticline pair at the range front (Figure 12 and 13).

LIJIAPUZI AND MIBO SHAN Lijiapuzi is located at the southern end of the Tianjin Shan (Figure 3). The major structure is a north-trending anticline (Figure 14) in which Oligocene gypsiferous red beds (Qinshuiyin Formation) strike approximately north-south. At the eastern range front, the red beds dip 30° to 40° east, and in one locality they become slightly overturned, dipping west at a steep angle (Deng et al., 1984). To the west, they dip west at angles 40° to 50°, but farther west, the dip of the red beds becomes more gentle to horizontal. South of Lijiapuzi, the anticline plunges south into the Quaternary loess. We infer that this fold is related to slip on a thrust fault at depth that dips west.

About 4 km south of the end of the Tianjin Shan is the Mibo Shan. These ranges are separated by an northwest-trending syncline filled with Quaternary rocks (Figure 2 and 3). The Mibo Shan consists of two left-stepping en echelon anticlines separated by a syncline. The anticlines are cored by Oligocene red beds of the Qinshuiyin Formation and locally by the Sikouzi Conglomerate. The folds in the Mibo Shan are

arcuate and trend northwest in their western parts and progressively more northerly to the southeast. They form a right-stepping pattern with the structures of the Tianjin Shan (Figures 2 and 14).

We mapped the westernmost part of the eastern anticline in the Mibo Shan where it is cored by the gypsum-bearing Oligocene Qinshuiyin Formation (Figures 14 and 15). Along the eastern foot of Mibo Shan, the Oligocene red beds dip steeply northward beneath the Quaternary loess, and alluvium and no evidence of faulting was found along this side of the Mibo Shan. To the south, the red beds dip more gently toward the south. Farther to the south, the overlying Miocene mudstone (Hongliugou Formation) is only gently warped and is nearly horizontal. The geometry of this anticline suggests that it is cored by a blind thrust ramp that dips west at depth. The anticline generally trends N30°-40°W and plunges moderately west. At its western end, the axial trace curves to the north before plunging beneath Quaternary alluvium (Figure 14) and forms a left-stepping offset with the anticlines at Lijiapuzi 5 km to the north (Figure 14).

THE YANTON SHAN FOLD AND THRUST FAULT ZONE

About 25 km northeast of the Tianjin Shan is the Yanton Shan arcuate thrust fault zone (Figures 2 and 3). Escarpments are clear on the Landsat imagery along eastern side of the Yanton Shan (Figure 3). Field investigations show that the Devonian red beds have been thrust eastward over the Tertiary red beds and Quaternary sediments along the northern part of the Yanton Shan fault zone (Ningxia Geological Bureau, 1976). The trend of this fault is about N40°W. To the south the trend of

the Yanton Shan changes to north-northwest, and the prominent thrust fault becomes a south-plunging anticline cored by Oligocene red beds. Farther to the south, the range trends about north-south, and another anticline that trends north-northwest is present. The geometry of structures in the Yanton Shan is similar to that in the Tianjin Shan and Mibo Shan (Figure 2). Where the pre-Cenozoic rocks are exposed, the deformation is dominated by thrust faulting. The trends of thrust faults are about N40°-50°W. The deformation in the Tertiary red beds, however, is dominated by folding, and the folds trend north-northwest then curve to become nearly north-south toward the southeast. These folds also form a right-stepped en echelon pattern.

THE NIUSHOU SHAN - DALOU SHAN FOLD AND FAULT ZONE

This fault zone is located northeast of the Yanton Shan (Figures 2 and 3). It is an area in the geology of Ningxia because it bounds two different geological terrains. North of the fault the Paleozoic stratigraphy is similar to that of the North China block, and south of the fault it similar to that of the Nanshan fold belt. Unfortunately the geological history of this fault zone has not been well studied. Currently, it forms southern boundary of the Yinchuan graben. Several earthquakes of magnitude 4 to 5 Ms, which have occurred at the southern end of the Yinchuan graben, may have been associated with movement on this fault.

In the Dalou Shan, a N20°-30°-trending thrust fault places Paleozoic rocks eastward over Miocene red beds. In the Niushou Shan, there are several thrust faults striking about N50°W and dipping

southwest. They make up a fault zone that bounds the eastern side of the Niushou Shan. These faults carry grey, green, and black slate of Ordovician age over Miocene orange silty mudstone, probably the equivalent of the Hongliugou Formation, and locally the slate is thrust over Quaternary gravel. A reconnaissance study by Liao Yuhua (1986, unpublished manuscript) has shown many sub-horizontal slickensides within the fault zone that indicate a left-lateral strike-slip component. Northwest of the Niushou Shan, Cretaceous rocks have been thrust over Miocene red beds, and farther northwest, the fault is covered by Quaternary sediments in the Gobi desert. Because this fault has not been well studied, its Cenozoic and recent kinematic history is poorly known, but the clear lineation on the Landsat imagery (Figure 3) and the horizontal slickensides suggest a large component of active strike-slip movement along this fault coupled with some thrust displacement.

THE YINCHUAN GRABEN AND THE HELAN SHAN HORST IN THE NORTHERN NINGXIA

North of the Niushou Shan - Dalou Shan fault, the dominant style of deformation includes a large component of normal faulting with a comparable, if not larger, right-lateral strike-slip component. The Helan Shan horst and Yinchuan graben are the major structural units that formed within the region (Figure 1 and 2).

The Helan Shan mountains trend north northeast and consist of rocks that range from Sinian (pre-Cambrian) to middle Mesozoic in age. The major deformational phase that forms the pre-Cenozoic structures of the Helan Shan occurred in Jurassic time (Wang et al., 1986; Liao Yuhua,

unpublished manuscript, 1986). At present, the Helan Shan is bounded on both sides by high-angle normal faults. The normal faults on the western side have not been studied. On the eastern side, the Cenozoic and Quaternary rocks are displaced by normal faults, the East Helan Shan faults, that dip steeply eastward at the foot of the Helan Shan. These same faults form the western boundary of the Yinchuan graben.

The Yinchuan basin is a typical graben that is bounded on both sides by normal faults that dip into the basin. It trends 160 km north-northeast and is 50 to 55 km wide in its east-west direction. The graben is bounded on the west by the East Helan Shan fault zone, which consists of several north-northeast-trending normal faults. One of the major strands along the west side of the graben at the eastern foot of the Helan Shan clearly forms a prominent range-front scarp (Figure 16). The alluvial fans are reported to have been cut by this fault. At one place, a small fan has been downdropped to the east with about 50 m of apparent normal separation (Liao et al., 1982). To the north, the continuation of this fault has offset a segment of the "Great Wall" that was built about 400 years ago with about 1.5 ± 0.5 m right-lateral offset and 0.9 ± 0.2 m vertical offset (He, 1982; Wang et al., 1982; Liao et al., 1982; Deng et al., 1984; Zhang et al., 1986). About 3 to 4 km east of the Helan Shan another fault scarp 16.5 km long is present west of Yinchuan. The scarp faces southeast and trends generally northeast (Figure 16). The vertical normal separation of the piedmont slop ranges from 2 to 4 m, and horizontal offset has been reported.

The major fault zone that bounds the eastern side of the graben is referred to as the Huanghe fault. Although there is no surface

outcrop to locate this fault, geophysical studies have demonstrated its existence (Liao Yuhua, unpublished manuscript, 1986; Zhang et al., 1986).

Geophysical studies and a borehole (more than 2000 m) have indicated that the basement of Yinchuan graben is formed mainly by Ordovician limestone, and the graben fill consists of 3000 - 3600 m of Paleogene, 2000 - 2500 m of Neogene, and 1000 - 1600 m of Quaternary sedimentary rocks. Thus, the total Cenozoic sedimentary accumulation ranges from 6000 m to 7700 m thick (Liao Yuhua, unpublished manuscript, 1986; Zhang et al., 1986). The Tertiary red beds within the graben can be correlated lithologically with those in southern Ningxia, suggesting that the floor of the Yinchuan graben was part of the large basin that was formed in Tertiary time in northwestern China before the graben formed. Tertiary rocks within the graben are thicker than rocks of the same age in other areas of Ningxia, suggesting that the Yinchuan graben was a site of rapid subsidence during the development of the large Tertiary basin. The elevation of the Helan Shan ranges from 2000 to 3000 m (maximum 3557 m) above sea level. The surface of the Yinchuan graben is about 1000 m above the sea level. Thus, the total minimum vertical separation of Paleozoic rocks ranges from 7000 m to 9700 m on opposite sides of the East Helan Shan fault zone.

When displacement on the Helan Shan faults began is poorly known. Tertiary gypsiferous red beds (possibly Oligocene in age and equivalent to the Qinshuiyin Formation) are preserved within southern part of the Helan Shan (Figure 17), which suggests that the uplift might not have begun during the deposition of the Oligocene gypsiferous red

beds. But inadequate knowledge of Tertiary deposition in the Helan Shan area makes it impossible to reasonably understand the history of the East Helan Shan fault. By assuming that uplift of the Helan Shan began in early Oligocene (36.5 Ma.), the minimum vertical slip rate on the East Helan Shan fault would be 0.19 - 0.27 mm/yr; if it began in latest Oligocene (23.5 Ma.), the minimum rate would be 0.30 - 0.41 mm/yr; and if it began in latest Pliocene time (about 2 Ma), the minimum rate would be 3.5 - 4.9 mm/yr.

DISCUSSION

The major deformational phases that occurred in the Haiyuan and Liupan Shan area began after deposition of Pliocene conglomerate (Ganhegou Formation) and before deposition of Quaternary deposits (Burchfiel et al., 1987; Zhang et al., 1987). In the Tianjin Shan and Mibo Shan, the youngest rocks involved in the folds and thrust faults are also the Pliocene tan conglomerate. Near Xiao Hong Gou the Quaternary conglomerate is involved in the folds, but it also unconformably overlies the Tertiary, probably Pliocene, conglomerate. This conglomerate could be derived from relief formed by the earliest part of the deformation that was later responsible for its deformation. The Pliocene tan conglomerate is not exposed in the Yanton Shan, Niushou Shan and Dalou Shan, but we still infer that deformation began after deposition of Pliocene conglomerate in this area because there is no unconformity between any of the other Tertiary formations and the youngest formation involved in each of the areas in the Miocene Hongliugou Formation. The onset of extension in the Yinchuan graben is

uncertain, but we think the deformation may also have begun after the formation of the Pliocene conglomerate.

The Cenozoic structures in the Haiyuan and Liupan Shan area suggest a thin-skinned deformation (see Zhang et al., 1987). The decollement zone beneath these structures cuts through structurally complex pre-Cenozoic rocks and structures in this region. If this thin-skinned geometry can be extended to include the folds and thrust faults in southern Ningxia, much of the late Cenozoic structural development would have a style similar to that of the Haiyuan and Liupan Shan area, where the earliest phase of deformation was southwest to northeast convergence and was followed by late left-slip along major fault zones. The displacement on the left-slip fault zone was transferred to a north- or northwest-trending zone of shortening.

The geometry of the Tianjin Shan - Mibo Shan fault zone is similar to that of the Haiyuan and Liupan Shan fault zone. Its western segment trends west-northwest to east-west. Pre-Cenozoic rocks exposed in the hanging wall of the western part of this zone contain structures that are dominated by thrust and reverse faults. Its eastern part trends north-northwest to north-south. The hanging wall consists mostly of Tertiary red beds, and the structures are dominated by frontal ramp anticlines parallel to the range front. The geometry of structures in the eastern segment of the Tianjin Shan - Mibo Shan fault zone is similar to structures in the eastern segment of the Yanton Shan, where the deformation is dominated by thrust faulting in pre-Cenozoic rocks and by folding in the Tertiary rocks, and the north-northwest to north-south trending folds in the eastern segments form a right-stepped en

echelon pattern. Recently, a left-lateral displacement of 3.6 ± 1 km has been reported west of our mapped area along the Tianjin Shan - Mibo Shan fault zone, but whether this displacement occurred after the thrust faulting and folding or in the early stage of deformation is uncertain. We suggest that the left-slip on the fault did follow the early stage of thrust faulting and folding because of very similar geometry between the Haiyuan - Liupan Shan fault zone and the Tianjin Shan - Mibo Shan fault zone. The only difference may be that the left-slip faulting on the Haiyuan fault offset old thrust faults and folds, but along the Tianjin Shan fault the left-slip faulting follows one of the thrust or reverse faults. Evidence for east-vergent shortening is present along the eastern segment of the Tianjin Shan - Mibo Shan fault zone and the northwest-trending Yanton Shan fault zone. We interpret the left-lateral offset along the western Tianjin Shan fault zone as being transferred into shortening in the eastern Tianjin Shan, Mibo Shan and Yanton Shan. Unfortunately, insufficient mapping in these areas does not allow us to calculate the amount of shortening across them as we did in the Haiyuan - Liupan Shan area (Zhang et al., 1987).

The evidence of northeastward thrust faulting is clear along the Niushou Shan and Dalou Shan fault zone. Their prominent lineation on the satellite imagery and recent reconnaissance work by Liao Yuhua (1986, unpublished manuscript) suggest there may be a large amount of left-lateral strike-slip component along this fault. This fault zone bounds the Yinchuan graben on the south. The Quaternary extension and opening of the Yinchuan graben are probably in part related to the evolution of this fault zone.

The amplitude of displacement and topographic relief on the convergent and strike-slip structures in southern Ningxia decreases to the northeast, and the evidence for active faulting also becomes less clear in the same direction, even though the sharpness of the topographic range fronts suggests active deformation. We suggest that the rate of deformation along these more northerly structural zones may be less than the rate in the Haiyuan and Liupan Shan area to the south. The average Quaternary left-lateral slip rate along the Haiyuan fault is 5 - 10 mm/yr (Burchfiel et al., 1987). The left-lateral displacement along the Tianjin Shan fault appears to be 3.6 ± 1 km. Burchfiel et al. (1987) suggest that the left-slip on the Haiyuan fault began near the end of Pliocene time or beginning of Pleistocene time (about 1.6 Ma). If we assume that the left-slip along the Tianjin Shan fault zone is contemporaneous with that on the Haiyuan fault, the average slip rate would be about 1.5 to 2.7 mm/yr. The amount of offset and rate of slip along the Niushou Shan and Dalou Shan fault zone are unknown, but some evidence suggests a left-lateral strike-slip component. The topography of the Niushou Shan and Dalou Shan is lower than that of the Liupan Shan, and even lower than that of the Tianjin Shan and Mibo Shan. Thus we suggest that the rate of slip on the Niushou Shan - Dalou Shan fault is probably less than that on the Tianjin Shan fault zone.

It appears that all the ranges in southern Ningxia have been subjected to the same deformation processes: early northeastward convergence followed by later increasing component of left-slip on east-west to northwest-southeast trending faults. The left-slip displacement is transferred into crustal shortening on the north-south trending

zones. The rates of deformation, however, can be inferred to be less in the northern range than in the southern ranges. Thus the northern ranges have not evolved as fast or as far as those in the Haiyuan and Liupan Shan area over the same period of time. Thus the tectonic evolution in the Haiyuan and Liupan Shan area probably foreshadows of the future deformation in the northern ranges. If the interpretation presented above is correct, it suggests the Ningxia region became the northeastern margin of the Tibetan Plateau in Pliocene time, and is being elevated by the irregular growth of convergent and oblique-slip structures. The plateau may continue to grow toward the northeast, but in an irregular way.

ACKNOWLEDGEMENTS

This paper represents collaboration under a protocol between the State Seismological Bureau of China and the U. S. Geological Survey and National Academy of Sciences of the United States. Specific support for this study was provided by the National Science Foundation grant number EAR - 8306863, and by the State Seismological Bureau of China. The American authors are particularly grateful to many Chinese workers, both scientific and non-scientific, for making their visits to China pleasant and productive.

REFERENCES

Burchfiel, B. C., Zhang, P., Wang, Y., Zhang, W., Jiao, D., Song, F., Deng, Q., Molnar, P., and L. Royden, Geology of the Haiyuan fault zone, Ningxia Autonomous Region, China and its relation to the evolution of the Northeastern margin of the Tibetan Plateau, submitted to J. Geophys. Res., 1987.

Deng, Q., Zhang, Y., Xu, G., and Fan, F., On the tectonic stress field in China and its relation to plate movement, Phys. Earth and Planet Interiors, 18, 257-273, 1979.

Deng, Q., Song, F., Zhu, S., Li, M., Wang, T., Zhang, W., Burchfiel, B. C., Molnar, P., and P. Zhang, Active faulting and tectonics of the Ningxia-Hui Autonomous Region, China, J. Geophys. Res., 89, 4427-4445, 1984.

He, S., On the dislocation of the Great Wall near the Schizuishan city, Ningxia Autonomous Region, in The Active Faults in China, Seismology Publiching House, Beijing, China, (in Chinese), 151-153, 1982.

Huang, T. K., An outline of the tectonic characteristics of China, Continental Tectonics, National Academic Press, 184-197, 1980.

Liao, Y., Wang, Y., Huai, F., Song, F., and Liu, P., A preliminary discussion on the active fault zone along the eastern piedmont Helan Shan mountain, in The Active Faults in China, Siesmology Publishing House, Beijing, China, (in Chinese), 162-166, 1982.

Molnar, P. and P. Tapponnier, Cenozoic tectonics of Asia: Effects of a continental collision, Science, 189, 419-426, 1975.

Molnar, P. and P. Tapponnier, Active tectonics of Tibet, J. Geophys. Res., 83, 5361-5374, 1978.

Ningxia Geological Bureau, Geological map of the Haiyuan area (1/200,000), Geological Press, 1959.

Ningxia Geological Bureau, Geological map of the Pingliang area (1/200,000), Geological Press, 1974.

Ningxia Geological Bureau, Geological map of the Zhongwei area (1/200,000), Geological Press, 1976.

Ningxia Geological Bureau, Stratigraphy of the Ningxia Hui Autonomous Region, Geological Press, 1980.

Tapponnier, P. and P. Molnar, Slip-line field theory and large scale continental tectonics, Nature, 264, 319-324, 1976.

Tapponnier, P. and P. Molnar, Active faulting and Cenozoic tectonics of China, J. Geophys. Res., 82, 2905-2930, 1977.

Wang, Y., Song, F., Liao, Y., Kui, F., and Liu, P., Some features of the active faults in the northern part of the Ningxia Hui Autonomous Region, in The Active Faults in China, Seismological Publishing House, Beijing, China, (in Chinese), 154-161, 1982.

Wang, Y., Song, F., Liao, Y., Zhang, W., Kuei, F., and P. Liu, Some characteristics of seismotectonics in North Ningxia, and the effects of uplifting of Tibetan Plateau to North China Block, Recent Crustal Movement, (in Chinese), 1985.

Zhang, B., Liao, Y., Guo, S., Wallace, R. E., Bucknam, R. C., and T. C. Hanks, Fault scarps related to the 1739 earthquake and seismicity of the Yinchuan graben, Ningxia Hui Autonomous Region, China, Bull. Seism. Soc. Am., 76, 1255-1287, 1986.

Zhang, P., Molnar, P., Burchfiel, B. C., Royden, L., Wang, Y., Deng, Q., Song, F., Zhang, W., and D. Jiao, A, Bounds on the Holocene slip rate of the Haiyuan fault, North-Central China, submitted to Quaternary Research, 1987.

Zhang, P., Molnar, P., Zhang, W., Deng, Q., Wang, Y., Burchfiel, B. C., Royden, L., and D. Jiao, B, Bounds on the recurrence interval of major earthquakes along the Haiyuan fault in North-Central China, submitted to Quaternary Research, 1987.

Zhang, W., Jiao, D., Zhang, P., Molnar, P., Burchfiel, B. C., Deng, Q., Wang, Y., and Song, F., Displacement along the Haiyuan fault associated with the great 1920 Haiyuan earthquake, Bull. Seism. Soc. Am., 77, 117-131, 1987.

Zhang, P., Burchfiel, B. C., Molnar, P., Zhang, W., Jiao, D., Deng, Q., Royden, L., and Song, F., C, Amount and style of late Cenozoic deformation in the Liupan Shan area, Ningxia Autonomous region, China, submitted to J. Geophys. Res., 1987.

Zhang, Z., Liou, J. G., and R. G. Coleman, An outline of the plate tectonics of China, Geol. Soc. Am. Bull., 95, 295-312, 1984.

FIGURE CAPTIONS

Figure 1, Regional tectonic map of north-central China. Three major crustal terrains are shown in this map. The Paleozoic Nanshan fold belt tectonically belongs to the Tibetan Plateau, and the Ordos block belongs to the North China Block. Only the major active faults are shown in this map, by thick lines. Thick lines with arrows are strike-slip faults, thick lines with ticks are normal faults, and the thick lines with solid triangles are thrust faults, with ticks and triangles pointing down dip. Location of Figure 2 is indicated.

Figure 2, Geological map of the Ningxia region (see Figure 1 for location). PK is pre-Cretaceous rocks. K1s is the Cretaceous Sanqiao Formation. K1h is the Cretaceous Heshangpu Formation. K1l is the Cretaceous Lisanwa Formation. K1m is the Cretaceous Madong Shan Formation. K1s is the Cretaceous Naijiahe Formation. Ors is the Eocene or Oligocene Sikouzi Formation. Orb is the Oligocene Qinshuiyin Formation. Mrb is the Miocene Hongliugou Formation. Pcg is the Pliocene Ganhegou Formation. Blank area is covered by loess and other Quaternary sediments. Dotted area covers Cenozoic extensional basin. Thick lines with ticks are normal faults, and thick lines with solid triangles are thrust or reverse faults. Thick lines with arrows are strike-slip faults. Dashed thick lines are inferred faults. Major folds are also shown with standard symbols. Letter A indicates the 3.6 ± 1 km left-lateral offset along the Tianjin

Shan fault zone.

Figure 3, Portion of Landsat imagery E-1492-03031-5 showing thrust, strike-slip,and normal faults in the transition between the Tianjin Shan and the Yinchuan graben (Figure 2). The mapped areas along the Tianjin Shan fault zone are also shown in this image. The steep escarpments on the northern or eastern sides of the Mibo Shan, the Tianjin Shan, the Yanton Shan, the Dalou Shan, and the Niushou Shan mark thrust fault zones that dip west or southwest but that also may include strike-slip components. The escarpment on the east side of the Dalou Shan seems to be part of the same fault zone east of the Niushou Shan that continues north-northwest to bound the southern ends of the Helan Shan and the Yinchuan graben. The large river in the top left part of the image is the Huang He (Yellow River).

Figure 4, Regional distribution of the Tertiary red beds (Oligocene to Pliocene) in the northeastern part of the Tibetan Plateau, China. Compiled from geological maps of that area.

Figure 5, Geological map of Hong Gou Liang along the Tianjin Shan. Cph is the Cambrian phyllite. Olm is the Ordovician limestone. Drb is the Devonian red beds. Cbs is the Carboniferous black shales and siltstone. Pss is the Permian sandstone. Ors is the Eocene or Oligocene red conglomerate (Sikouzi Formation). Orb is the Oligocene red beds (Qinshuiyin Formation). The thick lines are south dipping thrust and reverse faults. Dashed faults are inferred.

Figure 6, Stream offset of 6.2 ± 2 m near Hongouliang along the

Tianjin Shan and Mibo Shan fault zone. View is to the northeast. The stream flows from southwest to northeast, and the bottom of channel is very narrow (about 1 m). The dashed line with arrows marks the fault. The black object inside the cycle is a daybag.

Figure 7, Stream offset of 6.2 ± 2 m, adjacent to the one in Figure 5, near Hongouliang along the Tianjin Shan and Mibo Shan fault zone. View is the southeast. The dashed line with arrows marks the fault surface exposed on the ground. The stream flows from southwest to northeast. The upstream channel is shown at lower right conner of the photo as indicated by a single arrow. The bank of downstream shannel is at left bottom of the photo as indicated by a single arrow on left side of the fault, but the channel bottom is not shown in the photo. View is to the southeast.

Figure 8, Mountain front of the Tianjin Shan. The high mountain consists of Paleozoic rocks. The low foothills consist of Tertiary red beds. The mapped thrust and reverse faults are located between the high mountains and the low hills. The Tertiary red beds in the lower hills have been folded. An active fault is inferred at the front of the low hills. View is to the south.

Figure 9, Geological map near Qingeda along the Tianjin Shan - Mibo Shan fault zone. Olm is the Ordovician limestone. Drb is the Devonian red beds. Cbs is the Carboniferous black shale and siltstone. Ors is the Eocene or Oligocene red conglomerate

(Sikouzi Formation). Orb is the Oligocene red beds (Qinshuiyin Formation). The thick lines are faults, and dashed thick lines are inferred faults. Lines with dots are unconformities. AA shows location of Figure 9.

Figure 10, Sketch of cross-section in Qingeda. See Figure 8 for location. Olm is the Ordovician limestone. Drb is the Devonian red beds. Ors is Oligocene red conglomerate (Sikouzi Formation). Qal is the Quaternary alluvium.

Figure 11, Geological map near Xiao Hong Gou. Cbs is the Carboneferous black shale and siltstone. Pss is the Permian sandstone. Ocg is the old conglomerate of unknown age. Ors is the Eocene or Oligocene red conglomerate (Sikouzi Formation). Orm is the Oligocene - Miocene red beds (Qinshuiyin and Hongliugou Formations). Pcg is the Pliocene conglomerate (Ganhegou Formation). Qal is the Quaternary alluvium.

Figure 12, Sketch of cross-section to show the progressive deformation in Xiao Hong Gou. See Figure 10 for location.

Figure 13, Photo of cross-section in Figure 11. The view is to the southeast. The steeply dipping red beds in the right side of the photo are Miocene red beds and conglomerate. The gently dipping beds near the middle right edge of the photo are the tan conglomerate, of probable Pliocene age.

Figure 14, Geological map of Lijiapuzi and Mibo Shan area. Orb is the Oligocene red beds (Qinshuiyin Formation). Mrb is the Miocene red mudstone (Hongliugou Formation). Blank area is covered by loess and Quaternary alluvial sediments.

Figure 15, View to the southeast along the anticline at the front of the Mibo Shan. The core of the anticline is just along the peak in the middle of the photo. The Tertiary red beds in southwest slope of the peak dip to the southwest, and the same beds in northeast slope dip to the northeast.

Figure 16, Fault scarps of the East Helan Shan fault zone. The faults are present along the foot of the mountain. The scarp in the front part of the photo is also a fault scarp, which cut the alluvial fans. The heights of the scarp range from 1 to 3 m. This fault scarp extends about 16.5 km parallel to the Helan Shan mountain.

Figure 17, Oligocene gypsiferous red beds (Qinshuiyin Formation) preserved within southern Helan Shan mountain. The rocks on both sides of the photo are Paleozoic rock. The rocks in the middle of the photo are Oligocene gypsiferous red beds. The Oligocene gypsiferous red beds in the middle of the photo are bounded by normal faults, but whether they are active is unknown.

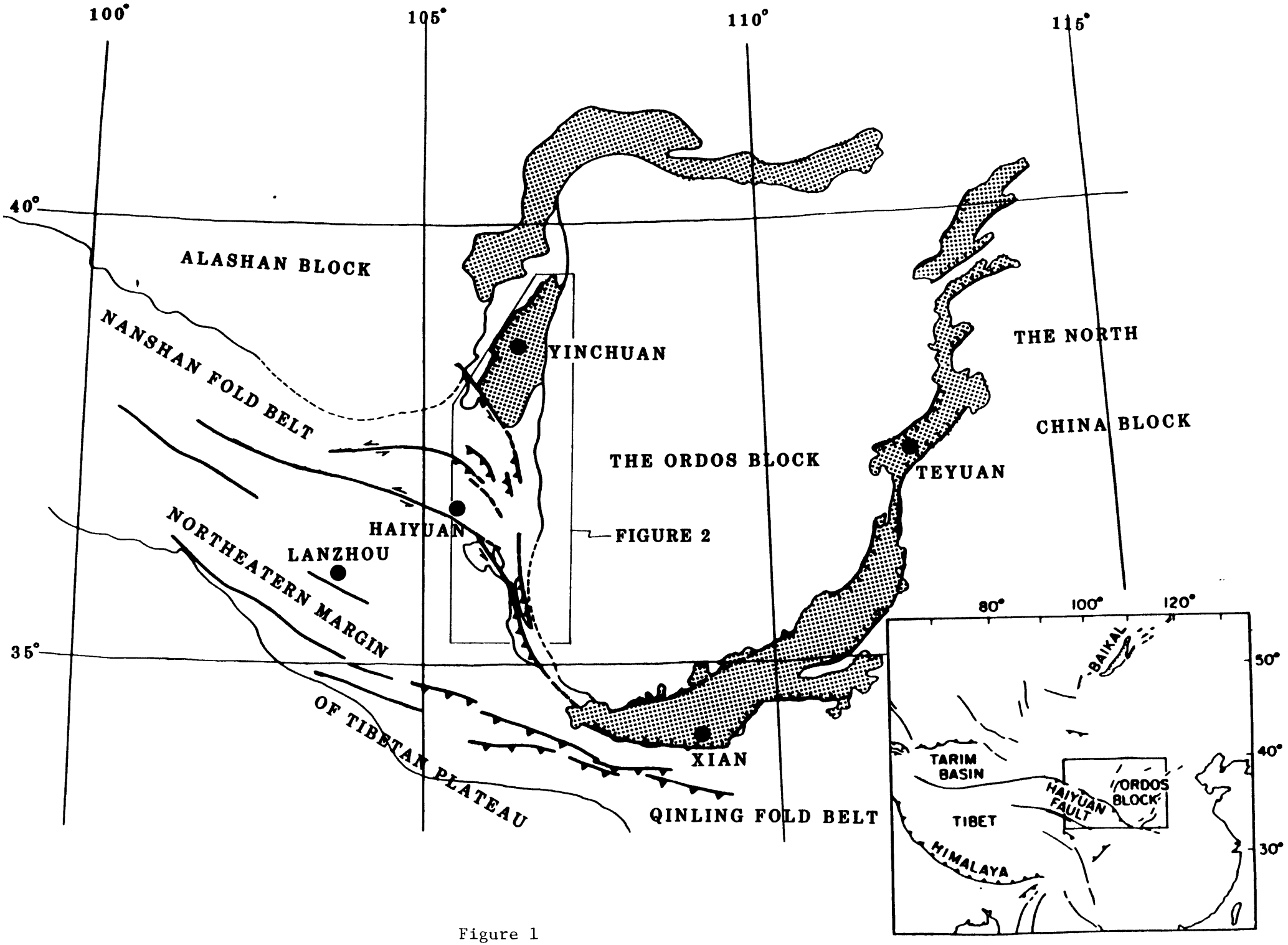
100°
105°
110°
115°
40°
35°
ALASHAN BLOCK
NANSHAN FOLD BELT
YINCHUAN
THE NORTH
CHINA BLOCK
THE ORDOS BLOCK
TEYUAN
HAIYUAN
FIGURE 2
LANZHOU
NORTHEATERN MARGIN
OF TIBETAN PLATEAU
XIAN
QINLING FOLD BELT
80°
100°
120°
50°
40°
30°
BAIKAL
TARIM BASIN
HAIYUAN FAULT
ORDOS BLOCK
TIBET
HIMALAYA

Figure 1

FIGURE 2

SEE THE FOLDED MAP SHEET

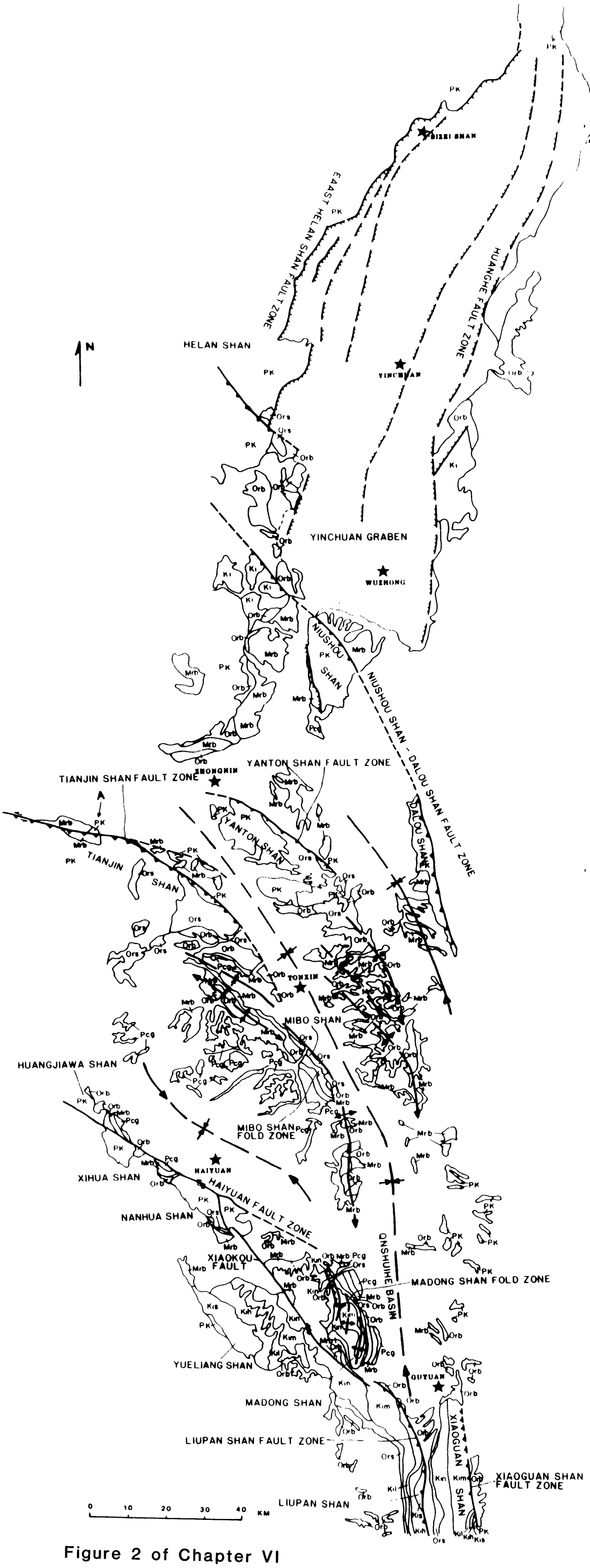

Figure 2 of Chapter VI

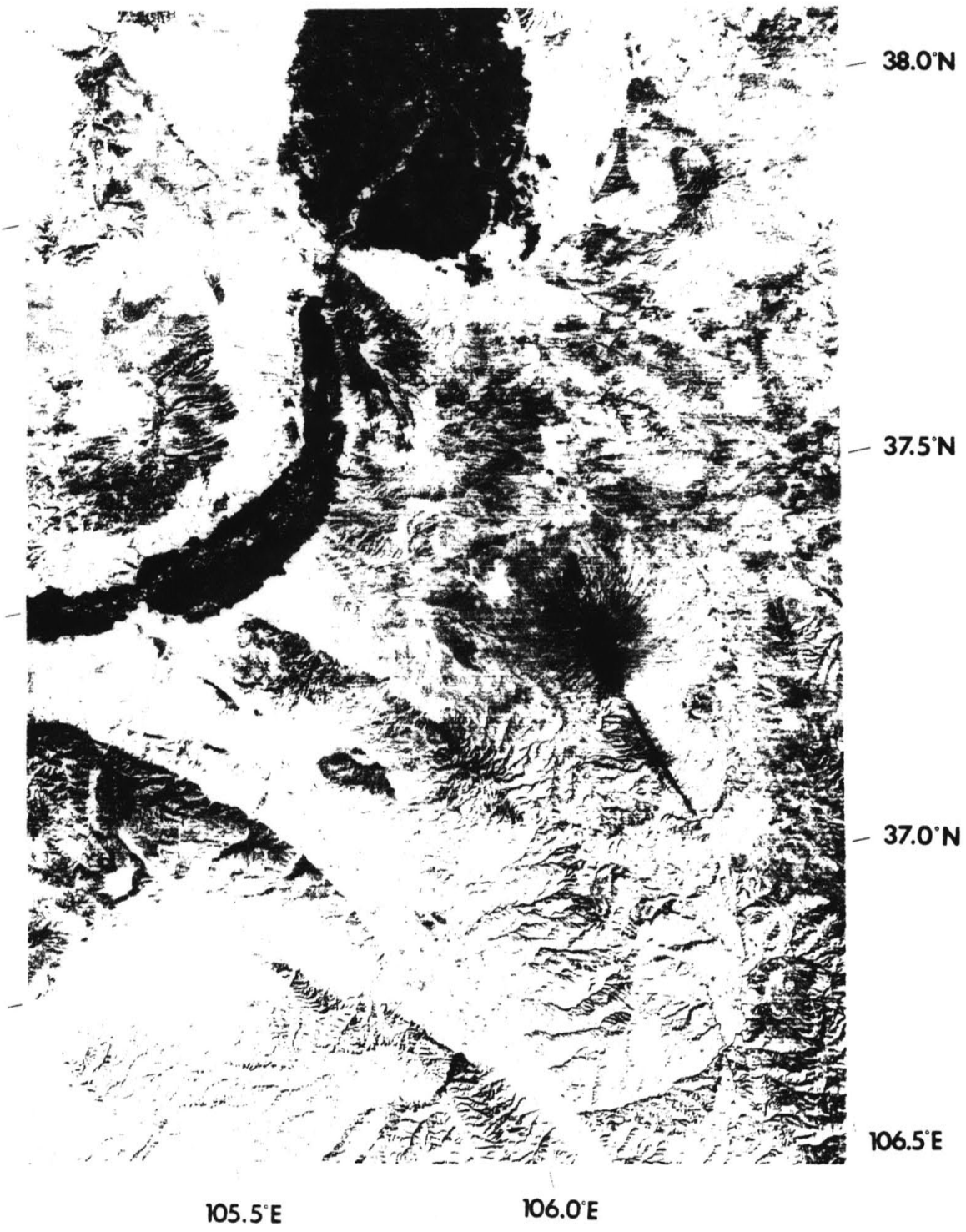

Fifure 3A

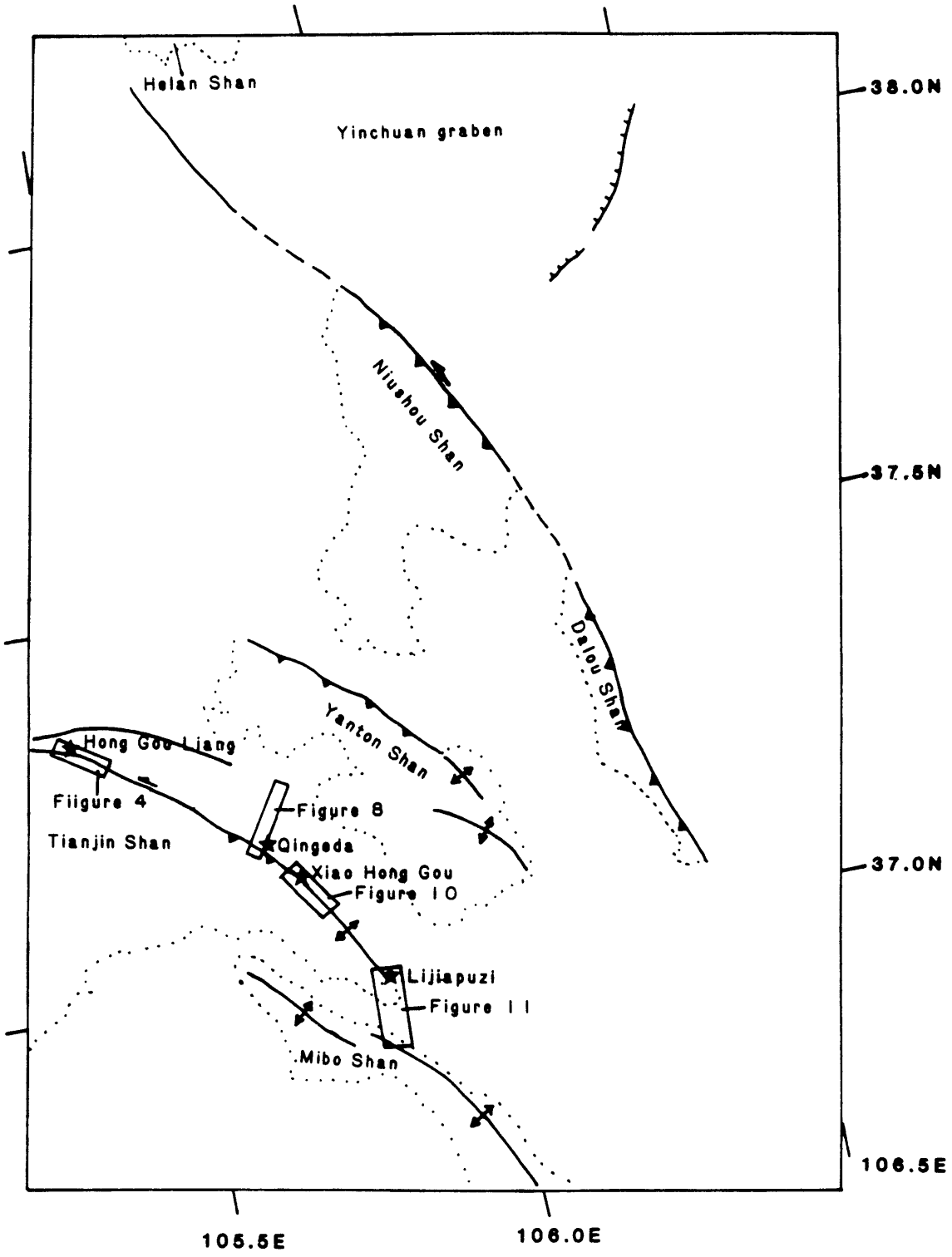
Helan Shan
Yinchuan graben
Niushou Shan
Daiou Shan
Yanton Shan
Hong Gou Liang
Fiigure 4
Figure 8
Tianjin Shan
Qingeda
Xiao Hong Gou
Figure 10
Lijiapuzi
Figure 11
Mibo Shan
38.0N
37.5N
37.0N
106.5E
105.5E
106.0E

Figure 3B

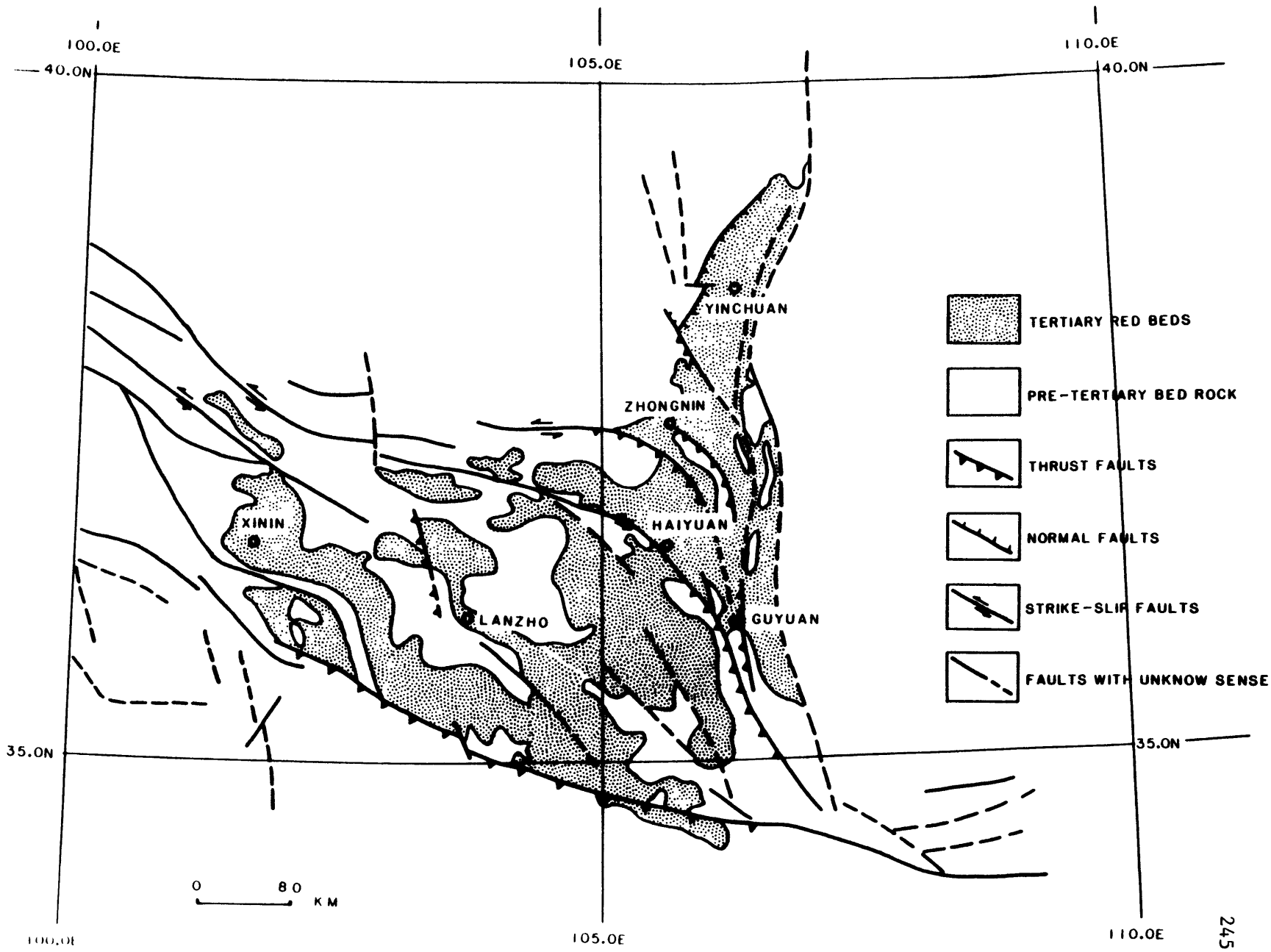
100.0E
105.0E
110.0E
40.0N
35.0N
YINCHUAN
ZHONGNIN
HAIYUAN
XININ
LANZHO
GUYUAN
TERTIARY RED BEDS
PRE-TERTIARY BED ROCK
THRUST FAULTS
NORMAL FAULTS
STRIKE-SLIP FAULTS
FAULTS WITH UNKNOW SENSE
0
80
KM

Figure 4

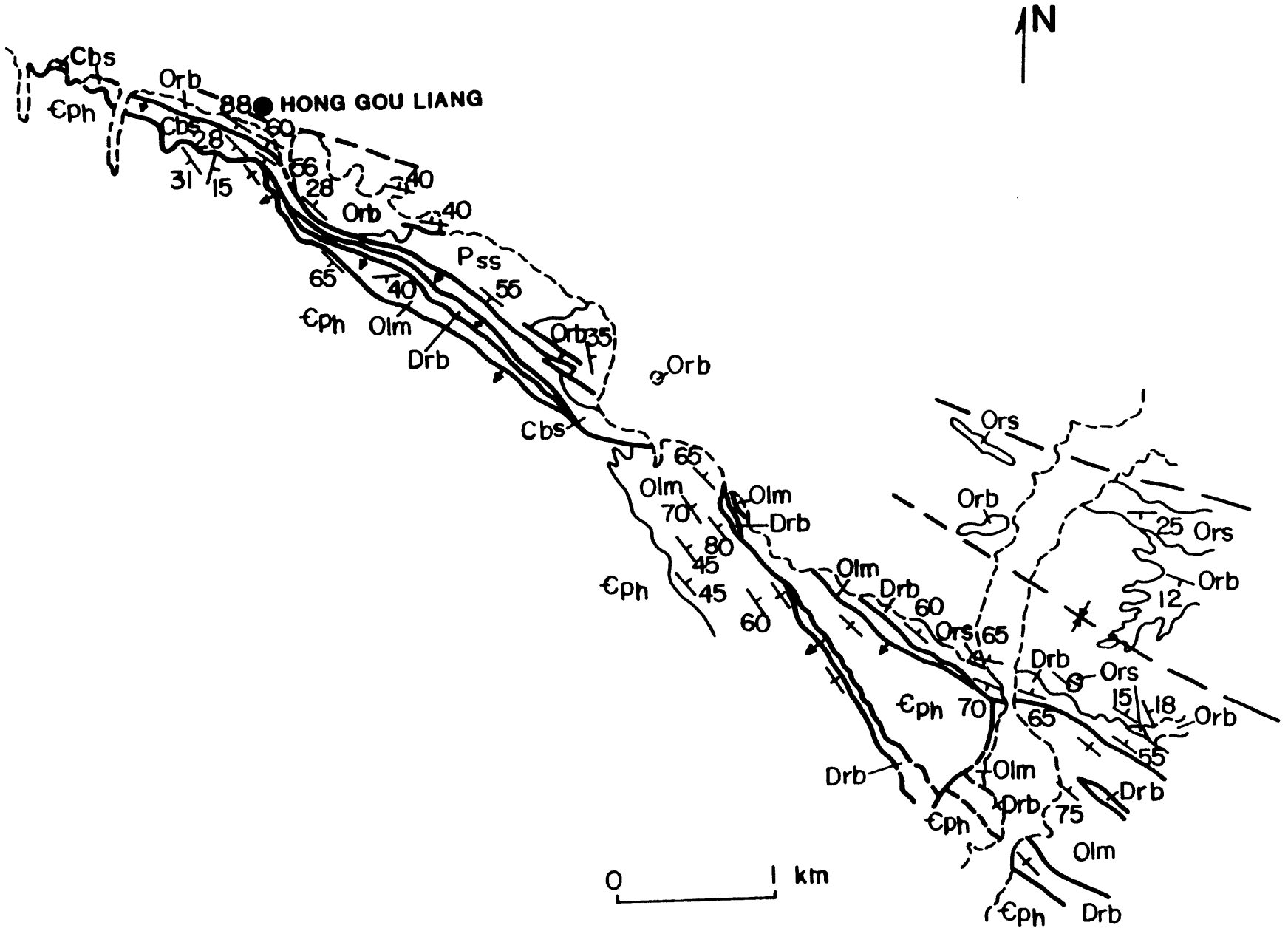

Figure 5

Figure 6

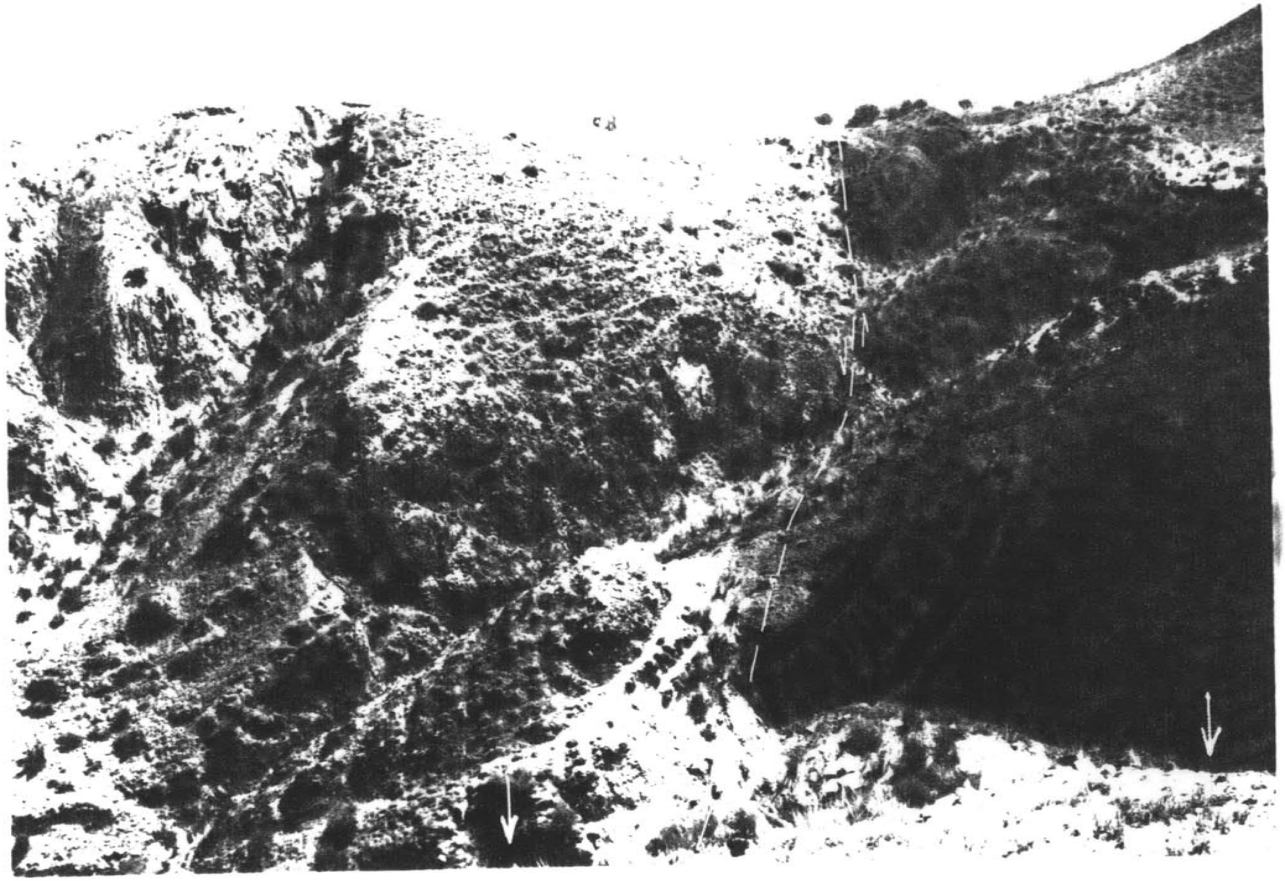

Figure 7

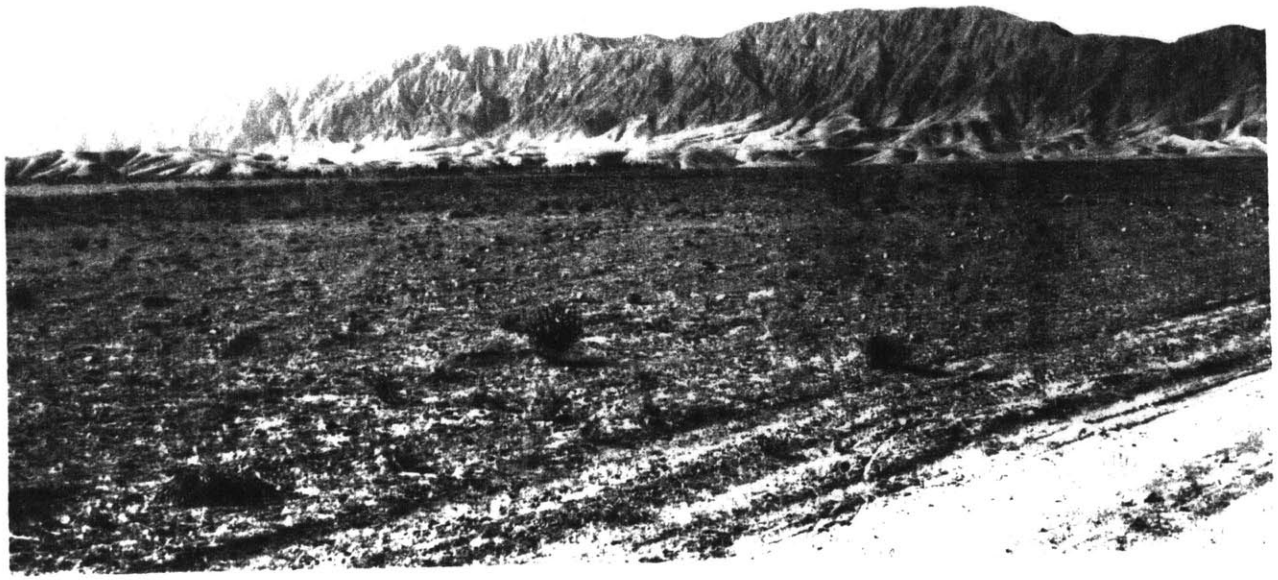

Figure 8


N
A
62
58
Drb
58
Ors
Ors
42
Ors
Ors
A
34
Olm
Ors
27
22
30
20
Ors
15
42
Ors
Ors
25
34
57
24
45
Olm
Olm
23
10
Ors
Cbs
45
59
Olm
22
Drb
QINGEDA
Ors
Cbs
25
20
Olm
20
11
78
Drb
Ors
Cbs
Olm
Cbs
13
26
58
Olm
Ors
72
70
30
Ors
70
Cbs
16
Ors
15
45
30
0
1 KM

Figure 9

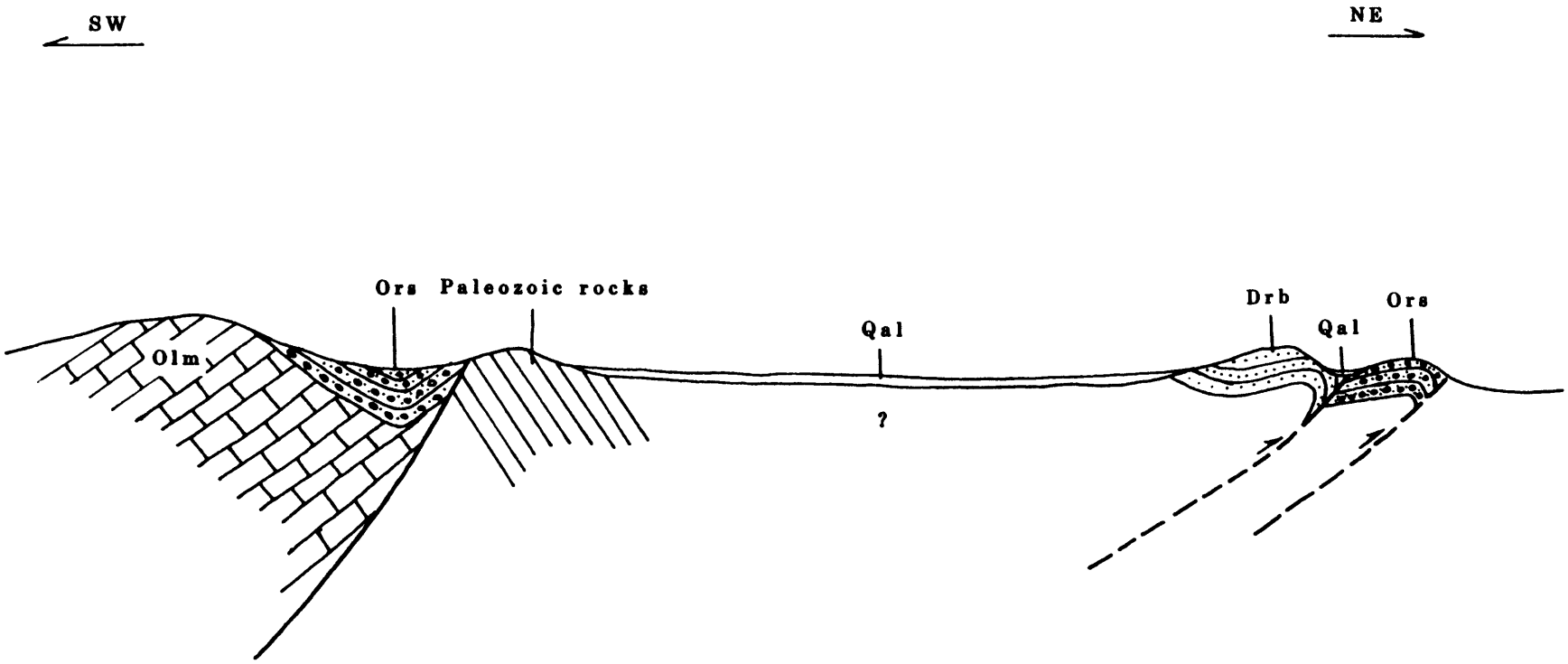

Figure 10

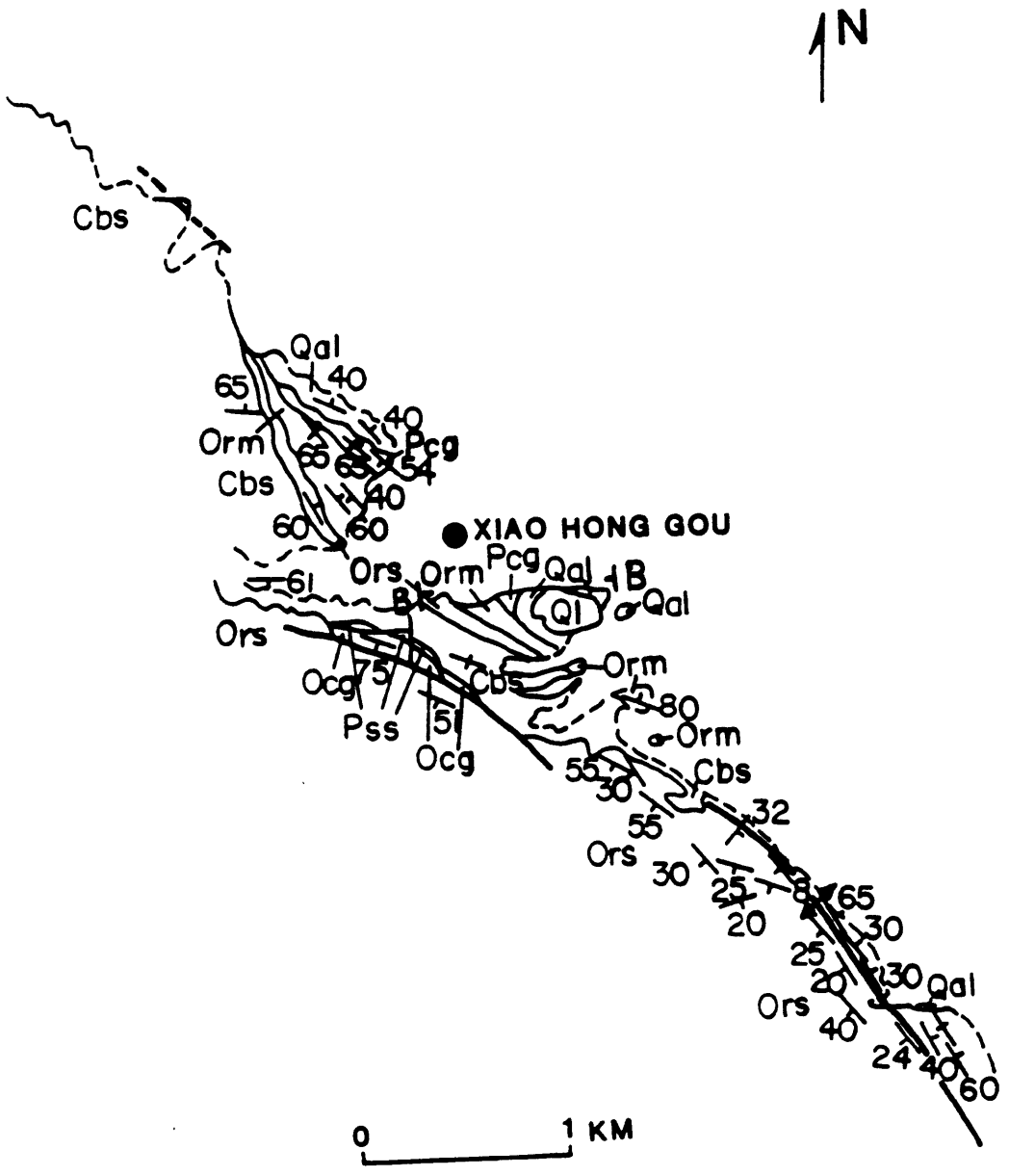
N
Cbs
Qal
65
40
Orm
Pcg
Cbs
60
XIAO HONG GOU
Ors
Orm
Pcg
Qal
B
Ql
Ors
Ocg
Pss
Cbs
Orm
80
Cbs
55
30
32
Ors
30
25
20
65
30
25
20
30
Qal
Ors
40
24
40
60
0
1 KM

Figure 11

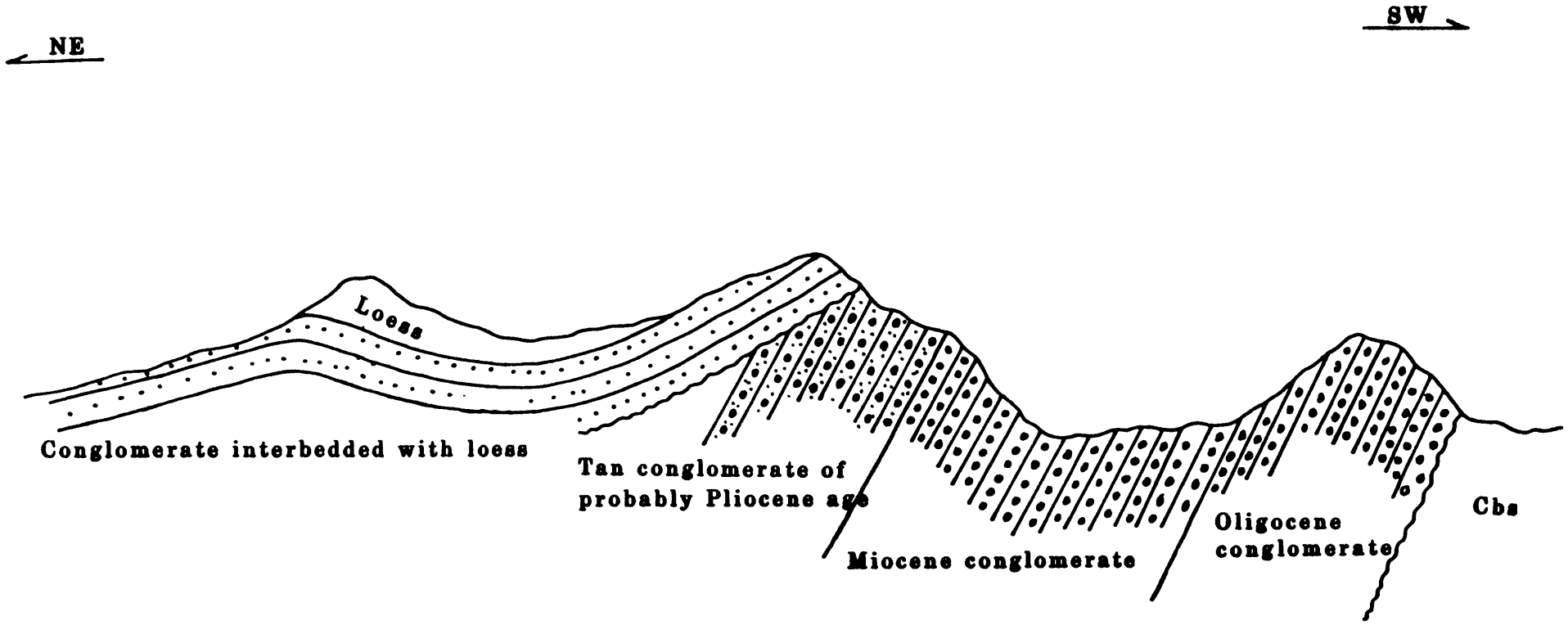
NE
SW
Loess
Conglomerate interbedded with loess
Tan conglomerate of
probably Pliocene age
Miocene conglomerate
Oligocene
conglomerate
Cbs

Figure 12

Figure 13

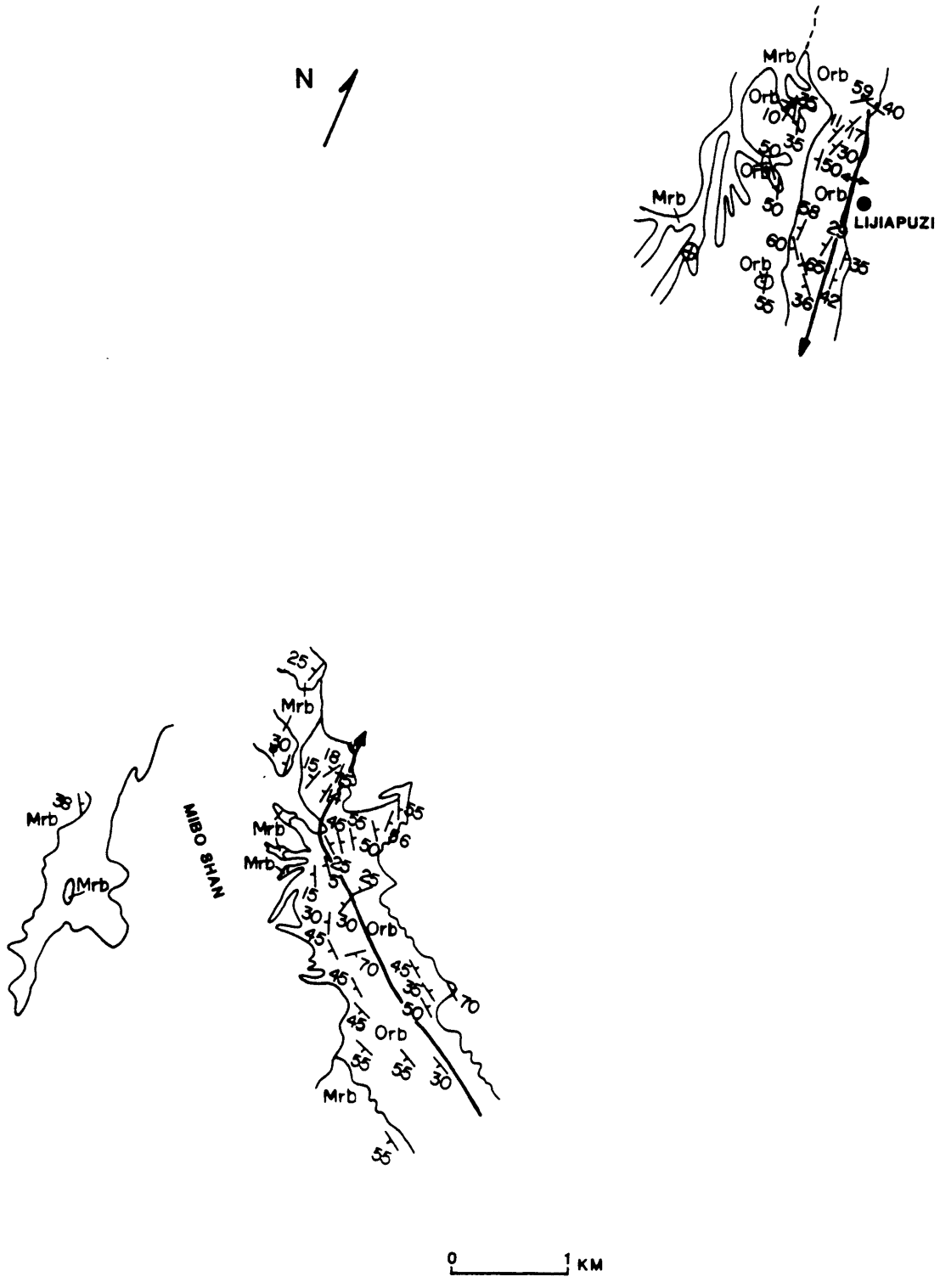

Figure 14

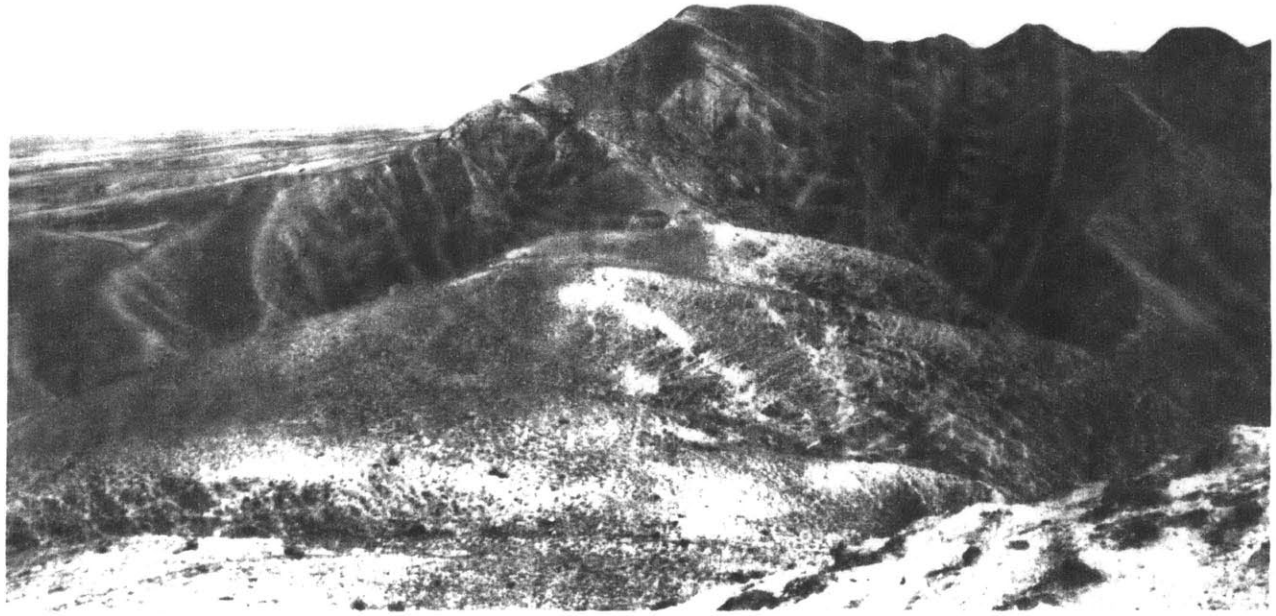

Figure 15

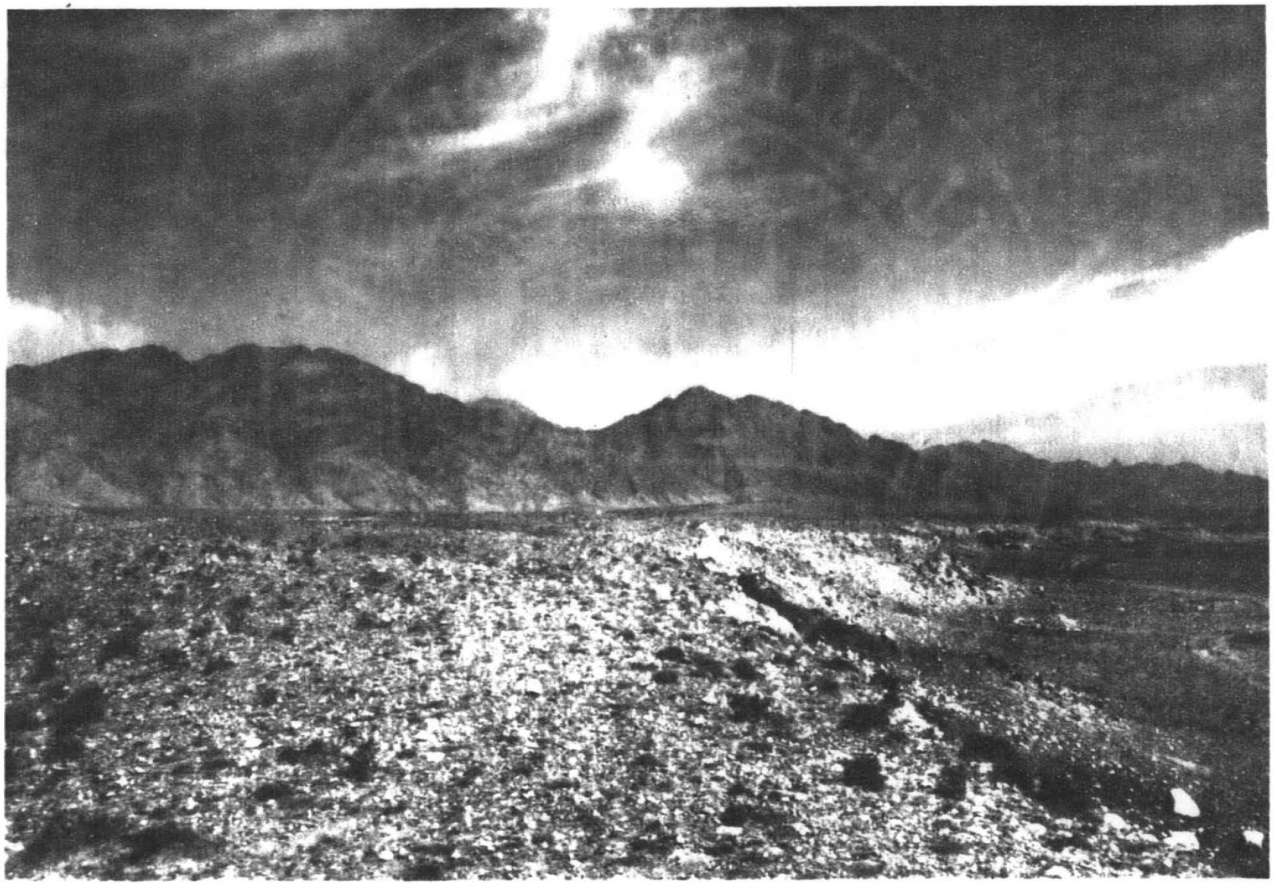

Figure 16

Figure 17